Characterization of r-protein variants in *Saccharomyces cerevisiae*

DISSERTATION

ZUR ERLANGUNG DES DOKTORGRADES DER
NATURWISSENSCHAFTEN (DR. RER. NAT.) DER
NATURWISSENSCHAFTLICHEN FAKULTÄT III
BIOLOGIE UND VORKLINISCHE MEDIZIN DER
UNIVERSITÄT REGENSBURG

vorgelegt von
Andreas Neueder
aus Bogen

Regensburg, 2010

Promotionsgesuch eingereicht am: 13.04.2010

Prüfungausschuss:

Vorsitzender:	Prof. Dr. A. Kurtz
1. Gutachter:	Prof. Dr. H. Tschochner
2. Gutachter:	Prof. Dr. R. Sterner
3. Prüfer:	Prof. Dr. W. Seufert
Ersatzprüfer:	Prof. Dr. T. Dresselhaus

Diese Arbeit wurde unter der Anleitung von Prof. Dr. Herbert Tschochner und Dr. Philipp Milkereit am Lehrstuhl für Biochemie III des Instituts für Mikrobiologie, Genetik und Biochemie der Universität Regensburg erstellt.

Ich erkläre hiermit, dass ich die vorliegende Arbeit ohne unzulässige Hilfe Dritter und ohne Benutzung anderer als der angegebenen Hilfsmittel angefertigt habe. Die aus anderen Quellen direkt oder indirekt übernommenen Daten und Konzepte sind unter Angabe der Quelle gekennzeichnet. Insbesondere habe ich nicht die entgeltliche Hilfe von Vermittlungs- bzw. Beratungsdiensten (Promotionsberater oder andere Personen) in Anspruch genommen. Niemand hat von mir unmittelbar oder mittelbar geldwerte Leistungen für Arbeit erhalten, die im Zusammenhang mit dem Inhalt der vorgelegten Dissertation stehen. Die Arbeit wurde bisher weder im In- noch im Ausland in gleicher oder ähnlicher Form einer anderen Prüfungsbehörde vorgelegt.

Regensburg, den

Table of contents

Table of figures

List of tables

Table of supplemental figures

List of supplemental tables

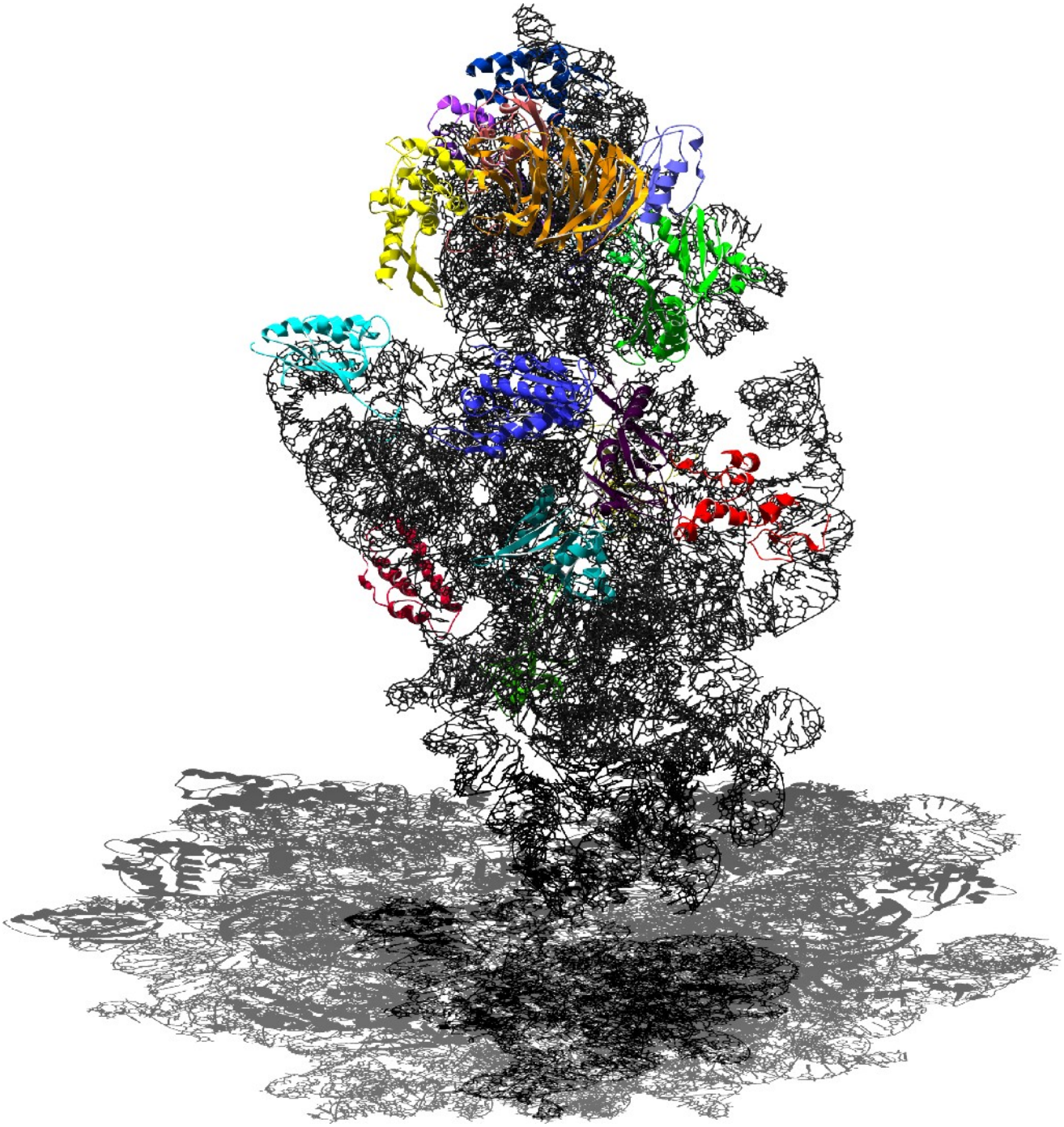

previous page

adapted from the latest structure of a eukaryotic 40S subunit from
Thermomyces lanuginosus
based on cryo-EM, resolution 8.9Å, pdb:3JYV
Taylor *et al.*, 2009

1 Introduction

1.1 The Ribosome

First described in the early 1950s as “microsomes”, particles which contain RNA and are involved in protein synthesis (Siekevitz, 1952), “ribosomes“ were born in 1958 on a meeting of the Biophysical Society at the MIT (Roberts, 1958). The syllable “ribo” was used to emphasize the RNA content of the microsomes. The term ribosomes was coined, because the conference participants liked the word as “it has a pleasant sound” (Roberts, 1958). At the same time extensive biochemical characterization of these particles was going on and the first cryo-electron microscopy images of ribosomes were taken. It soon became also clear that ribosomes are the molecular machines that produce polypeptides (Keller et al., 1954; McQuillen et al., 1959). Identification of the messenger RNA (mRNA) (Volkin and Astrachan, 1956; Jacob and Monod, 1961), transfer RNA (tRNA) bound amino acids (Hoagland et al., 1958) and decryption of the genetic code (Nirenberg and Matthaei, 1961; Morgan et al., 1966) completed the picture of the process of translation. Further milestones in the emergence of the up to date mechanistic model of translation were the identification of a third tRNA binding site (Rheinberger et al., 1981), the dissection of the single steps in the translation pathway (Rodnina et al., 1997; Pape et al., 1998) and atomic resolution structures of ribosomal subunits, which showed that RNA itself catalyzes the peptidyl-transferase reaction (among others (Ban et al., 2000; Wimberly et al., 2000; Schmeing et al., 2005)).

1.2 Ribosome structure

1.2.1 Composition

Ribosomes are large ribonucleoprotein (RNP) complexes, so by definition they consist of RNA (ribosomal RNA, rRNA) and proteins (ribosomal proteins, r-proteins). The general architecture is conserved between all three evolutionary kingdoms. The small ribosomal subunit (SSU, 30S/40S in prokaryotes/eukaryotes) consists of one RNA (16S/18S in prokaryotes/eukaryotes) and small ribosomal proteins (rpS). The large ribosomal subunit (LSU, 50S/60S in prokaryotes/eukaryotes) consists of two or three RNAs (5S and 23S in Bacteria; 5S, 5.8S and 25S in Archaea and Eukarya) and large ribosomal proteins (rpL). The core sequences of the ribosomal RNA species are conserved, while in the course of evolution archaeal and eukaryotic rRNAs gained additional parts, the so-called expansion segments. About two-thirds the number of small and half the number of large ribosomal proteins, which are able to build up a bacterial ribosome, have counterparts in one of the other evolutionary kingdoms (Figure 1, BAE). Additionally, a large number of r-proteins is conserved between Archaea and Eukarya (Figure 1, AE).

Ribosomal proteins were previously identified and labeled according to their migration

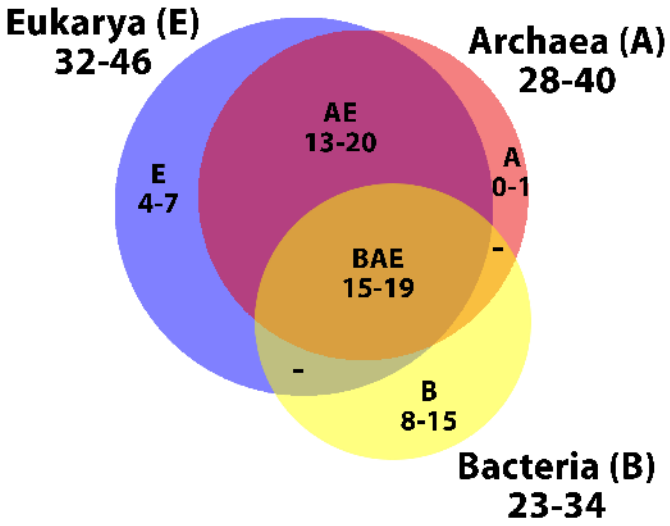

Figure 1. Venn diagram of ribosomal proteins from the three evolutionary kingdoms
The numbers show the average count of r-proteins in the respective evolutionary kingdom, e.g. Eukarya 32-46 means that an average eukaryotic ribosome is composed of 32 small ribosomal and 46 large ribosomal proteins. The numbers given in the intersections indicate the conserved r-proteins in the evolutionary kingdoms. BAE 15-19, for example means that 15 SSU and 19 LSU r-proteins are conserved between Bacteria, Archaea and Eukarya.

behavior in two-dimensional polyacrylamide gels. As a consequence many different nomenclatures came into existence, which is even more complicated as the prokaryotic and eukaryotic labeling was based on diverse abbreviations. For example the prokaryotic ribosomal protein of the small subunit S19 is the homologue of eukaryotic ribosomal protein rpS15, whose aliases are Rps21p, RIG-protein, S15, S21 and rp52. Whole genome sequencing of the eukaryotic model organism *S. cerevisiae* allowed for the first time to systematically assign protein names (Planta and Mager, 1998). This nomenclature is listed in table 1, together with the respective nomenclature of the prokaryotic counterparts. All ribosomal proteins described in this work are labeled according to this table. Recent advances in mass spectrometric analyses led to the discovery of a 33rd eukaryotic ribosomal protein of the small subunit, termed Asc1p in yeast and RACK1 (**r**eceptor for **a**ctivated **C**-**k**inase 1) in higher eukaryotes (Link et al., 1999; Gerbasi et al., 2004).

As mentioned before, the small subunit in prokaryotes contains the 16S rRNA, whose eukaryotic homologue is the 18S rRNA. The size difference between both is around 300 nucleotides (16S ca. 1500 bp, 18S ca. 1800 bp), for which the expansion segments account for. The 5.8S rRNA (ca. 160 bp), which exists in eukaryotes and some Archaea, is homologous to the 5'-end of prokaryotic 23S rRNA (Jacq, 1981). The secondary structure and the length (ca. 120 bp) of the 5S rRNA are very well conserved in all three evolutionary kingdoms (Szymanski et al., 2002). The biggest ribosomal RNA species can largely differ between species, but is usually about 2800 bp in Prokarya (23S) and about 3400 bp in Eukarya (25S). Some higher eukaryotic species posses an even larger 28S rRNA (ca. 4800 bp). In this case too, the size differences are originating from the evolutionary gained expansion segments.

	Eukarya		Archaea		Bacteria		
	H. sapiens	*S. cerevisiae*	*T. acidophilum*	*S. acidocaldarius*	*E. coli*	*T. thermophilus*	
RPSA	RPSA	RPS0A RPS0B	TA1190	Saci_0088	rpsB	TTHA0861	S2
RPS2	RPS2	RPS2	TA1251	Saci_0577	rpsE	TTHA1675	S5
RPS3	RPS3	RPS3	TA1265	Saci_0591	rpsC	TTHA1686	S3
RPS3A	RPS3A	RPS1A RPS1B	TA1167	Saci_0620			
RPS4	RPS4X RPS4Y	RPS4A RPS4B		Saci_0585			
RPS5	RPS5	RPS5	TA0092	Saci_0686	rpsG	TTHA1696	S7
RPS6	RPS6	RPS6A RPS6B	TA0323m	Saci_0831			
RPS8	RPS8	RPS8A RPS8B		Saci_0758			
RPS9	RPS9	RPS9A RPS9B	TA1032	Saci_0081	rpsD	TTHA1665	S4
RPS11	RPS11	RPS11A RPS11B	TA1262	Saci_0588	rpsQ	TTHA1683	S17
RPS13	RPS13	RPS13	TA1131	Saci_0829	rpsO	TTHA1138	S15
RPS14	RPS14	RPS14A RPS14B	TA1031	Saci_0082	rpsK	TTHA1666	S11
RPS15	RPS15	RPS15	TA1267	Saci_0593	rpsS	TTHA1688	S19
RPS15A	RPS15A	RPS22A RPS22B		Saci_0582	rpsH	TTHA1678	S8
RPS16	RPS16	RPS16A RPS16B	TA0432	Saci_0086	rpsI	TTHA1464	S9
RPS17	RPS17	RPS17A RPS17B	TA0589	Saci_0670			
RPS18	RPS18	RPS18A RPS18B		Saci_0080	rpsM	TTHA1667	S13
RPS19	RPS19	RPS19A RPS19B	TA0050	Saci_1469			
RPS20	RPS20	RPS20	TA0455	Saci_0684	rpsJ		S10
RPS23	RPS23	RPS23A RPS23B		Saci_0688	rpsL	TTHA1697	S12
RPS24	RPS24	RPS24A RPS24B	TA1092	Saci_0853			
RPS25	RPS25	RPS25A RPS25B					
RPS26	RPS26	RPS26A RPS26B		Saci_1554			
RPS27	RPS27	RPS27A RPS27B	TA1204	Saci_1276			
RPS27A	RPS27A	RPS31	TA1093				
RPS28	RPS28	RPS28A RPS28B		Saci_0698			
RPS29	RPS29	RPS29A RPS29B		Saci_0583	rpsN	TTHA1679	S14
RPS30	RPS30	RPS30A RPS30B		Saci_1348			

Table 1. Eukaryotic and prokaryotic nomenclature of SSU r-proteins

The genes are labeled according to the commonly used abbreviation in the corresponding organism. Left column is the eukaryotic nomenclature, right column the prokaryotic nomenclature. RpS25 is not conserved in the organisms listed (e.g. it is in *S. tokodaii* (ST0372)).

1.2.2 Structures of prokaryotic ribosomes

Early analyses of ribosome structures were purely based on electron microscopy images. In the late 1950s, the first pictures of ribosomes in a cell ((Palade, 1955), Figure 2 A), although they were not described as such, or as isolated RNPs were obtained (among others (Roberts, 1958), Figure 2 B). Electron microscopy techniques such as metal-shadowing and negative staining helped to improve the differentiation of substructures in isolated subunits ((Lake, 1976), Figure 2 C). The extremely complex X-ray diffraction patterns, caused by the giant mass of a ribosome (about 2.5 MDa prokaryotic; 4.2 MDa eukaryotic) prevented for a long time the solution of the atomic resolution structure. Finally in 2000, the crystal structures of both prokaryotic subunits were successfully obtained ((Ban et al., 2000; Wimberly et al., 2000), Figure 2 D and E). These structures were the basis for a molecular understanding of ribosome function and could be "used by scientists in order to develop new antibiotics, directly assisting the saving of lives and decreasing humanity's suffering" (The Royal Swedish Academy of Sciences, 2009).

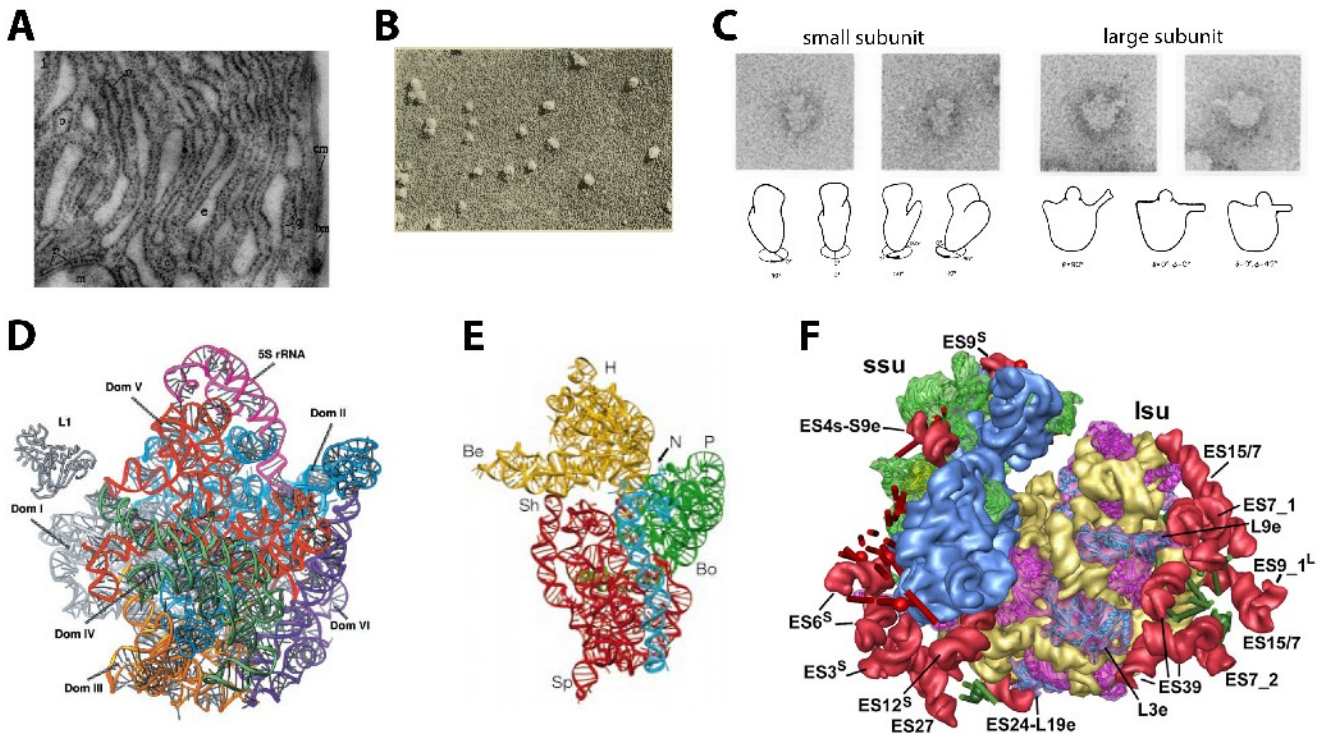

Figure 2. A brief history of ribosome structures
(**A**) Electron microscopy image of the basal region of an acinar cell of a rat pancreas (magnification 1:73000). Taken from Palade, 1955. (**B**) Electron microscopy image of purified RNP particles (magnification 1:170000). Taken from Prof. Kaesberg in Roberts, 1958. (**C**) Negatively contrasted isolated subunits of *E. coli* ribosomes and their diagrammatic representation. Modified from Lake, 1976. (**D**) Crown view of the LSU. Ribbon representation of the atomic resolution structure (2.4 Å) from *Haloarcula marismortui* subunits by Ban et al., 2000. (**E**) Ribbon representation of the atomic resolution structure (3 Å) from *Thermus thermophilus* small ribosomal subunits by Wimberley et al., 2000. (**F**) Ribbon representation of the cryo-electron microscopy based structure (8.7 Å) of a mammalian ribosome from *Canis lupus familiaris* by Chandramouli et al., 2008

The secondary structures of the different ribosomal RNAs were predicted way before the actual 3D structure was solved (Fox and Woese, 1975; Woese et al., 1980; Noller et al., 1981). In this studies it became also quite evident that *in vitro* and *in vivo* folding states of rRNAs differ, speaking for final folding changes upon stable incorporation in mature subunits. The secondary structure of the 16S rRNA can be clearly divided into 4 different regions (Figure 3 A and Figure 4 A). All subdomains are connected via the neck region (Figure 3 A, n). The 5'-domain and the central domain together form the body of the SSU. Some structural landmarks are easily distinguishable, namely the spur, the shoulder and the platform (Figure 3 A, s, sh and pt). Another easily visible subdomain is the 3'-major or head domain (Figure 3 A, h). A prominent feature of this domain is the beak region (Figure 3 A, bk). The 16S 3'-end is forming two helices (3'-minor domain), whereas the longer helix h44 is stretching almost over the whole body domain at the intersubunit side of the SSU. The ultimate 16S 3'-end (helix h45) however is localized between the platform and the head domain.

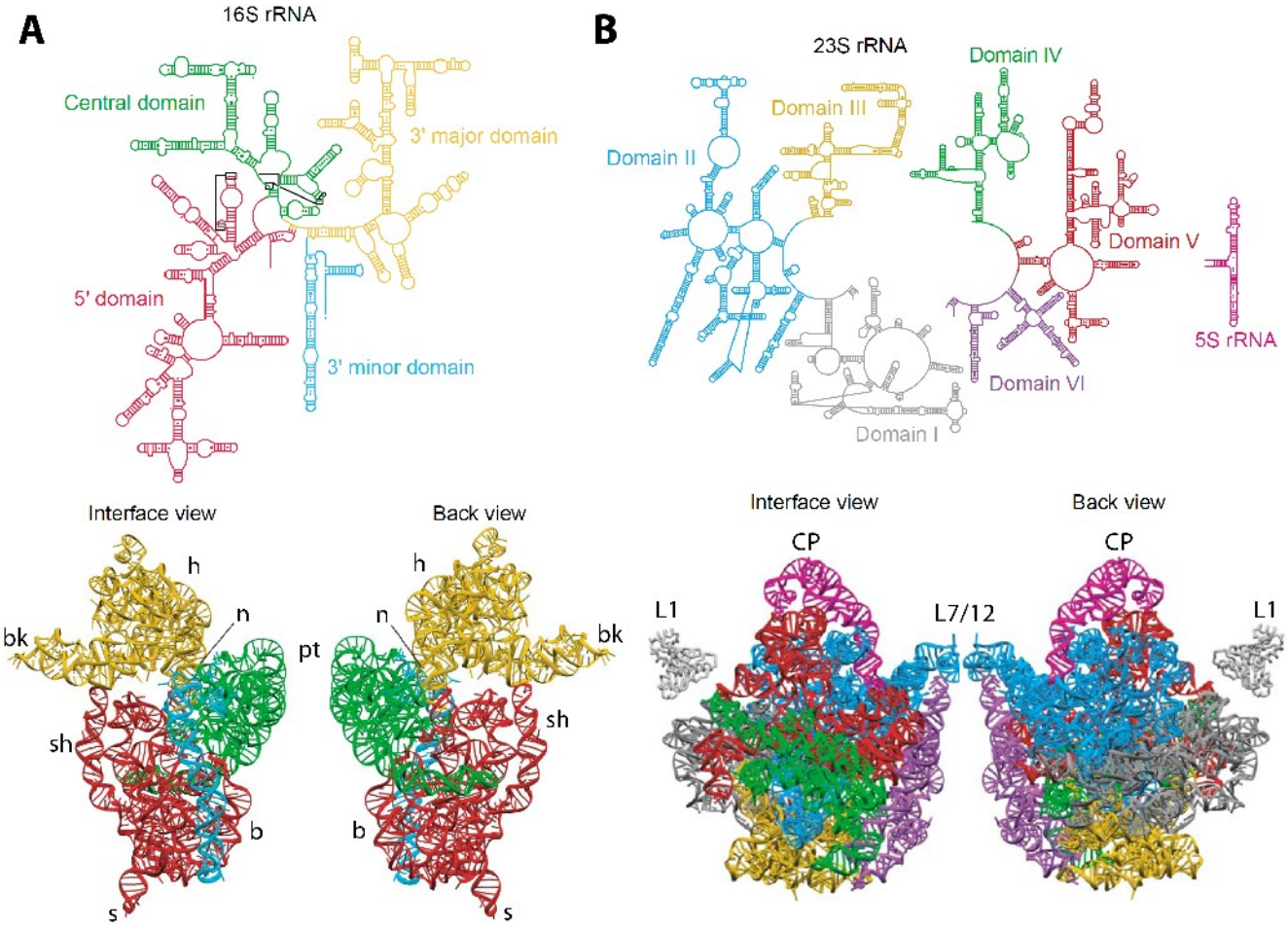

Figure 3. The structure of prokaryotic ribosomal subunits

(**A**) Structure of the SSU. The upper part displays the rRNA secondary structure, the lower part is the crystal structure from pdb:1J5E. Abbreviations: h – head; bk – beak; n – neck; p – platform; sh – shoulder; b – body; s – spur. (**B**) Structure of the LSU. The upper part displays the rRNA secondary structure, the lower part is the crystal structure from pdb:1FFK. Abbreviations: L1 – L1 stalk; CP – central protuberance; L7/12 – L7 and L12 stalk. (modified from Ramakrishnan and Moore, 2001)

The secondary structure of 23S rRNA can be divided into 6 subdomains (Figure 3 B). In the three dimensional structure on the other side, one can hardly see any of these subdomains, since the ribosomal rRNA is “intricately woven together” (Ramakrishnan and Moore, 2001). Hence only two structural landmarks, the L1 stalk and the L7/L12 stalk, are pointing out (Figure 3 B). The central protuberance is composed of the 5S RNP (Figure 3 B), which is binding “on top” of the large subunit.

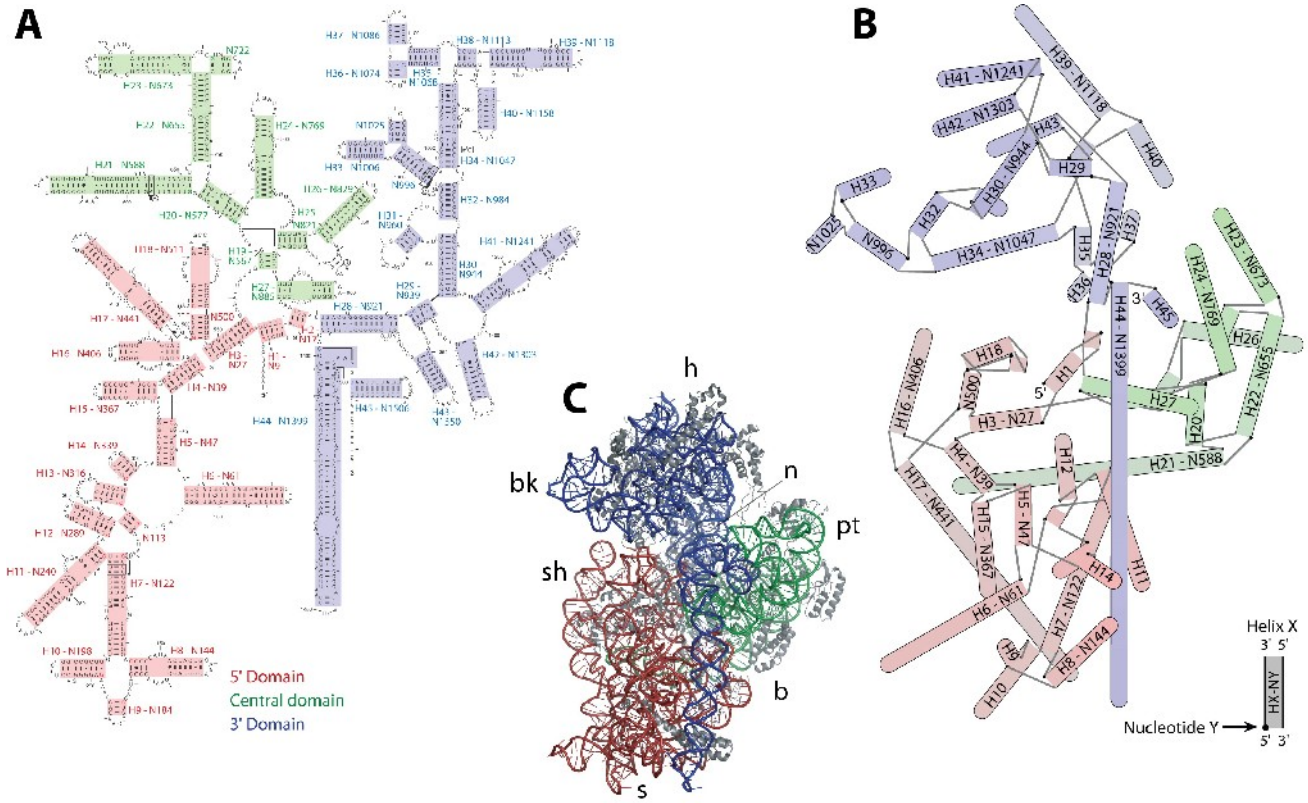

Figure 4. Different representations of the 30S subunit
(**A**) Secondary structure prediction of the 30S subunit, based on minimal free energy models. (**B**) A hybrid representation of the 30S subunit, in which the traditional flat secondary structure prediction is connected to the actual 3D structure by positioning the helices in their three dimensional constellation. (**C**) Crystal structure of the 30S subunit. Abbreviations: h – head; bk – beak; n – neck; pt – platform; sh – shoulder; b – body; s – spur. (**A**)-(**C**) 30S subunit folding domains (5'-, central and 3'-domain) are colored in the same way. (modified from Sykes and Williamson, 2009)

In this work, the molecular functions of ribosomal proteins exclusively from the small subunit have been assayed. As described before, the small subunit can be divided into 4 subdomains (in Figure 4 A the 3'-major and 3'-minor domain are subsumed as the 3'-domain). Recently a new representation of 16S rRNA has been proposed that connects 2D and 3D structure by positioning the secondary structure helices in their three dimensional constellation ((Sykes and Williamson, 2009), see Figure 4 B). So it is easily possible to position ribosomal proteins and map their rRNA interaction sites in a considerably more consistent way than projecting these contacts into the old secondary structure diagrams (Figure 5 A). Some of the obvious structural landmarks are stabilized/formed by a individual r-protein. For example the platform

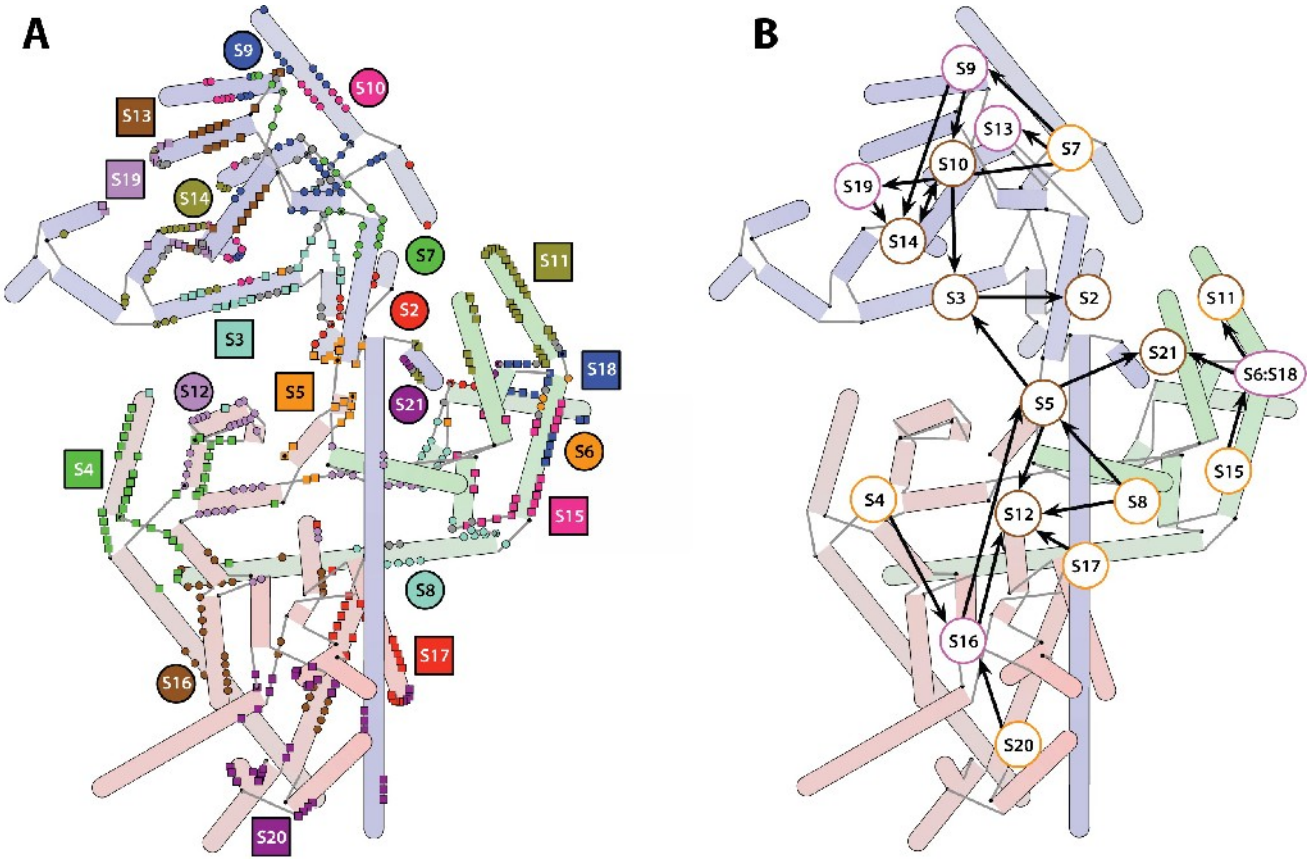

Figure 5. Ribosomal protein-RNA contacts
(**A**) The interaction sites of ribosomal proteins with rRNA are mapped into the hybrid representation of the 30S subunit (see Figure 4). (**B**) The Nomura assembly map (see Figure 16) is projected onto the hybrid representation of the 30S subunit. Arrows indicate the inter-dependencies of r-protein assembly. Subdomains are colored as in Figure 4. (modified from Sykes and Williamson, 2009)

is built up by S11 (rpS14 in eukaryotes), the shoulder by S4 (rpS9 in eukaryotes) and the spur by S20 (no eukaryotic homologue). The neck region is of special interest as it stabilizes the conformation of all major SSU subdomains to each other. The substantial contribution to this spatial organization is made by S5 (rpS2 in eukaryotes) (Figure 5 A). This r-protein mainly binds helices h1 and h2 (5'-domain) and orientates it towards helices h36 and h28 (3'-domain).

Many structures have been recently acquired of ribosomes complexed with tRNA, mRNA or various drugs. These structures allowed the exact determination of the respective binding sites and gave insights into structural changes during ribosome function and the mechanism of translation (for recent reviews see (Simonetti et al., 2009; Agirrezabala and Frank, 2009) and Figure 6, (Schmeing et al., 2009)). Another example of mechanistic insights into translation by analyses of ribosome structures is the ratchet-like rotation of the SSU relative to the LSU during translation elongation. This movement is induced by GTP hydrolysis of elongation factor G (EF-G) and was revealed by observations of cryo-electron microscopy based structures of a translating bacterial ribosome (Frank and Agrawal, 2000).

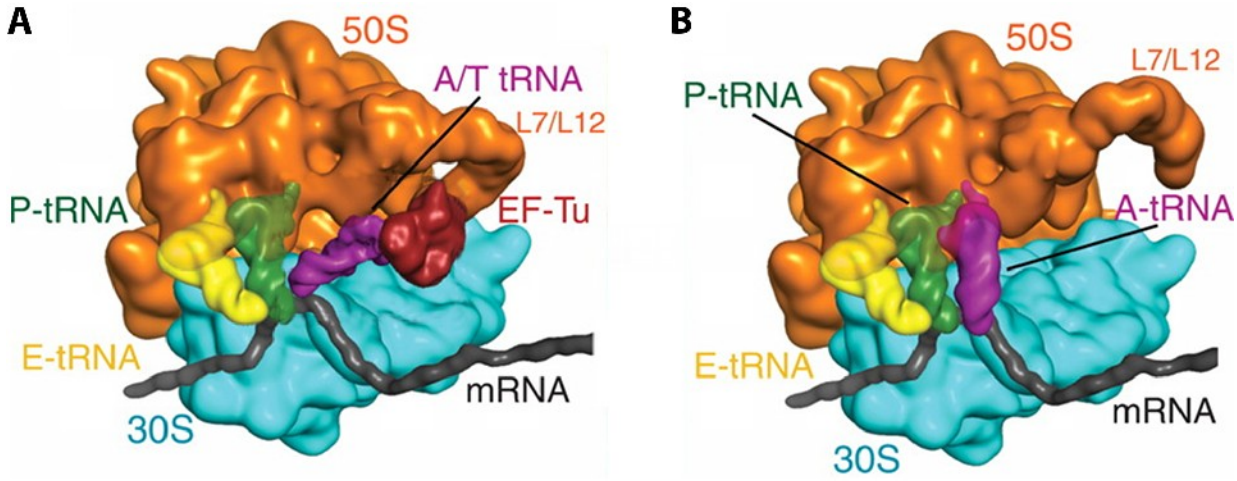

Figure 6. Schematic structure of the 70S ribosome with tRNAs and mRNA
A schematic representation of a crystal structure of the ribosome bound to EF-Tu and aminoacyl tRNAs; top view. pdb:2WRN, 2WRO, 2WRQ, 2WRR. (**A**) The L7/L12 stalk recruits the ternary complex (aminoacyltRNA•GTP•EF-Tu) to a ribosome with deacylated tRNA in the E site and peptidyl-tRNA in the P site. (**B**) After hydrolysis of GTP by EF-Tu, pi and EF-Tu are released and the tRNAs are accommodated. (modified from Schmeing et al., 2009).

1.2.3 Structures of eukaryotic ribosomes

The eukaryotic ribosome is almost twice as large as its prokaryotic counterpart. Therefore it hasn't been possible to solve any atomic resolution structures of eukaryotic ribosomes up to now. Nevertheless cryo-electron microscopy and single particle methods allowed a pretty detailed view of eukaryotic ribosomes. The overall architecture of both eukaryotic subunits is remarkably similar to the prokaryotic structure (compare Figure 3 and Figure 7). On the other hand, the dimensions of the subunits are increased due to the expansion segments, which are most likely stabilized by binding of eukaryotic specific ribosomal proteins (Chandramouli et al., 2008; Taylor et al., 2009).

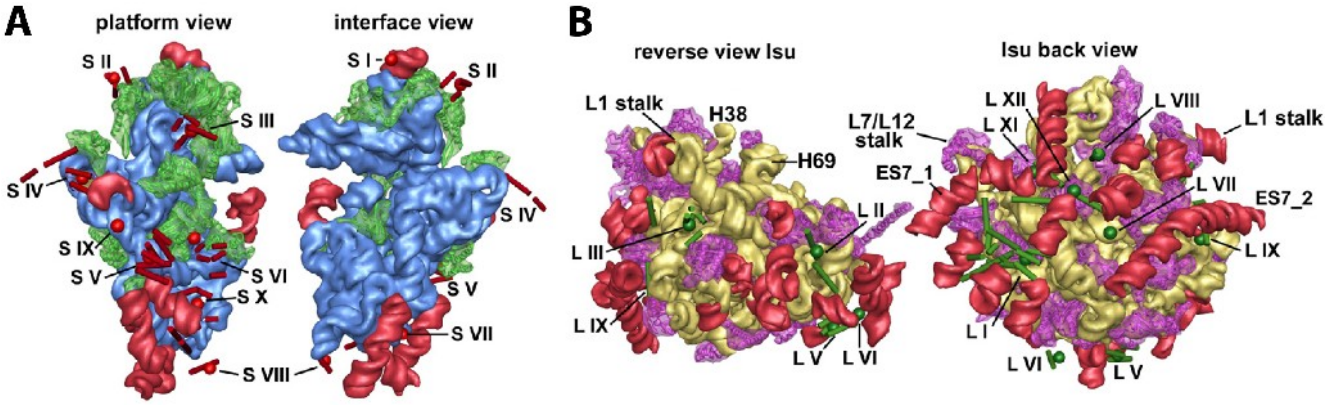

Figure 7. Structures of mammalian ribosomal subunits
8.7Å structure of the *Canis lupus familiaris* ribosome determined by cryo-electron microscopy (pdb:) (**A**) Novel proteins of the SSU are marked with red spheres and possible α-helices are indicated by red cylinders. The core rRNA and expansion segments (ES) are shown as blue and red ribbons, and the conserved proteins are shown in green. (**B**) Novel proteins of the LSU are marked with green spheres and possible α-helices are indicated by green cylinders. The core rRNA and expansion segments (ES) are shown as gold and red ribbons and the conserved proteins are colored magenta. (modified from Chandramouli et al., 2008)

15, respectively 19 eukaryotic r-proteins of the small and the large subunit are conserved in bacteria (see Figure 1 and Table 1). The structure of these proteins was modeled by homology and docked into the density maps. Hence, in all structures of eukaryotic ribosomes mostly the conserved r-proteins are localized (Figure 8 A). One of the two exceptions is rpS19, which could be assigned to a density at the top of the SSU head domain (Taylor et al., 2009). The other exception is Asc1p, the yeast ortholog of RACK1 (receptor for activated protein kinase C1), binding in the 3'-major domain (Figure 8 A). Asc1p is a stoichiometric constituent of the small subunit and is supposed to repress gene expression (Gerbasi et al., 2004).

One method to localize eukaryotic/archaeal specific r-proteins is based on bioinformatic analyses of the primary sequence conservation of bacterial specific SSU r-proteins. The found rRNA binding motifs were aligned with the primary sequence of eukaryotic specific r-proteins and by this possible orthologes were identified (Malygin and Karpova, 2009). In other approaches, crosslinking agents were used to identify protein-rRNA contacts (Takahashi et al., 2005; Pisarev et al., 2008a). These possible r-protein positions, by chance can be assigned to unattributed densities in cryo-EM maps (Taylor et al., 2009).

This way, rpS26 and rpS28 could be consistently localized next to rpS5 and rpS14 in the head-platform interface. RpS27 is probably binding in the body domain. The localization of rpS25 is indefinite as it has been localized both to the head-platform interface (Takahashi et al., 2005; Taylor et al., 2009) and the body next to the spur (Malygin et al., 2009).

Figure 8 B elucidates the SSU subdomains, which are assigned according to the secondary structure conservation with prokaryotic 16S rRNA. It is clearly visible that the conserved sequences form the SSU core structure, with the expansion segments being located more on the surface. In all available pseudo-atomic structures of eukaryotic SSUs the last 3 nucleotides of 18S rRNA are not modeled. Nevertheless it is clear that the 18S 3'-end has to be in the head-platform interface in close proximity to rpS5 and rpS14 (see also discussion in 3.2).

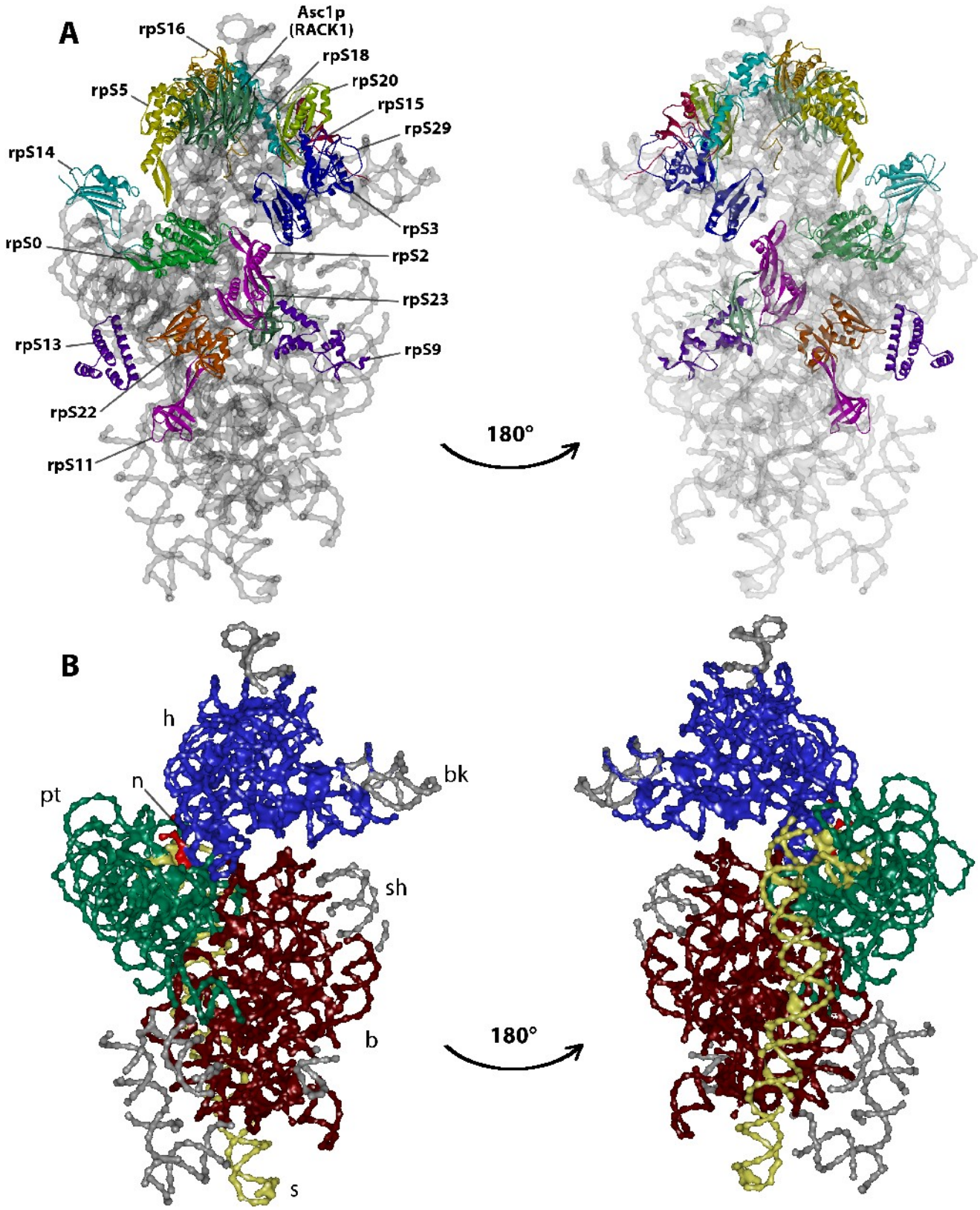

Figure 8. Cryo EM based structure of a eukaryotic 40S subunit and 40S rRNA subdomains
(**A**) The structure for the 40S subunit from *Canis lupus familiaris* (pdb:2ZKQ, Chandramouli et al., 2008) based on cryo electron-microscopy maps and homology modeling. The left panel is a cytoplasmic view of the SSU, right panel is inter-subunit view. (**B**) The colors show the subdomains of 40S rRNA. The 5'-domain is shown in brown, the central domain in green, the 3'-major domain in blue, the 3'-minor domain in beige, the last 3'-18S rRNA nucleotides after helix 45, which have been modeled, in red and rRNA expansion segments, which are unique to eukaryotes, in gray. Abbreviations: h – head; bk – beak; n – neck; pt – platform; sh – shoulder; b – body; s – spur.

1.2.4 Comparison and assessment of pro- and eukaryotic ribosome structures

The solution of atomic resolution structures of prokaryotic ribosomes has been one of the most important steps towards a molecular understanding of ribosome function. The doubled mass of an eukaryotic ribosome has prevented the achievement of crystal structures. During the first years of this thesis, the best available structure of an eukaryotic small subunit was determined with a resolution of 11.4 Å (Spahn et al., 2001). The biggest disadvantage of this structure is that the r-proteins, which were modeled by homology to their prokaryotic counterparts, were simply docked onto a 30S rRNA core from *T. thermophilus*. Thus, the complete structure of the SSU is distorted and especially protein-rRNA contacts are not accurate (Figure 9 A). The 18S rRNA in two newer cryo-EM based structures was modeled according to the actually observed densities and includes rRNA expansion segments (Chandramouli et al., 2008; Taylor et al., 2009). The r-protein core structures are quite similar of all three. On the other side, the unstructured N- or C-terminal protein parts of many r-proteins look fairly different (Figure 9 B and C).

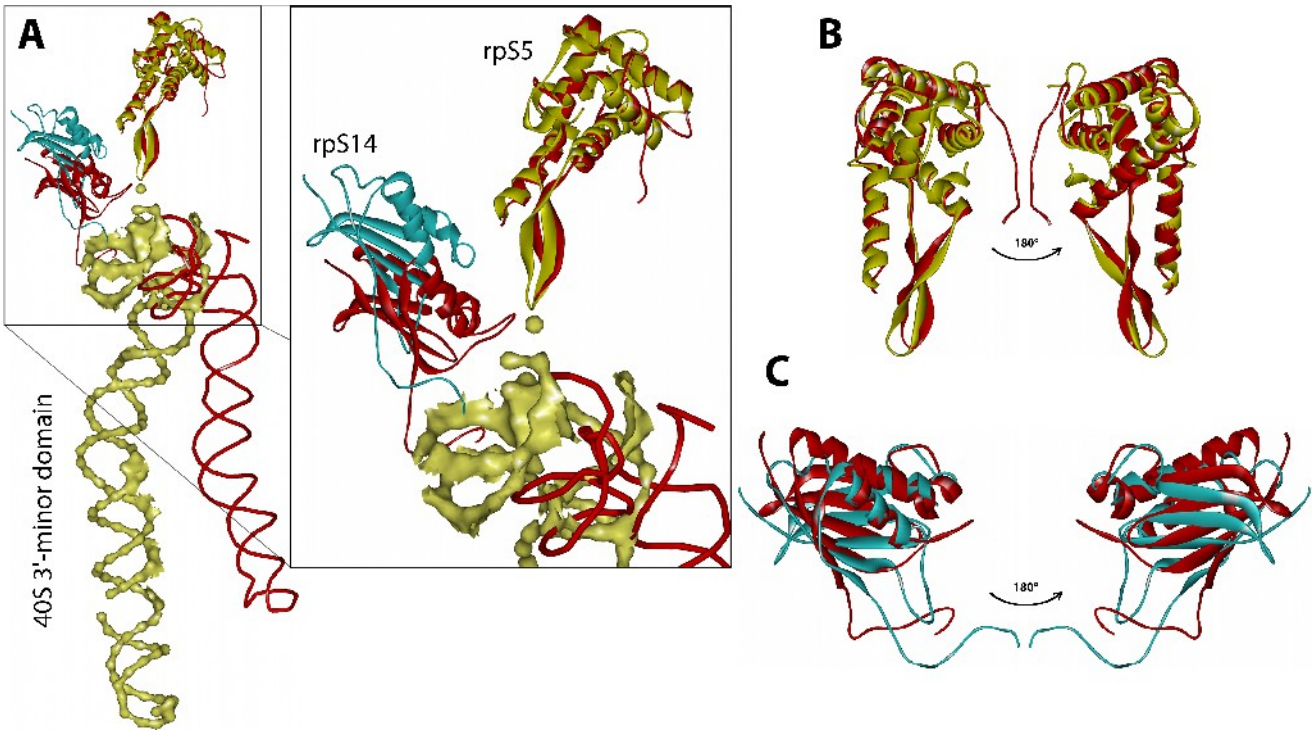

Figure 9. Comparison of different pseudo atomic structures of eukaryotic ribosomes
(**A**) Both structures shown are cryo EM modeling maps. The structure shown in red was obtained by Spahn et al, 2001 (pdb:1S1H). The other structure shown (rpS5 in yellow, rpS14 in light blue and 3'-minor domain in beige), was built by Chandramouli et al., 2008 (pdb:2ZKQ). The comparison has been obtained by fitting both rpS5 structures. (**B**) A comparison of rpS5 structures (red: Spahn et al.; yellow: Chandramouli et al.). (**C**) A comparison of rpS14 structures (red: Spahn et al.; light blue: Chandramouli et al.).

These uncertainties rendered it quite difficult to predict any protein-protein or protein-rRNA contact site. For example S7 (rpS5) interacts via its non-conserved C-terminus with S11 (rpS14) in the prokaryotic ribosome (Robert and Brakier-Gingras, 2003). In the structure by Spahn, there is a possible interaction of rpS14 with the hairpin of rpS5 (Figure 9 A). The

structure obtained by Chandramouli et al. shows a protein-protein contact of rpS14 with the C-terminus of rpS5 (Figure 9 A, see also Figure 39). The most up to date structure of Taylor and colleagues separates the two proteins again to a distance of about 7.9 Å (data not shown). All structural models presented in this work are therefore rather predictions than absolute statements. Definite answers to all these questions will eventually be given by an atomic resolution structure of an eukaryotic ribosome.

1.3 Ribosome function

Ribosomes catalyze the fundamental process of translation. In other words, ribosomes translate the genetic information, which is saved in the DNA and delivered by the messenger RNAs, into polypeptides. The process of translation and peptide bond formation is quite conserved in all evolutionary kingdoms (see 1.3.2). In contrast to this, translation initiation differs greatly between Eukarya and Prokarya (see 1.3.1).

translation step	Bacteria	Archaea	Eukarya	translation step	Bacteria	Archaea	Eukarya
initiation	IF1	aIF1A	eIF1A	elongation	EF-Tu	aEF1α	eEF1A
	IF2	aIF5B	eIF5B		EF-Ts	aEF1B	eEF1B (2 or 3 subunits)
	IF3	aIF1	eIF1		SelB	SelB	eEFSec
		aIF2α	eIF2α				SBP2
		aIF2β	eIF2β		EF-G	aEF2	eEF2
		aIF2γ	eIF2γ				
		aIF2Bα	eIF2Bα	termination	RF1	aRF1	eRF1
			eIF2Bβ		RF2		
			eIF2Bγ		RF3		eRF3
		aIF2Bδ	eIF2Bδ				
			eIF2Bε	recycling	RRF		
			eIF3 (13 subunits)		EF-G		
		aIF4A	eIF4A				eIF3
			eIF4B				eIF3j
			eIF4E				eIF1A
			eIF4G				eIF1
			eIF4H				
		aIF5	eIF5				
		aIF6	eIF6				
			PABP				

Table 2. Translation factors in all three evolutionary kingdoms
Orthologous or functionally homologous factors are aligned. (adapted from Rodnina and Wintermeyer, 2009)

1.3.1 Translation initiation

It is not much known about the mechanism of translation initiation in Archaea, but it seems that it is a “mosaic of eukaryal and bacterial features” (Bell and Jackson, 1998). Many eukaryotic translation initiation factors have homologues in Archaea (see Table 2, (Rodnina and Wintermeyer, 2009)), but mRNA binding and start codon recognition is Bacteria-like (reviewed in (Benelli and Londei, 2009)).

In Bacteria (Figure 10 B), all three initiation factors (see Table 2) bind the 30S subunit. Subsequently the complex binds mRNA, predominantly interacting with the Shine-Dalgarno sequence. The correct positioning of mRNA is achieved by binding of the initiator tRNA in the P site, partially displacing IF3. After subunit joining, GTP is hydrolyzed by IF2 that triggers conformational changes of IF2 itself. This in turn promotes dissociation of initiation factors

and accommodation of the initiator tRNA.

In contrast to Bacteria, the initiator tRNA in Eukarya is bound in a ternary complex with eIF2 and GTP (Figure 10 A). The ternary complex together with eIF1, eIF1A, eIF3 and the 40S subunits forms the 43S initiation complex. The modifications of eukaryotic mRNAs, namely a 5'-cap structure (7-methylguanosine) and 3'-polyadenylation, aid the formation of a circular structure. The modifications are bound by the cap-binding protein eIF4E, the scaffolding factor eIF4G and the poly(A)-binding protein (PABP). The 43S initiation complex binds to this structure and subsequently scans along the mRNA for the start codon. During scanning GTP is maybe hydrolyzed by eIF2, but the phosphate is not released until start codon recognition. The release triggers conformational changes that lead to dissociation of eIF1, eIF2 and eIF5 from the complex and simultaneous joining of eIF5B·GTP. The 60S subunit is binding and upon GTP hydrolysis by eIF5B the remaining initiation factors are released and the initiator

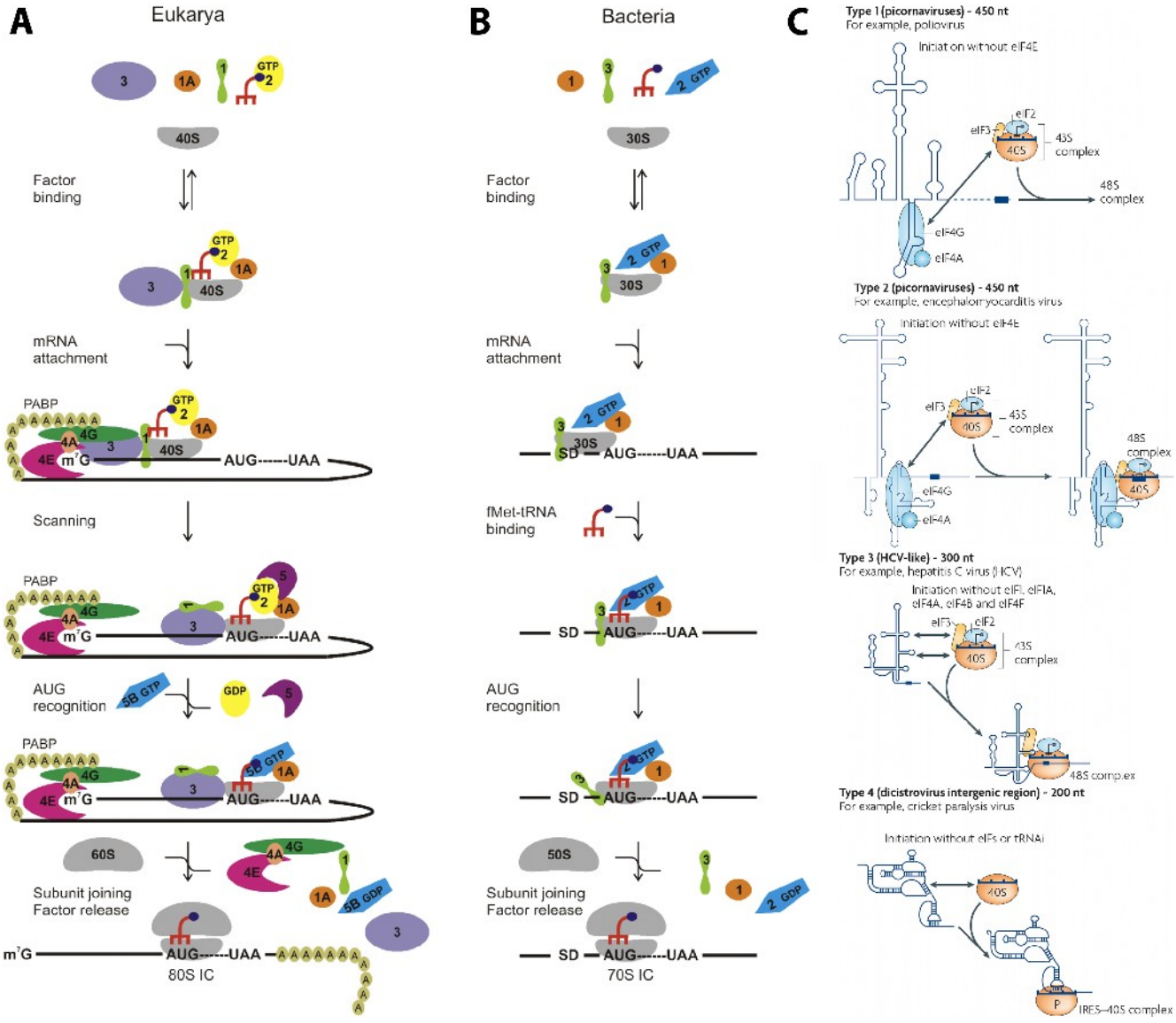

Figure 10. Translation initiation in Bacteria and Eukarya
Canonical translation initiation in Eukarya (**A**) and Bacteria (**B**). (modified from Rodnina and Wintermeyer, 2009) (**C**) IRES dependent translation initiation in eukaryotes. (modified from Jackson et al., 2010) (**A**)-(**C**) for details see text

tRNA accommodates in the P site.

Interestingly, eukaryotic ribosomes are able to initiate translation independent of mRNA modifications very much like bacterial ribosomes (Figure 10 C, (Jackson et al., 2010)). 40S/43S initiation complexes bind to mRNA secondary structures named IRES (**i**nternal **r**ibosome **e**ntry **s**ites). These were first identified by analysis of translation initiation of naturally uncapped polio- and picornavirus mRNAs (Pelletier and Sonenberg, 1988; Jang et al., 1988). Up to now, there are four different types of viral IRES-43S/40S initation complex known (see Figure 10 C), which involve different subsets of initiation factors. Remarkably, the type 4 (dicistrovirus intergenic region) IRES dependent initiation is completely independent of any translation initiation factors or initiator tRNAs. Here, an IRES secondary sequence element mimics the tRNA in the P site.

Many non-viral mRNAs have been identified that contain an IRES sequence, though they can also be translated in the canonical, cap-dependent way (Johannes et al., 1999). These include most notably stress response mRNAs and apoptosis related mRNAs (Henis-Korenblit et al., 2000; Mitchell et al., 2001). The key player to switch from cap-dependent to IRES initiation might be eIF4G, which is not only highly over expressed in cancer tissues (Braunstein et al., 2007; Silvera et al., 2009), but in addition its mRNA contains an IRES sequence itself (Johannes and Sarnow, 1998). The translational feedback mechanism of eIF4G expression might shift the translation initiation toward IRES dependent upon high levels of eIF4G and vice versa.

1.3.2 Translation elongation

Translation elongation, as well as termination follows the same principles throughout all living organisms. The tRNAs are bound by an elongation factor/GTP (EF-Tu in Bacteria, for homologues see Table 2) and associate with the ribosome at the A site (Figure 11 A, (Steitz, 2008)), which leads to release of the tRNA from the E site. The correct codon-anticodon pairing triggers GTP hydrolysis and simultaneously the ribosome is subjected to a conformational change that accommodates the A and P site tRNAs in the optimal position for the peptidyl-transferase reaction to occur (see also Figure 6). The transferase reaction itself is catalyzed by universally conserved nucleotides in the 23S/25S rRNA and the tRNA (reviewed in (Beringer and Rodnina, 2007)). The translocation from the pre (A and P site occupied) to the post (P and E site occupied) state is facilitated by binding and GTP hydrolysis of another elongation factor (EF-G in Bacteria).

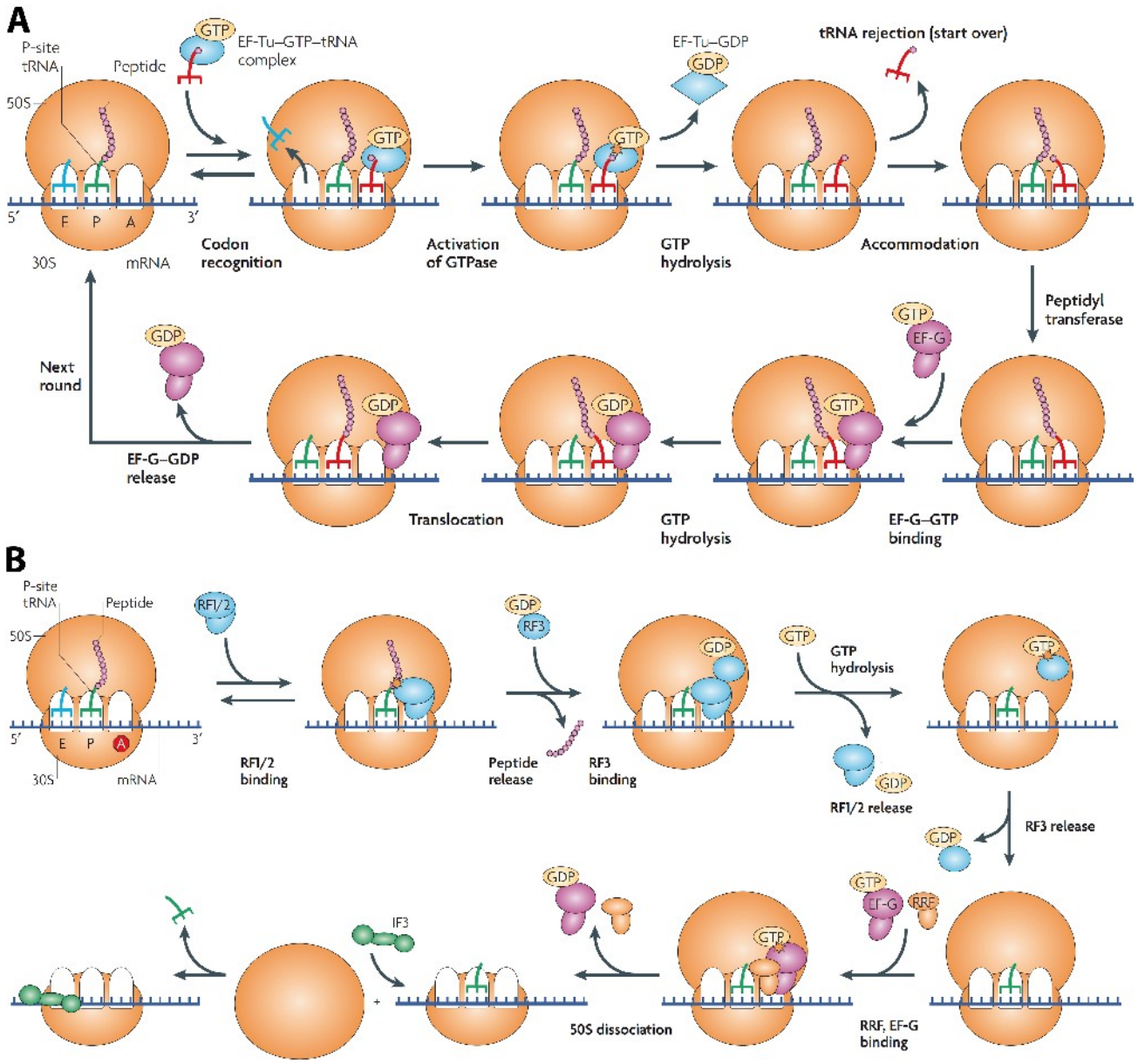

Figure 11. Translation elongation and termination in prokaryotes
(**A**) Translation elongation cycles in prokaryotes. (**B**) Translation termination and recycling in prokaryotes. (**A**) and (**B**) for details see text. (modified from Steitz, 2008)

1.3.3 Translation termination and recycling

As soon as a stop codon is positioned at the A site, release factors bind (RF1 or RF2 in Bacteria, for homologues see Table 2). This causes hydrolysis and release of the tRNA-polypeptide at the P site (Figure 11 B). Binding of another factor in complex with GDP (RF3 in Bacteria), followed by exchange of GDP to GTP and subsequent hydrolysis results in dissociation of the release factors and the ribosome. In this post-termination complex (post-TC), the ribosome is still bound to mRNA and a tRNA is left at the P site. The complete dissassembly is facilitated by ribosome release factors (RRF and EF-G in Bacteria). In eukaryotes, this process is conducted by initiation factors (eIF3, eIF3j, eIF1A, eIF1).

1.4 Ribosome biogenesis

1.4.1 Production of ribosomal constituents

1.4.1.1 Synthesis of rRNA

The rDNA genes of eukaryotes are usually arranged in multi-copy gene clusters. In yeast, the rDNA genes are localized on chromosome 12 in about 150 copies. One rDNA gene is composed of a 35S gene and a 5S gene, which are transcribed by DNA-dependent RNA polymerase I (Pol I) and DNA-dependent RNA polymerase III (Pol III), respectively (Figure 12). The 35S gene codes for a 35S rRNA that is the precursor transcript for the mature 18S, 5.8S and 25S rRNAs (for processing details see 1.4.3).

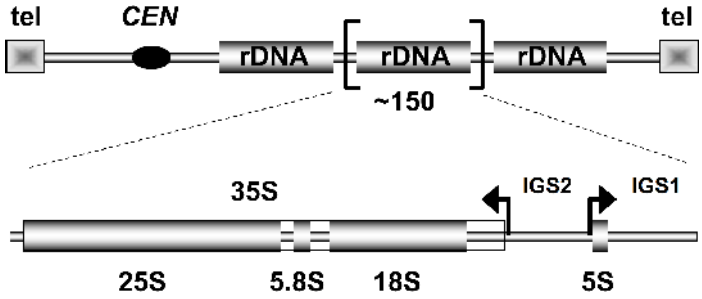

Figure 12. rDNA locus of *S. cerevisiae*
The rDNA locus of *S. cerevisiae* is at chromosome 12 in a multicopy gene array. One copy is composed of a 35S gene and a 5S gene, both with their own promoters (indicated by the arrows). Abbreviations: tel – telomer; CEN – centromer, IGSX – intergenic spacer X. (modified from Goetze et al., 2010)

The Pol I promoter region is located in the intergenic spacer 2 (IGS2) with an enhancer region in the IGS1 region. The later one stimulates transcription by Pol I over 15 fold (Elion and Warner, 1986). The promoter region itself consists of a core element (CE) and a upstream element (UE). In the current model of transcription initiation (reviewed in (Moss et al., 2007)), the multiprotein complex upstream activating factor (UAF; consists of Rrn5p, Rrn9p, Rrn10p, Uaf30p and histones H3 and H4) is binding first to the upstream element. Bridged by the TATA-box binding protein (TBP), the core factor (CF; consists of Rrn6p, Rrn7p and Rrn11p) is binding next. Pol I is only able to initiate transcription in complex with Rrn3p that binds to the A43 subunit of Pol I and the core factor subunit Rrn6p (Figure 13). The switch from initiation to elongation mode involves dissociation of Rrn3p and possibly also of TBP and the core factor. 90% of transcription termination occurs at a binding site for the factor Reb1p in the IGS1. The remaining polymerases, reading through the normal termination site, are stopped next to the replication folk barrier (RFB), an element in the IGS1 region that inhibits DNA replication in the direction opposite to rDNA transcription.

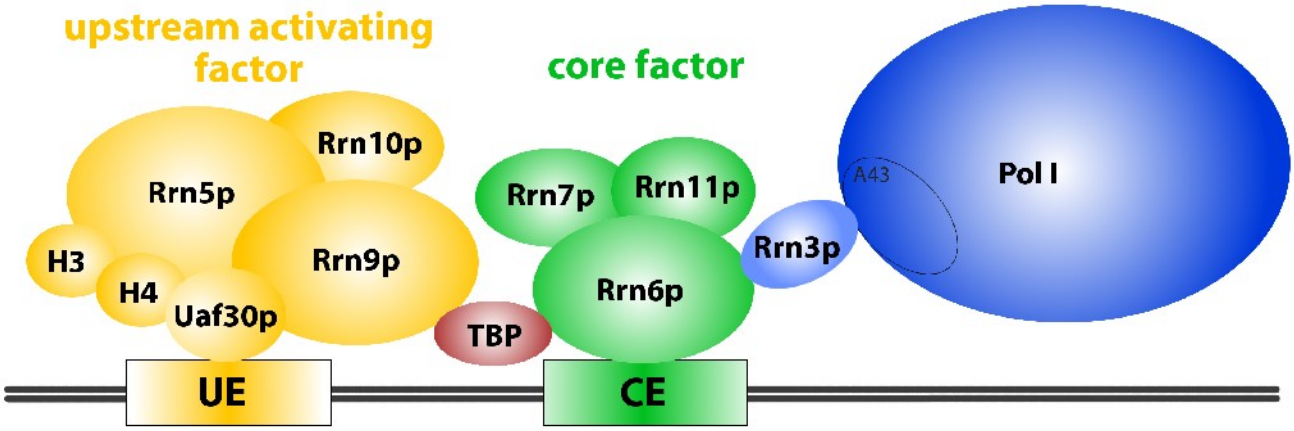

Figure 13. Pol I initiation complex in *S. cerevisiae*
The Pol I initiation complex in its active form. Abbreviations: UE – upstream element; CE – core element; TBP – TATA-box binding protein.

In addition to the mentioned basal transcription factors, Net1p and Hmo1p seem to play a role in stimulation of Pol I transcription. Net1p binds directly to Pol I (Shou et al., 2001), while Hmo1p is found all over the 35S rDNA locus (Gadal et al., 2002). Interestingly Hmo1p also binds to the promoters of many r-proteins, thus providing a potential link between rRNA and r-protein production (Hall et al., 2006) (see also 1.4.6).

Only about half of the rDNA repeats in a normal growing yeast cell are in an active state, i.e. these repeats are almost devoid of nucleosomes and heavily transcribed (Merz et al., 2008). The inactive repeats on the other side are transcriptionally silenced by tight packaging into heterochromatin (Dammann et al., 1995).

1.4.1.2 Synthesis of ribosomal proteins

The third DNA dependent RNA polymerase – Pol II – transcribes the genes of ribosomal proteins in eukaryotes. These genes are spread all over the genome and are not arranged in clusters as in prokaryotes (Mager et al., 1977). Interestingly, despite the fact that the half-lifes of messenger RNAs of r-proteins are very short (Moore et al., 1995), it seems that eukaryotic r-proteins are expressed in excess. This mechanism was suggested to assure that r-protein production is never the rate limiting step in ribosome biogenesis (Lam et al., 2007).

1.4.2 Ribosome biogenesis factors and snoRNPs

The main difference between bacterial and eukaryotic (archaeal) ribosome biogenesis is the requirement of a vast number of non-ribosomal proteins and small nucleolar RNAs (snoRNA) in the production of ribosomes.

Prokaryotic ribosomal RNA species are nevertheless modified. They are subjected to isomerization of uridine to pseudouridine and chemically modified by addition of methyl groups, just like the archaeal and eukaryotic ones (see 1.4.3.2, reviewed in (Kaczanowska and Rydén-Aulin, 2007)). Though the mechanism of pseudouridine formation is independent of snoRNAs in Bacteria (Charette and Gray, 2000). And in addition, most of the chemical

modifications, with exception of some 23S modification in the proximity of the peptidyl-transferase center, are dispensable (Krzyzosiak et al., 1987; Green and Noller, 1996). Complete *in vitro* reconstitution of prokaryotic ribosomes from *E. coli* is independent of any non-ribosomal factors. But, to create functional subunits, heating steps are required that most likely prevent the rRNAs from blundering in thermodynamically folding traps (Mizushima and Nomura, 1970; Herold and Nierhaus, 1987). *In vivo*, ribosome maturation factors probably assume responsibility for correct folding. There are about 50 known biogenesis factors in *E. coli*, however most of them are non-essential (reviewed in (Kaczanowska et al., 2007)).

A common feature of Archaea and Eukarya is that selectivity of base modification is achieved using small non-coding RNAs, the snoRNAs. The increasing number of sequenced archaeal genomes since the turn of the millennium allowed the identification of first C/D-box snoRNAs (called sRNA in Archaea) and later also H/ACA type snoRNAs (among others (Gaspin et al., 2000; Omer et al., 2000a; Tang, Bachellerie, et al., 2002)). The C/D-box snoRNAs are complementary in sequence to the respective modification site and “guide” the RNP, which methylates nucleotides in rRNA and tRNA species. The mechanism of target site selection of H/ACA type snoRNAs is the same as of C/D-box snoRNAs, but the consequence of RNP binding is the isomerization of uridine to pseudouridine (reviewed in (Dennis et al., 2001)).

The first steps in eukaryotic rRNA processing (see 1.4.3.1) largely depend on the U3 snoRNA (Hughes and Ares, 1991a). This snoRNA together with about 30 proteins form the 90S pre-ribosome, also named SSU processome in yeast, because it consists of mostly SSU biogenesis factors (Dragon et al., 2002a). Further modification of the ribosomal RNAs involves about 70 additional snoRNPs (reviewed in (Henras et al., 2008)). Like in prokaryotes, most of the single modifications are not essential, though absence of a subset alters e.g. ribosome fidelity and/or function (King et al., 2003; Liang et al., 2007) (see also 1.4.3.2).

The U3 snoRNP is thought to assemble co-transcriptionally at the nascent 35S pre-rRNA transcript, forming a 90S particle, which is visible in Miller chromatin spreads of actively transcribed rRNA genes as “terminal balls” (Dragon et al., 2002a). Mainly biogenesis factors that are required for maturation of the SSU are associated within this 90S pre-ribosomes. Endonucleolytic processing in the internal transcribed spacer 1 (ITS1) region (see 1.4.3.1) splits the following maturation pathways of pre-40S and pre-60S particles. In general, biogenesis factors can be divided into many different classes: endoribonucleases (e.g. RNase MRP, maybe Nob1p), exoribonucleases (e.g. Rat1p, Xrn1p), helicases (e.g. Dbp2p, Prp43p), kinases (e.g. Hrr25p), ATPases (e.g. Rea1p), GTPases (e.g. Nog1p, Nog2p), methyl-transferases (e.g. Nop2p, Dim1p), peptidyl-proline-isomerases (e.g. Fpr3p), r-protein assembly factors (e.g. Rrp7p), intra-nucleolar/nuclear transport factors (e.g. Noc1p, Noc2p, Noc3p) and nuclear-export factors (e.g. Crm1p, Rrp12p, Mex67p/Mtr2p, Ltv1p).

In total about 150 non-ribosomal trans-acting factors are engaged in eukaryotic ribosome biogenesis (reviewed in (Tschochner and Hurt, 2003; Nazar, 2004; Henras et al., 2008)).

Recent analysis in yeast showed that the high efficiency in ribosome production is maybe boosted by association of biogenesis factors with pre-ribosomes not as single proteins, but as multiprotein “building blocks” (Merl et al., 2010). These protein complexes seem to assemble independent of pre-rRNA and offer kinetic advantages in contrast to a sequential binding of each component. One putative multiprotein complex of particular interest in this work was purified via Rio2p. Rio2p itself is a serine kinase that efficiently co-purifies 20S pre-rRNA and is required for final cytoplasmic pre-18S rRNA processing (Vanrobays et al., 2003; Geerlings et al., 2003). TAP-tag purification and subsequent protein analysis by mass spectrometry identified 6 proteins (Krr1p, Ltv1p, Enp1p, Tsr1p, Dim1p, Hrr25p) that associate independent on pre-rRNA with Rio2p. Several components of this complex are required for late pre-40S biogenesis (Gelperin et al., 2001; Seiser et al., 2006a). Nob1p and Pno1p/Dim2p were constantly co-purified but their stable association is dependent on concurrent pre-rRNA incorporation into the Rio2p-RNP (Merl et al., 2010). Pno1p (**p**artner of **No**b1p), alias Dim2p, is a nucleolar/nuclear-cytoplasmic shuttling protein with homology to Krr1p and involved in pre-18S rRNA processing and modification events (Vanrobays et al., 2004). Up to now, there is no absolute evidence of the endoribonuclease that mediates final pre-18S rRNA processing (see 1.4.3.1). One of the two proposed ribonucleases is Fap7p, because it was found to transiently interact with rpS14, a component of the head-platform interface in proximity to the 18S 3'-end and to exhibit NTPase activity (Granneman et al., 2005). The other, more likely candidate is Nob1p, which contains a PIN domain and co-purifies with pre-SSU particles. Additionally Nob1p interacts *in vitro* with rpS14 and rpS5, both localized in the head-platform interface (Fatica et al., 2003, 2004). Recently it was shown that Nob1p is able to bind solely with certain specifity to artificial RNA constructs that mimic its potential substrate, though its endonucleolytic activity is rather low under these conditions (Lamanna and Karbstein, 2009; Pertschy et al., 2009a).

In a genetic suppressor screen of the cold-sensitive phenotype caused by depletion of Ltv1p, Nob1p, Prp43 and Pfa1p were found (Pertschy et al., 2009b). The helicase Prp43p and its co-factor Pfa1p participate in spliceosome dissasembly (Arenas and Abelson, 1997; Martin et al., 2002), are needed to break up snoRNA-rRNA hybrids (Bohnsack et al., 2009) and maybe are involved in a conformational change of pre-40S subunits, preceding final 18S maturation (Pertschy et al., 2009a).

1.4.3 Maturation of ribosomal RNAs

1.4.3.1 pre-rRNA processing events

The architecture of bacterial and archaeal rRNA operons is strikingly similar (Figure 14). The rRNA genes are clustered and the precursor transcript contains the coding sequences for 16S, 23S and 5S rRNAs, but also codes for some tRNAs.

In the bacterial model organism *E. coli* (Figure 14 A), the precursors of the ribosomal 16S and 23S RNAs are released by the action of RNase III, which is also required for further processing of 23S precursor species (Dunn and Studier, 1973). The precursor of the 5S rRNA is released by RNase E (Szeberényi et al., 1984). The mature 3'-ends of 23S rRNA and 5S rRNA are formed by RNase T (Li and Deutscher, 1995; Li et al., 1999a), while the processing enzymes for the 5'-ends are still unknown. The 16S 3'-end processing enzyme is yet unknown, too. The functional related ribonucleases RNase E and RNase G finally generate the 16S 5'-end (Li et al., 1999b).

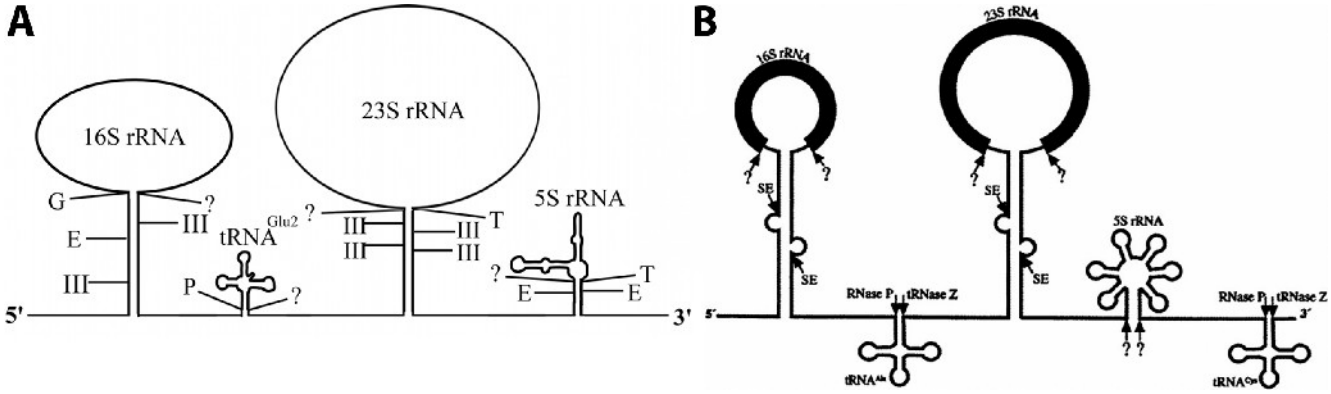

Figure 14. rRNA processing in Prokarya
(**A**) rRNA processing in Bacteria. The *rrnB* operon of *E. coli* is shown. The processing sites of the ribonucleases are indicated: III - RNase III, G – RNase, E – RNase E, P – RNase P, T – RNase T, ? – unknown RNase. (modified from Kaczanowska and Rydén-Aulin, 2007). (**B**) rRNA processing in Archaea. One of the rRNA operons of *Haloferax volcanii* is shown. The processing sites of the ribonucleases are indicated: SE – splicing endonuclease, ? – unknown RNase. (modified from Hölzle et al., 2008)

Ribosomal RNA processing in Archaea, was analyzed in different model organisms (among others (Durovic and Dennis, 1994a; Morrissey and Tollervey, 1995; Ciammaruconi and Londei, 2001; Tang, Rozhdestvensky, et al., 2002)) and seems to follow a common pathway, illustrated in Figure 14 B. Well defined secondary structure elements, called bulge-helix-bulge motifs, are recognized the RNA splicing endonuclease, which releases the rRNA precursor and simultaneously ligates the arising ends (Kjems and Garrett, 1988, 1991). The potential endonuclease that processes the 5S 5'-end has been recently identified (Hölzle et al., 2008). Also involved in tRNA maturation, the endonuclease tRNase Z recognizes a tRNA-like secondary structure motif, 5' of the 5S rRNA sequence and successively generates the mature 5S 5'-end.

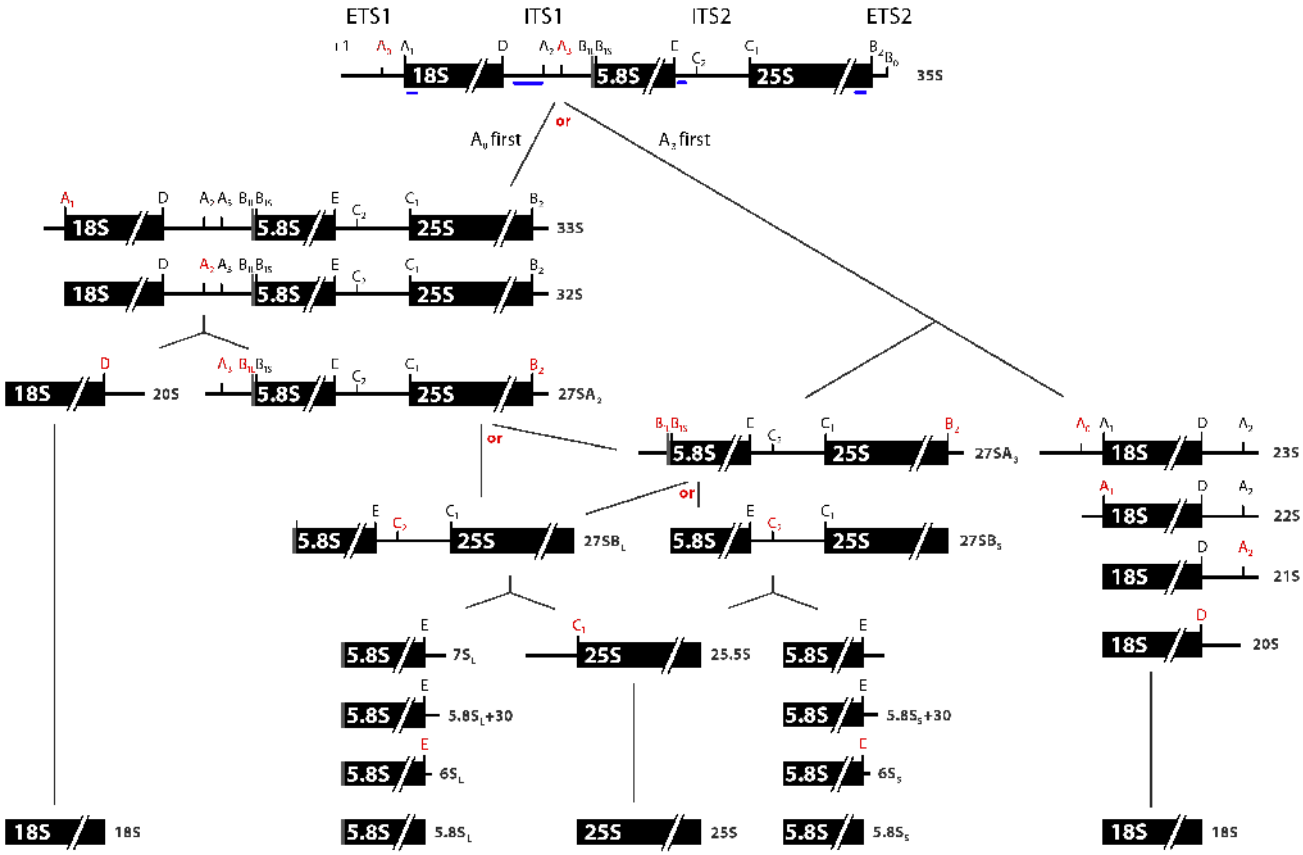

Figure 15. The rRNA processing pathway of *S. cerevisiae*
At the very top, the first detectable Pol I transcript – the 35S pre-rRNA is shown. The processing sites are illustrated (+1, A_0, A_1, etc.). The blue bars illustrate the Northern blot probes used in this work. Abbreviations: ETS X – external transcribed spacer X, ITS X – internal transcribed spacer X. The processing sites, leading to the next pre-rRNA species are marked in red. If two precursors are produced by a cleavage step, the lines are dividing. Two lines that are labeled with "or" indicate alternative processing pathways.

Pre-rRNA processing in eukaryotes commonly deploys the same principles. A large, polycistronic precursor transcript (see 1.4.1.1), which contains the coding sequences for 3 of the 4 rRNAs, is processed by endo- and exoribonucleases. In addition about 150 non-ribosomal factors and over 70 snoRNPs are involved to form the mature rRNAs (see 1.4.2). The eukaryotic pre-rRNA processing pathway has been extensively analyzed in the model organism *S. cerevisiae* (Figure 15). Based on this maturation pathway, the general principles are covered below. For comprehensive and detailed description of each processing step see (Granneman and Baserga, 2004; Nazar, 2004; Henras et al., 2008) and references therein.

The first detectable pre-rRNA transcript (35S) is thought to be co-transcriptionally cleaved by the endonuclease Rnt1p, the eukaryotic homologue of RNase III at site B_0 (Henras et al., 2004). Under normal conditions, U3 snoRNP (see 1.4.2) dependent endonucleolytic cleavages at sites A_0, A_1 and A_2 occur next. These processing events are strongly coupled and involve base pairing of U3 snoRNA with ETS1 and 18S rRNA sequences (among others (Hughes and Ares, 1991b; Beltrame and Tollervey, 1992)). A (sub-) population of the nascent transcripts might actually be processed co-transcriptionally at the mentioned sites (Henras et

al., 2004; Koš and Tollervey, 2010). Processing at site A_2 finally leads to separation of small and large subunit precursors. An alternative processing pathway utilizes processing at site A3 to separate the SSU and LSU precursor rRNAs, especially if processing at A_0, A_1 or A_2 is hindered (Ferreira-Cerca et al., 2005).

The majority of the originating $27SA_2$ pre-rRNA is cleaved by the endonuclease RNase MRP (functionally related to RNase P, see before) at site A3 to form $27SA_3$. This new 5'-end is recognized by one of the homologous 5'→3' exonucleases Xrn1p or Rat1p and the precursor of the short version of the mature 5.8S rRNA ($27SB_S$, resulting in $5.8S_S$) is generated. The longer version ($27SB_L$, resulting in $5.8S_L$) is formed by cleavage of an unknown endonuclease at site $B1_L$. The 3'-end of the 27SB species is concomitant processed by Rex1p, a 3'→5' exonuclease. Through cleavage at site C2 by an unknown endonuclease, the precursors of 25S (25.5S) and 5.8S ($7S_S$ or $7S_L$) are separated. Xrn1p or Rat1p form the mature 5'-end of 25S rRNA by exonucleolytic processing. Final maturation of the 7S pre-rRNAs involves several intermediates (see Figure 15). The exosome, a multiprotein complex with 3'→5' exonuclease activity, the homologous 3'→5' exonucleases Rex1p and Rex2p and the potential endonuclease Ngl2p are needed to produce the two mature forms of 5.8S rRNA.

The third RNA constituent of the LSU, the 5S rRNA is transcribed already with its mature 5'-end, but is extended by a few nucleotides at the 3'-end. The concerted activity of the 3'→5' exonucleases Rex1p, Rex2p and Rex3p generates the mature 5S 3'-end (van Hoof et al., 2000).

The 23S pre-rRNA, which is produced upon processing at site A_3 (see before), is most likely further matured at sites A_0, A_1 and A_2, resulting in 20S pre-rRNA.

The mature 3'-end of any 20S pre-rRNA is generated by an endonucleolytic cleavage step at site D. Previous work suggested that the cis-elements, which are necessary for efficient D site processing, are located in the immediate proximity of the mature 18S 3'-end itself (Liang and Fournier, 1997; van Beekvelt, Jeeninga, et al., 2001). As described before (1.4.2), Nob1p is the presumable endonuclease mediating this final 18S rRNA maturation step. Remarkably, it was demonstrated that the homologous processing step in Bacteria might happen after translation initiation or even during the first round of translation (Mangiarotti et al., 1974; Hayes and Vasseur, 1976) (see also discussion in 3.3).

For virtually all processing events during ribosomal RNA maturation it is not known, how they are regulated. It is of course possible that the ribonuclease's activity itself is regulated, e.g. by a co-factor. For some exonucleases the stopp signal might be composed of secondary rRNA structure elements and/or r-proteins (Lee and Nazar, 1997). A regulatory mechanism, in which activity of the processing enzyme is in all probabilities modulated by the correct substrate conformation, has been proposed for the maturation of 5S rRNA by RNase M5 [43,44] and 23S rRNA by RNase Mini-III [45] in *Bacillus subtilis*. In this organism L18

respective L3 binding is a prerequisite for occurrence of the corresponding cut, by shaping the RNP into a conformation that is the correct substrate for the processing nuclease (Pace et al., 1984; Stahl et al., 1984; Redko and Condon, 2009) (see also discussion in 3.2).

1.4.3.2 Modification of rRNAs

Ribosomal RNAs of practically all living organisms are covalently modified. The modifications are isomerization of uridine to pseudouridine and methylation of riboses (2'-O-ribose methylation) and bases. Methylation and pseudouridinylation are carried out by specific proteins in Bacteria and in Archaea and Eukaryotes additionally by snoRNPs (see also 1.4.2). In eukaryotes, many of these modifications seem to occur already co-transcriptional (Retèl et al., 1969; Ni et al., 1997).

The role of these modifications, although the modification sites are quite well conserved, is still rather obscure. Block of the modification sites or mutation of the modifying enzymes result in specific phenotypes, while in all cases ribosome biogenesis seems to be unaffected (among others (Tollervey et al., 1993; Zebarjadian et al., 1999)). Thus the modifications are most probably essential for ribosome function, rather than for ribosome biogenesis. In addition, the modification sites cluster around the decoding and peptidyl-transferase center (King et al., 2003; Baxter-Roshek et al., 2007; Liang et al., 2007). However, the modifications could be structural checkpoints, since the binding sites for some r-proteins of biogenesis factors might be formed only if the modification mark is set (Song and Nazar, 2002).

1.4.4 Folding of precursor subunits and assembly of r-proteins

The *in vitro* reconstitution of translational active ribosomal subunits from naked rRNA and purified components was one of the biggest breakthroughs in understanding how cells produce ribosomes (Hosokawa et al., 1966; Traub and Nomura, 1968; Nomura and Erdmann, 1970). Although the assembly and folding process of the large ribosomal subunit is more complex and probably involves many intermediates, the general principles of assembly and folding of both subunits are the same (Nomura et al., 1970; Herold et al., 1987). These will be elucidated hereafter, based on the excessive studies of SSU folding and assembly (reviewed in (Woodson, 2008; Sykes et al., 2009)).

The *in vitro* studies showed that the ribosome is a self-assembling RNP, since reconstitution of both subunits required no additional factors. In addition, the primary sequence of the 16S itself, in particular of the 5'-domain was sufficient to form many of the interactions observed in the three-dimensional structures (Stern et al., 1989; Adilakshmi et al., 2005). Nevertheless, thermodynamically traps of rRNA folding are greatly reduced upon r-protein binding (Semrad et al., 2004; Woodson, 2008) and *in vivo* most probably also by biogenesis factors (among others (El Hage et al., 2001; Maki and Culver, 2005; Hoffmann et al., 2010; Bunner, Nord, et al., 2010a)).

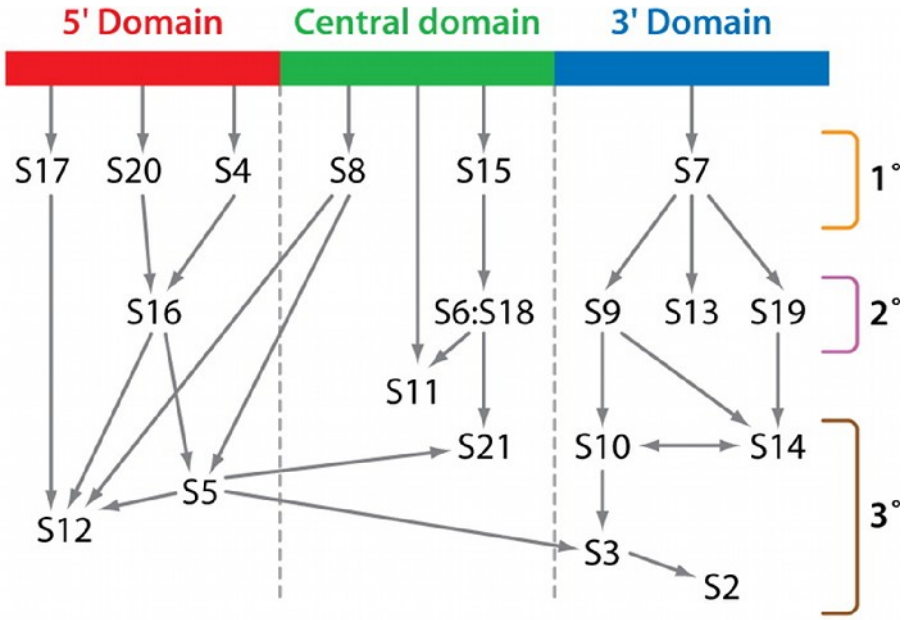

Figure 16. The Nomura assembly map for the 30S subunit
The assembly map shows the order of r-proteins in respect of their hierarchy of binding to the different subdomains of 30S subunits. Primary binders are indicated with 1°, secondary binders with 2° and tertiary binders with 3°. For a projection into 3D see Figure 5. (modified from Sykes and Williamson, 2009)

Another observation during the reconstitution experiments was that assembly of r-proteins seems to follow a hierarchy. In other words, the binding of some r-proteins is the prerequisite for stable incorporation of others. The r-proteins were grouped into three categories: primary binders – required for initial folding of rRNA, bind first; secondary binders – stable incorporation depends on the preceding incorporation of primary binders; tertiary binders – largely depend on primary and secondary binders (Figure 16).

Strikingly, the hierarchical assembly of the SSU subdomains (see 1.2.2) is, with minor exceptions, independent of each other (Figure 16). The electron micrographs in Figure 17 nicely illustrate the interplay of 16S rRNA folding and r-protein assembly

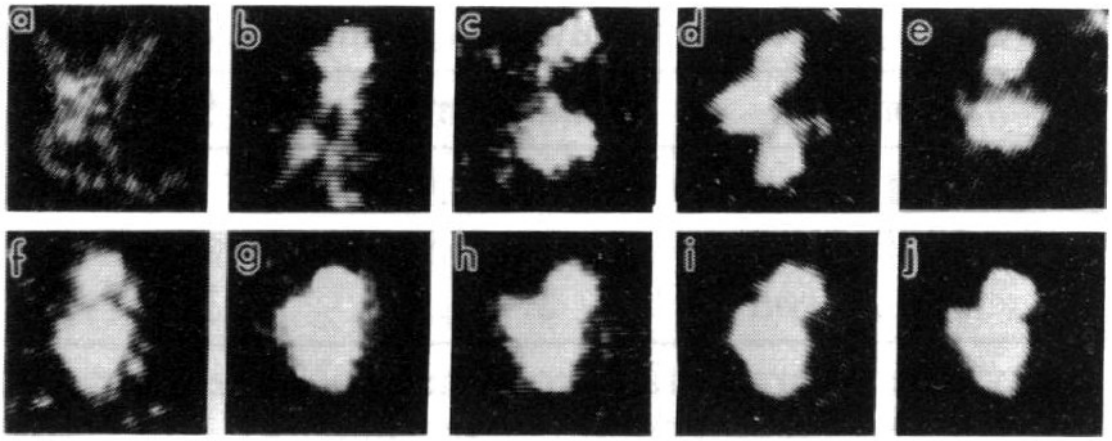

Figure 17. Electron micrographs taken during the *in vitro* assembly process of *E. coli* SSUs
30Å EM images taken during the *in vitro* reconstitution of the *E. coli* 30S ribosomal subunit. (a) free 16S rRNA. (b) 16S rRNA and primary binding r-proteins (16S rRNA and S4, S8, S15, S20, S17, S7). (c)-(g) Subsequent assembly of the missing r-proteins. (h) and (i) fully *in vitro* assembled SSU (16S rRNA and 20 r-proteins or 16S rRNA and TP30, respectively). (j) native *E. coli* SSU. (modified from Mandiyan et al., 1991)

(Mandiyan et al., 1991). See particularly Figure 17 (d), in which all three subdomains are already distinguishable by assembly of the primary (S4, S8, S15, S20, S16/17, S7) and secondary (S16, S19, S13, S9, S18, S6) binding r-proteins. Recent work showed that this autonomous subdomain folding simultaneously starts at different sites all over the 16S rRNA and is generally clustered in the SSU subdomains (Talkington et al., 2005; Adilakshmi et al., 2008). It has even been possible to almost fully reconstitute the SSU subdomains independently, starting from 16S rRNA fragments and the respective r-proteins (Weitzmann et al., 1993; Samaha et al., 1994; Agalarov et al., 1998).

The binding of r-proteins apparently follows most likely an induced fit model (Adilakshmi et al., 2008). The first interaction of one r-protein part induces re-folding of the local rRNA environment, which in turn creates the binding site for another protein part or another r-protein. By this mechanism it is possible that r-proteins of different levels in the assembly hierarchy bind cooperatively. They maybe initially contact rRNA simultaneously, but stable binding of secondary or tertiary binders through induced fit requires structural re-arrangement by the primary binder.

The results of the *in vitro* dependency map (Mizushima et al., 1970), pulse-chase experiments with labeled r-proteins during reconstitution (Talkington et al., 2005; Bunner, Beck, et al., 2010) and time-resolved hydroxyl radical footprinting (Adilakshmi et al., 2008) all lead to the following two conclusions: first, the hierarchy of r-protein binding correlates mostly with the temporal order of assembly and second, the 5'-domain is faster decorated with r-proteins than the central or 3'-domain. In addition, the transcription of rDNA genes *in vivo* and the assembly of r-proteins most probably is coupled (Chooi and Leiby, 1981; Gallagher et al., 2004; Koš et al., 2010). Transcription is 5' to 3' directed and the binding sites of many primary binders are at the 5'-ends of 16S and 23S rRNA. These observations led to the postulation of the so-called “assembly gradient” (Nierhaus, 1991).

This hypothesis is nevertheless challenged by the facts that nucleation of folding simultaneously starts at many different sites (Adilakshmi et al., 2008) and initial binding of a subset of r-proteins (5'-, and central domain and/or primary binder of the 3'-domains) does not enhance the assembly of other 3'-domain binding proteins (Bunner, Beck, et al., 2010). Interestingly, the wildtype-like array of the subdomains of each subunit in the rRNA operons is not essential *in vivo*. *E. coli* strains, in which the subdomains were permuted, were able to grow and exhibited fully assembled ribosomal subunits (Kitahara and Suzuki, 2009).

The knowledge about the hierarchy of r-protein assembly in eukaryotes is rather limited. Two systematic knockout screen in *S. cerevisiae* showed that r-proteins that bind in the 5'- and central domain of the small subunit were required for early processing steps (A_0, A_1, A_2) and proteins of the head domain were required for efficient D site cut processing (Ferreira-Cerca et al., 2005). This clear clustering is however not true for r-proteins of the large ribosomal subunit (Pöll et al., 2009). A detailed *in vivo* analysis of head domain assembly in yeast

demonstrated a broad homology between the eukaryotic and bacterial r-protein assembly pathway in this SSU subdomain (Ferreira-Cerca et al., 2007). Depletion of the primary binder of the head domain rpS5 (S7 in Bacteria) consequently led to loss of stable binding of other head domain r-proteins, while the 5'- and central domains were normally assembled. The second level in the hierarchy of assembly might be as well conserved, since depletion of rpS15 (S19 in Bacteria) led to loss of stable binding of only a smaller subset of r-proteins.

Although many of the r-proteins are able to associate already with nascent SSUs in the nucleus (among others (Ferreira-Cerca et al., 2005, 2007; Krüger et al., 2007)), their final, stable incorporation could be dependent on cytoplasmic maturation events (see before: induced fit model). One well studied example is rpS3, whose stable incorporation into nascent SSU depends on a phosphorylation/dephosphorylation cycle in which the cytoplasmic kinase Hrr25p is involved (Schäfer et al., 2006). Other examples are rpL10, rpL24 and the phospho-stalk protein P0, all incorporated into pre-60S subunits after biogenesis factor displacement in the cytoplasm (among others (West et al., 2005; Pertschy et al., 2007; Kemmler et al., 2009)). Early work in the late 1970s identified potential late binding r-proteins by comparison of the incorporation of labeled r-proteins into ribosomal subunits after short or long pulse times (Kruiswijk et al., 1978; Auger-Buendia et al., 1979). They found rpS10, rpS25, rpS27, rpS31, rpS32, rpS33 and rpS34 respectively rpS7, rpS9, rpS20 and rpS26 to associate with nascent subunits at a late stage of ribosome assembly. The major difficulty here is the assignment of the ribosomal proteins (see 1.2.1) according to the particular migration behavior in the 2D gels (McConkey et al., 1979). Each laboratory used its own protocol for the gel-electrophoresis, so e.g. rpS33 could be rpS28, rpS9 could be rpS10, and so forth. Taken together, these data imply nevertheless a correlation of the rRNA processing phenotype upon depletion of the r-protein and its stage of stable assembly (see before: the “assembly gradient”).

In all evolutionary kingdoms a class of biogenesis factors exists that is thought to improve/accelerate the assembly of r-proteins onto nascent subunits. A recent study used labeled protein pulse–chase experiments monitored by quantitative mass spectrometry, to analyze the effects of these assembly factors on *in vitro* reconstitution kinetics of bacterial 30S subunits (Bunner et al., 2010b). They concluded that assembly factors facilitate the binding of r-proteins through induced conformational changes, RNA chaperone-like activity or inhibition of unproductive r-protein assembly by physically blocking the binding site. In eukaryotes, the phenotypes observed upon depletion of some r-protein assembly factors can be (partially) suppressed by overexpression of the respective r-protein (among others (Baudin-Baillieu et al., 1997a; Loar et al., 2004; Buchhaupt et al., 2006)). These assembly factors are therefore not utterly required for r-protein binding, but they accelerate stable incorporation and thereby ribosome biogenesis.

1.4.5 Transport of precursor subunits

The nucleolus, a subcompartiment of an eukaryotic nucleus, has versatile functions in regulation of mitosis, cell cylce progression, proliferation, stress response and biogenesis of several RNPs (reviewed in (Boisvert et al., 2007; Sirri et al., 2008)). It is also and what's more, the site of rDNA transcription by Pol I and Pol III (see 1.4.1.1). In the nucleolus three subregions can be distinguished: the fibrillar centers (Figure 18 B, FC), the dense fibrillar components (Figure 18 B, DFC) and the granular compartment (Figure 18 B, GC. Transcription by Pol I largely takes place at the border between the FC and the DFC regions. Further processing and modification of pre-rRNAs occurs in the DFC. Final assembly is accomplished mostly in the granular component.

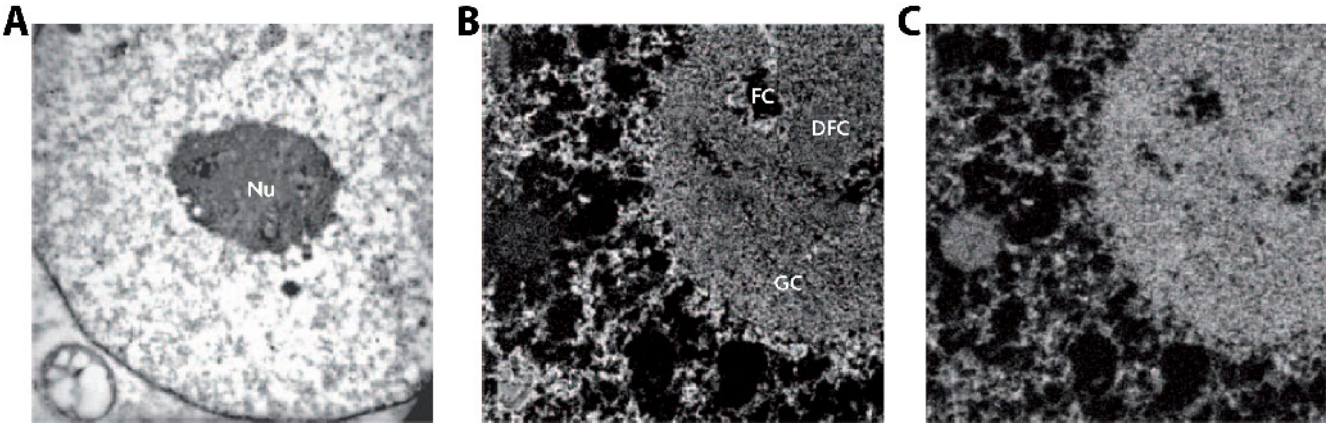

Figure 18. Ultrastructural images of nucleoli
(**A**) A HeLa cell with a nucleolus (Nu). Uranyl-acetate-stained cell section visualized by transmission EM. (**B**) and (**C**) Electron spectroscopic imaging pictures. Phosphorus (nucleic-acid) enriched (**B**) or nitrogen (protein) enriched (**C**). Abbreviations: FC – fibrillar center; DFC – dense fibrillar component; GC – granular component. (modified from Boisvert et al., 2007)

The proteins required for ribosome biogenesis quite likely diffuse plainly into the nucleolar subregions and are probably sequestered at their site of action (among others (Chen and Huang, 2001; Dundr et al., 2004; Louvet et al., 2005)). After separation of the 90S pre-ribosome into the two precursor particles (pre-60S and pre-40S, see 1.4.3.1), the pre-60S subunits runs through multiple nuclear processing, assembly and folding events, but is very likely moving through diffusion (Politz et al., 2003). The same mechanism of movement seems to be true for the majority of the pre-40S particles, but recent data suggested that a subpopulation of the precursors are actively transported, meaning dependent on motor proteins (nuclear myosin I) and energy (Cisterna et al., 2006, 2009).

The nuclear pore complex (NPC) is a large (60 to 125 MDa) multiprotein complex that allows passage of cargos in and out of the nucleus (for recent reviews see (Peters, 2005; Fiserova and Goldberg, 2010)). The NPC is composed of nucleoporins (NUPs), which often posses large hydrophobic stretches, the FG-repeats (phenylalanine and glycine rich sequences). The actual molecular mechanism of translocation is unknown, but current models discuss the FG-repeats as a selectivity barrier (reviewed in (Fiserova et al., 2010)). The import and

export adapter proteins are members of the so-called karyopherin protein family. These proteins bind to nuclear import (NLS) or nuclear export (NES) sequences of their cargo and mediate an initial contact with the NPC.

The only known karyopherin involved in nuclear export of ribosomal subunits and whose function is conserved between all eukaryotes is Crm1p (Xpo1 in higher eukaryotes) (Ho et al., 2000; Moy and Silver, 1999; Thomas and Kutay, 2003). Crm1p doesn't bind to the ribosomal subunits directly, but recognizes NES sequences on adapter proteins. For the large subunit this adapter protein is Nmd3p (Ho et al., 2000). For the small subunit, up to now three adapters are known: Ltv1p, DIM2 and RIO2 (the later ones were identified in higher eukaryotes) (Seiser et al., 2006b; Vanrobays et al., 2008; Zemp et al., 2009). The role of Ltv1p as a Crm1p adapter protein was recently questioned, since deletion of its NES sequence did not result in a nuclear retention of Ltv1p. Nevertheless, export of SSU precursors was diminished in this case, probably due to lack of biogenesis factor displacement by fully functional Ltv1p (Fassio et al., 2010a).

Next to the karyopherin Crm1p, various other proteins are known to promote nuclear export of ribosomal subunits. Rrp12 was shown to be required for efficient export of both subunits. This protein contains HEAT repeats (**H**untington-**e**longation-**A** subunit-**T**OR), a motif, which is also found in other FG-repeat interacting proteins (Oeffinger et al., 2004). Another export adapter for the large subunit is the heterodimer Mex67p-Mtr2p, which is a general mRNA export factor (Yao et al., 2007). Probably other factors, like for example Arx1p, which can bind both, ribosomal subunits and the FG-repeats of the NPC, facilitate nuclear export of pre-ribosomal subunits (Bradatsch et al., 2007; Hung et al., 2008).

This high redundancy in ribosomal subunit export is probably necessary to cope with the vast quantity of nascent ribosomes (Warner, 1999). This redundancy is as well reflected in the fact that Crm1p itself is not essential for nuclear export. Fusion of several proteins, which are involved in mRNA or tRNA export to Nmd3p resulted in Crm1p independent export of ribosomal subunits. Even the export adapter Nmd3p is exchangeable, thus a fusion of its NES to rpL3 promoted export of LSU precursors (Lo and Johnson, 2009).

In general, export competence and a certain r-protein assembly state of precursor subunits go hand in hand. Consequently, lack of various r-proteins results in nuclear retention of precursor subunits (Léger-Silvestre et al., 2004; Ferreira-Cerca et al., 2005; Robledo et al., 2008; Pöll et al., 2009). Several possible underlying mechanisms will be discussed in chapter 1.5.2.

1.4.6 Regulation, quality control and homeostasis of ribosome production

Ribosome synthesis devours vast amounts of energy and amino acids in a growing cell. It is therefore easy to understand that ribosome biogenesis has to be tightly regulated. Prokaryotic cells mainly regulate ribosome synthesis at the level of rDNA transcription and translational feedback mechanisms (for recent reviews see (Wagner, 2002; Dennis et al., 2004; Magnusson et al., 2005; Suthers et al., 2007; Kaczanowska et al., 2007)). Eukaryotic cells regulate ribosome biogenesis basically in the same manner, but the way this is achieved is quite different (see further down).

Each prokaryotic cell has to deal with fast changing environmental conditions. Nutrient depletion, in particular amino acid starvation triggers the so-called “stringent response” on ribosome biogenesis. The binding of deacetylated amino acids to the ribosome, which appear due to amino acid deprivation, causes the synthesis of (p)ppGpp (guanosine 3'-diphosphate 5'-(tri)diphosphate). The induction of (p)ppGPP synthesis can be also a result of carbon or energy source deprivation. Finally, (p)ppGpp binds to the RNA polymerase and shuts down transcription, yet the exact mechanism is still under discussion.

Steady-state or in other words, growth rate regulation enables bacterial cells to adapt to the overall growth conditions. In contrast to the stringent response, steady-state regulation is achieved by varying the number of ribosomes. Feedback loops of r-protein mRNA translation and attenuation or intensification of rDNA synthesis facilitate the change in ribosome number. Free ribosomal proteins were shown to bind their messenger RNA, thus translational repressing their own expression. This excess of free ribosomal proteins is reflecting an imbalance of rRNA to r-proteins, thereby linking translation to ongoing transcription and r-protein assembly. The molecular signals that result in modification of RNA polymerase activity are still unclear, but (p)ppGpp might again be the main effector molecule. Somehow ongoing translation by functional ribosomes results in a decrease of (p)ppGpp levels and thereby in an increase of RNA polymerase activity.

Eukaryotes seem to have a similar pathway to the stringent response in Bacteria. There is no known small effector molecule like (p)ppGpp, but a specialized protein family was identified (GCN, **g**eneral **c**ontrol **n**on-derepressible proteins). Upon amino acid deprivation, they initiate a response that leads to a general reduction in protein synthesis, but on the other hand to an upregulation of amino acid anabolism (reviewed in (Hinnebusch, 2005)). Regulation of r-protein expression could be mediated by protein kinase A (PKA), rather than the GCN protein family, since only mutations in the PKA and not in Gcn1p or Gcn4p show a deregulation of expression (Moehle and Hinnebusch, 1991; Klein and Struhl, 1994).

The common pathway in eukaryotes of sensing nutrient availability and other environmental conditions, is mediated by the TOR (target of rapamycin) kinase ((Powers and Walter, 1999) reviewed in (Lempiäinen and Shore, 2009)). The current model of TOR dependent ribosome biogenesis regulation is illustrated in Figure 19 A. The TOR kinase is found in two structural

and functional diverse complexes termed TORC1 and TORC2 (TOR kinase complex 1 or 2). The TORC2 main functions are regulation of the cytoskeleton dynamics and the AGC kinase family (protein kinase A, G, C) (reviewed in (Cybulski and Hall, 2009)). The TORC1 is sensitive to stress and lack of nutrients (mimicked by the drug rapamycin). These stimuli block the activation (phosphorylation) of various effector molecules, like the Sch9p kinase or Sfp1p (Figure 19 A). This in turn shuts down the transcription of r-protein or the Ribi (**ri**bosome **bi**ogenesis) regulon genes, which encompasses the genes coding for ribosome biogenesis factors and snoRNAs.

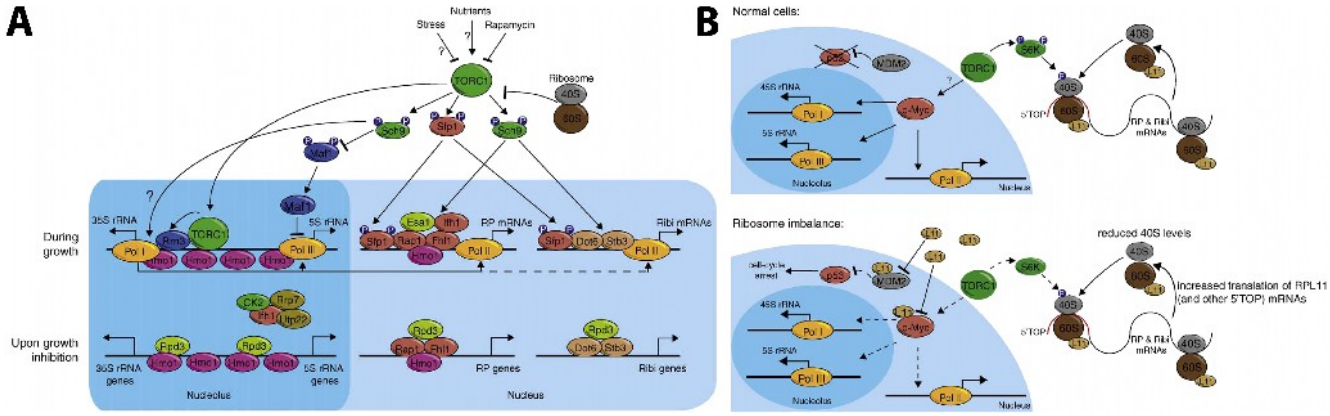

Figure 19. Control of ribosome biogenesis in eukaryotes
(**A**) The TOR pathway in yeast. The TOR complex 1 (TORC1) and the downstream effector proteins are shown. The upper panel illustrates the situation during growth, the lower panel upon growth inhibition. (**B**) The regulation of transcription and translation of ribosomal components in mammalian cells. (**A**) and (**B**) For simplification, not all pathway components and connections are shown. Question marks indicate poorly understood connections. Further details are elucidate in the main text. (modified from Lempiäinen and Shore, 2009)

Coordination of rDNA transcription and r-protein/Ribi gene transcription is maybe achieved through a common factor to all three RNA polymerases – Hmo1p (UBF1 in higher eukaryotes) (Hall et al., 2006; Berger et al., 2007). In addition TOR was found to directly bind to Pol I promoters at the rDNA locus (Li et al., 2006) and probably regulation the core transcription factor Rrn3p (TIF1A in higher eukaryotes) (Claypool et al., 2004; Mayer et al., 2004). Processing of pre-rRNA and assembly of r-proteins might as well be coupled to transcription of r-protein and Ribi genes. In yeast, the essential Pol II transcription factor Ifh1p is found in a second complex with casein kinase 2, Utp22p, and Rrp7p, termed the CURI complex (Rudra et al., 2007). Utp22p and Rrp7p are both components of the 90S pre-ribosome and necessary for early pre-rRNA processing and assembly events (Baudin-Baillieu et al., 1997b; Dragon et al., 2002b).

On the other hand, it was claimed that ribosomal proteins in HeLa cells are produced in excess, compensated by constitutive degradation of non-assembled r-proteins (Lam et al., 2007). Furthermore, in yeast, inhibition of the TOR kinase leads to severely reduced levels of newly synthesized ribosomal subunits without preceding impairment of Pol I transcription (Reiter, Steinbauer, Philippi et al., 2010, unpublished). Thus, the amount of available free r-proteins could control the rate of ribosome production.

In contrast to yeast cells, mammals seem to prefer post-transcriptional control of ribosome biogenesis (Figure 19 B). An imbalance in ribosomal subunit stoichiometry causes upregulation of transcription of a subset of mRNAs, containing a 5'-TOP (poly-pyrimidine) motif (Fumagalli et al., 2009). Among these is e.g. rpL11, which was shown to inhibit the transcription factor c-myc (Dai et al., 2007, 2010), but also binds to MDM2 and induces p53 dependent cell cycle arrest (Zhang et al., 2003; Fumagalli et al., 2009).

Furthermore, there is rising evidence that in eukaryotes ribosome biogenesis is regulated in multiple additional layers, like e.g. changes in chromatin structure (Murayama et al., 2008) or plasticity of rDNA repeat numbers (Nomura, 1999).

Many quality control pathways assure that the error-prone process of ribosome biogenesis finally results in functional mature ribosomes. During eukaryotic ribosome biogenesis, misfolded or misassembled precursors are detected, polyadenylated by the TRAMP (**Tr**f4p-**A**ir1/2p-**M**tr4p **p**olyadenylation) complex and subsequently degraded by the exosome (among others (Dez et al., 2006; Schneider et al., 2007; Wery et al., 2009)). The ultimate way of regulating a cell's ribosome content is the degradation of ribosomes themselves. Ribosomes that carry a potentially lethal defect in the rRNA, are normally matured, but become rapidly degraded in the cytoplasm by the so-called NRD (**n**on functional **r**RNA **d**ecay) pathways (LaRiviere et al., 2006; Cole et al., 2009). These pathways are thought to recognize stalled ribosomes and independently degrade the defective SSUs and LSUs, respectively (reviewed in (Lafontaine, 2010)). 18S NRD most probably is initiated by endonucleolytic cleavage of 18S rRNA, followed by complete exonucleolytic digest. 25S NRD on the other hand, is carried out by tagging defective LSUs (associated) components with ubiquitin, followed by proteasomal degradation.

Two specialized forms of autophagy, the ribophagy and PMN (**p**iecemal **m**icroautophagy of the **n**ucleus) lead to bulk degradation of mature and pre-ribosomes, respectively, upon nutrient depletion. PMN isn't yet well characterized, though it might result in vacuolar degradation of nucleolar pre-ribosomes (Roberts et al., 2003). Ribophagy most probably is promoted via deubiquitylation of unidentified ribosome associated factors, leading to selective uptake of mature subunits into the vacuole. Like in the NRD pathways, ribophagy of the SSU and the LSU seem to be independently regulated (Kraft et al., 2008; Kraft and Peter, 2008).

1.5 Ribosomal proteins

1.5.1 The roles of r-proteins in mature ribosomes

The ribosome is a ribozyme. Both, the decoding (18S rRNA) and the peptidyl-transferase reaction (25S rRNA, tRNA) are mediated by RNA residues. Despite this fact, ribosomal proteins accomplish many and important tasks in ribosome function (Table 3). For example, several small ribosomal proteins are required for binding and correct positioning of the mRNA. S12 (rpS23) is part of the decoding center and influence ribosome accuracy. Ribosomal proteins of the large subunits orientate tRNAs and are often the site of translation factor binding (see Table 3, reviewed in (Brodersen and Nissen, 2005; Wilson and Nierhaus, 2005; Dresios et al., 2006)).

ribosomal protein		**function(s)**
Bacteria	Eukarya	
S1		Suggested to bring the mRNA into the proximity of the ribosome during initiation.
S3, S4, S5		Form the mRNA entry pore and may have a helicase activity to unwind mRNA secondary structure encountered during translation.
S4	rpS9	Mutations increase the error during the decoding process.
S12	rpS23	Involved in decoding of the second and third codon positions at the A site. Mutations in S12 confer resistance against streptomycin, increase accuracy of the decoding process and, in most cases, concomitantly decrease the rate of translation. The lack of S12 in reconstituted particles also increases accuracy.
S13		Interacts with P site tRNA.
	rpS25	Essential for translation initiation by the Dicistroviridae and hepatitis C viral IRESs.
	Asc1p (RACK1)	Involved in various signaling pathways. Deletion leads to increased drug sensitivity affecting cell wall biosynthesis and translation eleongation. The mRNA binding protein Scp160p fails to associate with ribosomes upon Asc1p depletion.
L1	rpL1	Probably involved in the removal of deacylated tRNA from the E site.
L2, L3		Required for peptidyl-transferase reaction
L4		Mutations in L4 can confer resistance against macrolide antibiotics such as erythromycin by indirectly interfering with drug binding; role in rRNA transcription antitermination.
L5		Interacts with P site tRNA. Integral part of the 5S RNP.
L7/L12		Involved in elongation-factor binding and GTPase activation.
L9		Mutations in L9 effect the efficiency of translational bypassing.
L11		Mutations in L11 or lack of the complete protein confer resistance against thiostrepton, an antibiotic that blocks the ribosomal transition from the pre- to post-translocational state and vice versa. During the stringent response this protein senses the presence of a deacylated tRNA in the A site; mutations or the absence of the protein can cause a relaxed phenotype (relC) resulting from loss of stringent control.
L16	rpL10	May be involved in correct positioning of the acceptor stem of A- and P-site tRNAs as well as RRF on the ribosome. Eukaryotic rpL10 interacts with rpS6 and is required for subunit joining.
L22		May interact with specific nascent chains to regulate translation.
L23, L24	rpL25	Present at the tunnel exit site and has been shown to be a component of the chaperone trigger factor binding site on the ribosome.
L27		Bacterial-specific protein implicated in the placement of the acceptor stem of P-site tRNA and binding of the ribosome recycling factor on the 50S subunit.
L29		Is located close to the tunnel exit site and may constitute part of the binding site for the signal recognition particle.
	rpL44	Interacts with tRNA at the E site.

Table 3. The roles of selected r-proteins in ribosome function

The ribosomal protein(s) with their respective function(s) are listed. If the functions were addressed using the bacterial r-protein, the bacterial nomenclature is used, if the eukaryotic r-protein was used, vice versa. If the function was prooved to be conserved, both names are given. (mainly adapted from Brodersen and Nissen, 2005; Wilson and Nierhaus, 2005, Dresios et al., 2006)

Much of the current knowledge arose from potent *in vitro* reconstitution and translation assays of prokaryotic ribosomes and the availability of atomic resolution structures. Nevertheless, recent studies suggested certain roles of eukaryotic r-proteins in the translational process (Table 3). Most probably the known functions of prokaryotic r-proteins in translation are conserved, too (among others (Alksne et al., 1993a; Synetos et al., 1996a; Eisinger et al., 1997; Rauch et al., 2005; Fei et al., 2008)).

Hereafter, the functions in translation of the small ribosomal proteins, which have been explicitly analyzed in this work, will be explained in more detail.

RpS17 has no homologue in Bacteria and nothing is known about a potential function in translation.

S5 the prokaryotic homologue of rpS2 is one of the three proteins, together with S3 (rpS3) and S4 (rpS9), which forms the mRNA entry pore and orientates it in a correct way (Kurkcuoglu et al., 2008a). Mutants of S5 (*ram* – **r**ibosomal **a**mbiguity **m**utations) are known to reduce the accuracy of translation (Rosset and Gorini, 1969; Piepersberg et al., 1975a; Cabezón et al., 1976). It probably also facilitates conformational changes in rRNA structure that might act as a switch from accurate to error-prone translation (Piepersberg et al., 1975b; Lodmell and Dahlberg, 1997; Kirthi et al., 2006). Mutations in eukaryotic ribosomal protein rpS2, the so-called SUP44 mutants are known as omnipotent suppressors of all three classes of nonsense mutations in yeast and show a similar phenotype to the prokaryotic *ram*-mutants (Alksne et al., 1993b; Synetos et al., 1996b). Crosslinking experiments suggested that rpS2 contributes, like S5, to the formation of the mRNA entry pore (Pisarev et al., 2008b). Very interestingly, the role of rpS2 in maintaining the accuracy of translation could be regulated by phosphorylation in eukaryotes. The kinase Ctk1p (CDK9 in higher eukaryotes), which phosphorylates rpS2, has been shown to interact with Pol I, as well as Pol II. Thereby, another potential link between rDNA transcription and translation could be established (Bouchoux et al., 2004; Röther and Strässer, 2007).

Crosslinks of the intersubunit r-protein S19, the prokaryotic homologue of rpS15, implies that it helps to orientate the P site tRNA (Rosen et al., 1993). Eukaryotic rpS15 on the other hand seems to contact more the surrounding of the A site (Bulygin et al., 2002; Pisarev et al., 2006, 2008c).

The head domain rpS20 is localized at the cytoplasmic site of the small subunit (see Figure 8 A) and apparently does not contribute directly to translation.

RpS5 and rpS14 are both components of the head-platform interface (see Figure 8 A). This region is important for translation factor binding, as well as tRNA and mRNA orientation. For a more detailed description of their roles in translation see 3.3.

1.5.2 The roles of r-proteins in ribosome biogenesis

Ribosomal proteins bind and accompany a nascent ribosomal subunit most probably starting with transcription in the nucleolus until final maturation in the cytoplasm. Therefore it is easily imaginable that they undertake tasks in several steps of ribosome biogenesis (see 1.4).

Since prokaryotes lack this complex process of eukaryotic ribosome biogenesis, r-proteins in these organisms are mainly needed to stabilize newly built rRNA structures or help forming them (see 1.4.4). Some prokaryotic r-proteins are required for efficient generation of ribosomal subunits, but curiously enough are dispensable for ribosome function. Nevertheless, they remain assembled in the mature subunits, maybe to improve stability of flexibility of the ribosome (Nierhaus, 1991).

In vivo, this stabilization of (pre)-rRNA structures, which is true for prokaryotic, as well as for eukaryotic r-proteins (see 1.4.4), might be the prerequisite for ongoing ribosome biogenesis. Thereby biogenesis factor binding sites might be established or the r-protein acts as a docking sites itself (e.g. rpl10 for NMD3, see 1.4.5). It is also possible that a certain assembly state creates the proper substrate for a pre-rRNA processing enzyme (see 3.2) or modification by a snoRNP (see 1.4.3.2). Two large scale screens, which analyzed the ribosome biogenesis phenotypes caused by depletion of a ribosomal protein, showed that indeed different subsets of r-proteins are required for specific pre-rRNA processing steps ((Ferreira-Cerca et al., 2005; Pöll et al., 2009), see also among others (Moritz et al., 1990; Demianova et al., 1996; Tabb-Massey et al., 2003; Léger-Silvestre et al., 2004; Rosado et al., 2007; Chaudhuri et al., 2007)). Interestingly, the roles of some eukaryotic r-proteins in ribosome biogenesis changed during the course of evolution. Systematic siRNA knockdown in human HeLa cells indicated that ribosome biogenesis, in particular pre-rRNA processing is blocked at different stages, when compared to yeast, upon lack of a specific r-protein (Robledo et al., 2008). For example rpS7, which isn't needed for mature 18S production in yeast, exhibited a strong processing defect of a 18S precursor rRNA species (30S respectively 26S, equivalent of 23S in yeast), when depleted in HeLa cells. The function of rpS15 is controversial. While one study stated that the roles of rpS15 are conserved between yeast and mammals (Rouquette et al., 2005), another one claimed that rpS15 is dispensable for rRNA processing and nuclear export (Robledo et al., 2008).

A eukaryotic specific process in ribosome biogenesis is the nuclear export of precursor subunits. Up to now, several ribosome biogenesis factors are known that participate and are required for efficient nuclear export (see 1.4.5). What's more, the depletion of many r-proteins results in export block or delay of precursor subunits (Jakovljevic et al., 2004; Léger-Silvestre et al., 2004; Rouquette et al., 2005; Ferreira-Cerca et al., 2005; Robledo et al., 2008; Pöll et al., 2009). One could imagine different ways, in which way r-proteins are able to promote nuclear export. First, a certain r-protein assembly state of precursor subunits or the r-protein itself represents the binding sites for export factors. Second, r-proteins themselves mediate

the passage through the NPC by interacting with the hydrophobic nucleoporins, thereby vanquishing the entropic barrier to allow transport (Weis, 2007). Another possibility is that a window of opportunity exists, in which the precursors can be further matured and acquire export competence, otherwise they are recognized by the surveillance machinery and become degraded (see 1.4.6).

The *in vitro* reconstitution experiments in Bacteria demonstrated a hierarchical kind of r-protein assembly (see 1.4.4). The analysis of different SSU head domain assembly states, after depletion of the primary binder rpS5 and the secondary binder rpS15, revealed that the hierarchical mode and the separation into subdomains of r-protein assembly is conserved (Ferreira-Cerca et al., 2007). Furthermore, a direct correlation between a certain r-protein assembly state of pre-SSUs and efficient nuclear export was shown.

The involvement of r-proteins in several ribosome biogenesis steps is mostly know, since depletion of a particular r-protein leads to specific defects (see before). However, detailed analyses of their molecular functions in these processes are few and far between. For example, a C-terminally truncated version of rpL5 is still able to form the 5S RNP, but is defective in assembly into pre-60S subunits (Moradi et al., 2008). For the late binding r-protein rpL10, the regions critical for Nmd3p release from the pre-60S subunits were determined (Hofer et al., 2007). Furthermore, the specific protein parts of rpL25, required for efficient processing of different rRNA precursors, were identified (van Beekvelt, de Graaff-Vincent, et al., 2001). Interestingly, some protein parts of rpL25 seem to be necessary for U3-dependent cleavages, in particular at site A_0. This suggests that efficient ETS1 and ITS2 processing might be coupled, like it was proposed for ETS1 and ITS1 (Venema and Tollervey, 1995) or ITS1 and ETS2 (Allmang and Tollervey, 1998). The only detailed analysis of a small subunit ribosomal protein is about rpS14 (Jakovljevic et al., 2004). RpS14 is one of the primary binding proteins of the 18S central domain and is needed for processing at sites A_0, A_1 and A_2. A C-terminally mutated variant of rpS14 partially suppressed this phenotype. The 40S precursors were exported and 20S pre-rRNA was produced.

1.5.3 Extra-ribosomal functions

Observations in Bacteria indicated early on that r-proteins do not only have roles in ribosome function, but are involved in several other cellular processes. The two most striking extra-ribosomal functions of bacterial r-proteins are the translational feedback control of r-protein expression and participation in the RNA polymerase anti-termination complex. The feedback-regulation of r-protein expression is one of the ways Bacteria assure a stoichiometric production of r-proteins and rRNA. One r-protein of each operon is able to bind its mRNA and translational represses the expression (reviewed in (Wilson et al., 2005), see also 1.4.6). In Bacteria, if transcription and translation becomes uncoupled, which is the case for the non-translated rRNAs, transcription would normally stop. To prevent premature

transcription termination of rRNA genes, anti-termination complexes are formed on the rRNA leader sequences. These are comprised of the Nus proteins and ribosomal proteins like S1 (prokaryotic specific), S4 (rpS9) or S10 (rpS20) (reviewed in (Squires and Zaporojets, 2000; Roberts et al., 2008)).

“Moonlighting is particularly widespread among ribosomal proteins, many of which have extraribosomal ‘‘employment’’ in addition to their daytime jobs as components of the translation machinery” (Weisberg, 2008). This statement is as well, and in particular true for eukaryotic ribosomal proteins (reviewed in (Lindström, 2009; Warner and McIntosh, 2009)). Defects in ribosome biogenesis result in all likelihood in an imbalance of rRNA to r-proteins. For some examples of free r-proteins, it was shown that they participate in regulatory feedback-loops, similar to those of Bacteria (Table 4). Free ribosomal proteins can also bind to MDM2 in mammals (HDM2 in humans), thereby inducing p53 dependent cell cycle arrest (Table 4). Contributions to many other processes are proposed, but not yet or only poorly confirmed (Table 4). Only in a few cases, extra-ribosomal functions were directly demonstrated (Table 4, fully extra-ribosomal).

Haploinsuffiency of r-proteins was shown to lead to increased lifespan (among others (Hansen et al., 2007; Chiocchetti et al., 2007; Steffen et al., 2008)) but might also propagate cancer or developmental abnormalities (among others (Pellagatti et al., 2008; Ruggero and Pandolfi, 2003; Derenzini et al., 2009)). Mutations in various r-proteins or ribosome biogenesis related factors were linked to several inherited bone marrow failure syndromes with a high predisposition to leukemia (reviewed in (Ganapathi and Shimamura, 2008)).

r-protein	extra-ribosomal function	r-protein	extra-ribosomal function
autoregulation of r-protein synthesis		**fully extra-ribosomal**	
L30 (*S.c.*)	inhibits its own mRNA splicing	L7 (archaea)	snoRNP
S14 (*S.c.*)	inhibits its own mRNA splicing	RACK1 (all?)	cell signaling
L2 (*S.c.*)	shortens its own mRNA halftime	L13a (*H.s.*)	inhibits mRNA translation (GAIT complex)
S28 (*S.c.*)	shortens its own mRNA halftime		
L12 and others? (*C.e.*)	inhibits its own mRNA splicing	S3 (*H.s., D.m.*)	DNA endonuclease
		S3 (*H.s.*)	binds NFκB
S13 (*H.s.*)	inhibits its own mRNA splicing	L10 (*A.th.*)	antiviral
ribosome biosynthesis sentinels (mammals)		L10 (*H.s.*)	binds c-jun
L5	sequesters M/HDM2	**interesting possibilities**	
L11	sequesters M/HDM2	S20 (*S.c.*)	influences Pol III transcription
L23	sequesters M/HDM2	L6 (*S.c.*)	influences Pol III transcription
S7	sequesters M/HDM2	L22 (and others) (*D.m.*)	binds Histone H1 (affects transcription?)
L11	sequesters c-myc		
L26	promotes p53 translation	L22 (*H.s.*)	binds EBER-1 RNA (of EB virus)
L23	sequesters nucleophosmin from Miz1	S26 (*H.s.*)	susceptibility to diabetes (?)

Table 4. Extra-ribosomal functions of eukaryotic proteins
Abbreviations: *S.c. S. cerevisiae*; *C.e. Caenorhabditis elegans; H.s. Homo sapiens; A.th. Arabidopsis thaliana; D.m. Drosophila melaongaster.* (adapted from Warner and McIntosh, 2009, see references therein)

1.6 Objectives

Saccharomyces cerevisiae is a frequently used and well studied eukaryotic model organism. Ribosomes are among the most intricate ribonucleoprotein complexes. They consist of 4 ribosomal RNAs and over 70 ribosomal proteins. For synthesis of eukaryotic ribosomes, more than 100 non-ribosomal proteins and over 70 snoRNPs are needed. Studying ribosome biogenesis in yeast can therefore reveal general functions and mechanisms of RNP production. The coordinated binding and subsequent incorporation of r-proteins into the nascent subunits is crucial to generate functional ribosomes. Other important steps in eukaryotic ribosome biogenesis are the trimming of precursor sequences of ribosomal RNAs and nucleo-cytoplasmic transport of nascent ribosomes. Individual r-protein assembly events were previously shown to be required for specific rRNA processing steps and/or nuclear export of pre-ribosomes. Yet, the molecular functions of r-proteins in these processes remained unclear.

A main objective of this work was to create and identify partially functional r-protein variants. A previously established genetic system that allows to conditionally shutdown the expression of a specific r-protein (Ferreira-Cerca et al., 2005) was used to assay these variant r-proteins. Decoupling of functional aspects of a r-protein could consequently help to characterize its molecular functions in a specific process. Furthermore, bypassing the first essential role of the particular ribosomal protein might elucidate potential additional functions in the complex process of ribosome biogenesis.

One of the approaches used to create variant r-proteins was based on the primary sequence conservation of r-proteins in the three evolutionary kingdoms. Particularly Archaea share a large set of homologous ribosomal proteins with Eukarya. Due to the non-perfect sequence match and often missing, eukaryotic specific protein parts, archaeal r-proteins can be considered as variants of eukaryotic r-proteins. Archaeal r-proteins should be expressed and functionally characterized in the conditional yeast r-protein knockout strains. This might allow the identification of conserved or eukaryotic specific features of the respective eukaryotic ribosomal protein. In the light of this screen, it is for example of interest, whether *prokaryotic* ribosomal proteins are able to promote nuclear export of precursor subunits, as was observed for their eukaryotic counterparts.

In a parallel approach, eukaryotic ribosomal proteins should be modified, either by site directed mutagenesis or partial truncation. To determine, which regions should be modified, current atomic structure models of ribosomal subunits were used. In order to ascertain the significance and function of individual protein parts and reveal possible further roles of the respective r-protein, its variants should be assayed in several ways. In particular, (pre-) rRNA interaction, promotion of nuclear export, impact on pre-rRNA maturation and on protein compositions of several RNPs involved in ribosome biogenesis should be analyzed.

2 Results

2.1 General strategies to design variant r-protein alleles for functional studies in *S. cerevisiae*

2.1.1 General considerations

The primary aim of this work was to elucidate the molecular functions of small ribosomal subunit r-proteins in ribosome biogenesis. The depletion phenotypes of most ribosomal proteins are well studied in yeast (Ferreira-Cerca et al., 2005; Pöll et al., 2009), but partially also known in humans (Robledo et al., 2008). Nevertheless, the molecular functions of the respective r-protein in the affected steps of ribosome biogenesis are hardly, if at all known (see 1.5.2). It is also easily imaginable that many r-proteins might have additional functions in other steps of ribosome biogenesis or ribosome function, different from their first, essential one. To reveal these potential second functions and to characterize the known contribution of r-proteins to different ribosome biogenesis steps in detail, it is necessary to create and analyze variants with partial functionality. Thus it might be possible to uncouple e.g. (pre-) rRNA assembly of the r-protein variant from processing, transport of precursors, interaction with biogenesis factors, etc., which could lead to a molecular understanding of the r-protein's function.

In this work r-protein variants were created using basically two approaches: creation of variants based on evolutionary conservation or diversification of primary structure elements of r-proteins or creation of mutants based on tertiary structure features of r-proteins.

In the first approach, the large number of conserved r-proteins between the evolutionary kingdoms (see Figure 1) was used to study gain or loss of r-protein functions during the course of evolution. Ribosomal proteins, which are derived from evolutionary distant species (see 2.1.2), were expressed in the eukaryotic model organism *S. cerevisiae*. Characterization of these r-proteins could lead to identification of evolutionary gained tasks, which the eukaryotic r-protein is able to overtake, yet the prokaryotic is not. Nevertheless, due to a certain sequence conservation, they might still be able to conduct the basal, “old” r-protein functions. In the light of this partial conservation of function, it is of special interest, whether prokaryotic r-proteins are perhaps able to participate in eukaryotic specific processes, like for example nucleo-cytoplasmic transport. Taking advantage of bioinformatic tools, like multiple sequence alignments, which are a fast way to analyze the primary structure diversification of proteins, it is evident that many eukaryotic r-proteins gained additional sequences in comparison to their prokaryotic counterparts. Deletion of these extended protein parts might again result in a loss of function if deleted, or when fused to a prokaryotic homologue, in a gain of function (see 2.1.3).

In the second approach, the growing number of (pseudo-) atomic structures of ribosomes was used to explicitly characterize certain r-protein parts, possibly even pinpointing the function of one specific amino acid. Attenuation of protein-protein or protein-RNA interfaces, by mutating the amino acids predicted to be required for the interaction, led to another set of r-protein variants. Such mutations might be subtle and hence result as well in partially functional r-proteins variants, which are defective in performing certain tasks in ribosome biogenesis (see 2.1.4). Localization of the mutation in regard to the ribosome bound r-protein could shed light on the molecular function of the mutated part. For example, predicted rRNA-interacting parts are maybe required to establish a certain assembly state, while protein parts on the surface side of the ribosome are more likely required for recruitment of biogenesis factors.

In the course of the systematic analyses of r-protein depletion phenotypes (Ferreira-Cerca et al., 2005; Pöll et al., 2009), yeast strains were created, in which the genomic copies of most r-proteins are replaced by a heterologous marker and the respective ribosomal protein is expressed under control of a galactose inducible promoter (pGAL-RPSX, Figure 20). The r-protein variants created in this work were constitutive expressed (FLAG/HA-variant, Figure 20) and transformed into the respective conditional r-protein knockout strain. After shutdown of wildtype r-protein expression on glucose, the variants were characterized, concerning their function in pre-rRNA processing, transport of precursor particles and biogenesis factor recruitment/release.

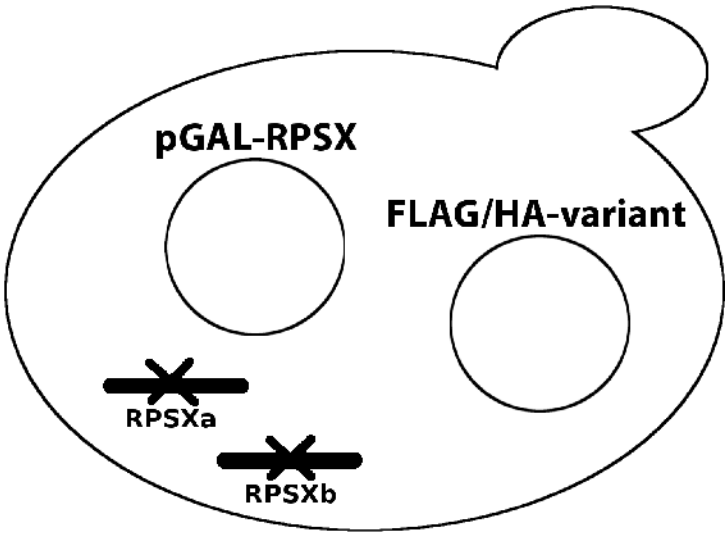

Figure 20. The genetic system used to analyze the r-protein variants
The genomic copies of the respective r-protein are knocked out. The strains contain in addition an ectopically expressed, galactose inducible copy of the wildtype r-protein and a constitutive expressed, FLAG- or HA-epitope tagged copy of the r-protein variant

2.1.2 Expression of archaeal homologues of r-proteins in *S. cerevisiae*

Thermoplasma acidophilum and *Sulfolobus acidocaldarius* are both thermophilic archaeons, which live in extremely acidic environments at a pH of 2 to 3 (Darland et al., 1970; Brock et al., 1972). Both genomes have already been sequenced (Ruepp et al., 2000; Chen et al., 2005). *S. acidocaldarius* is one of the archeal model organisms. Similarities between the eukaryotic and archeal transcription machinery (Zillig et al., 1979; Prangishvilli et al., 1982; Schnabel et al., 1984; Langer et al., 1995), as well as DNA repair mechanisms (Koulis et al., 1996; Jacobs and Grogan, 1997; Wood et al., 1997; Skorvaga et al., 1998) and cell cylce control (Bernander and Poplawski, 1997; Hjort and Bernander, 2001), have been extensively studied in *S. acidocaldarius*. Sequencing of *T. acidophilum* showed many homologies to members of the genus Sulfolobus, which might be due to extensive lateral gene transfer between the different species, which live in the same habitate (Ruepp et al., 2000). A histone-like molecule, actin- and myosin-like proteins, a primitive respiration machinery and possibly the facility of endocytosis, turned *T. acidophilum* into good candidate for the “ancestor” of a eukaryotic cell (Searcy et al., 1978; Stein and Searcy, 1978; Wolf et al., 1993; Roeben et al., 2006), nonetheless this is controversial discussed (Ruepp et al., 2000). A very unique feature of *T. acidophilum* is its rDNA organization. The rDNA is not clustered as in most other organisms, but there is only a single copy of each gene coding for 5S, 16S and 23S rRNA spread in the genome (Tu and Zillig, 1982; Ree et al., 1989; Ree and Zimmermann, 1990). In most archeons, as well as in *S. acidocaldarius*, the precursor transcript of the rDNA operon is multiply processed and modified by snoRNPs ((Durovic and Dennis, 1994b; Potter, Durovic, and Dennis, 1995; Potter, Durovic, Russell, et al., 1995; Omer et al., 2000b), see also 1.4). Since the rRNA species of *T. acidophilum* are transcribed separately, only final trimming of 5' and 3' extended 23S occurs (Ree et al., 1990).

T. acidophilum	Archaea – Euryarchaeota – Thermoplasmata – Thermoplasmatales – Thermoplasmataceae – Thermoplasma
S. acidocaldarius	Archaea – Crenarchaeota – Thermoprotei – Sulfolobales – Sulfolobaceae – Sulfolobus

Table 5. Taxonomy of *T. acidophilum* and *S. acidocaldarius*

Ribosomal proteins from both species exhibit a broad primary sequence conservation, when compared to yeast r-proteins. The full length alleles of 18 r-proteins from the small subunit of *T. acidophilum* (TAS) and 11 r-proteins from the small subunit of *S. acidocaldarius* (SAS) were cloned into ectopic multicopy yeast vectors. These archaeal r-proteins were tested first, whether they can fully substitute their yeast homologue in the corresponding conditional r-protein knockout strains. Surprisingly one, out of the 29 archaeal r-proteins tested, was able to fully overtake all essential functions of its eukaryotic counterpart (see 2.2.6). Many TAS and SAS were, despite a lack of some necessary functions, able to interact with pre-rRNA in yeast (data not shown, see diploma thesis of the author) and some could at least partially complement the loss of their eukaryotic homologue (see also 2.2.1, 2.2.2, 2.2.6).

2.1.3 Truncation and fusion mutants of yeast r-proteins

Based on multiple sequence alignments, yeast r-proteins have been analyzed for any non-conserved primary sequence parts. As described before, these parts might have eukaryotic specific functions. The truncated alleles of these r-proteins were cloned into ectopic multicopy yeast vectors and analyzed in the corresponding conditional r-protein knockout strains.

The remaining, evolutionary conserved parts are homologous to the archaeal r-proteins. A fusion of the archaeal r-protein with the non-conserved eukaryotic specific sequence might result in a variant similar to the eukaryotic r-protein. These fusion proteins were created using the splicing by overlap extension (SOE) PCR method (see 5.2.4.1). In the first PCR step each part is separately amplified with a certain overlap to the other part. In the second PCR step the amplicons from the first step are used as templates and the full length fusion allele is created. These alleles were also cloned into ectopic multicopy yeast vectors and analyzed in the corresponding conditional r-protein knockout strains.

2.1.4 Amino acid substitution mutants of yeast r-proteins

Point mutations were introduced in r-proteins to weaken protein-protein or protein-RNA interactions. Pseudo atomic structures of eukaryotic ribosomes or crystal structures of prokaryotic ribosomes were used as basis for determination of the (predicted) amino acids, involved in the interface (see 1.2.1). Only hydrogen bond and electrostatic mediated interactions were considered in this work, since the predicted hydrophobic interactions are hardly accurate due to the non-atomic resolution of the available structures (see 1.2.4). Especially arginine and lysine residues in r-proteins were mutated, because they possess conformational flexible side chains, which are in addition capable of interacting with RNA.

2.1.5 Table of described variant r-proteins in this work

For detailed description of the variants see the appropriate chapter.

variant of	name	background
rpS2 (2.2.3)	rpS2-ΔN	deletion of eukaryotic specific N-terminus
	rpS2-Δloop	attenuation of predicted head-body interaction
	rpS2-short-loop	attenuation of predicted head-body interaction
	rpS2-loop::APA	attenuation of predicted head-body interaction
	rpS2-RRAA	attenuation of predicted head-body interaction
	rpS2-KRRAAA	attenuation of predicted head-body interaction
rpS5 (2.2.4)	rpS5-ΔN	deletion of eukaryotic specific N-terminus
	rpS5-ΔC	deletion of highly conserved C-terminus
	rpS5-Δloop	alteration of r-protein fold; only globular domain left
	rpS5-short-loop	alteration of r-protein fold; only globular domain left
rpS14 (2.2.5)	rpS14-KKRAAA	attenuation of possible rpS14-ITS1 interaction
	rpS14-KKAA	attenuation of possible rpS14-ITS1 interaction
rpS15 (2.2.1)	TAS15	archaeal homologue of rpS15 (*T. acidophilum*)
	SAS15	archaeal homologue of rpS15 (*S. acidocaldarius*)
rpS17 (2.2.2)	rpS17-ΔC	deletion of eukaryotic specific C-terminus
	TAS17	archaeal homologue of rpS17 (*T. acidophilum*)
	rpS17-chimera	fusion protein of archaeal TAS17 and C-terminus of yeast rpS17
rpS20 (2.2.6)	TAS20	archaeal homologue of rpS20 (*T. acidophilum*)
	SAS20	archaeal homologue of rpS20 (*S. acidocaldarius*)
	SAS20-chimera1	partial exchange of TAS20 and SAS20 primary sequences
	SAS20-chimera2	partial exchange of TAS20 and SAS20 primary sequences
	SAS20-chimera3	partial exchange of TAS20 and SAS20 primary sequences
	SAS20-KKTT	point mutations in the tip of the SAS20 hairpin
	SAS20-K59S	point mutations in the tip of the SAS20 hairpin
	SAS20-K59T	point mutations in the tip of the SAS20 hairpin
	SAS20-K61T	point mutations in the tip of the SAS20 hairpin

Table 6. Overview of described variant r-proteins in this work

2.2 Characterization of r-protein variants in *S. cerevisiae*

2.2.1 rpS15 and its variants

RpS15 and rpS18 are the only known r-proteins in the head domain of the small subunit that bind at the interface site of SSU and LSU (see Figure 8 A and Figure 21 A). Many of the rRNA interacting amino acids of rpS15 are well conserved in all three evolutionary kingdoms (e.g *S. cerevisiae* H79, R81, Y97, G99 or K100, Figure 21 C).

In vivo depletion of rpS15 results in a block of 18S rRNA processing at site D (see 1.4.3.1) and accumulation of 20S pre-rRNA (Léger-Silvestre et al., 2004; Ferreira-Cerca et al., 2005) (see also Figure 22 C, compare lanes 1 and 2). In addition nucleo-cytoplasmic transport of precursor subunits is strongly delayed (Léger-Silvestre et al., 2004; Ferreira-Cerca et al., 2005) (see also Figure 23, vector).

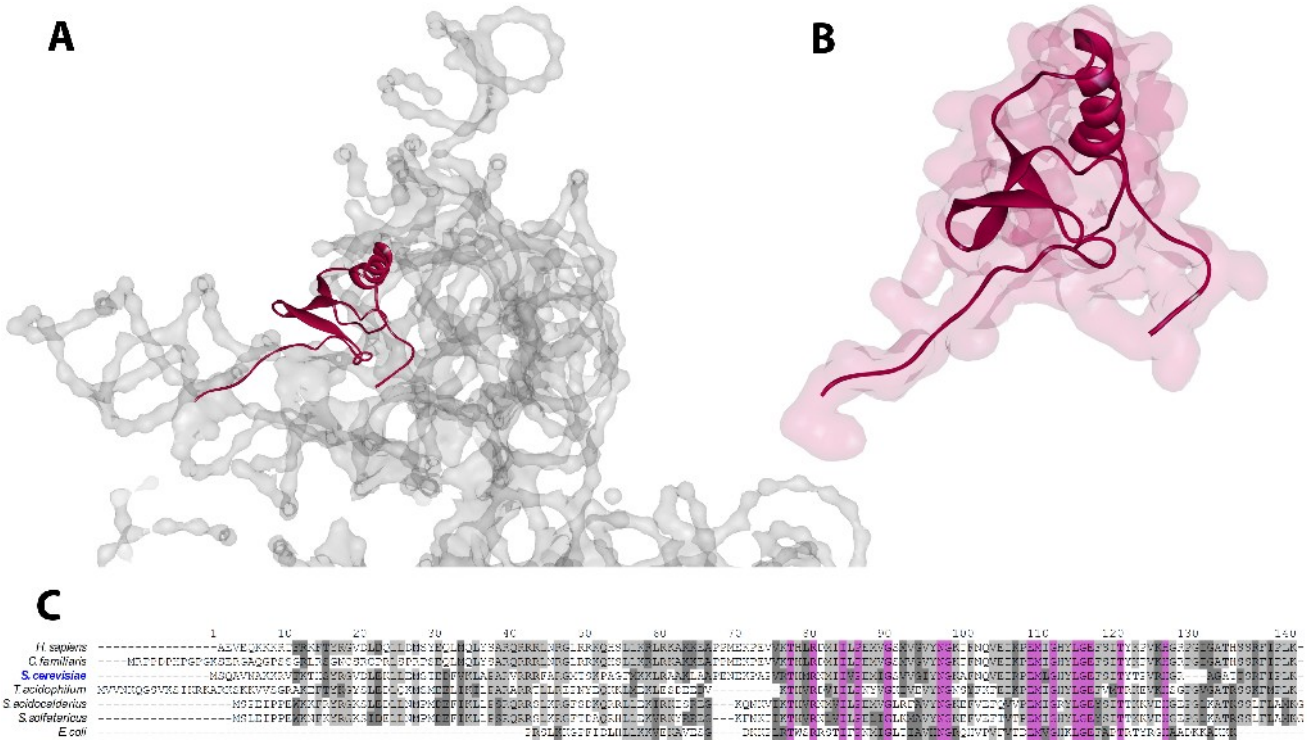

Figure 21. RpS15 localization, structure and protein sequence conservation
(**A**) Localization of rpS15 on the 40S subunit (Chandramouli et al., 2008; pdb:2ZKQ), inter-subunit view (see also Figure 8). (**B**) Ribbon representation of rpS15 structure with the calculated surface laid underneath. Amino acids 43 to 130 of 145 in total are modeled. (**C**) Multiple sequence alignment of yeast rpS15 primary structure (AlignX, Vector NTI, Invitrogen, ClustalW algorithm and blosum score-matrix). Protein sequences of representative organisms from all three evolutionary kingdoms are shown (sequences were obtained from NCBI (http://www.ncbi.nlm.nih.gov/protein)). The color code illustrates amino acid conservation: identical - purple; conserved – gray; block of similar – dark-gray. The numbers give the positions of *S. cerevisiae* amino acids.

name	background	mutation	database (ToP)
rpS15	*S. cerevisiae* full length allele (wildtype)	-/-	Nt-FLAG: 1004 Nt-HA : 1176
TAS15	archaeal homologue of rpS15 (*T. acidophilum*)	-/-	Nt-FLAG: 506 Nt-HA : 1174
SAS15	archaeal homologue of rpS15 (*S. acidocaldarius*)	-/-	Nt-FLAG: 708 Nt-HA : 1175

Table 7. List of rpS15 variants

2.2.1.1 The archaeal homologues of rpS15 partially complemented the loss of their eukaryotic counterpart in S. cerevisiae

S19, the prokaryotic homologue of yeast rpS15, from *T. acidophilum* (hereafter termed TAS15) exhibits about 32% of identical amino acids with yeast rpS15 (47% of amino acids with side chains of the same chemical properties). S19 from *S. acidocaldarius* (hereafter termed SAS15) exhibits about 35% identical amino acids (50% of amino acids with side chains of the same chemical properties). Both proteins were ectopically expressed as FLAG- or HA-epitope fusion proteins under the control of a constitutive promoter in the conditional rpS15 knockout strains.

While none of the archaeal alleles was able to fully complement the loss of rpS15 at the normal yeast cultivation temperature of 30°C or below, the expression of SAS15 – and at a very low level also the expression of TAS15 – restored partial growth at 37°C (Figure 22 A). The complementation effect could be dependent on protein expression levels, since either the expression level of SAS15 goes up, or the protein is stabilized at 37°C (Figure 22 B, compare lanes 4 and 8).

2.2.1.2 The archaeal homologues of rpS15 were efficiently incorporated into SSU precursors

Both, FLAG-tagged TAS15 and SAS15 efficiently co-precipitated SSU precursor rRNA species (Figure 22 D, see probe ITS1) at 30°C and 37°C. The interaction of SAS15 with pre-40S precursors was in addition quite salt resistant, the interaction of TAS15 with 40S precursors on the other side was weakened upon salt increase (Figure 22 D and E, compare 20S co-precipitation). The rather high co-precipitation of 27S (precursor rRNA of 25S and 5.8S, see 1.4.3.1) by TAS15 could be eliminated with higher salt conditions (Figure 22 D and E, compare probe E/C2). The incorporation of both variants in mature ribosomes was more stable at 37°C, than at 30°C (Figure 22 D and E, compare 25S and 18S, input vs. IP), although to an overall lesser extent compared to lower salt concentrations (Figure 22 D and E, compare probes 25S and 18S). At more physiological salt concentrations of 200 mM KCl (Alberts et al., 1989), SAS15 was far better assembled into mature subunits at 37°C (Figure 22 D, see probe ITS1), which might correlate with its ability to partially complement the growth defect due to loss of rpS15 (Figure 22 A).

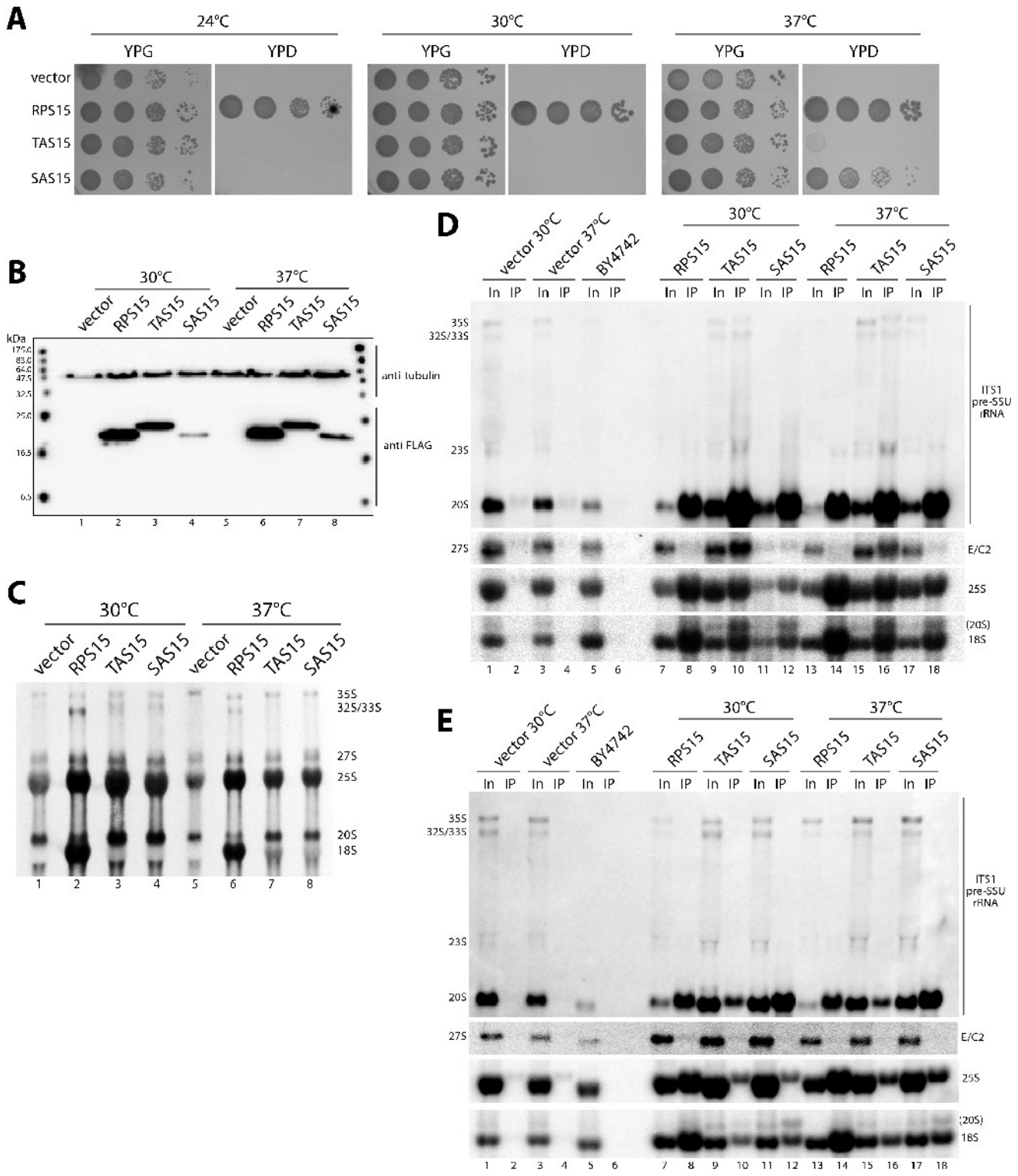

Figure 22. Growth phenotypes of rpS15 variants, expression levels, pre-rRNA processing analyses and incorporation into SSU precursors

(**A**)-(**E**) All experiments were performed in yeast strain pGAL-RPS15 (ToY89), in which full length rpS15 is encoded under the control of the galactose inducible GAL1 promoter. The strain was either transformed with an empty vector (YEplac195) or vectors coding for FLAG-tagged full length rpS15 (ToP1004), TAS15 (ToP506) or SAS15 (ToP708) under the control of a constitutive promoter. (**A**) Serial dilutions of the indicated transformants on galactose (YPG) or glucose (YPD) containing plates. Plates were incubated for 3 days. (**B**)-(**E**) Cells were grown overnight in selective media containing galactose, diluted in YP-galactose and subsequently expression of pGAL-RPS15 was shut down for 2 hours in YP-glucose medium. The cultures were cultivated at the respective temperature of the later experiment. (**B**) Western blot analysis of the indicated transformants, using a monoclonal

anti FLAG antibody. Tubulin was used as loading control. (**C**) 5',6'-[^{3}H] uracil metabolic labeling of newly synthesized RNA. Cells were pulsed for 30 minutes at 30°C or 37°C. Total RNA was extracted and separated by gel electrophoresis, radio-labeled RNA was visualized by fluorography as indicated in Materials and Methods. (**D**) and (**E**) Northern blot analysis of RNA co-purified with the indicated FLAG-tagged rpS15 variants. RNA was extracted from Input (In) and immuno-purified (IP) fractions. Wildtype strain BY4742 served as background control for immuno-purification. Probes used for detection of (pre-) rRNA species are depicted right-hand. In (**D**) 200 mM salt (KCl, see 5.2.5.3) was used for cell breakage, binding and washing of the immunoprecipitations. In (**E**) 400 mM salt (KCl) was used.

2.2.1.3 Expression of the archaeal homologues of rpS15 could not rescue the pre-rRNA processing defects caused by rpS15 depletion

At both temperatures used, depletion of rpS15 led to inhibited D-site cut processing and accumulation of 20S pre-rRNA (Figure 22 C, vector). 20S pre-rRNA still accumulated when the archaeal homologues TAS15 and SAS15 were expressed (Figure 22 C, 20S). Nevertheless, the expression of both archaeal r-proteins promoted production of some 18S rRNA (Figure 22 C, 18S). Although 18S rRNA was produced only on a small scale, the amount, at least at 37°C, seems to be enough to allow growth. On the other hand, 20S pre-rRNA might be able to form translation competent ribosomes (see discussion in 3.3). Upon expression of the archaeal rpS15 variants, 20S pre-rRNA never reached the levels of mature 18S rRNA (compare 20S to 18S levels with probe 18S in Figure 22 C or D, lanes 13, 15 and 17), contradicting this hypothesis under these conditions.

2.2.1.4 Expression of the archaeal homologues of rpS15 enhanced nuclear export of SSU precursor particles

As already reported (Léger-Silvestre et al., 2004; Ferreira-Cerca et al., 2005), depletion of rpS15 caused a very strong delay in nucleo-cytoplasmic transport of pre-40S subunits (see also Figure 23 A and B, vector). Remarkably this export defect was cured by the expression of each of the two archaeal variants. FISH analysis clearly showed a bright cytoplasmic signal for ITS1 containing particles when expressing TAS15 or SAS15 (Figure 23 A, TAS15, SAS15). Confirming this result, 20S pre-rRNA appeared in substantial amounts in the cytoplasmic fractions in the strains expressing any archaeal r-protein (Figure 23 A, TAS15 and SAS15). The elevated levels of 20S (in the strains expressing TAS15 or SAS15, compared to rpS15), which was visible in the sub-cellular fractionation, correspond to higher ITS1 signal levels in FISH analysis (compare Figure 23 A and B) and accumulation of 20S pre-rRNA in pulse experiments (compare Figure 22 C, 20S).

Most interestingly, prokaryotic r-proteins, evolved in cells having no nucleo-cytoplasmic compartmentalisation, are able to substitute an eukaryotic r-protein in its role in nuclear export of small subunit precursors. The properties of rpS15, which support nuclear export of pre-40S particles, are apparently evolutionary conserved. Since any interactions of archaeal r-proteins with the eukaryotic export machinery seem unlikely, yet can not be directly ruled out, most probably rpS15 assembly itself renders the precursors export competent (for discussion see 3.3).

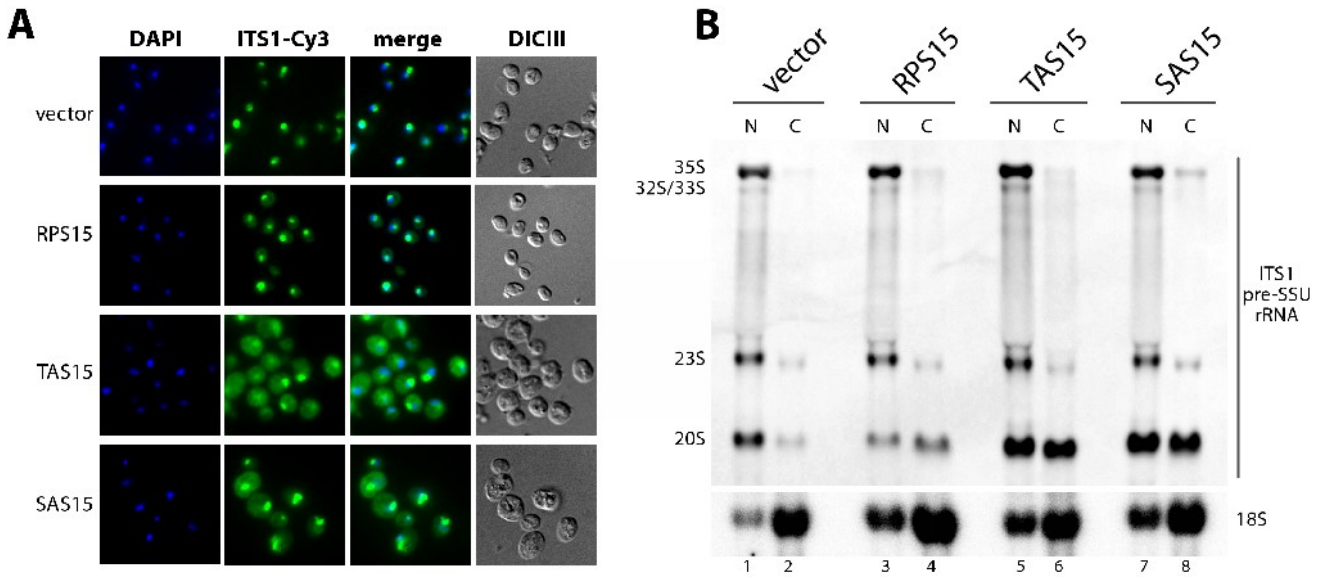

Figure 23. Analyses of nuclear export of SSU precursors containing rpS15 variants
(**A**)-(**B**) All experiments were performed in yeast strain pGAL-RPS15 (ToY89), in which full length rpS15 is encoded under the control of the galactose inducible GAL1 promoter. The strain was either transformed with an empty vector (YEplac195) or vectors coding for FLAG-tagged full length rpS15 (ToP1004), TAS15 (ToP506) or SAS15 (ToP708) under the control of a constitutive promoter. (**A**) FISH analysis of steady state distribution of precursor subunits. Cells were grown overnight in selective media containing galactose, diluted in YP-galactose and expression of pGAL-RPS15 was shut down for 2 hours in YP-glucose medium. Total DNA (DAPI) and rRNA precursors containing ITS1-sequences between site D and A2 (ITS1-Cy3) were detected as described in 5.2.6.2. (**B**) Steady state analysis of pre-rRNA in sub-cellular fractions. Cells were grown for 1.5 hours in YPD before nucleo-cytoplasmic fractionation (see 5.2.5.5). Cells were spheroplasted and subsequently fractionated in nuclei (N) and cytoplasm (C). RNA was extracted and 2.4 times more volume of nuclear than cytoplasmic fractions were separated by gel electrophoresis and analyzed by northern blotting. Probes for detection of rRNA species are depicted right-hand.

2.2.1.5 Expression of the archaeal homologues of rpS15 improved the in vivo assembly state of some head domain r-proteins

Most likely r-protein assembly events, following rpS15 assembly, are a prerequisite for nuclear export of SSU precursors (Ferreira-Cerca et al., 2005, 2007). *In vivo* assembly of rpS15 was found to be required for stable incorporation of a subset of head domain r-proteins (Ferreira-Cerca et al., 2007). The two r-proteins, whose binding was mostly destabilized are rpS3 and rpS19.

Interaction of these two proteins with (pre-) rRNA was analyzed in strains expressing HA-tagged TAS15 and SAS15 or no rpS15 (vector) after shutdown of rpS15 expression (for verification of the phenotype of HA-tagged archaeal rpS15 variants see Supplemental Figure 3). Confirming the published results, the dependency of stable incorporation of rpS3 and rpS19 on the presence of rpS15 could be shown (Figure 24 A and B, vector). Expression of TAS15, as well as SAS15, clearly improved the stable assembly of rpS3 and rpS19 into pre-SSU particles (Figure 24, compare 20S co-precipitation levels, see also quantification below).

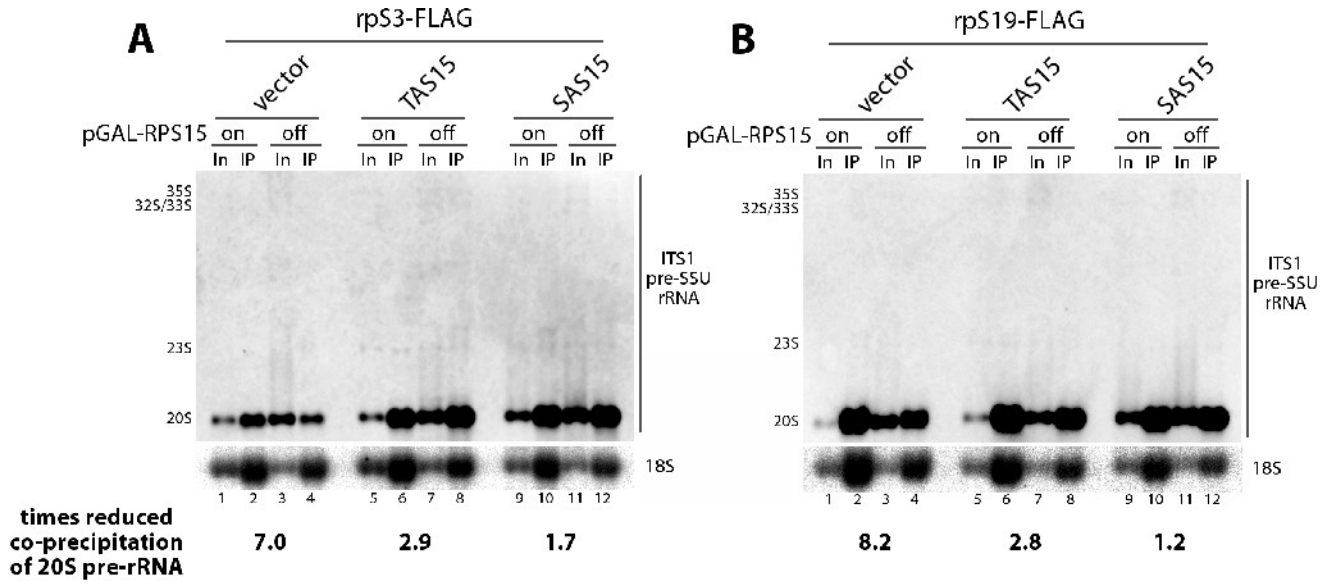

Figure 24. Analysis of r-protein interactions with SSU precursors containing rpS15 variants
(**A**) and (**B**) All experiments were performed in yeast strain ToY1217, in which full length rpS15 is encoded under the control of the galactose inducible GAL1 promoter. The strain was transformed with vectors supporting the constitutive expression of FLAG-tagged rpS3 (ToP994) and rpS19 (ToP1008) and in addition, with an empty vector (YEplac181) or vectors coding for HA-tagged TAS15 (ToP1171) or SAS15 (ToP1172) under the control of a constitutive promoter. Transformants were grown overnight in selective media containing galactose and on the next day diluted in YP-galactose medium. The cultures were split, one half was further grown in YP-galactose (on, wildtype rpS15 is expressed), in the other half of the culture expression of pGAL-RPS15 was shut down for 3 hours in YP-glucose medium (off). 200 mM salt (KCl, see 5.2.5.3) was used for cell breakage, binding and washing of the immunoprecipitations. (**A**) Northern blot analysis of SSU (pre-) RNA co-purified with FLAG-tagged rpS3 in cells expressing TAS15, SAS15 or no rpS15 (vector). RNA was extracted from Input (In) and immuno-purified (IP) fractions. Probes used for detection of (pre-) rRNA species are depicted right-hand. (**B**) Same as (**A**) but the IP was done by purifying FLAG-rpS19. (**A**) and (**B**) The factor of reduced 20S co-precipitation was calculated as follows: (%IP20S / %IP18S)**on** / (%IP20S / %IP18S)**off**. Quantification was done, using LAS3000, FLA3000 and MultiGauge software (FujiFilm).

Deduced from these results, the expression of any archaeal homologue of rpS15 might be sufficient to promote the subsequent assembly of other head domain r-proteins and thus allow nuclear export of precursor subunits. The main role of rpS15 in nuclear export of SSU precursors might therefore be to facilitate assembly of other head domain r-proteins. These in turn possibly interact directly with the export machinery, create binding sites for biogenesis factors, or are themselves required for assembly of other r-proteins (see 1.4.5 and 3.3).

2.2.2 rpS17 and its variants

Eukaryotic ribosomal protein rpS17 is only conserved in Archaea (see Table 1), whereby it has not been mapped in any cryo-EM based eukaryotic ribosome structure (see 1.2.3). In 2008 a solution structure of rpS17 from *Methanobacterium thermoautotrophicum* was solved (Wu et al., 2008). The structure showed rpS17 as a three-helix bundle protein with a novel phosphopeptide-binding fold (Figure 25 A). Only the N-terminal primary sequence of rpS17 is conserved (Figure 25 C), the C-terminal half is eukaryotic specific. Using the web-based secondary structure prediction program PHYRE (Kelley and Sternberg, 2009), the complete sequence of rpS17 was analyzed (Figure 25 B). The prediction stated that the C-terminus of rpS17 is composed of two helices and three beta sheets and maybe contains a hairpin (aa 85 to 105). Based on the secondary structure predictions, the C-terminus might fold similar to an inverse classical RNP fold of the spliceosomal protein U1A (Orengo and Thornton, 1993; Nagai, Oubridge, Ito, Jessen, et al., 1995; Nagai, Oubridge, Ito, Avis, et al., 1995) and is therefore possibly involved in RNA binding.

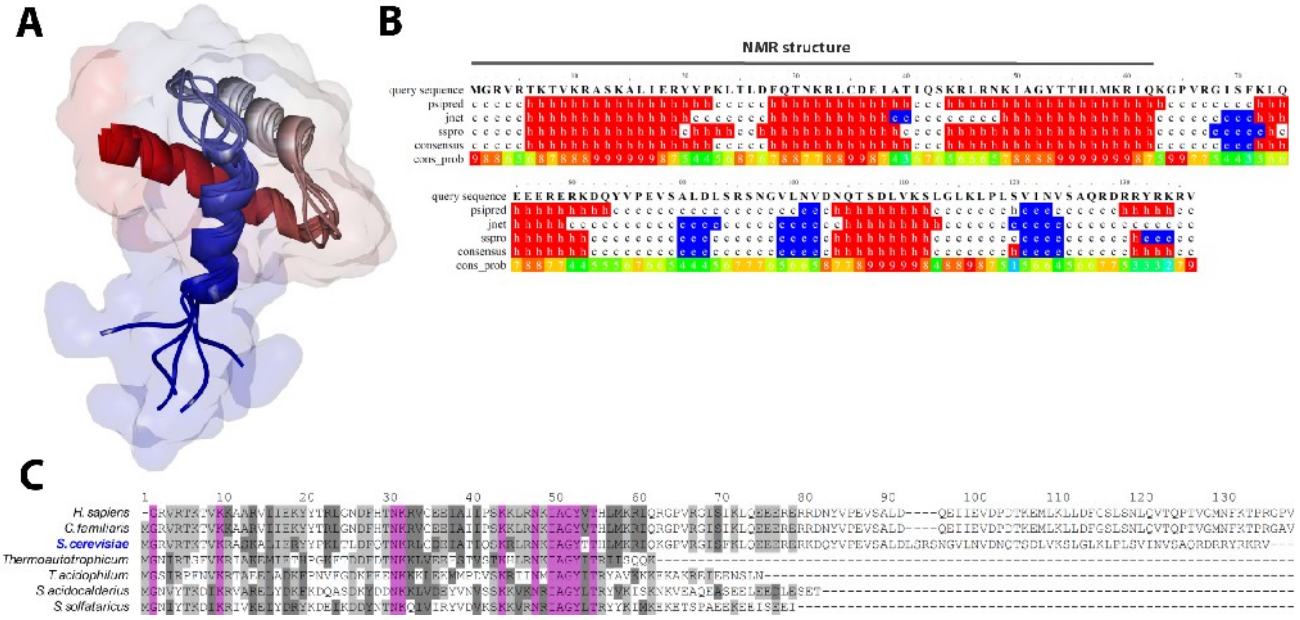

Figure 25. RpS17 structure and protein sequence conservation
(**A**) Ribbon representation of five rpS17 solution structures from *Methanobacterium thermoautotrophicum* (pdb:1RQ6; Wu et al., 2008) with the calculated surface laid underneath (color code: N-terminus - red, C-terminus - blue). Amino acids 1 to 62 of 136 in total are modeled. (**B**) Secondary structure prediction for yeast rpS17 protein sequence. The calculation was done with the PHYRE 2.0 – Protein Homology/analogY Recognition Engine (Kelley and Sternberg, 2009), a web based interface to predict secondary structure elements from primary sequences. Query sequence is the rpS17 primary sequence; psipred, jnet, sspro are prediction programs (c stands for coil, h for helices and e for beta strands); cons_prob gives the probability of a secondary structure element at the corresponding position. On top, the sequence used for NMR solution structure by Wu et al., is indicated. (**C**) Multiple sequence alignment of yeast rpS17 primary structure (AlignX, Vector NTI, Invitrogen, ClustalW algorithm and blosum score-matrix). Protein sequences of representative organisms from Eukarya and Archaea are shown (sequences were obtained from NCBI (http://www.ncbi.nlm.nih.gov/protein)). The color code illustrates amino acid conservation: identical - purple; conserved – gray; block of similar – dark-gray. The numbers give the positions of *S. cerevisiae* amino acids. RpS17 is not conserved in Bacteria and therefore not modeled into any Cryo EM based structure (see Figure 8).

RpS17 depletion mirrors the phenotype of rpS19 depletion in a human cell line and both are needed for processing of nuclear pre-18S rRNA species (Robledo et al., 2008). RpS17 deletion has not been analyzed in yeast before.

2.2.2.1 The depletion phenotype of rpS17

RpS17 is encoded by two almost identical, interchangeable gene copies in yeast (Abovich and Rosbash, 1984; Abovich et al., 1985). Expression of at least one gene copy is required, so the single knockouts of RPS17A or RPS17B, respectively, are viable, the double knockout is lethal (Figure 26 A, vector). All the experiments were performed in yeast strain ToY566, in which both copies of RPS17 are knocked out and RPS17A is ectopically encoded under control of the GAL1-promoter (ToP479). Upon rpS17 depletion, D-site cut processing (see 1.4.3.1) was blocked and 20S pre-rRNA was slightly accumulating (Figure 26 C, vector). FISH signals of this 20S rRNA containing precursor were highly concentrated in the nucleus, arguing for a very strong nuclear export delay (Figure 27, vector). All of the these described phenotypes could be rescued by expression of a rpS17 wildtype copy in strain ToY566 (Figure 26 and Figure 27, RPS17).

name	background	mutation	database (ToP)
rpS17	*S. cerevisiae* full length allele (wildtype)	-/-	Nt-FLAG: 1006
rpS17-ΔC	deletion of eukaryotic specific C-terminus	ΔE75-V136	Nt-FLAG: 517
TAS17	archaeal homologue of rpS17 (*T. acidophilum*)	-/-	Nt-FLAG: 551
rpS17-chimera	fusion protein of archaeal TAS17 and C-terminus (E75-V136) of yeast rpS17	-/-	Nt-FLAG: 575

Table 8. List of rpS17 variants
Amino acid positions are given, according to the primary sequence of RPS17A gene product

2.2.2.2 All analyzed rpS17 variants were efficiently incorporated into SSU precursors

As described before (2.1.1), eukaryotic specific protein parts might have gained additional functions during the course of evolution. A C-terminal truncated version of rpS17 (rpS17-ΔC), in which amino acids E75 to V136 were deleted (see Figure 25 C), was still able to interact with SSU precursors (Figure 26 D, probe ITS1). This interaction was in addition fairly stable, since rpS17-ΔC still precipitated 20S pre-rRNA fairly well under high salt conditions (Figure 26 D and E, compare always 20S levels in lanes 5 and 6). The archaeal homologue of rpS17 from *T. acidophilum* (TAS17) co-precipitated 20S pre-rRNA, but this interaction was not salt resistant (Figure 26 D and E, compare always 20S levels in lanes 7 and 8). TAS17 is one example which illustrates the fact that expression level (under detection limit, see Figure 26 B, lane 4) and rRNA interaction are not directly related (for another example see 2.2.6.2). Most probably all other variants are highly over-expressed due to the multicopy vector

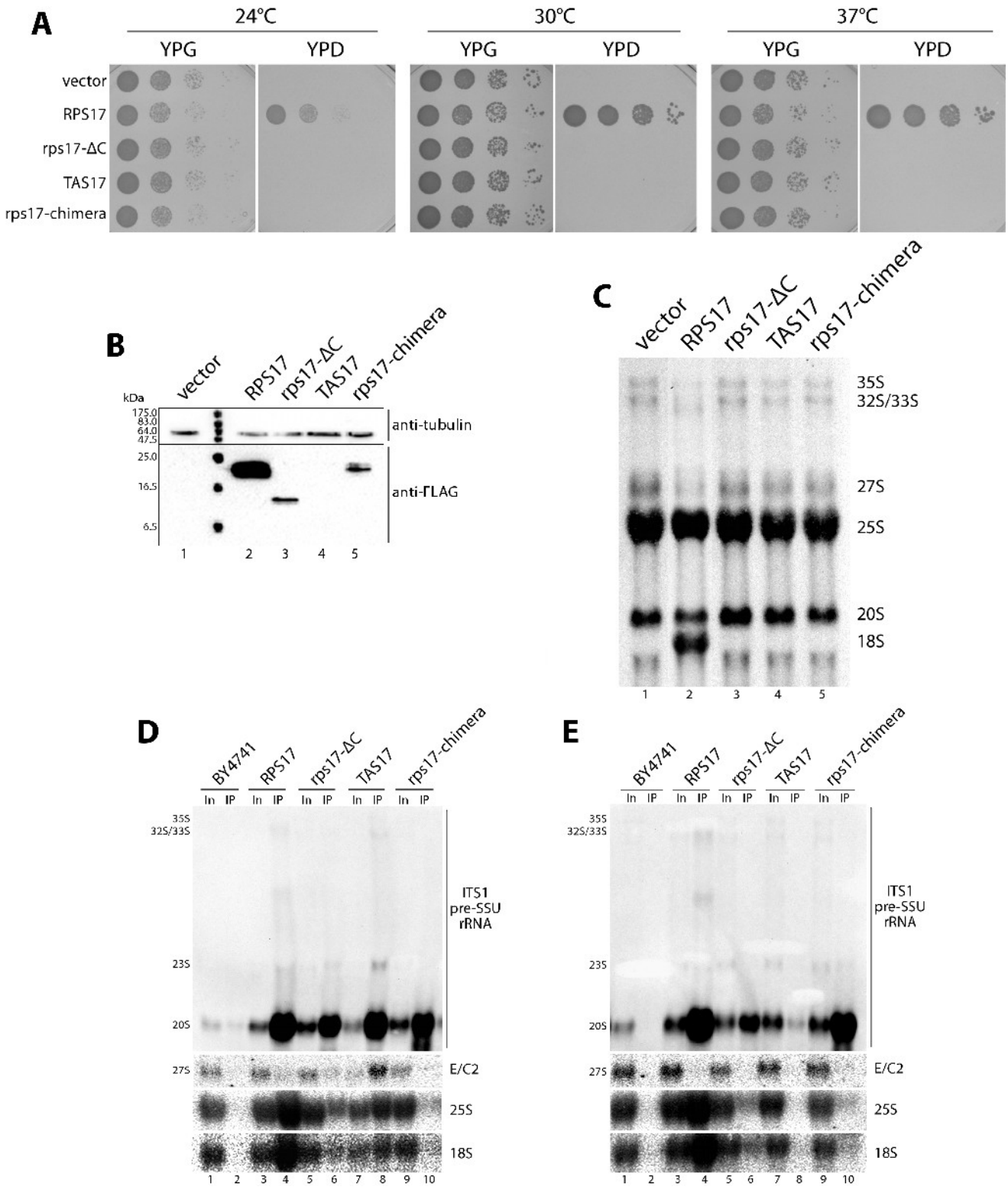

Figure 26. Growth phenotypes of rpS17 variants, expression levels, pre-rRNA processing analyses and incorporation into SSU precursors

(**A**)-(**E**) All experiments were performed in yeast strain pGAL-RPS17 (ToY566), in which full length rpS17 is encoded under the control of the galactose inducible GAL1 promoter. The strain was either transformed with an empty vector (YEplac195) or vectors coding for FLAG-tagged full length rpS17 (ToP1006), rpS17-ΔC (ToP517), TAS17 (ToP551) or rpS17-chimera (ToP575) under the control of a constitutive promoter. (**A**) Serial dilutions of the indicated transformants on galactose (YPG) or glucose (YPD) containing plates. Plates were incubated for 3 days. (**B**)-(**E**) Cells were grown overnight in selective media containing galactose, diluted in YP-galactose and subsequently expression of pGAL-RPS17 was shut down for 2 hours in YP-glucose medium. (**B**) Western blot

analysis of the indicated transformants, using a monoclonal anti FLAG antibody. Tubulin was used as loading control. (**C**) 5',6'-[^{3}H] uracil metabolic labeling of newly synthesized RNA. Cells were pulsed for 30 minutes at 30°C. Total RNA was extracted and separated by gel electrophoresis, radio-labeled RNA was visualized by fluorography. (**D**) and (**E**) Northern blot analysis of RNA co-purified with the indicated FLAG-tagged rpS17 variants. RNA was extracted from Input (In) and immuno-purified (IP) fractions. Wildtype strain BY4741 served as background control for immuno-purification. Probes used for detection of (pre-) rRNA species are depicted right-hand. In (**D**) 200 mM salt (KCl, see 5.2.5.3) was used for cell breakage, binding and washing of the immunoprecipitations. In (**E**) 400 mM salt (KCl) was used.

system and only a sub-population of the proteins is incorporated into precursor subunits (compare Figure 26 B and D). A chimeric protein of TAS17, whose part resembles the N-terminal portion of rpS17 and the C-terminus of rpS17, which is missing in the rpS17-ΔC variant, artificially restores a full length rpS17-like protein (rpS17-chimera). This variant strongly interacted with SSU precursor rRNAs (Figure 26 D and E, compare always 20S levels in lanes 9 and 10). In addition the chimeric protein, in comparison to TAS17 alone, was more salt stable incorporated into 20S pre-rRNA containing precursors (Figure 26 E, compare 20S in lanes 8 and 10), indicating actually RNA binding ability of rpS17's C-terminal part (see 2.2.2).

Expression of neither of the rpS17 variants abrogated the pre-rRNA processing phenotypes, observed upon rpS17 depletion. In all variants 3'-18S rRNA maturation was hindered (Figure 26 C, lanes 3 to 5). Only full length rpS17 expression restored wildtype like pre-rRNA maturation (Figure 26 C, lane 2).

2.2.2.3 The C-terminal part of rpS17 is required for stable incorporation into mature ribosomes

Both, the archaeal rpS17 variant TAS17 and rpS17-ΔC, which consists only of the conserved N-terminal part of rpS17, were incorporated into mature ribosomes with clearly lower efficiency than yeast full length rpS17 (Figure 26 D and E, compare always 25S and 18S levels in lanes 3 and 4 versus 5 and 6). The fusion of TAS17 and the C-terminus of rpS17 (rpS17-chimera) improved the salt stable incorporation of the variant into precursors (see before), but surprisingly not into mature ribosomes (Figure 26 D and E, compare 25S and 18S co-precipitations of the different variants). In conclusion, non-conserved features of the N-terminal part of rpS17 seem to be required for incorporation of rpS17 into mature ribosomes. The C-terminus, on the other hand, enhances salt resistant interaction with SSU precursors and is required for 18S 3'-end processing.

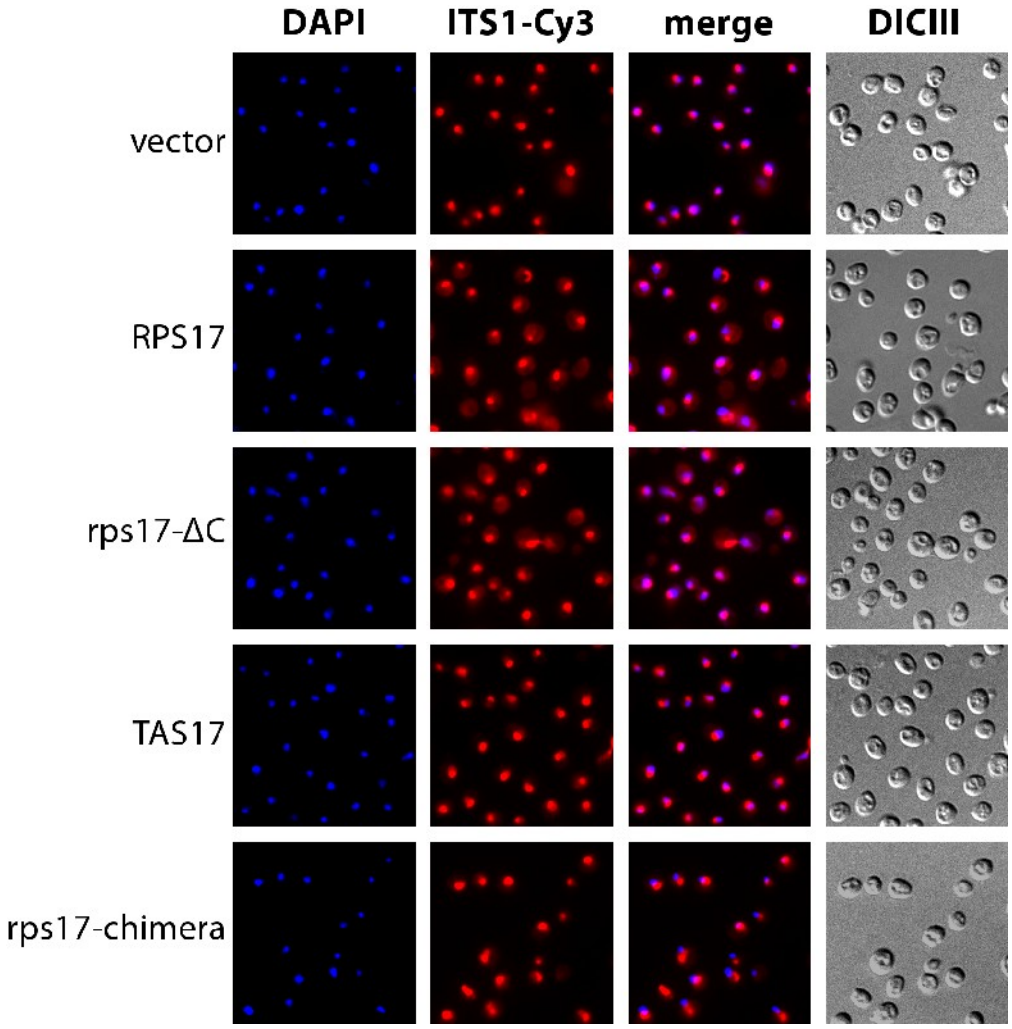

Figure 27. Analyses of nuclear export of SSU precursors containing rpS17 variants
FISH analysis was performed in yeast strain pGAL-RPS17 (ToY566), in which full length rpS17 is encoded under the control of the galactose inducible GAL1 promoter. The strain was either transformed with an empty vector (YEplac195) or vectors coding for FLAG-tagged full length rpS17 (ToP1006), rpS17-ΔC (ToP517), TAS17 (ToP551) or rpS17-chimera (ToP575) under the control of a constitutive promoter. Cells were grown overnight in selective media containing galactose, diluted in YP-galactose and subsequently expression of pGAL-RPS17 was shut down for 2 hours in YP-glucose medium. Total DNA (DAPI) and rRNA precursors containing ITS1-sequences between site D and A2 (ITS1-Cy3) were detected as described in 5.2.6.2.

2.2.2.4 The conserved N-terminal part of rpS17 is sufficient to allow nuclear export of SSU precursor particles

Depletion of rpS17 caused a strong accumulation of ITS1-containing precursors in the nucleus (Figure 27, vector, see ITS1-Cy3). Expression of full length rpS17 or the C-terminal truncated variant rpS17-ΔC restored nucleo-cytoplasmic transport (Figure 27, RPS17 and rps17-ΔC). TAS17, the archaeal homologue of rpS17, which lacks the eukaryote specific C-terminal domain of yeast rpS17, led to an intermediate phenotype. Here, a stronger ITS1 signal was visible in the cytoplasm, compared to the rpS17 depletion situation (compare vectorand TAS17 in Figure 27). The same was true for the chimeric rpS17 variant (Figure 27, rps17-chimera). Expression of both, rpS17 or rpS17-ΔC resulted in readily detectable ITS1-signals in the cytoplasm (Figure 27, rpS17 and rpS17-ΔC).

TAS17 is another example for a prokaryotic r-protein (see also rpS15 variants, 2.2.1.4), whose expression is sufficient to enhance nuclear export of pre-40S subunits. It remains again unclear, whether this prokaryotic protein can interact with the eukaryotic export machinery, “shield” the pre-SSUs during passage of the nuclear pore complex, or the “old” protein core is sufficient to stabilize assembly of other r-proteins and by this promote nuclear export of precursor particles.

Taken together, these results suggest that the evolutionary conserved N-terminal part of rpS17 is sufficient to allow stable incorporation into pre-SSUs and promote nuclear export of these precursor particles. The C-terminal part of rpS17 is required for stable assembly into mature ribosomes and for final cytoplasmic 18S rRNA 3'-end maturation.

2.2.3 rpS2 and its variants

The head domain helices h35 and h36 pack against the body/head transition helix h28 and thereby build the neck region of the small subunit (see Figure 4). The two ribosomal proteins which bind in this area are rpS0 and rpS2 (see Figure 8). The main part of rpS2 is localized in the body domain, but it forms extensive contacts to the head domain with a hairpin, especially with helices h34, h35 and h36, which build the lower part of the head domain (Figure 28 A and B, see also Figure 5). Deduced from current pseudo-atomic structures, three candidate amino acids in the hairpin of rpS2 have been identified, which are in the right 3D conformation to be capable of interacting with rRNA (Figure 28 B and C). The two arginines R91 and R95 of yeast rpS2 are only conserved in eukaryotes. Lysin K88 on the other hand is highly conserved in all evolutionary kingdoms (Figure 28 C).

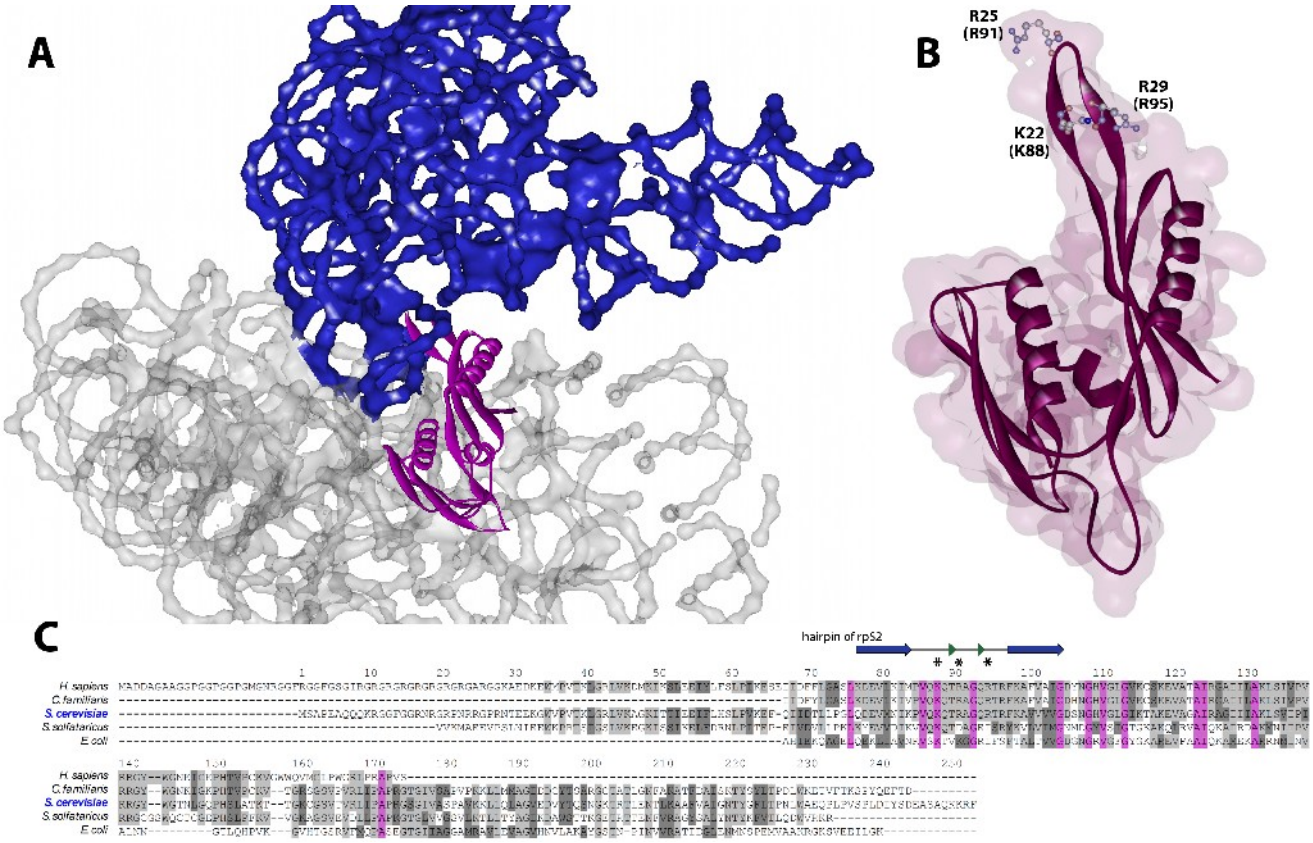

Figure 28. RpS2 localization, structure and protein sequence conservation
(A) Localization of rpS2 on the 40S subunit (Chandramouli et al., 2008; pdb:2ZKQ), cytoplasmic view (see also). The 40S rRNA 3'-major domain is colored in blue, other 40S rRNA sequences in gray (B) Ribbon representation of rpS2 structure with the calculated surface laid underneath. Amino acids 9 to 157 of 179 in total are modeled. Three amino acids, capable of interacting with RNA are highlighted. The position is given according to the C. familiaris nomenclature with S. cerevisiae position in brackets. (C) Multiple sequence alignment of yeast rpS2 primary structure (AlignX, Vector NTI, Invitrogen, ClustalW algorithm and blosum score-matrix). Protein sequences of representative organisms from all three evolutionary kingdoms are shown (sequences were obtained from NCBI (http://www.ncbi.nlm.nih.gov/protein)). The color code illustrates amino acid conservation: identical - purple; conserved – gray; block of similar – dark-gray. The numbers give the positions of S. cerevisiae amino acids. The asterisks show the amino acids highlighted in (B), which are located in a predicted hairpin (Chandramouli et al., 2008) (blue arrows indicate part of a beta sheet, green triangles are residues in an isolated beta-bridge).

In vivo depletion of rpS2 in *S. cerevisiae* resulted in block of 18S rRNA processing at site D and slight accumulation of 20S pre-rRNA. While the steady state distribution of pre-40S particles after shutdown of rpS2 showed no strong nuclear export defect, newly synthesized pre-SSUs were exported with delayed kinetics (Ferreira-Cerca et al., 2005).

name	background	mutation	database (ToP)
rpS2	*S. cerevisiae* full length allele (wildtype)	-/-	Nt-FLAG: 993
rpS2-ΔN	deletion of eukaryotic specific N-terminus	ΔM1-E31	Nt-FLAG: 515
rpS2-Δloop	attenuation of predicted head-body interaction; deletion of complete hairpin	ΔK84-F98	Nt-FLAG: 1104
rpS2-short-loop	attenuation of predicted head-body interaction; shortening of the hairpin	ΔP85-Q87 and ΔT96-R97	Nt-FLAG: 1106
rpS2-loop::APA	attenuation of predicted head-body interaction; deletion of complete hairpin by insertion of APA	K84-F98::APA	Nt-FLAG: 1105
rpS2-RRAA	attenuation of predicted head-body interaction	R91A, R95A	Nt-FLAG: 1070
rpS2-KRRAAA	attenuation of predicted head-body interaction	K88A, R91A, R95A	Nt-FLAG: 1107

Table 9. List of rpS2 variants

2.2.3.1 A N-terminal truncation of rpS2 impaired growth under sub-optimal conditions

Some N-terminal arginines of rpS2 are methylated by Rmt1p/PRMT3 in Eukarya (Bachand and Silver, 2004; Lipson et al., 2010). It was supposed that “[...] the methylation of the 40S ribosomal protein S2 could potentially regulate the translationability of specific cellular transcripts in a temporal fashion” ((Bachand et al., 2004), see also “ribosome filter hypothesis”, 3.1).

Roughly the first 65 amino acids of rpS2 are conserved between Eukarya and Archaea. Nearly the first 30 amino acids are eukaryotic specific. Deletion of the first 31 amino acids of the primary sequence of yeast rpS2 in a strain, solely depending on this truncated rpS2 allele (rpS2-ΔN, yeast strain ToY1501), led to no obvious phenotype under optimal growth conditions (Figure 29 A, 30°C, YPD). Changes of carbon source or growth temperature resulted in minor (temperature) or major (galactose vs. glucose) impairments of cell growth, compared to wildtype rpS2 expression (Figure 29 A, compare RPS2 and rps2-ΔN). The truncated variant was well expressed (Figure 29 B), incorporated into pre- and mature ribosomal 40S subunits (Figure 29 C) and leads to no major (pre-) rRNA processing phenotype (Figure 29 D).

Taken together, these results imply that the growth impairments under non-optimal conditions due to expression of a N-terminally truncated rpS2 variant, are not caused by a ribosome biogenesis defect. Since rpS2 is most probably involved in formation of the mRNA entry pore (see 1.5.1), the growth defects are likely a result of a negative impact by the truncation on translation fidelity.

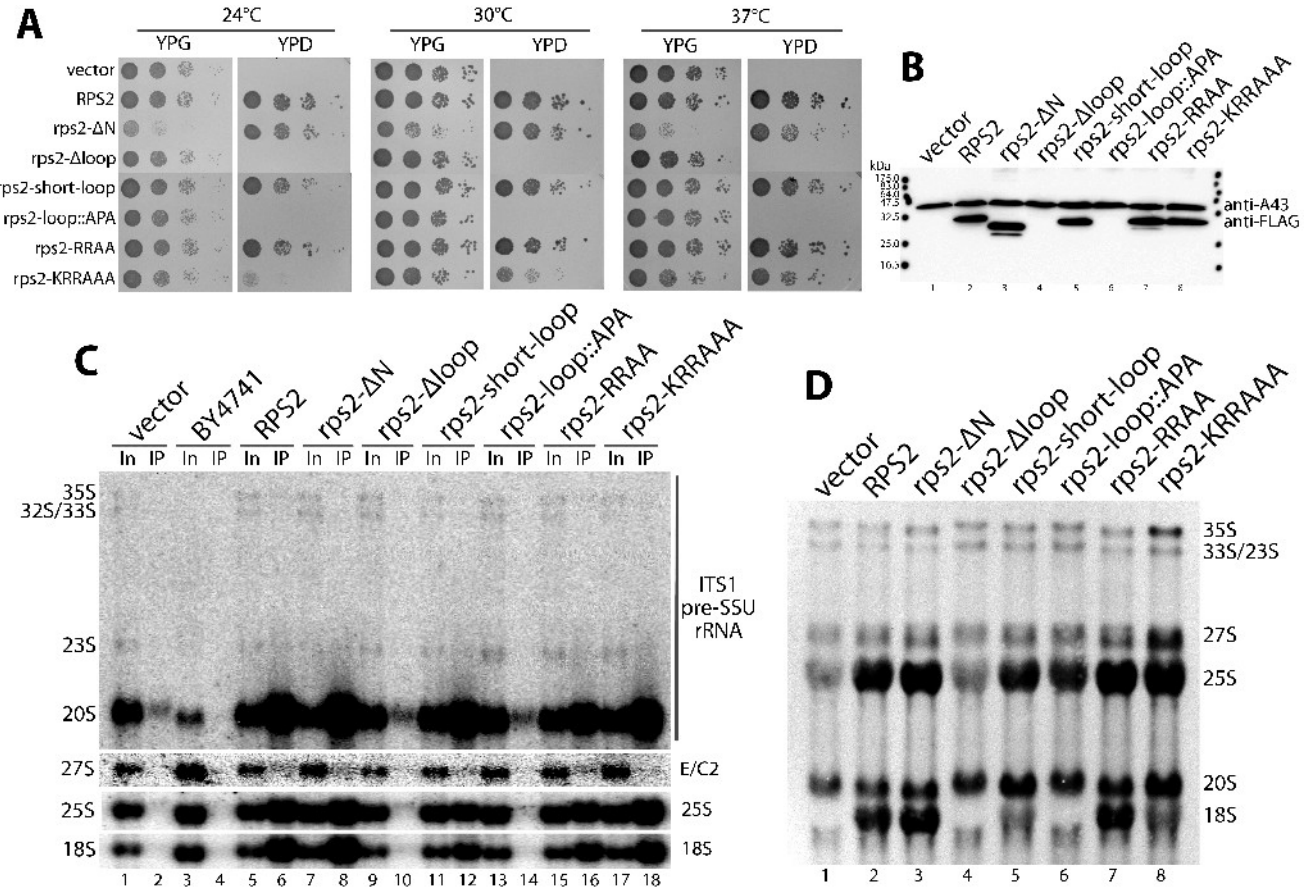

Figure 29. Growth phenotypes of rpS2 variants, expression levels, pre-rRNA processing analyses and incorporation into SSU precursors

(A)-(D) All experiments were performed in yeast strain pGAL-RPS2 (ToY286), in which full length rpS2 is encoded under the control of the galactose inducible GAL1 promoter. The strain was either transformed with an empty vector (YEplac195) or vectors coding for FLAG-tagged full length rpS2 (ToP993), rpS2-ΔN (ToP515), rpS2-Δloop (ToP1104), rpS2-short-loop (ToP1106), rpS2-loop::APA (ToP1105), rpS2-RRAA (ToP1070) or rpS2-KRRAAA (ToP1107) under the control of a constitutive promoter. (A) Serial dilutions of the indicated transformants on galactose (YPG) or glucose (YPD) containing plates. Plates were incubated for 3 days. The strain expressing FLAG-rpS2-ΔN is ToY1501, which solely depends on the FLAG-rpS2-ΔN variant to support growth. (B)-(D) Cells were grown overnight in selective media containing galactose, diluted in YP-galactose and subsequently expression of pGAL-RPS2 was shut down for 2 hours in YP-glucose medium. (B) Western blot analysis of the indicated transformants, using a monoclonal anti FLAG antibody. Anti-A43 antibodies, detecting A43 subunit of RNA polymerase I, were used as loading control. (C) Northern blot analysis of RNA co-purified with the indicated FLAG-tagged rpS2 variants. RNA was extracted from Input (In) and immuno-purified (IP) fractions. Wildtype strain BY4741 served as background control for immuno-purification. Probes used for detection of (pre-) rRNA species are depicted right-hand. 200 mM salt (KCl, see) was used for cell breakage, binding and washing of the immunoprecipitations. (D) 5',6'-[3H] uracil metabolic labeling of newly synthesized RNA. Cells were pulsed for 30 minutes at 30°C. Total RNA was extracted and separated by gel electrophoresis, radio-labeled RNA was visualized by fluorography.

2.2.3.2 The interaction of rpS2 with the head domain is required for efficient final 3'-end maturation of 18S rRNA precursors

A deletion of the complete hairpin (hereafter hairpin and loop are used as synonyms) of rpS2 (rpS2-Δloop), or replacement by an artificial sequence (rpS2-loop::APA) led to strongly reduced steady state levels of the variants (Figure 29 B). Expression of both variants didn't support growth (Figure 29 A). They were not incorporated into any ribosomal particle, nor rescued the processing phenotype defects upon rpS2 deletion (Figure 29 C and D). In the rpS2 variant termed rpS2-short-loop, two (ΔT96-R97), respectively three residues (ΔP85-Q87) between the beta sheet and the beta bridge in the hairpin were deleted (see Figure 28 C), leading to a smaller hairpin, shortened by about 5 Å. This contraction possibly affects some of the predicted interactions of rpS2, especially the ones of K88 and R95 with rRNA, by simply moving them out of reach. Although the expression of this variant supported growth after shutdown of rpS2 expression (Figure 29 A and B) and the variant was well incorporated into SSU precursors and mature ribosomes (Figure 29 C), final 3'-end maturation of 18S rRNA precursors was delayed (Figure 29 D, compare 20S to 18S in lanes 2 and 5). Mutation of the arginines R91 and R95 to alanines (rpS2-RRAA) had no effect whatsoever (Figure 29 A-D). If, based on this variant, in addition lysine K88 was mutated to alanine (rpS2-KRRAAA), meaning all potential rpS2 hairpin-rRNA contacts were mutated, 20S pre-rRNA processing was impeded (Figure 29 D, compare 20S to 18S in lanes 2 and 8) and the cells grew in a cold-sensitive manner (Figure 29 A). Nonetheless the variant was expressed and incorporated into ribosomal particles (Figure 29 B and C).

These results suggest that the interaction of the rpS2 hairpin with the head domain rRNA is important to allow efficient final 3'-end processing of 18S rRNA. A mechanism, by which the conformation of rpS2 is communicated, will be subsequently discussed (see 3.2).

2.2.3.3 Steady state distribution of SSU precursors was not altered upon expression of rpS2 variants

In vivo depletion of rpS2 impairs export of newly made pre SSUs, but doesn't alter the steady state distribution of pre-40S particles (Ferreira-Cerca et al., 2005). All of the just mentioned rpS2 variants displayed no dominant negative effect on steady state distribution of 20S containing precursor particles after shutdown of rpS2 expression. In each strain, ITS-Cy3 signals could be detected in the cytoplasm (Figure 30). Sub-cellular fractionation after metabolic labeling, which usually gives indication of export rates of newly synthesized subunits, was not conclusive with already published results, since even the expression of wildtype rpS2, due to unknown reasons, could not restore 18S production (data not shown).

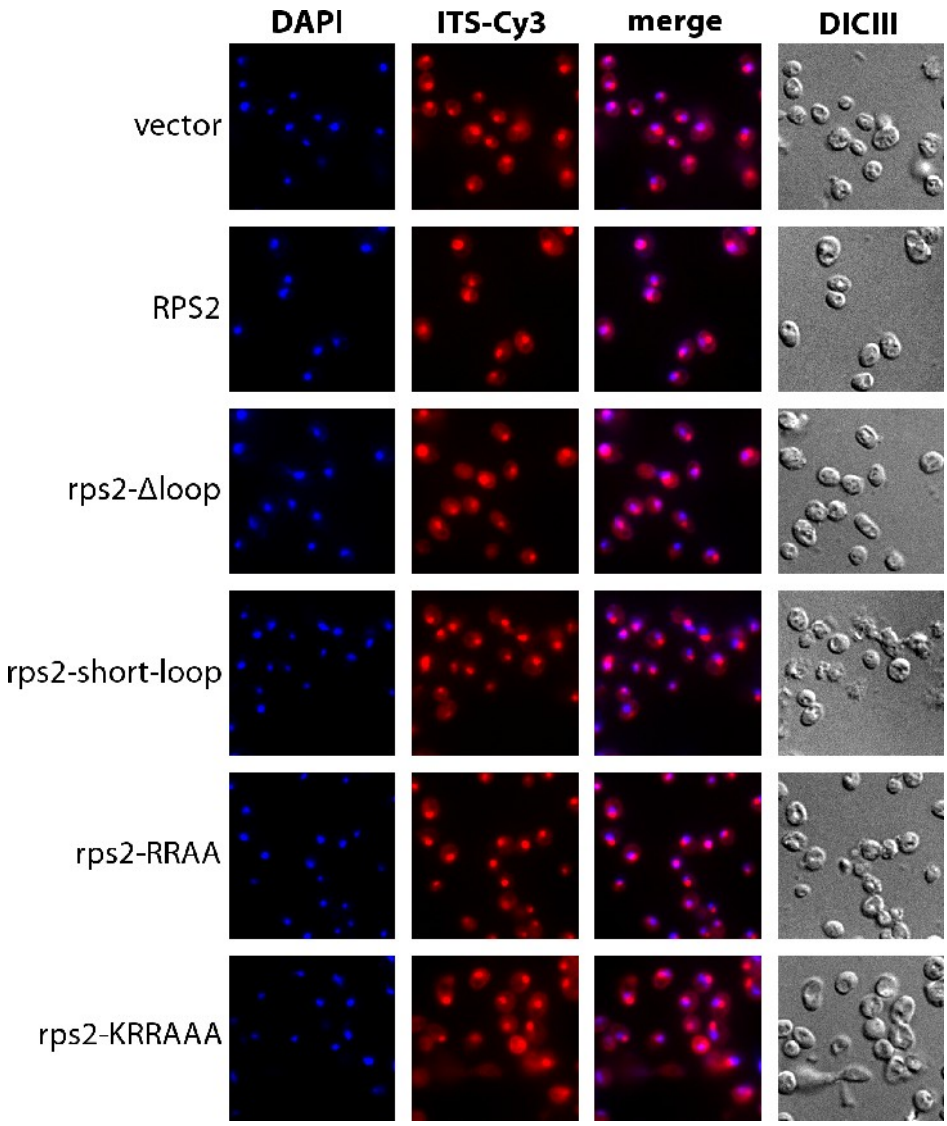

Figure 30. Analyses of nuclear export of SSU precursors containing rpS2 variants
All experiments were performed in yeast strain pGAL-RPS2 (ToY286), in which full length rpS2 is encoded under the control of the galactose inducible GAL1 promoter. The strain was either transformed with an empty vector (YEplac195) or vectors coding for FLAG-tagged full length rpS2 (ToP993), rpS2-Δloop (ToP1104), rpS2-short-loop (ToP1106), rpS2-RRAA (ToP1070) or rpS2-KRRAAA (ToP1107) under the control of a constitutive promoter.
FISH analysis of steady state distribution of precursor subunits. Cells were grown overnight in selective media containing galactose, diluted in YP-galactose and expression of pGAL-RPS2 was shut down for 2 hours in YP-glucose medium. Total DNA (DAPI) and rRNA precursors containing ITS1-sequences between site D and A2 (ITS1-Cy3) were detected as described in 5.2.6.2.

2.2.4 rpS5 and its variants

The prokaryotic homologue of rpS5 (S7) is the primary *in vitro* binder of the head domain (see 1.4.4). Consistently, *in vivo* assembly of yeast rpS5 is required for stable incorporation of other head r-proteins into precursor subunits (Ferreira-Cerca et al., 2007). Its binding site is opposite of the platform component rpS14 (see Figure 8 A and Figure 39 and discussion in 3.2). The protein itself is comprised of a triangular shaped helical domain and a long protruding hairpin. The C-terminus is pointing towards rpS14, but is not in the right conformation, according to current structure models, to interact with mature 18S rRNA (Figure 31 A and B).

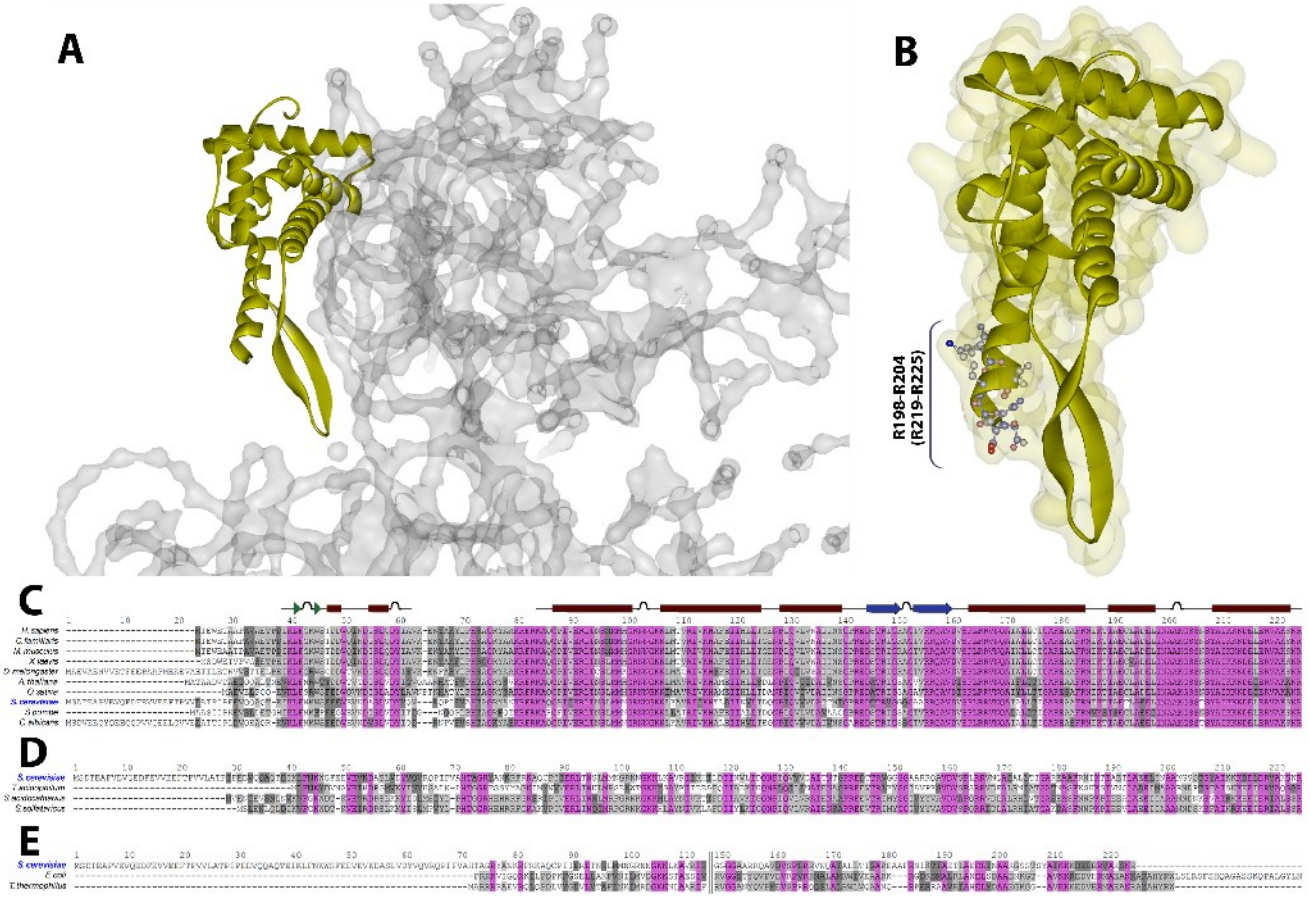

Figure 31. RpS5 localization, structure and protein sequence conservation
(**A**) Localization of rpS5 on the 40S subunit (Chandramouli et al., 2008; pdb:2ZKQ), cytoplasmic view (see also Figure 8). (**B**) Ribbon representation of rpS5 structure with the calculated surface laid underneath. Amino acids 17 to 40 and 63 to 204 of 204 in total are modeled. The highly conserved last 7 C-terminal amino acids are shown with their side chains. The position is given according to the *C. familiaris* nomenclature with *S. cerevisiae* position in brackets. (**C**) Multiple sequence alignment of yeast rpS5 primary structure (AlignX, Vector NTI, Invitrogen, ClustalW algorithm and blosum score-matrix). Protein sequences of representative eukaryotic organisms are shown (sequences were obtained from NCBI (http://www.ncbi.nlm.nih.gov/protein)). The predicted secondary structure elements (Chandramouli et al., 2008) are shown on top (blue arrows indicate part of a beta sheet; green triangles are residues in an isolated beta-bridge; brown rectangle indicate an alpha helix; black semicircles are hydrogen bonded turns). (**D**) Multiple sequence alignment of yeast rpS5 primary structure with representative archaeal homologues. (**E**) Multiple sequence alignment of yeast rpS5 primary structure with representative bacterial homologues. (**C**)-(**E**) The color code illustrates amino acid conservation: identical - purple; conserved – gray; block of similar – dark-gray. The numbers give the positions of *S. cerevisiae* amino acids.

As known from analyses of S7, the prokaryotic homologue of rpS5, most of the protein-rRNA interactions are mediated by the triangular shaped helical domain, while the protruding hairpin is mainly required for tRNA orientation at the E-site (Döring et al., 1994). Crosslinking studies suggested that both, S7 and rpS5 are part of the mRNA channel (Dontsova et al., 1991; Brandt and Gualerzi, 1992; Pisarev et al., 2006, 2008a). The primary sequence of rpS5 is well conserved in Archaea (Figure 31 D). When compared to bacteria (Figure 31 E), it is obvious that the N-terminus of rpS5 is specific to eukaryotes and only to some extent conserved in Archaea (see Figure 31 D). A characteristic C-terminal extension of varying length is only found in Bacteria (Figure 31 E, starting after yeast R225). It was proposed that this C-terminal extension stabilizes the orientation of the S7 hairpin towards the helical domain (Brodersen et al., 2002) and that this extension in addition contacts S11 (rpS14) in Bacteria (Robert et al., 2003).

In vivo depletion of yeast rpS5 results in a very strong A_0, A_1, A_2 processing delay and hardly any detectable newly synthesized 20S pre-rRNA. Pre-40S subunit precursor become trapped in the nucleus (Ferreira-Cerca et al., 2005). In addition, as mentioned above, stable head domain assembly of other r-proteins is massively perturbed upon rpS5 depletion (Ferreira-Cerca et al., 2007).

name	background	mutation	database (ToP)
rpS5	*S. cerevisiae* full length allele (wildtype)	-/-	Nt-FLAG: 996 Nt-HA : 1162
rpS5-ΔN	deletion of eukaryotic specific N-terminus	ΔM1-K41	Nt-FLAG: 572
rpS5-ΔC	deletion of highly conserved C-terminus	ΔR219-R225	Nt-FLAG: 1101 Nt-HA : 1156
rpS5-Δloop	alteration of r-protein fold; only globular domain left by deletion of hairpin	ΔR143-V162	Nt-FLAG: 1098 Nt-HA : 1157
rpS5-short-loop	alteration of r-protein fold; only globular domain left by shortening of hairpin	ΔR143-G151 and ΔA154-V162	Nt-FLAG: 1099 Nt-HA : 1158

Table 10. List of rpS5 variants

2.2.4.1 Deletion of the eukaryotic specific N-terminal part did not affect essential functions of rpS5 in vivo

RpS5 was N-terminally truncated by 41 amino acids (M1 to K41, rpS5-ΔN), to create a variant in which only the conserved part between Archaea and Eukarya is left (Figure 31 C and D). This truncated protein was still able to adopt all the essential roles of full length rpS5 in ribosome biogenesis and function (Figure 32 A). The variant was well expressed (Figure 32 B), efficiently incorporated into precursor and mature ribosomes (Figure 32 C) and its expression led to no major rRNA processing defect (Figure 32 D, compare lanes 2 and 3). Since the N-terminal part is only weakly conserved, even between eukaryotes (Figure 31 C), it is therefore hardly surprising that it has no essential function. A recent report argues that some other N-terminally truncated rpS5 variants, although able to complement all essential

functions of full length rpS5, have minor effects on translation, in particular translation initiation and initiation factor binding (Lumsden et al., 2009).

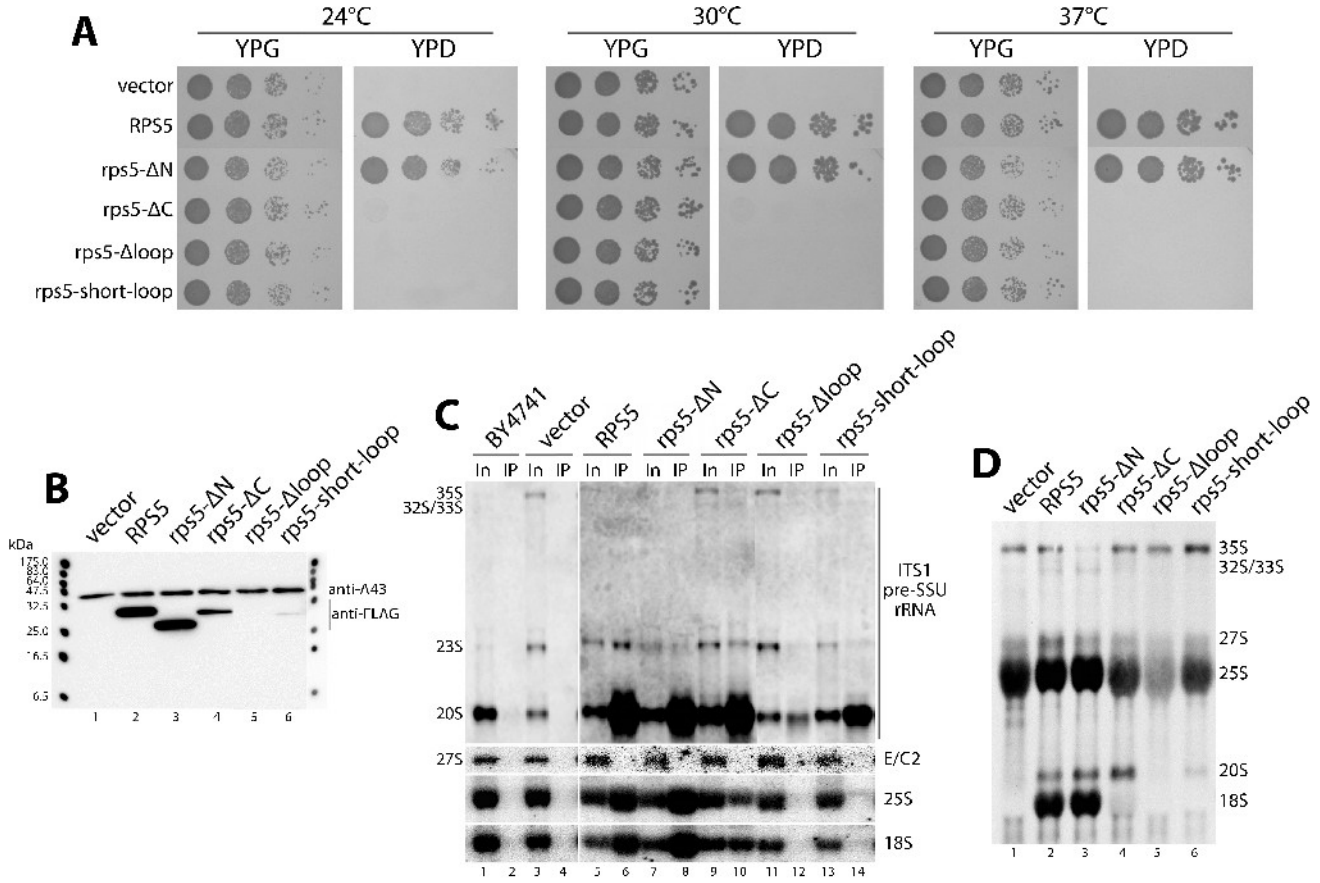

Figure 32. Growth phenotypes of rpS5 variants, expression levels, pre-rRNA processing analyses and incorporation into SSU precursors

(**A**)-(**D**) All experiments were performed in yeast strain pGAL-RPS5 (ToY323), in which full length rpS5 is encoded under the control of the galactose inducible GAL1 promoter. The strain was either transformed with an empty vector (YEplac195) or vectors coding for FLAG-tagged full length rpS5 (ToP996), rpS5-ΔN (ToP572), rpS5-ΔC (ToP1101), rpS5-Δloop (ToP1098) or rpS5-short-loop (ToP1099) under the control of a constitutive promoter. (**A**) Serial dilutions of the indicated transformants on galactose (YPG) or glucose (YPD) containing plates. Plates were incubated for 3 days. (**B**)-(**D**) Cells were grown overnight in selective media containing galactose, diluted in YP-galactose and subsequently expression of pGAL-RPS5 was shut down for 2 hours in YP-glucose medium. (**B**) Western blot analysis of the indicated transformants, using a monoclonal anti FLAG antibody. Anti-A43 antibodies, detecting A43 subunit of RNA polymerase I, were used as loading control. (**C**) Northern blot analysis of RNA co-purified with the indicated FLAG-tagged rpS5 variants. RNA was extracted from Input (In) and immuno-purified (IP) fractions. Wildtype strain BY4741 served as background control for immuno-purification. Probes used for detection of (pre-) rRNA species are depicted right-hand. 200 mM salt (KCl, see 5.2.5.3) was used for cell breakage, binding and washing of the immunoprecipitations. (**D**) 5',6'-[^{3}H] uracil metabolic labeling of newly synthesized RNA. Cells were pulsed for 30 minutes at 30°C. Total RNA was extracted and separated by gel electrophoresis, radio-labeled RNA was visualized by fluorography.

2.2.4.2 The molecular structure of the rpS5 hairpin is essential for stable incorporation of rpS5 into pre-40S subunits

As previously mentioned, rpS5 is composed of a globular folded domain and a long protruding hairpin (see Figure 31 A and B) (hereafter hairpin and loop are used as synonyms). A variant lacking this loop (rpS5-Δloop) was not able to complement the growth phenotype of the conditional pGAL-RPS5 strain (Figure 32 A). The steady state protein levels

of this variant were below the detection limit (Figure 32 B, lane 5). Thus rpS5-Δloop mimicked the depletion phenotype of rpS5 regarding rRNA processing defects (Figure 32 D, compare lanes 1 and 5) and RNA co-immunoprecipitation showed only minor interaction of rpS5-Δloop with 20S pre-rRNA containing SSU precursors (Figure 32 C, see lane 12).

In contrast to the complete deletion of the hairpin, a deletion of the hairpin's branches (see Table 10, rpS5-short-loop), possibly better preserving the overall protein structure, resulted in slight production of 20S pre-rRNA (Figure 32 D, lane 6) and higher accumulation of steady state 20S pre-rRNA levels (Figure 32 C, lanes 11 and 13). The variant rpS5-short-loop was poorly expressed (Figure 32 B), yet it precipitated 20S pre-rRNA in good amounts (Figure 32 C). Although the variant was incorporated into pre-40S particles, it didn't assemble into mature ribosomes (Figure 32 C, compare 25S and 18S vs. 20S co-precipitation).

2.2.4.3 The C-terminal seven amino acids of rpS5 are specifically required for efficient final 3' end maturation of 18S rRNA precursors

A highly conserved part of rpS5 is its C-terminal helix (see Figure 31 C). Truncation of the seven C-terminal amino acids (R219 to R225, rpS5-ΔC) moderately decreased the expression level of the variant (Figure 32 B) and the variant was still efficiently incorporated into 40S precursor particles at almost the same level as the full length protein (Figure 32 C, see ITS1 probe, compare lanes 6 and 10). But rpS5-ΔC was apparently less well incorporated into 18S rRNA containing mature ribosomes than full length rpS5 (Figure 32 C, compare 18S and 25S levels in lanes 6 and 10). Expression of the rpS5-ΔC variant led to efficient production of 20S pre-rRNA after shutdown of full length rpS5 expression (Figure 32 D), clearly abrogating the A_0, A_1, A_2 processing defects seen when wildtype rpS5 is missing. On the other hand, the newly produced 20S pre-rRNA was not efficiently converted into mature 18S rRNA (Figure 32 D, compare lanes 2 and 4, 20S and 18S).

In addition, steady state levels of 20S pre-rRNA, which was produced upon rpS5-ΔC expression, slightly accumulated compared to 20S levels in wildtype situation (see Figure 31 C, lanes 5 and 9, 20S and Figure 32 D, lanes 2 and 4, 20S). Accordingly, the C-terminal 7 amino acids of rpS5 seem to be required for the efficient endonucleolytic cleavage at site D, converting 20S pre-rRNA into mature 18S rRNA.

2.2.4.4 Nuclear export of SSU precursor particles was partially restored upon expression of some rpS5 variants

In cells depleted for rpS5, a probe against the ITS1 sequences, hybridizing with 20S pre-rRNA and its precursors, detected strictly nucleolar and nuclear signals indicating nuclear retention of SSU precursors (Figure 33 A, vector). Steady state analysis of (pre-) rRNA distribution in sub-cellular fractionation indicated the same strong nuclear export delay (Figure 33 B, vector). The 20S pre-rRNA amount in the cytoplasmic fraction was at the same level as the 35S pre-rRNA amounts (Figure 33 B, lane 2), both most probably derived from nuclei broken up during the experimental procedure. Expression of the variant rpS5-Δloop led

to no obvious nuclear export of precursor subunits (Figure 33, rpS5-Δloop), resembling the phenotype observed upon rpS5 depletion.

Expression of full length rpS5 and its variants rpS5-ΔC as well as rpS5-short-loop resulted in readily detectable additional cytoplasmic ITS1 signals (Figure 33 A), indicating that SSU precursors reach the cytoplasmic compartment in these strains. Expression of rpS5-ΔC led to an even stronger cytoplasmic ITS1 signal than expression of full length rpS5 (Figure 33 A, see also 20S levels in Figure 32 C, lanes 5 and 9), which might correlate with a reduced rate

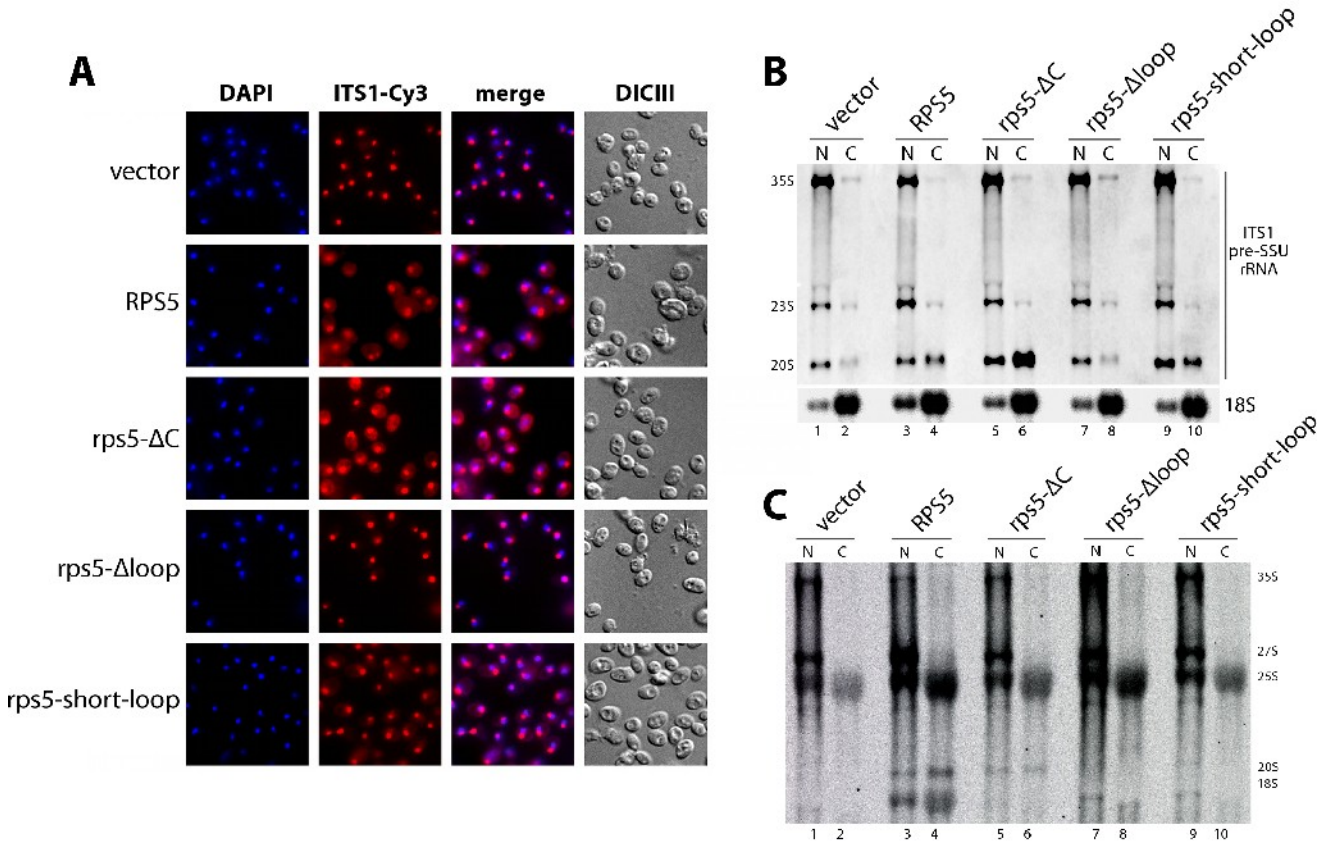

Figure 33. Analyses of nuclear export of SSU precursors containing rpS5 variants
(**A**)-(**C**) All experiments were performed in yeast strain pGAL-RPS5 (ToY323), in which full length rpS5 is encoded under the control of the galactose inducible GAL1 promoter. The strain was either transformed with an empty vector (YEplac195) or vectors coding for FLAG-tagged full length rpS5 (ToP996), rpS5-ΔC (ToP1101), rpS5-Δloop (ToP1098) or rpS5-short-loop (ToP1099) under the control of a constitutive promoter. (**A**) FISH analysis of steady state distribution of precursor subunits. Cells were grown overnight in selective media containing galactose, diluted in YP-galactose and expression of pGAL-RPS5 was shut down for 2 hours in YP-glucose medium. Total DNA (DAPI) and rRNA precursors containing ITS1-sequences between site D and A2 (ITS1-Cy3) were detected as described in 5.2.6.2. (**B**) Steady state analysis of pre-rRNA in sub-cellular fractions. Cells were grown overnight in selective media containing galactose, diluted in YP-galactose (YPG) and expression of pGAL-RPS5 was shut down for 1.5 hours in YPD before starting with the fractionation protocol (see 5.2.5.5). Cells were spheroplasted and subsequently fractionated in nuclei (N) and cytoplasm (C). RNA was extracted and 2.4 times more volume of nuclear than cytoplasmic fractions were separated by gel electrophoresis and analyzed by northern blotting. Probes for detection of rRNA species are depicted right-hand. (**C**) Cell fractionation after metabolic RNA labeling. Cells were grown overnight in in YP-galactose media, diluted in YP-galactose, spheroplasted and expression of pGAL-RPS5 was shut down. Newly synthesized RNA was labeled with 5',6'-[^{3}H] uracil for 20 minutes. Nuclear (N) and cytoplasmic (C) cellular fractions were subsequently separated, RNA was extracted, separated by gel electrophoresis and newly synthesized RNA was visualized by fluorography. Same volume percentage of nuclear and cytoplasmic fractions were loaded on the gel.

in the conversion of 20S pre-rRNA to mature 18S rRNA. The cytoplasmic signal intensity for ITS1 containing precursor particles in the strain expressing rpS5-short-loop rather resembles those of full length rpS5 (Figure 33 A), reflecting also the minor production or degradation of 20S pre-rRNA (Figure 32 C, compare 20S levels in lanes 5, 9 and 13). Steady state analysis of (pre-) rRNA distribution in sub-cellular fractions confirmed these results (Figure 32 B).

Expression of the variant rpS5-ΔC led to increased amounts of 20S pre-rRNA in the cytoplasmic fraction, compared to those of full length rpS5, in which processing of 20S to 18S was still going on (Figure 33 B, compare lanes 4 and 6). Expression of the variant rpS5-short-loop displayed an intermediate pre-SSU distribution in nuclear and cytoplasmic fractions (Figure 33 B, compare lanes 4, 6 and 10).

Cell fractionation after metabolic RNA labeling was used to more directly assess the dynamics of nuclear export of newly synthesized SSU precursors. In agreement with the FISH analyses and sub-cellular fractionation experiments, no cytoplasmic accumulation of newly synthesized 18S rRNA or its precursors was detectable, when full length rpS5 was depleted. Only negligible amounts of nascent nuclear 20S pre-rRNA could be detected (Figure 33 D, vector). In contrast, in both strains expressing either rpS5 or its variant rpS5-ΔC, newly synthesized 20S-pre-rRNA reached the cytoplasm (Figure 33 D, lanes 4 and 6). In agreement with the previous pulse experiments (see Figure 32 D), newly synthesized cytoplasmic 20S pre-rRNA was only efficiently converted into 18S rRNA when rpS5, however not rpS5-ΔC was expressed. In addition, while rpS5-ΔC clearly supported nuclear export of newly synthesized SSU precursors, the low ratio of nascent cytoplasmic versus nuclear SSU (pre-) rRNAs argues that its incorporation in SSU precursors leads either to a delay in nucleo-cytoplasmic transport or to a distinct cytoplasmic destabilization of SSU precursors. This delay/destabilization was even more evident in the strain expressing the variant rpS5-short-loop. While newly synthesized nuclear 20S pre-rRNA could be observed, 20S was hardly detectable in the cytoplasmic fraction (Figure 33 D, lanes 9 and 10).

RpS5 without its shortened hairpin was sufficient to allow slight production of 20S pre-rRNA and minor nuclear export of pre-40S particles (Figure 32 and Figure 33, rpS5-short-loop). The last seven amino acids of rpS5 were not strictly required to form export competent precursor SSUs, containing 20S pre-rRNA. Instead their absence only slightly decelerated the export kinetics of nuclear-cytoplasmic transport, but almost completely blocked 18S rRNA 3'-end maturation (Figure 32 and Figure 33, rpS5-ΔC).

2.2.4.5 The correct molecular structure of the rpS5 hairpin is required for stable assembly of some head domain r-proteins

Similar to what was previously observed in *in vitro* reconstitution experiments with prokaryotic SSU components, in *S. cerevisiae,* rpS5 is required for stable incorporation of many ribosomal proteins located in the SSU head domain (Ferreira-Cerca et al., 2007). Establishment of a robust head domain assembly status correlated with efficient cytoplasmic

accumulation of SSU precursors, at the same time several r-proteins of the head domain are specifically required for cytoplasmic conversion of 20S pre-rRNA into 18S rRNA.

Expression of the rpS5-short-loop variant resulted in a 20S pre-rRNA containing precursor particles, which further on were exported, though with apparently strongly reduced efficiency (see 2.2.4.2 and 2.2.4.4). It was speculated before that a well assembled SSU head domain is a prerequisite for efficient nuclear export. To analyze the assembly status of nascent SSUs, FLAG-epitope affinity purifications of ectopically co-expressed functional FLAG-fusion alleles of various small ribosomal subunit proteins, in the absence of rpS5 or presence of rpS5 variants, were performed. The amount of pre-rRNA co-purifying with FLAG-tagged ribosomal proteins was compared before or after shut down of GAL1-promoter driven RPS5 expression for two hours.

As previously observed (Figure 32 C, lane 3), *in vivo* depletion of rpS5 led to some accumulation of 23S rRNA and to a reduction of 20S pre-rRNA steady state levels, caused by a delay, but not complete block of endonucleolytic cleavages at sites A_0, A_1 and A_2 (Figure 34 A, vector, compare input lanes in “on” and “off” conditions). Flag-tagged r-proteins co-purified 20S pre-rRNA with similar efficiency as mature 18S rRNA when rpS5 was present (Figure 34 A, vector, compare input and IP in “on” condition). Upon rpS5 depletion the ratio of 20S pre-rRNA to 18S rRNA co-purifying with Flag-tagged SSU head domain r-proteins (rpS3, rpS15, rpS16, rpS19, rpS20 and rpS29) including rpS10 and rpS28, which presumably bind in the head domain, strongly decreased (Figure 34 A, vector; quantified in Figure 34 B, vector). This decrease confirmed the dependencies of stable incorporation into nascent SSU of these r-proteins on the *in vivo* assembly of rpS5. On the other hand, the stable assembly of the platform component rpS14 was independent on the presence of rpS5 (Figure 34).

Expression of the variant rpS5-short-loop led to stabilized incorporation of a subset of r-proteins (Figure 34, rpS10, rpS19, rpS20 and rpS29) into pre-SSUs. The incorporation of the other analyzed r-proteins remained largely destabilized (Figure 34, rpS3, rpS15, rpS16 and rpS28). All in all, the full length hairpin of rpS5 is not strictly required for production of 20S pre-rRNA or nuclear export of SSU precursor particles, but through the deletion, both processes occur with strongly decreased efficiency.

2.2.4.6 The C-terminal seven amino acids of rpS5 have minor impact on the SSU head domain r-protein assembly status

Remarkably, the assembly phenotypes of most of the r-proteins observed upon depletion of rpS5 were largely relieved by expression of rpS5-ΔC (Figure 34 A, rpS5-ΔC; quantified in Figure 34 B, rpS5-ΔC). Interestingly, the assembly phenotype of Flag-tagged rpS28 was only slightly suppressed. In conclusion, the last C-terminal seven amino acids of rpS5 seem to have minor impact on global SSU head domain assembly events. They are not strictly required for rpS5 function in nuclear export of SSU precursors, but are crucial for final cytoplasmic 3’ maturation of pre-18S rRNAs.

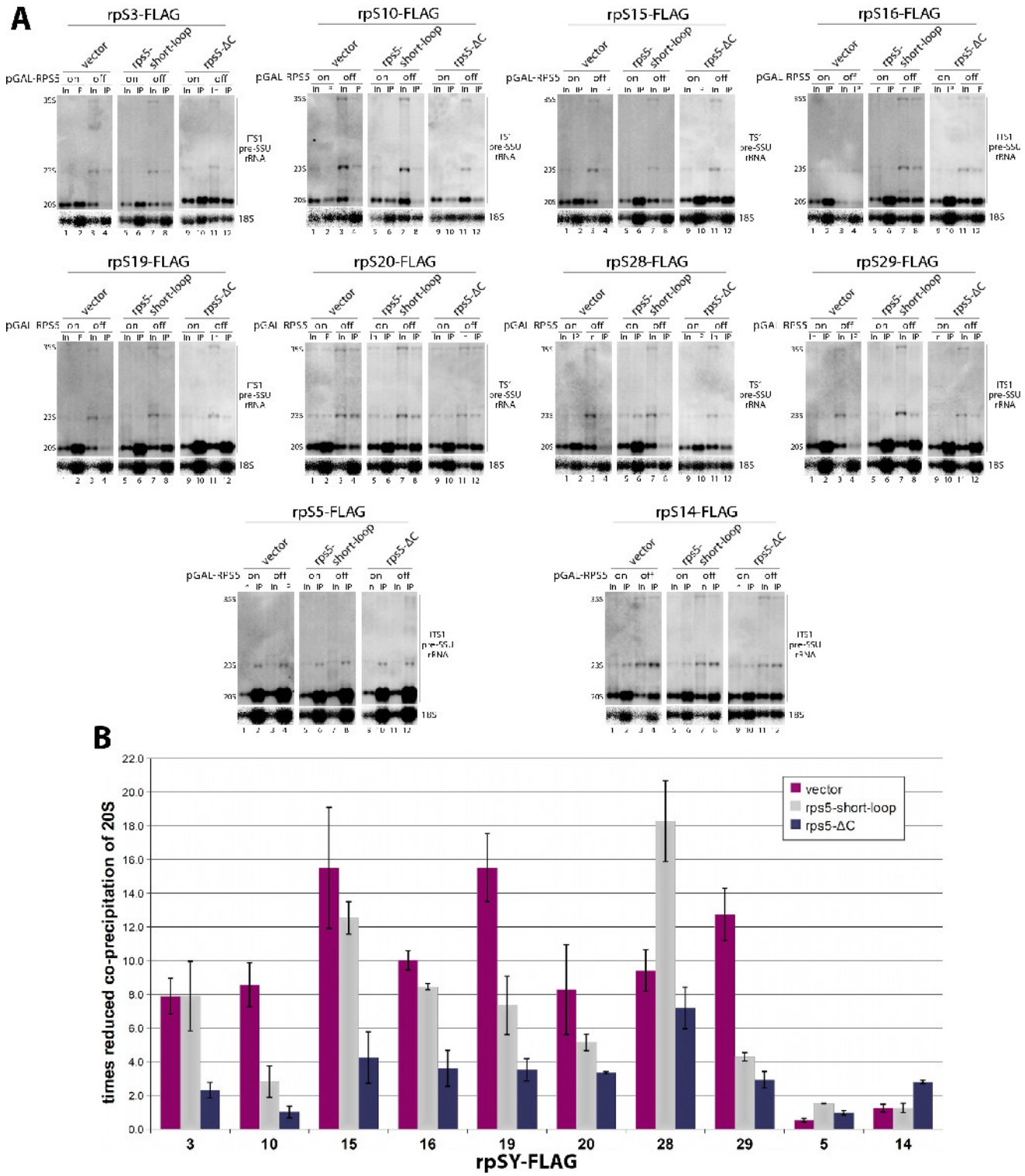

Figure 34. Analysis of r-protein interactions with SSU precursors containing rpS5 variants

(**A**) Northern blot analysis of SSU (pre-) RNA co-purifying with the FLAG-tagged r-proteins in precursors containing rpS5 variants. All experiments were performed in yeast strain ToY1659, in which full length rpS5 is encoded under the control of the galactose inducible GAL1 promoter. The strain was transformed with vectors supporting the constitutive expression of indicated FLAG-tagged r-proteins and in addition, with an empty vector (YEplac181) or vectors coding for HA-tagged rpS5-ΔC (ToP1156) or rpS5-short-loop (ToP1158) under the control of a constitutive promoter. Transformants were grown overnight in selective media containing galactose and on the next day diluted in YP-galactose medium. The cultures were split, one half was further grown in YP-galactose (on, wildtype rpS5 is expressed), in the other half of the culture expression of pGAL-RPS5 was shut down for 2 hours in YP-glucose medium (off). 200 mM salt (KCl, see 5.2.5.3) was used for cell breakage, binding and washing of the

immunoprecipitations. RNA was extracted from Input (In) and immuno-purified (IP) fractions. Probes used for detection of (pre-) rRNA species are depicted right-hand. (**B**) Quantification of r-protein interaction with SSU precursors containing rpS5-ΔC, rpS5-short-loop or no rpS5 (vector). Each data point was derived from 2 biological replicates (representative Northern blot shown in (**A**)). The factor of reduced 20S pre-rRNA co-precipitation was calculated as follows: (%IP20S / %IP18S)**on** / (%IP20S / %IP18S)**off**. Quantification was done, using LAS3000, FLA3000 and MultiGauge software (FujiFilm).

2.2.4.7 Nob1p and other factors required for final 3'-end maturation of pre-18S rRNA were present in SSU precursor particles containing rpS5-ΔC or rpS5-short-loop

Many r-proteins and several biogenesis factors, including Nob1p, the putative endonuclease, mediating final 3'-end 18S maturation, are needed to allow cytoplasmic 18S rRNA 3'-end maturation (see 1.4.2). Since both rpS5 variants, rpS5-ΔC and rpS5-short-loop gave rise to cytoplasmic, 20S pre-rRNA containing pre-SSU particles, the question arose, whether Nob1p and other ribosome biogenesis factors are still incorporated into these nascent 40S subunits.

By precipitation of the FLAG-tagged rpS5 variants, it was possible to purify associated RNPs and to analyze the protein content of these particles. The associated proteins were eluted, digested with trypsin and identified by mass spectrometry (see 5.2.7.1 and 5.2.7.2). The identified SSU biogenesis factors are listed in Table 11 and Table 12 (for the complete list, including factor description see Fehler: Referenz nicht gefunden and Supplemental Table 2). Many biogenesis factors, which are specifically required for late cytoplasmic maturation of pre-40S subunits, in particular Nob1p, the putative endonuclease mediating the 18S rRNA 3’-end processing, were identified in the affinity purified particles.

To compare the protein contents of SSU precursor particles, which incorporated either wildtype rpS5 or one of its variants, a quantitative mass spectrometry approach was used (iTRAQ®, Applied Biosystems). The pre-SSUs were purified via TAP-tagged Rio2p in the corresponding yeast strains. Rio2p is a component of cytoplasmic pre-40S subunits (Vanrobays et al., 2003), and still strongly interacted with 20S pre-rRNA after shutdown of rpS5 expression, in the yeast strains constitutive expressing HA-tagged rpS5, rpS5-ΔC or rpS5-short-loop (Figure 35 B, for detailed analysis and verification of the phenotypes of the HA-tagged variants, see Supplemental Figure 1). The associated proteins were digested with trypsin, labeled with the iTRAQ reagents and analyzed by mass spectrometry (MALDI TOF/TOF).

Early acting biogenesis factors, like components of the SSU processome (Nop58p, Nop1p, Utp6p, Krr1p, Snu13p) and a H/ACA-type snoRNP associated protein (Nop10p), were highly enriched in the Rio2p-TAP purification in the strain expressing rpS5-ΔC compared to the purification in the strain expressing rpS5 (Figure 35 A). These data suggest that due to truncation of the last seven amino acids of rpS5, a larger population of Rio2p-TAP associated RNPs is decorated with early biogenesis factors, probably because of delayed pre-rRNA processing or nuclear export kinetics.

protein	peptides	total ion score %
Arb1p	3	100
Bfr2p	1	79.4
Bms1p	2	100
Dbp2p	9	100
Dim1p	1	99.8
Ecm16p (Dhr1p)	1	94.4
Enp1p	2	100
Kre33p	2	100
Kri1p	1	92.5
Krr1p	2	100
Ltv1p	5	100
Mrt4p	2	100
Nob1p	2	100
Nop1p	1	96.1
Nop56p (Sik1p)	1	90
Nop58p (Nop5p)	1	100
Pno1p (Dim2p)	2	100
Prp43p	2	100
Rio2p	2	100
Sof1p	1	100
Tsr1p	4	100
Utp2p (Noc5p)	1	100
Utp12p (Dip2p)	1	96.7
Utp14p	1	100
Utp15p	1	95.5
Utp21p	1	100
Utp22p	2	100

Table 11. FLAG-rpS5-ΔC associated SSU biogenesis factors

protein	peptides	total ion score %
Arb1p	1	100
Enp1p	7	100
Ltv1p	4	100
Nob1p	3	100
Nop58p (Nop5p)	1	99.5
Rio2p	3	100
Tsr1p	4	100

Table 12. FLAG-rpS5-short-loop associated SSU biogenesis factors

Nevertheless the majority of co-purified particles was by all means of cytoplasmic nature (compare peptide numbers in Figure 35 A). Virtually all known late biogenesis factors, which are required for late pre-SSU maturation, were identified in the strain expressing rpS5-ΔC (Figure 35 A), confirming the analysis of FLAG-purified RNPs (see Table 11). Only relatively minor (less than 50%) differences in the amounts of individual tryptic peptides of Nob1p and other ribosome biogenesis factors co-purifying with Rio2p-RNPs could be observed.

Altogether these data indicate that the analyzed biogenesis factors, in particular Nob1p, can interact with rpS5-ΔC containing SSU precursors. As mentioned before, yeast Nob1p harbors presumably the endonuclease activity converting 20S pre-rRNA into 18S rRNA. Accordingly, these results support the assumption that the poor efficiency of pre-18S rRNA maturation in rpS5-ΔC containing SSU precursors is not due to the absence of the endonuclease Nob1p.

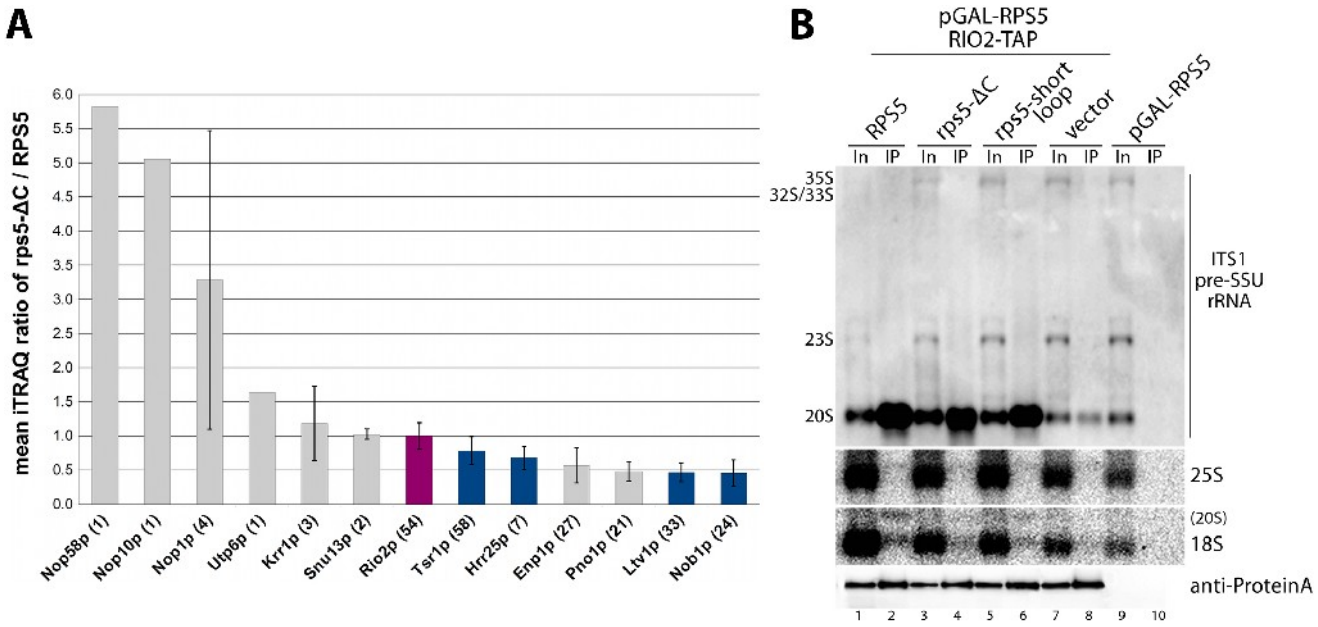

Figure 35. Analyses of the protein composition of SSU precursors containing rpS5-ΔC
(**A**) and (**B**) All experiments were performed in yeast strain ToY1739, in which full length rpS5 is encoded under the control of the galactose inducible GAL1 promoter and Rio2p is TAP-tagged. The strain was transformed with vectors supporting the constitutive expression of HA-tagged full length rpS5 (ToP1162) or rpS5-ΔC (ToP1156) and in (**B**) additional with an empty vector (YEplac181) and HA-tagged, constitutive expressed rpS5-Δloop (ToP1157) or rpS5-short-loop (ToP1158). Cells were grown overnight in selective media, diluted in YP-galactose and expression of pGAL-RPS5 was shut down for 2 hours in YP-glucose medium. (**A**) Analysis of biogenesis factors co-purified with Rio2p-TAP associated SSU precursors. Rio2p-TAP associated SSU precursors were affinity purified from both transformants and their protein composition was compared in a semi-quantitative way using the iTRAQ method as described in 5.2.7.1 and 5.2.7.3. The mean values (normalized to the Rio2p iTRAQ ratio) and standard deviations of three independent biological replicates (five technical replicates) are shown. The number of tryptic peptides for each protein is given in brackets after the protein name. Color code: magenta – Rio2p-TAP bait protein; dark-blue – biogenesis factors involved in 20S pre-rRNA containing precursor maturation. (**B**) Rio2p-TAP was affinity purified and SSU pre-rRNA contained in Input (In) and immuno-purified (IP) fractions was analyzed by Northern blotting. Probes used for detection of (pre-) rRNA species are depicted right-hand.

The same observations were true for the rpS5-short-loop containing pre-40S subunits. Rio2p-TAP purifications in this strain showed enrichment of a SSU processome component, compared to the Rio2p-TAP purification in the strain expressing rpS5 (Figure 36, Krr1p). This again argues for a larger nuclear population of Rio2p-TAP containing RNPs. Many late acting biogenesis factors, including Nob1p, were purified with similar efficiencies (less than 50% difference) in both strains (Figure 36).

Both variants, rpS5-short-loop and in particular rpS5-ΔC support the formation of a cytoplasmic 20S pre-rRNA containing particle, which is mostly assembled with head domain r-proteins and late acting biogenesis factors. Possible explanations, why final 18S 3'-end maturation after all is not occurring in both strains, will be discussed later (see 3.2).

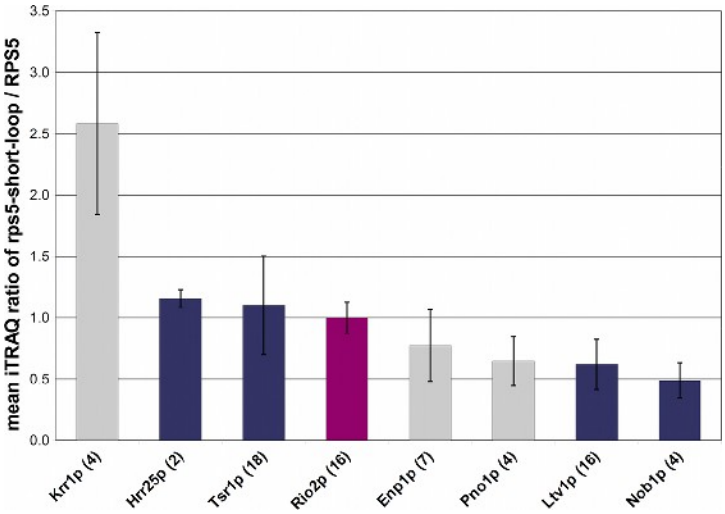

Figure 36. Analyses of the protein composition of SSU precursors containing rpS5-short-loop
All experiments were performed in yeast strain ToY1739, in which full length rpS5 is encoded under the control of the galactose inducible GAL1 promoter and Rio2p is TAP-tagged. The strain was transformed with vectors supporting the constitutive expression of HA-tagged full length rpS5 (ToP1162) or rpS5-short-loop (ToP1158). Cells were grown overnight in selective media, diluted in YP-galactose and expression of pGAL-RPS5 was shut down for 2 hours in YP-glucose medium. Rio2p-TAP associated SSU precursors were affinity purified from both transformants and their protein composition was compared in a semi-quantitative way using the iTRAQ method as described in 5.2.7.1 and 5.2.7.3. The mean values (normalized to the Rio2p iTRAQ ratio) and standard deviations of two independent biological replicates are shown. The number of tryptic peptides for each protein is given in brackets after the protein name. Color code: magenta – Rio2p-TAP bait protein; dark-blue – biogenesis factors involved in 20S pre-rRNA containing precursor maturation.

2.2.4.8 Polysome profiles of strains expressing rpS5-ΔC, full length rpS5 or no rpS5

A recent publication suggested that "immature small ribosomal subunits can engage in translation initiation in *Saccharomyces cerevisiae*". It was shown that a sub-population of 20S pre-rRNA containing pre-40S subunits co-sedimented with translating ribosomes, even in wildtype conditions. Inhibition of D-site cut processing led to a shift of the major population of cytoplasmic 20S pre-rRNA, now co-sedimenting mainly with 80S ribosomes, but also with polysomes (Soudet et al., 2010).

Expression of full length rpS5 after 2 hours shutdown of pGAL-RPS5 rescued the 60S accumulation seen upon rpS5 depletion (Figure 37 A), but still a relatively large amount of free subunits was visible when compared to wildtype (Figure 37 B and data not shown). In addition 20S pre-rRNA co-sedimented in large amounts in the range of 60S to 80S particles (Figure 37 B, 20S in fractions 5 to 10).

Depletion of rpS5 resulted in strongly decreased levels of nuclear restricted 20S pre-rRNA. This in conclusion led to a drastic drop of mature 40S subunits and therefore to a relative accumulation of free 60S subunits (Ferreira-Cerca et al., 2005) (see also Figure 37 A). The remaining 20S pre-rRNA peaked at fraction 7, which is about the size of a 60S or 70S particle (Figure 37 A).

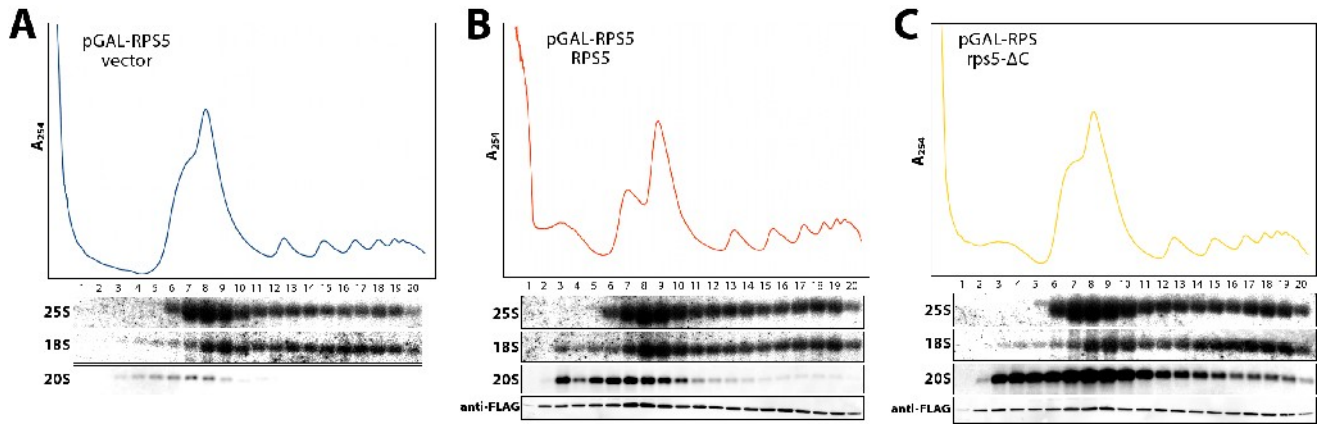

Figure 37. Polysome profiles of strains expressing rpS5 variants

(**A**)-(**C**) Polysome profiles were performed as described in 5.2.5.6. RNA and Proteins were extracted from the fractions, same volume percentage of fractions was loaded on the gels and analyzed by Northern or Western blotting. Probes used for detection of (pre-) rRNA species are depicted left-hand. Cycloheximide was added in all experiments. Yeast strain pGAL-RPS5 (ToY323), in which full length rpS5 is encoded under the control of the galactose inducible GAL1 promoter was either transformed with an empty vector (YEplac195) or vectors coding for FLAG-tagged full length rpS5 (ToP996) or rpS5-ΔC (ToP1101) under the control of a constitutive promoter. Cells were grown overnight in selective media containing galactose, diluted in YP-galactose and expression of pGAL-RPS5 was shut down for 2 hours in YP-glucose medium.

This particle might be a transition state from 90S to 43S pre-ribosomes, a 20S pre-rRNA trapped by a degradation machinery like e.g. the TRAMP-complex and the exosome (see 1.4.6) or a 43S pre-ribosome dimer, which might form under the salt conditions used.

Upon expression of the rpS5-ΔC variant, 20S pre-rRNA was accumulating and a large portion of this precursor rRNA was co-sedimenting with 80S ribosomes (Figure 37 C), like it was reported for other mutants blocking D-site cut processing (Soudet et al., 2010). In addition a 40S/43S peak was visible (Figure 37 C, fractions 2 to 4). The 20S pre-rRNA was not only peaking at a 70S to 80S particle size, but also co-sedimented with polysomes (Figure 37 C, fractions 11 to 20), again confirming recent findings (Soudet et al., 2010). It would be interesting to see, whether the 20S pre-rRNA in the polysomal fractions disappears if cycloheximide is omitted and elongating ribosomes can run off the mRNAs (Soudet et al., 2010). This would be an additional hint that 20S pre-rRNA is really associated with polysomes and possibly engages in translation under these conditions.

2.2.5 rpS14 and its variants

RpS14 is one of the primary binders of the central 18S rRNA domain and is localized at the platform next to the 18S 3'-end, opposite of rpS5 (see Figure 8, Figure 16 and Figure 38 A). The protein itself consists of a α/β-sandwich domain and a protruding C-terminus (Figure 38 B), whose positively charged residues are responsible for interactions with helix h45 in the 3'-minor 18S rRNA domain (see Figure 39 C). RpS14 is well conserved in all three evolutionary kingdoms, especially the two arginines (R132, R133) at the C-terminus, contacting h45 (Figure 38 C).

RpS14, together with rpS5 (see also 2.2.4), possibly forms an interface, which probably binds rRNA, since both r-proteins exhibit positively residues in this region, capable of building a RNA binding pocket (Figure 38 B and Figure 39 B). This interface might be additionally stabilized by a direct protein-protein contact of rpS14 and rpS5 (Figure 39 A, see also discussion in 3.2).

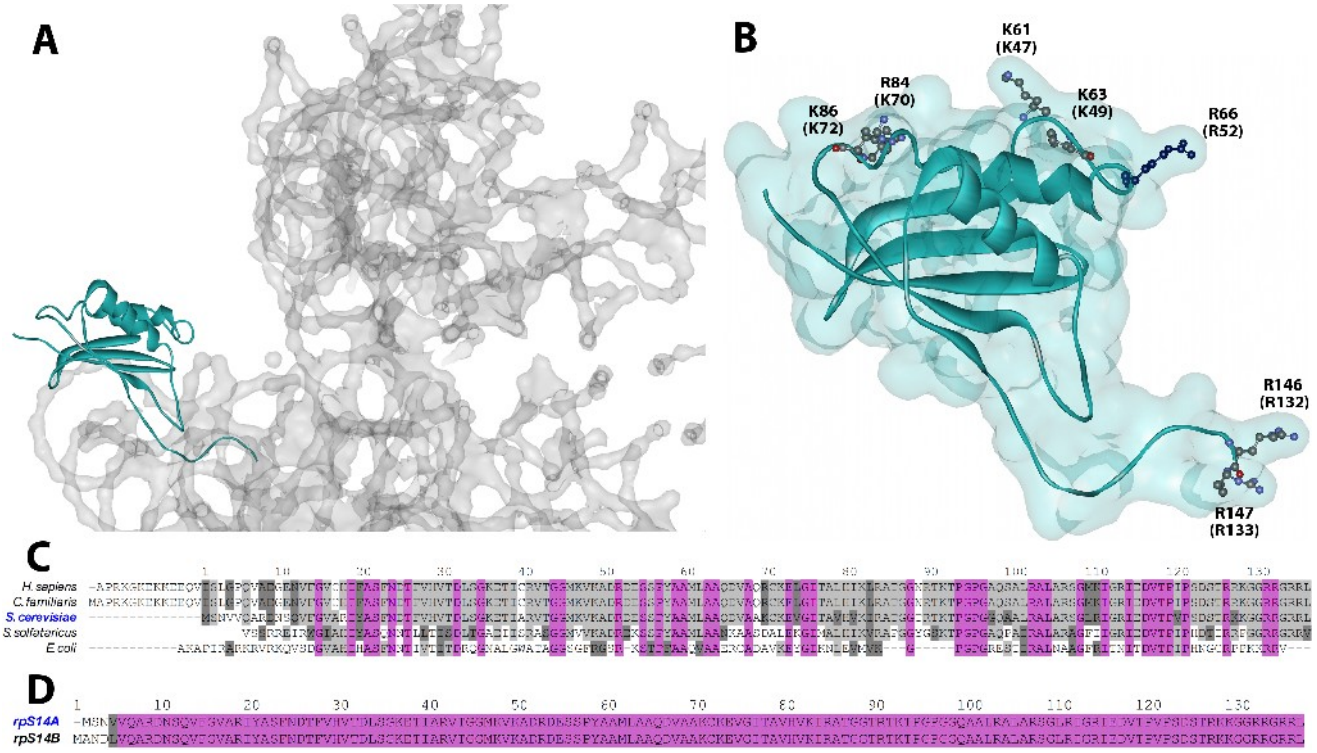

Figure 38. RpS14 localization, structure and protein sequence conservation
(**A**) Localization of rpS14 on the 40S subunit (Chandramouli et al., 2008; pdb:2ZKQ), cytoplasmic view (see also Figure 8). (**B**) Ribbon representation of rpS14 structure with the calculated surface laid underneath. Amino acids 23 to 147 of 151 in total are modeled. Seven amino acids, capable of interacting with RNA are highlighted. The position is given according to the *C. familiaris* nomenclature with *S. cerevisiae* position in brackets. (**C**) Multiple sequence alignment of yeast rpS14 primary structure (AlignX, Vector NTI, Invitrogen, ClustalW algorithm and blosum score-matrix). Protein sequences of representative organisms from all three evolutionary kingdoms are shown (sequences were obtained from NCBI (http://www.ncbi.nlm.nih.gov/protein)). (**D**) Multiple sequence alignment of yeast rpS14, encoded either by RPS14A or RPS14B. (**C**) and (**D**) The color code illustrates amino acid conservation: identical - purple; conserved – gray; block of similar – dark-gray. The numbers give the positions of *S. cerevisiae* amino acids.

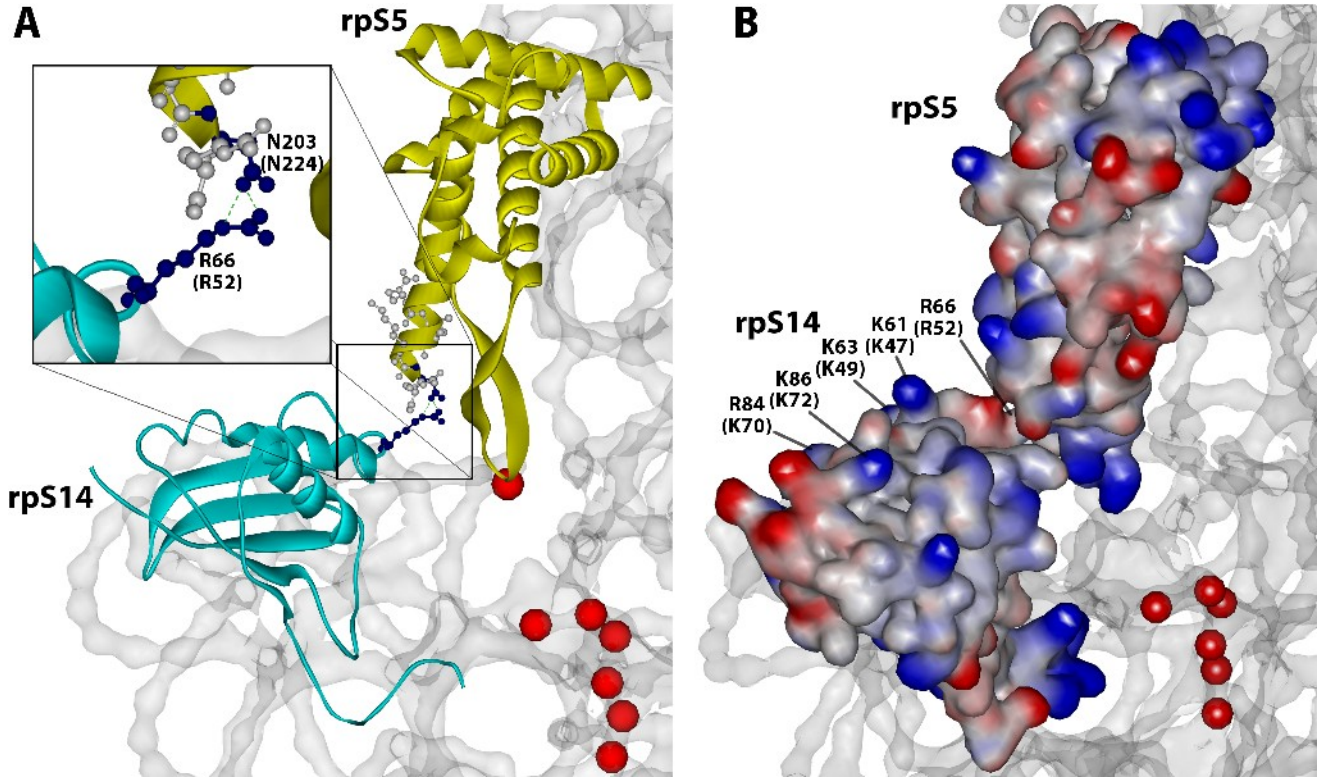

Figure 39. The local environment of rpS5 and rpS14
(**A**) and (**B**) All structures are taken from pdb:2ZKQ (Chandramouli et al., 2008). The position of amino acids is given according to the C. familiaris nomenclature with S. cerevisiae position (RPS14A) in brackets. (**A**) Cytoplasmic view of the rpS5 – rpS14 protein interface. RpS5 is colored in yellow, rpS14 in light blue, the last 3'-18S rRNA nucleotides with red dots and other 18S rRNA in gray. The last seven amino acids, which are missing in rpS5-ΔC (see 2.2.4) and R52 of rpS14 are shown with their side chains. The possible interaction site of rpS5 and rpS14 is magnified. (**B**) Same view as in (**A**), but proteins are shown with their calculated surfaces. The surface is colored according to partial charges: blue surfaces – partial positive charge, red surface – partial negative charge. Mutated amino acids of rpS14 variants are highlighted.

name	background	mutation	database (ToP)
rpS14	*S. cerevisiae* full length allele (wildtype)	-/-	Nt-FLAG: 1003
rpS14-KKRAAA	attenuation of possible rpS14-ITS1 interaction	K47A, K49A, R52A	Nt-FLAG: 1109
rpS14-KKAA	attenuation of possible rpS14-ITS1 interaction	K70A, K72A	Nt-FLAG: 1110

Table 13. List of rpS14 variants
Amino acid positions are given, according to the primary sequence of RPS14A gene product

In vivo depletion of yeast rpS14 results in a block of processing at sites A_0, A_1, A_2 and nucleolar accumulation of pre-SSU particles (Ferreira-Cerca et al., 2005) (see also Figure 40 and Figure 41, vector).

A rps14 variant, in which lysines K70 and K72 were mutated to alanines (rpS14-KKAA), both located in the interface between rpS14 and rpS5, showed no obvious phenotype (Figure 40).

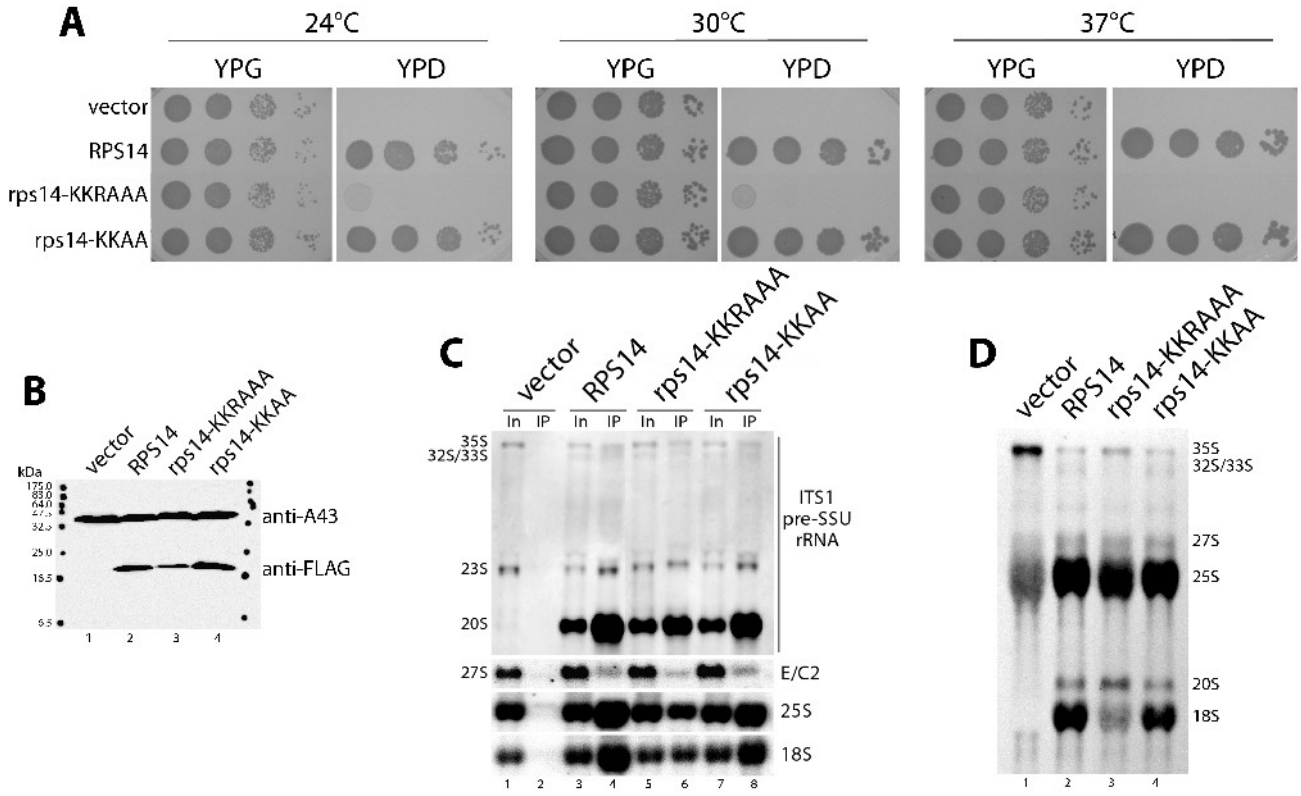

Figure 40. Growth phenotypes of rpS14 variants, expression levels, pre-rRNA processing analyses and incorporation into SSU precursors

(**A**)-(**D**) All experiments were performed in yeast strain pGAL-RPS14A (ToY399), in which full length rpS14 is encoded under the control of the galactose inducible GAL1 promoter. The strain was either transformed with an empty vector (YEplac195) or vectors coding for FLAG-tagged full length rpS14 (ToP1003), rpS14-KKRAAA (ToP1109) or rpS14-KKAA (ToP1110) under the control of a constitutive promoter. All RPS14 alleles were based on the sequence of RPS14A, whose gene product is 1 amino acid smaller than RPS14B. (**A**) Serial dilutions of the indicated transformants on galactose (YPG) or glucose (YPD) containing plates. Plates were incubated for 3 days. (**B**)-(**D**) Cells were grown overnight in selective media containing galactose, diluted in YP-galactose and subsequently expression of pGAL-RPS14 was shut down for 2 hours in YP-glucose medium. (**B**) Western blot analysis of the indicated transformants, using a monoclonal anti FLAG antibody. Anti-A43 antibodies, detecting A43 subunit of RNA polymerase I, were used as loading control. (**C**) Northern blot analysis of RNA co-purified with the indicated FLAG-tagged rpS14 variants. RNA was extracted from Input (In) and immuno-purified (IP) fractions. Probes used for detection of (pre-) rRNA species are depicted right-hand. 200 mM salt (KCl, see 5.2.5.3) was used for cell breakage, binding and washing of the immunoprecipitations. (**D**) 5',6'-[^{3}H] uracil metabolic labeling of newly synthesized RNA. Cells were pulsed for 30 minutes at 30°C. Total RNA was extracted and separated by gel electrophoresis, radio-labeled RNA was visualized by fluorography.

In contrast, a variant in which lysines K47, K49 and arginine R52 were mutated to alanines (rpS14-KKRAAA), could not complement the loss of rpS14 (Figure 40 A). Although the variant was well expressed (Figure 40 B) and incorporated into pre- and mature ribosomes, albeit with reduced stability (Figure 40 C, compare 18S input vs. IP levels for rpS2 and rpS2-KRRAAA), 18S rRNA 3'-end maturation was clearly delayed (Figure 40 D, lane 4). 20S pre-rRNA containing pre-40S subunits seem to be of cytoplasmic nature, as FISH analysis displayed cytoplasmic localization of ITS1 containing precursor particles (Figure 41).

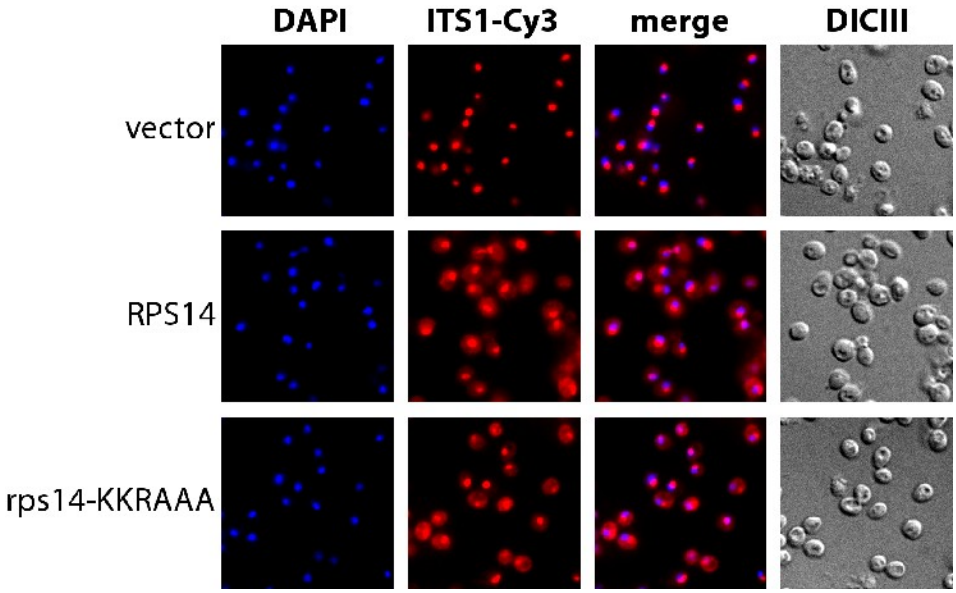

Figure 41. Analyses of nuclear export of SSU precursors containing rpS14 variants
FISH analysis was performed in yeast strain pGAL-RPS14 (ToY399), in which full length rpS14 is encoded under the control of the galactose inducible GAL1 promoter. The strain was either transformed with an empty vector (YEplac195) or vectors coding for FLAG-tagged full length rpS14 (ToP1003) or rpS14-KKRAAA (ToP1109) under the control of a constitutive promoter. Cells were grown overnight in selective media containing galactose, diluted in YP-galactose and subsequently expression of pGAL-RPS14 was shut down for 2 hours in YP-glucose medium. Total DNA (DAPI) and rRNA precursors containing ITS1-sequences between site D and A2 (ITS1-Cy3) were detected as described in 5.2.6.2.

Taken together, some of the positively charged amino acids in the interface region of rpS14 and rpS5 are specifically required for efficient late cytoplasmic 20S pre-rRNA processing. Probably destabilized rRNA binding in this rpS14 variant, through reduction of its interaction sites, can only establishes a suboptimal conformation of the precursor particle, required for efficient processing (see discussion in 3.2). This effect could be further enhanced by the deletion of the potential protein-protein contact site of rpS14 and rpS5 (see Figure 39 A).

2.2.6 rpS20 and its variants

RpS20 is binding in the head domain, next to the beak (Figure 42 A) and it features the typical r-protein fold, namely a globular structure with a protruding hairpin (Figure 42 B). Amino acids located in such hairpins are very often responsible for protein-RNA interactions. The globular domain of S10 builds one side of a groove, in which helix h39 is tightly bound (Clemons et al., 1999; Brodersen et al., 2002; Chandramouli et al., 2008; Taylor et al., 2009). The other side of the groove is built by S9 (rpS16 in eukaryotes) (see also Figure 8 A). Helices h31, h34, h41 and h43 are contacted through the protruding loop, while especially the tip of the loop is responsible for many interactions. RpS29 and rpS3, both involved in the beak formation (see (Schäfer et al., 2006) and Figures 8 and 16), are in close vicinity to rpS20 and very likely interact with each other (Figure 42 C). The primary sequence of rpS20 is well conserved in all evolutionary kingdoms and shows no large eukaryotic specific parts (Figure 42 D and E).

In vivo depletion of rpS20 results in a block of 18S rRNA processing at site D and accumulation of 20S pre-rRNA ((Ferreira-Cerca et al., 2005), see also Figure 43 D, compare lanes 1 and 2). Effects on nucleo cytoplasmic transport of precursor subunits lacking rpS20 could not be detected ((Ferreira-Cerca et al., 2005), see also Figure 44, vector).

name	background	mutation	database (ToP)
rpS20	*S. cerevisiae* full length allele (wildtype)	-/-	Nt-FLAG: 1009
TAS20	archaeal homologue of rpS20 (*T. acidophilum*)	-/-	Nt-FLAG: 510 HA : 1278
SAS20	archaeal homologue of rpS20 (*S. acidocaldarius*)	-/-	Nt-FLAG: 664 HA : 1279
SAS20-chimera1	partial exchange of TAS20 and SAS20 primary sequences (ultimate N-terminus)	(SAS20 M1-N18) :: (TAS20 M1-D19)	Nt-FLAG: 752
SAS20-chimera2	partial exchange of TAS20 and SAS20 primary sequences (N-terminus)	(SAS20 M1-L53) :: (TAS20 M1-S54)	Nt-FLAG: 753
SAS20-chimera3	partial exchange of TAS20 and SAS20 primary sequences (hairpin)	(SAS20 T44-K68) :: (TAS20 K45-R69)	Nt-FLAG: 754
SAS20-KKTT	point mutations in the tip of the SAS20 hairpin	K59T, K61T	Nt-FLAG: 1177
SAS20-K59S	point mutations in the tip of the SAS20 hairpin	K59S	Nt-FLAG: 1178
SAS20-K59T	point mutations in the tip of the SAS20 hairpin	K59T	Nt-FLAG: 1179
SAS20-K61T	point mutations in the tip of the SAS20 hairpin	K61T	Nt-FLAG: 1180

Table 14. List of rpS20 variants

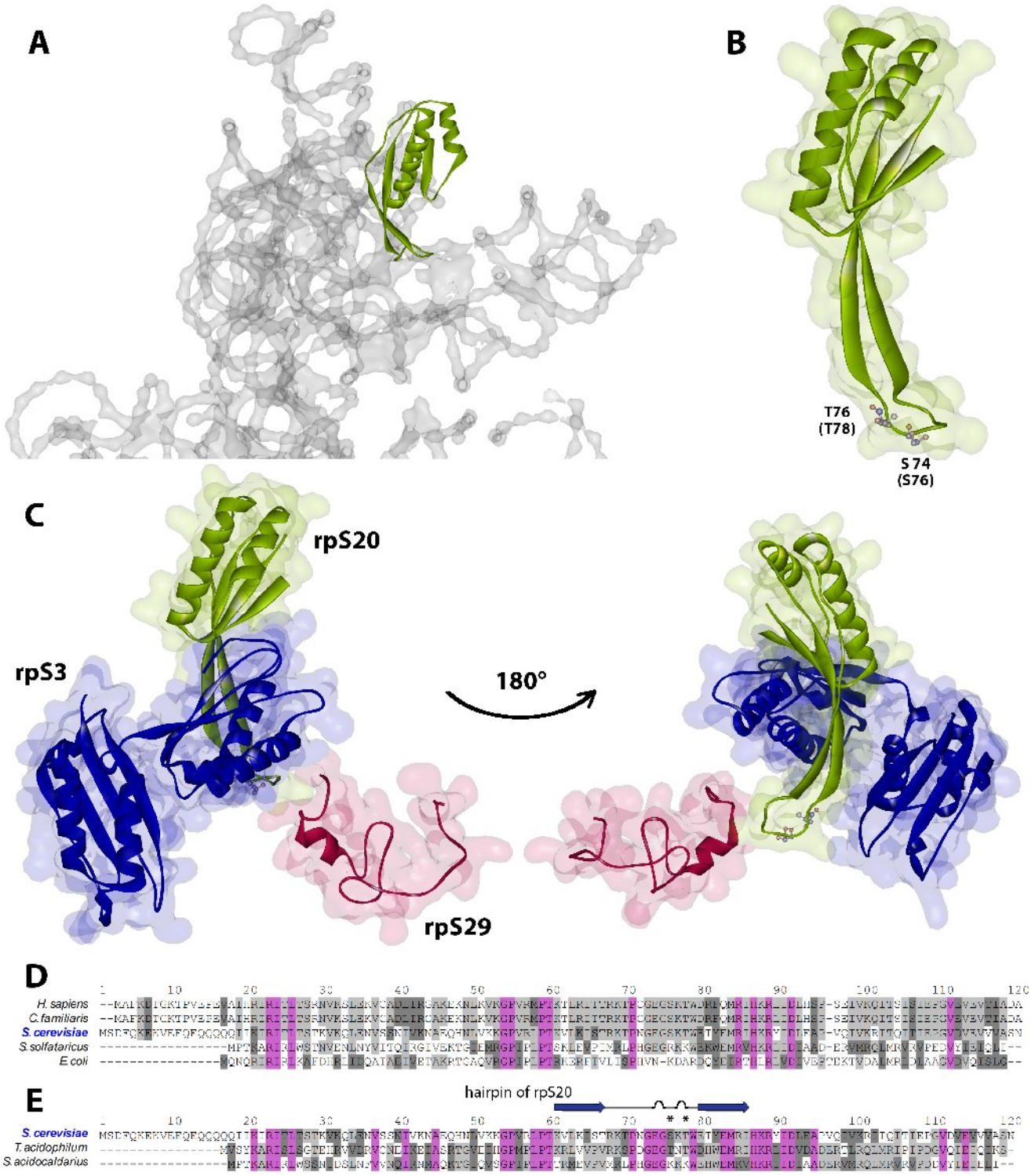

Figure 42. RpS20 localization, structure and protein sequence conservation

(**A**) Localization of rpS20 on the 40S subunit (Chandramouli et al., 2008; pdb:2ZKQ), cytoplasmic side view (see also Figure 8). (**B**) Ribbon representation of rpS20 structure with the calculated surface laid underneath. Amino acids 19 to 115 of 119 in total are modeled. Two amino acids in the tip of the hairpin are highlighted. The position is given according to the *C. familiaris* nomenclature with *S. cerevisiae* position in brackets. (**C**) The rpS3, rpS20, rpS29 protein cluster. (**D**) Multiple sequence alignment of yeast rpS20 primary structure (AlignX, Vector NTI, Invitrogen, ClustalW algorithm and blosum score-matrix). Protein sequences of representative organisms from all three evolutionary kingdoms are shown (sequences were obtained from NCBI (http://www.ncbi.nlm.nih.gov/protein)). (**E**) Multiple sequence alignment of yeast rpS20 primary structure with S10 (prokaryotic homologue of rpS20) from *Thermoplasma acidophilum* (TAS20) and *Sulfolobus solfataricus* (SAS20). The predicted secondary structure of the rpS20 hairpin (Chandramouli et al., 2008) is shown on top (blue arrows

indicate part of a beta sheet; black semicircles are hydrogen bonded turns). Asterisks indicate the position of the in (**B**) highlighted amino acids. (**D**) and (**E**) The color code illustrates amino acid conservation: identical - purple; conserved – gray; block of similar – dark-gray. The numbers give the positions of *S. cerevisiae* amino acids.

2.2.6.1 The archaeal r-protein S10 from T. acidophilum is able to substitute rpS20 in vivo in yeast

The archaeal homologues of rpS20 from *T. acidophilum* (TAS20) and *S. acidocaldarius* (SAS20) share around 32% respectively 25% of identical amino acids (49% respectively 43% of amino acids with side chains of the same chemical properties) (Figure 42 E). The only archaeal r-protein out of 29 tested (see 2.1.2), which was able to fully complement the loss of its eukaryotic counterpart, was TAS20, the rpS20 homologue of *T. acidophilum* (Figure 43 A, TAS20). In contrast, expression SAS20, the rpS20 homologue of *S. acidocaldarius* in yeast could not rescue the lethal phenotype of rpS20 deletion (Figure 43 A, SAS20). Expression levels of both proteins particular differed greatly from each other. TAS20 was highly expressed, while SAS20 expression was very low (Figure 43 B, compare lanes 3 and 4). Nevertheless SAS20 was, as well as yeast rpS20 or TAS20, incorporated into SSU precursor particles (Figure 43 C, compare input and IP lanes 20S), but hardly co-precipitated mature subunits (Figure 43 C, compare input and IP lanes 25S and 18S). A special phenomenon of rpS20 (and some variants) was the great amount of co-purified 27S pre-rRNA (Figure 43 C, probe E/C2). This precipitation is an indication for relatively high unspecific binding under the salt conditions used. This strong precipitation of 27S might be due to the fact that about 25% of rpS20's surface area contributes to RNA binding (Brodersen et al., 2002), or 27S pre-rRNA exhibits a RNA fold that resembles the binding site of rpS20. Furthermore, expression of TAS20 in yeast promoted to a large extent restoration of mature 18S production (Figure 43 D, lanes 2 and 3), while expression of SAS20 did not (Figure 43 D, lanes 1 and 4).

RpS20 depletion didn't detectably affect nucleo-cytoplasmic trafficking ((Ferreira-Cerca et al., 2005) and Figure 44, vector). Neither TAS20, nor SAS20 expression indicated a dominant negative effect on nuclear export after shutdown of rpS20 (Figure 44). In both strains, the 20S pre-rRNA containing pre-SSU particles were most likely localized in the cytoplasm.

TAS20 and SAS20 share about 48% of identical amino acids (67% of amino acids with side chains of the same chemical properties), so the question arose, why can TAS20 complement the functions of rpS20 and SAS20 can not?

2.2.6.2 Exchange of two amino acids in the hairpin of S. acidocaldarius rpS20 homologue rendered the variant functional in yeast 18S rRNA 3'-end maturation

To answer this, chimeric proteins were constructed in which parts of SAS20 were exchanged with TAS20 sequences. In neither case exchange of N-terminal parts could rescue the loss of yeast rpS20 (Figure 43 SAS20-chimera1 and SAS20-chimera2). Nevertheless, these variants were efficiently incorporated into SSU precursors (Figure 43 C, probe ITS1).

However an exchange of the SAS20 hairpin with the one from TAS20 allowed production of mature 18S rRNA and this variant was furthermore incorporated into mature ribosomes (Figure 43, SAS20-chimera3).

In-depth analysis of multiple sequence alignments of the rpS20 hairpin sequence revealed two additional positively charged amino acids in the primary sequence of SAS20, located in the tip of the hairpin (Figure 42 E). K59 and K61 of SAS20 are not conserved in eukaryotes (K59 is S76 and K61 is T78 in yeast, Figure 42 B and E). A variant, in which both lysines of SAS20 were mutated to threonines (situation in TAS20), again complemented the essential functions of yeast rpS20 (Figure 43, SAS20-KKTT).

Variants, in which only a single amino acid was mutated at a time, could only partially substitute yeast rpS20 (Figure 43, SAS20-K59S, SAS20-K59T and SAS20-K61T). These variants were well incorporated into SSU precursors, but poorly into mature ribosomes (Figure 43 D, lanes 13-16) and allowed only very low new synthesis of 18S rRNA at 30°C (Figure 43 D, lanes 8 and 9).

Taken together these variants imply that the hairpin of rpS20, in particular its tip is required for proper rpS20 function in final 18S 3'-end maturation. A possible mechanism by which the subtle changes in the hairpin are communicated, to allow or block D-site cut processing (distance of rpS20 hairpin to 18S 3'-end is more than 50Å), will be discussed later (see 3.2).

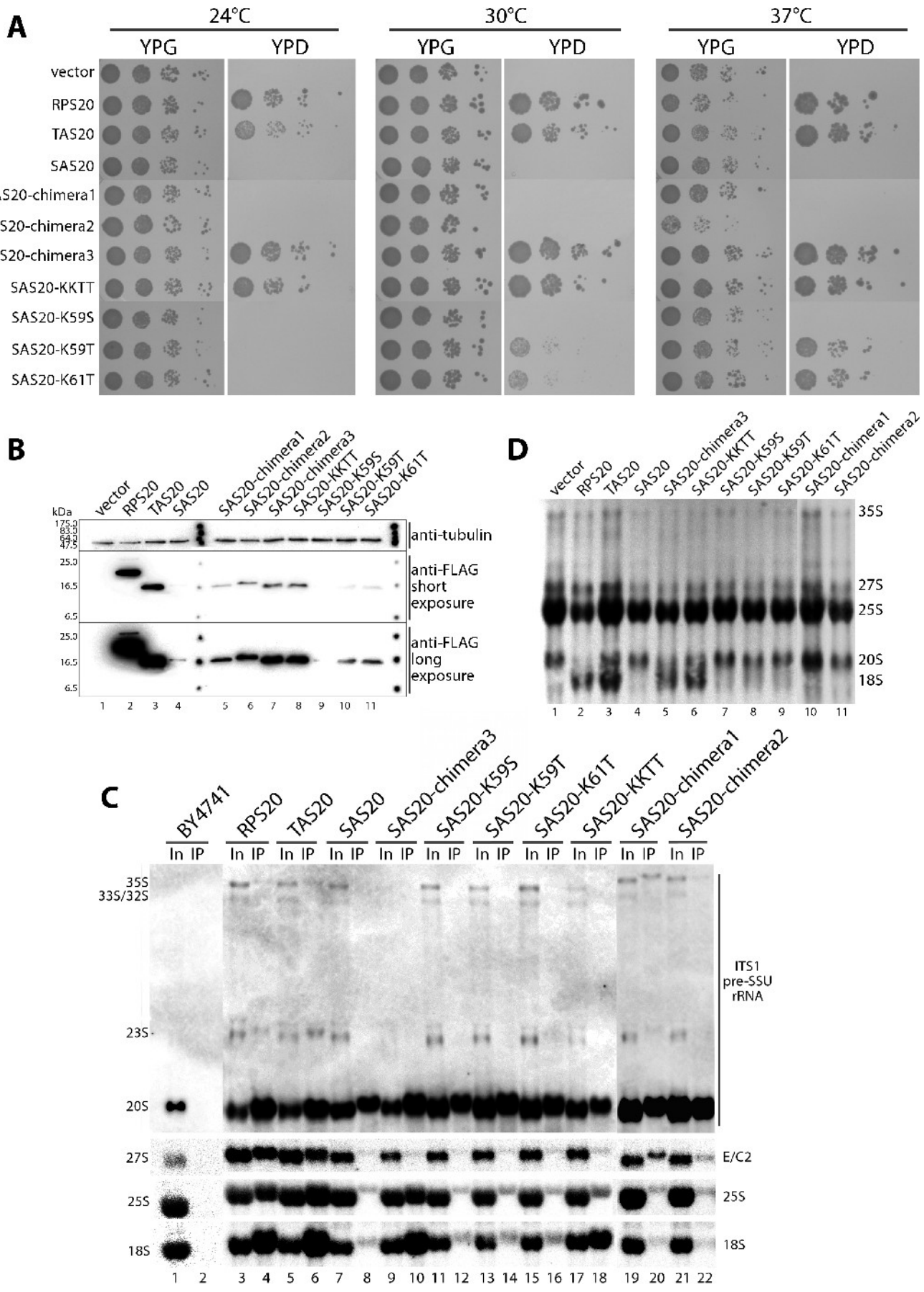

Figure 43. Growth phenotypes of rpS20 variants, expression levels, pre-rRNA processing analyses and incorporation into SSU precursors

(**A**) Yeast strain pGAL-RPS20 (ToY262), in which full length rpS20 is encoded under the control of the galactose inducible GAL1 promoter. The strain was either transformed with an empty vector (YEplac195) or vectors coding for FLAG-tagged full length rpS20 (ToP1009), TAS20 (ToP510), SAS20 (ToP664), SAS20-chimera1 (ToP752), SAS20-chimera2 (ToP753), SAS20-chimera3 (ToP754), SAS20-KKTT (ToP1177), SAS20-K59S (ToP1178), SAS20-K59T (ToP1179), SAS20-K61T (ToP1180) or rpS20-S76K (ToP1181) under the control of a constitutive promoter. Serial dilutions of the indicated transformants on galactose (YPG) or glucose (YPD) containing plates were incubated for 3 days at the respective temperature. (**B**)-(**D**) All experiments were performed in yeast strain pGAL-RPS20 (ToY845), in which full length rpS20 is encoded under the control of the galactose inducible GAL1 promoter. The strain was either transformed with an empty vector (YEplac195) or vectors coding for constitutive expressed FLAG-tagged rpS20 variants as described in (**A**). Cells were grown overnight in selective media containing galactose, diluted in YP-galactose and subsequently expression of pGAL-RPS20 was shut down for 4 hours in YP-glucose medium. (**B**) Western blot analysis of the indicated transformants, using a monoclonal anti FLAG antibody. Tubulin was used as loading control. (**C**) Northern blot analysis of RNA co-purified with the indicated FLAG-tagged rpS20 variants. RNA was extracted from Input (In) and immuno-purified (IP) fractions. Wildtype strain BY4741 served as background control for immuno-purification. Probes used for detection of (pre-) rRNA species are depicted right-hand. 200 mM salt (KCl, see 5.2.5.3) was used for cell breakage, binding and washing of the immunoprecipitations. (**D**) 5',6'-[^{3}H] uracil metabolic labeling of newly synthesized RNA. Cells were pulsed for 30 minutes at 30°C. Total RNA was extracted and separated by gel electrophoresis, radio-labeled RNA was visualized by fluorography.

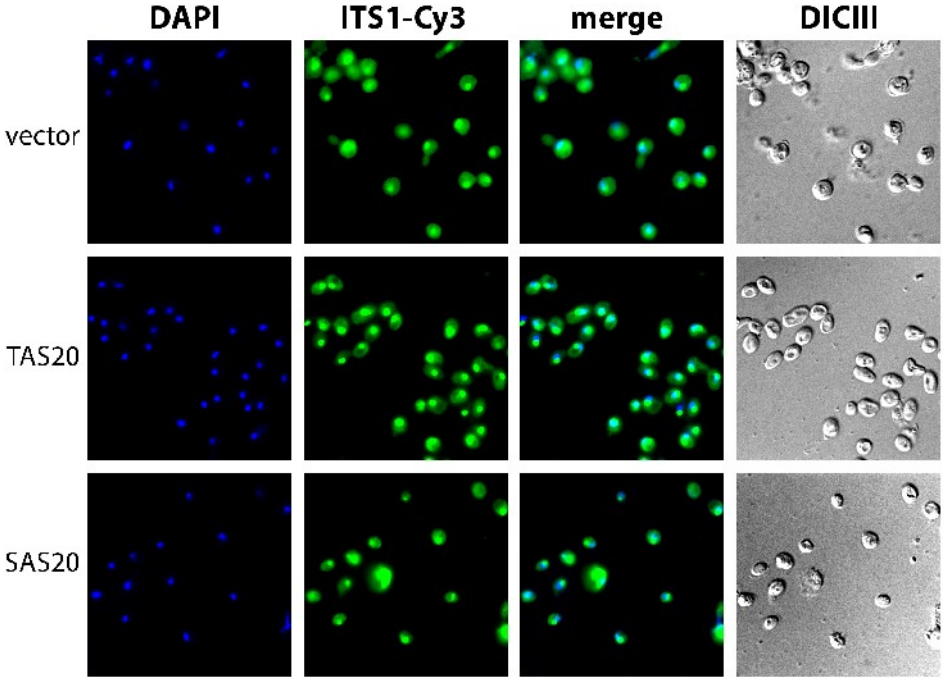

Figure 44. Analyses of nuclear export of SSU precursors containing rpS20 variants
FISH analysis was performed in yeast strain pGAL-RPS20 (ToY845), in which full length rpS20 is encoded under the control of the galactose inducible GAL1 promoter. The strain was either transformed with an empty vector (YEplac195) or vectors coding for FLAG-tagged TAS20 (ToP510), SAS20 (ToP664) under the control of a constitutive promoter. Cells were grown overnight in selective media containing galactose, diluted in YP-galactose and subsequently expression of pGAL-RPS20 was shut down for 4 hours in YP-glucose medium. Total DNA (DAPI) and rRNA precursors containing ITS1-sequences between site D and A2 (ITS1-Cy3) were detected as described in 5.2.6.2.

2.2.6.3 Depletion of rpS20 caused only slight changes in the r-protein assembly state of the SSU head domain

In vitro reconstitution experiments of prokaryotic ribosomes demonstrated that S10, the homologue of rpS20, is a tertiary binder (see Figure 16). Yet its incorporation into nascent SSUs is required for proper assembly of S14 (rpS29) and S3 (rpS3) (Mizushima et al., 1970) (see also Figure 16).

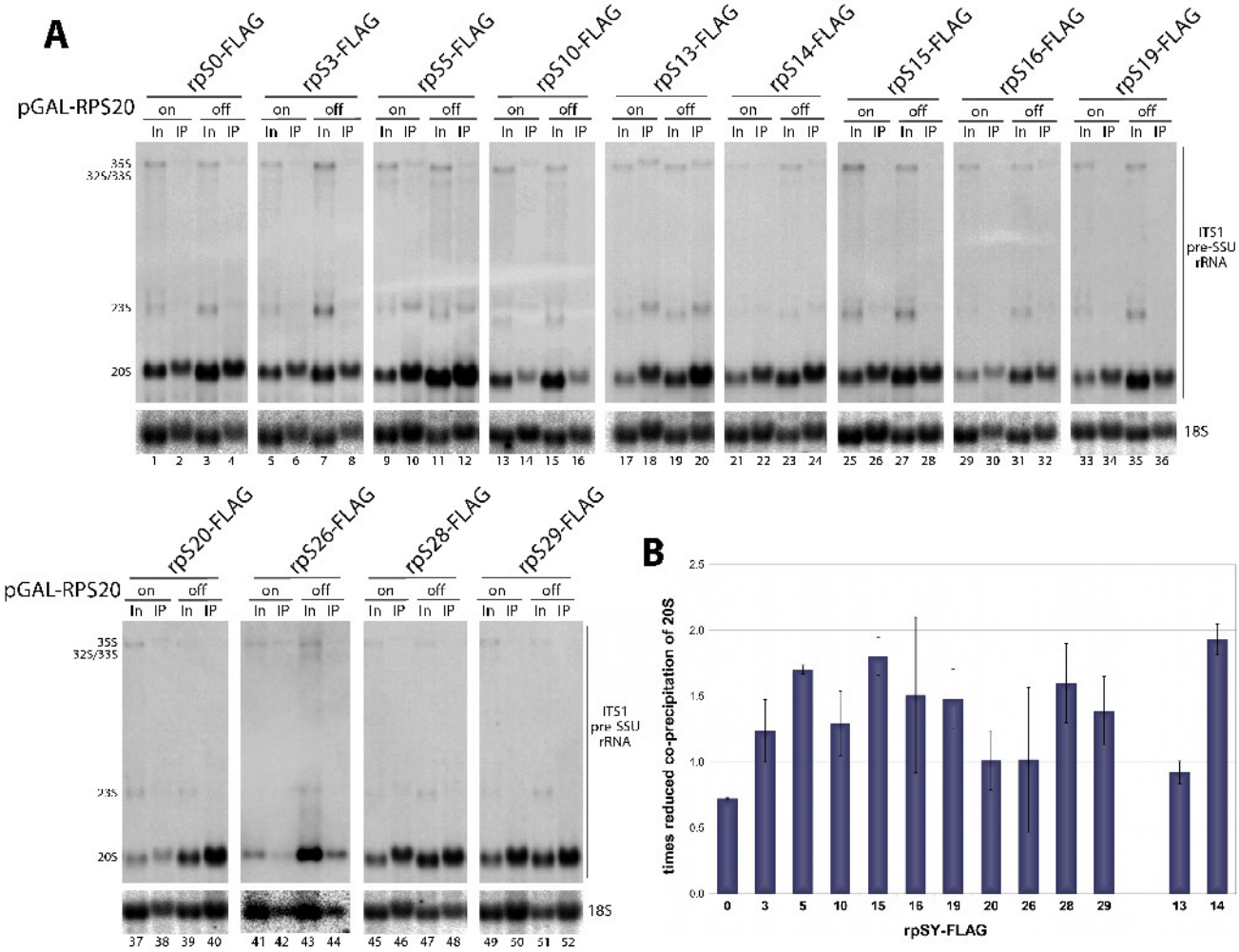

Figure 45. Analysis of r-protein interactions with SSU precursors before and after rpS20 depletion

(**A**) Northern blot analysis of SSU (pre-) RNA co-purifying with the indicated FLAG-tagged r-proteins before and after rpS20 depletion. The experiments were performed in yeast strain ToY262 or ToY845, in which full length rpS20 is encoded under the control of the galactose inducible GAL1 promoter. The strain was transformed with vectors supporting the constitutive expression of indicated FLAG-tagged r-proteins. Transformants were grown overnight in selective media containing galactose and on the next day diluted in YP-galactose medium. The cultures were split, one half was further grown in YP-galactose (on, wildtype rpS20 is expressed), in the other half of the culture expression of pGAL-RPS20 was shut down for 2 hours (ToY262) or 4 hours (ToY845) in YP-glucose medium (off). 200 mM salt (KCl, see 5.2.5.3) was used for cell breakage, binding and washing of the immunoprecipitations. RNA was extracted from Input (In) and immuno-purified (IP) fractions. Probes used for detection of (pre-) rRNA species are depicted right-hand. (**B**) Quantification of r-protein interaction with SSU precursors before and after rpS20 depletion. Each data point was derived from at least 2 biological replicates (representative Northern blot shown in (**A**)). The factor of reduced 20S co-precipitation was calculated as follows: (%IP20S / %IP18S)**on** / (%IP20S / %IP18S)**off**. Quantification was done, using LAS3000, FLA3000 and MultiGauge software (FujiFilm).

To elucidate the *in vivo* dependencies of stable incorporation of r-proteins with nascent subunits on the presence of rpS20, FLAG-tagged r-proteins were immuno-purified and the co-precipitated (pre-) rRNA was analyzed. To summarize the experiments, in contrast to what was found after *in vivo* depletion of the primary binder rpS5, no strong impact on the r-protein assembly state of nascent SSUs lacking rpS20 could be detected by this approach (compare Y-axis scales in Figure 45 B and Figure 34 B).

In particular a major destabilization of binding of rps3 and rpS29, the homologues of S3 and S14 (see before), was not visible (Figure 45 A, quantification in B). On the other hand, recently obtained data of mass spectrometric analyses of purified SSU precursor particles indicated small changes in the r-protein assembly state of yeast cells depleted of rpS20 (see 2.2.6.4 and data not shown).

In summary, the changes in the r-protein assembly state of SSU precursors upon depletion of the tertiary binder rpS20 are relatively low, compared to the changes caused by depletion of the primary binder rpS5. Nevertheless, small changes in the stable incorporation of some late binding r-proteins can not be ruled out.

2.2.6.4 Characterization of nascent SSUs that contained SAS20 showed no major interference in r-protein and biogenesis factors assembly state

Only slight changes in r-protein assembly state of nascent SSUs were induced by *in vivo* depletion of rpS20 (see 2.2.6.3). The r-protein assembly state of SSU precursors containing SAS20 was analyzed in a semi-quantitative way by using a mass spectrometric approach, comparing their protein composition to SSU precursors containing the rpS5-ΔC variant. The assembly state of the latter one was analyzed in detail and showed no major impairment in r-protein binding (see 2.2.4.6).

Pre-ribosomal particles that incorporated the FLAG-tagged variants were affinity purified via the FLAG-epitope of the variants, the associated proteins were digested with trypsin, labeled with the iTRAQ reagents (iTRAQ®, Applied Biosystems) and analyzed by mass spectrometry (MALDI TOF/TOF).

In this case, the enrichment of rpS20 and SAS20 could be used as an internal control for assessment of the obtained data (Figure 46, light blue bars). SAS20 was not present in the purification of the rpS5-ΔC containing particles and rpS20 was depleted in the strain expressing SAS20. Thus, the enrichment of rpS20 was very high in the purification of FLAG-tagged rpS5-ΔC compared to FLAG-tagged SAS20 (Figure 46, left side) and accordingly, SAS20 was highly depleted (Figure 46, right side). With the exception of rpS29, all analyzed SSU r-proteins seem to be incorporated in precursors containing SAS20. The stable incorporation of rpS29 into SAS20 containing particles might be affected, but this observation needs to be confirmed by repetition of the experiment (see the very high standard deviation of rpS29 iTRAQ ratio in Figure 46).

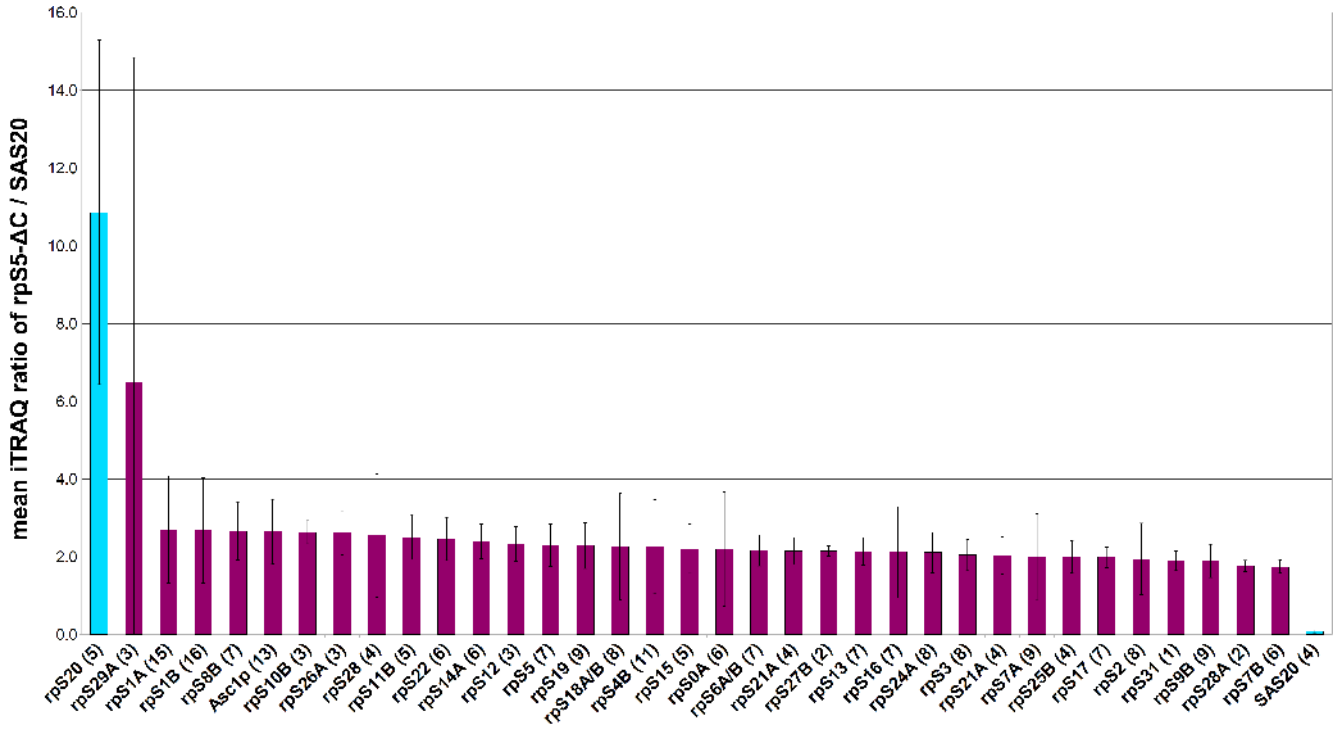

Figure 46. Analyses of r-protein composition of SSU precursors containing rpS5-ΔC or SAS20
The experiment was performed in yeast strains ToY323 and ToY845, in which full length rpS5 or rpS20 is encoded under the control of the galactose inducible GAL1 promoter. The strains were transformed with vectors supporting the constitutive expression of FLAG-tagged rpS5-ΔC (ToP1101 in ToY323) or SAS20 (ToP664 in ToY845). Cells were grown overnight in selective media, diluted in YP-galactose and expression of pGAL-RPS5 or pGAL-RPS20 was shut down for 2, respectively 4 hours in YP-glucose medium. FLAG-tagged variants were affinity purified from both transformants and their protein composition was compared in a semi-quantitative way using the iTRAQ method as described in 5.2.7.1 and 5.2.7.3. The mean values and standard deviations are shown. The number of tryptic peptides for each protein is given in brackets after the protein name. Color code: magenta – SSU r-proteins; light blue – rpS20 or SAS20.

Next to Nob1p, the putative endonuclease, mediating final 18S 3'-end maturation several other biogenesis factors are needed to allow cytoplasmic D-site processing (see 1.4.2).

To analyze the protein content of precursor particles, (pre-) SSUs were purified by precipitation of FLAG-tagged SAS20. The associated proteins were eluted, digested with trypsin and identified by mass spectrometry (see 5.2.7.1 and 5.2.7.2). The identified SSU biogenesis factors are listed in Table 15 (for the complete list, including factor description see Supplemental Table 3). Many biogenesis factors, emphasizing the co-purification of Nob1p, which are specifically required for late cytoplasmic maturation of pre-40S subunits were found in the SAS20-FLAG

protein	peptides	total ion score %
Arb1p	7	100
Bfr2p	1	100
Dbp2p	6	100
Ecm16p (Dhr1p)	1	97.5
Enp1p	10	100
Gar1p	1	100
Kre33p	3	100
Ltv1p	6	100
Nob1p	9	100
Nop58p (Nop5p)	1	100
Pno1p (Dim2p)	4	100
Rio2p	8	100
Rrp3p	2	100
Rrp8p	1	100
Rrp12p	2	100
Tsr1p	9	100

Table 15. FLAG-SAS20 associated SSU biogenesis factors

containing SSU precursors (46 peptides vs. 25 peptides of other proteins).

TAS20 could complement all essential functions of yeast rpS20, while SAS20 was unable to overtake its role in 18S rRNA 3'-end maturation (see 2.2.6.1). To get a more quantitative picture of the protein content of SSUs, which contained TAS20 or SAS20, TAP-tag purifications of Rio2p in the corresponding yeast strains were performed. The associated proteins were digested with trypsin, labeled with the iTRAQ reagents (iTRAQ®, Applied Biosystems) and analyzed by mass spectrometry (MALDI TOF/TOF).

TAP-tagged Rio2p, a component of cytoplasmic pre-40S subunits (Vanrobays et al., 2003), still strongly interacted with 20S pre-rRNA after shutdown of rpS20 expression, in both yeast strains expressing HA-tagged TAS20 or SAS20 (Figure 47 B, for growth phenotype of HA-tagged TAS20 and SAS20 see Supplemental Figure 2).

Only six peptides of SSU components were found (Figure 47 A, Krr1p, Nop1p, Snu13p, Nop58p). Enp1p and Pno1p are components of 90S pre-ribosomes, but most probably stay longer associated, since both precipitate high amounts of 20S pre-rRNA (Chen et al., 2003; Vanrobays et al., 2004) and at least Enp1p can be also localized in the cytoplasm (Léger-Silvestre et al., 2004). The majority of peptides was derived from biogenesis factors, acting at

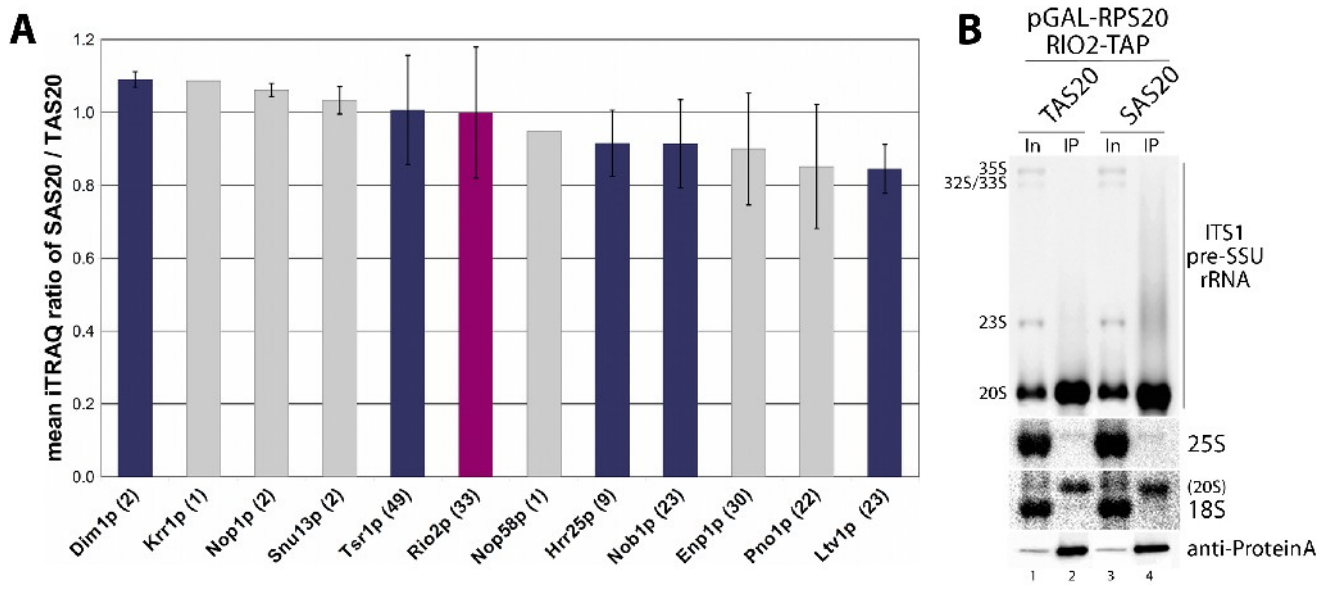

Figure 47. Analyses of the protein composition of SSU precursors containing TAS20 or SAS20
(**A**) and (**B**) All experiments were performed in yeast strain ToY845, in which full length rpS20 is encoded under the control of the galactose inducible GAL1 promoter and Rio2p is TAP-tagged. The strain was transformed with vectors supporting the constitutive expression of HA-tagged TAS20 (ToP1278) or SAS20 (ToP1279). Cells were grown overnight in selective media, diluted in YP-galactose and expression of pGAL-RPS20 was shut down for 4 hours in YP-glucose medium. (**A**) Analysis of biogenesis factors co-purified with Rio2p-TAP associated SSU precursors. Rio2p-TAP associated SSU precursors were affinity purified from both transformants and their protein composition was compared in a semi-quantitative way using the iTRAQ method as described in 5.2.7.1 and 5.2.7.3. The mean values (normalized to the Rio2p iTRAQ ratio) and standard deviations of two technical replicates are shown. The number of tryptic peptides for each protein is given in brackets after the protein name. Color code: magenta – Rio2p-TAP bait protein; dark-blue – biogenesis factors involved in 20S pre-rRNA containing precursor maturation. (**B**) Rio2p-TAP was affinity purified and SSU pre-rRNA contained in Input (In) and immuno-purified (IP) fractions was analyzed by Northern blotting. Probes used for detection of (pre-) rRNA species are depicted right-hand.

a later stage of pre-40S subunit maturation, which is consistent with the unaffected export of pre-SSUs after rpS20 depletion (see Figure 44). All of these biogenesis factors (see also 2.2.4.7), in particular Nob1p, remain associated with the Rio2p-RNP after rpS20 shutdown (Figure 47 A).

Both kinds of purifying (pre-) SSUs, by FLAG-tagged SAS20 or TAP-tagged Rio2p, indicate that none of the biogenesis factors required for D-site cut processing is missing in nascent SSUs containing SAS20. Supporting this hypothesis, the identified crucial amino acids in the SAS20 variant are localized in the tip of its hairpin and not on the surface side of SAS20 (see Figure 42). Thus it is unlikely that interaction with any factor is disturbed.

Taken together, the data suggest that the strong delay in 20S pre-rRNA processing, observed in the strain expressing SAS20, is not due to missing r-proteins or biogenesis factors, but rather based on conformational changes in subunit structure, which in turn leads to suboptimal processing (see also discussion in 3.2).

2.3 Nob1p interaction with precursor subunits

2.3.1 Nob1p co-purified pre-SSU rRNA independent of the *in vivo* assembly of some platform or head domain r-proteins

As previously mentioned, yeast Nob1p presumably harbors the endonuclease activity converting 20S pre-rRNA into mature 18S rRNA. To directly address the association of Nob1p after shutdown of various r-proteins of the small subunit, pre-rRNAs co-purifying with TAP-tagged Nob1p in the corresponding pGAL-RPSX strains were analyzed (Figure 48 A-E).

The C-terminal fusion of Nob1p with the TAP-epitope obviously resulted in a phenotype itself. Either by indirect or direct influence of the TAP-tag, final 18S rRNA maturation was slowed down and 20S pre-RNA was heavily accumulating (Figure 48 F and G, compare always lane 1 and 5). This observation might be the reason that TAP-tagged Nob1p in the pGAL-RPS5 strain led to roughly 20% lowered doubling times (Supplemental Figure 1 A). Upon *in vivo* depletion of rpS5 or rpS14 for at least 2 hours, only strongly reduced levels of 20S pre-rRNA were detectable (Figure 48 F and G, compare 20S in lanes 1 to 4). TAP-fusion of Nob1p in these strain delayed occurrence of the depletion phenotype by more than twice the normal time (Figure 48 F and G, compare always 20S in lanes 2 and 6, 3 and 7, etc.).

In summary, TAP-tagged Nob1p still co-purified very efficiently 20S pre-rRNA after shutdown of rpS2, rpS5, rpS14 and rpS20 (Figure 48 A-D). Additionally, the immunoprecipitation efficiencies suggest that Nob1p exists only sub-stoichiometrically amounts in yeast. A high level of 20S pre-rRNA in the input fractions did not correlate with an elevated rate of co-precipitation. The IP ratio rather looks like Nob1p-TAP could be saturated with 20S pre-rRNA and could only co-precipitate a certain amount of 20S pre-rRNA (Figure 48 A-D, compare 20S levels in IP lanes).

To further characterize the interaction of Nob1p with precursor subunits after shutdown of rpS5, Nob1p-TAP associated pre-rRNAs were purified in a yeast strain expressing HA-tagged alleles of rpS5, rpS5-ΔC, rpS5-Δloop or rpS5-short-loop (Figure 48 E). As shown before, Nob1p was able to interact with pre-SSU rRNA independent of *in vivo* assembly of rpS5 (Figure 48 B). Co-expression of the HA-tagged variants didn't alter this co-precipitation pattern (Figure 48 E).

These results support the data obtained by mass spectrometry (see 2.2.4.7 and 2.2.6.4), namely that the virtually blocked conversion of 20S pre-rRNA to mature 18S rRNA in the rpS5-ΔC (and rpS5-short-loop) as well as SAS20 containing SSU precursors is not due to the absence of the putative endonuclease Nob1p.

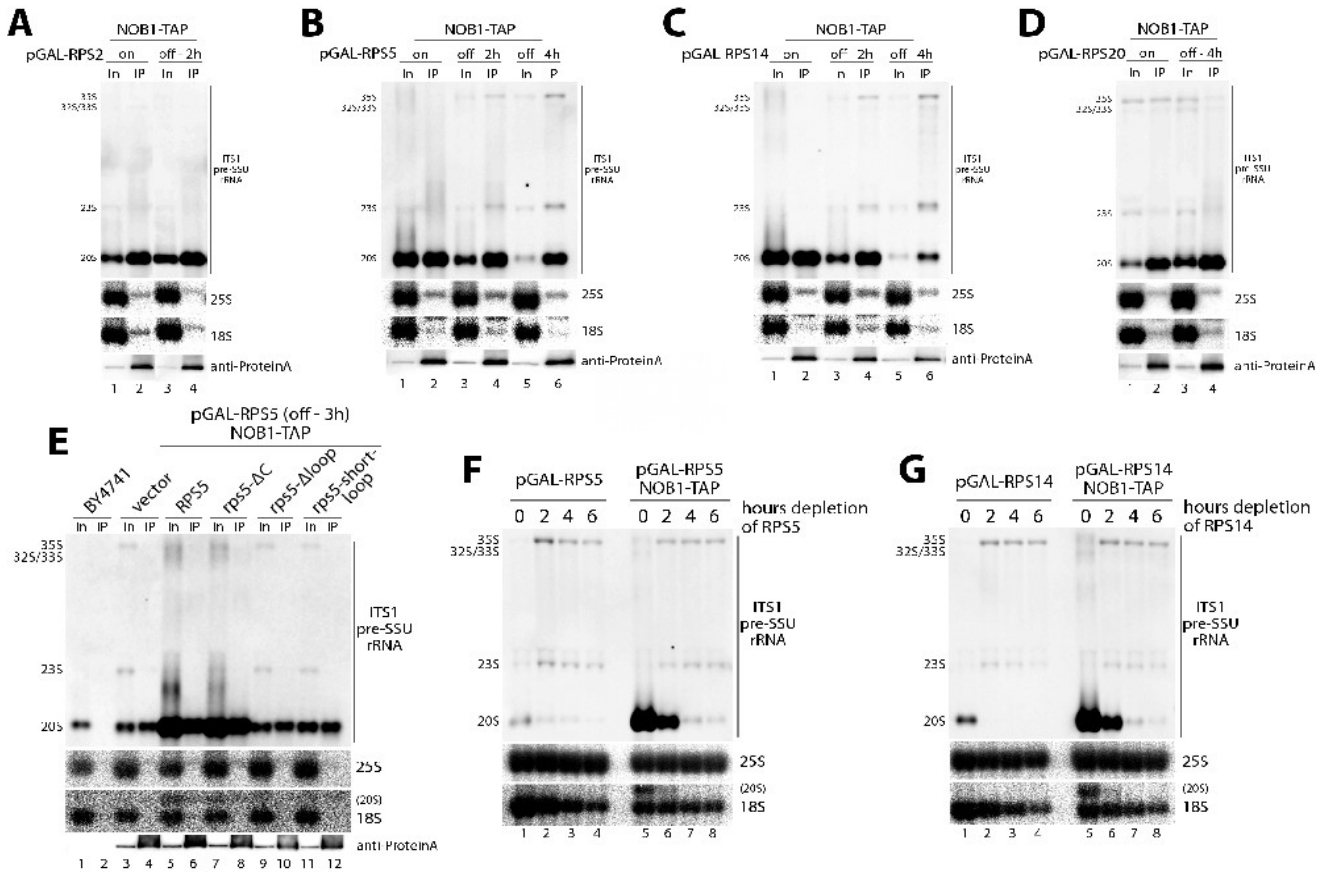

Figure 48. Analysis of Nob1p-TAP interactions with SSU precursors after depletion of various r-proteins of the small subunit

(**A**)-(**E**) Northern blot analysis of RNA co-purified with TAP-tagged Nob1p. RNA was extracted from Input (In) and immuno-purified (IP) fractions. Probes used for detection of (pre-) rRNA species are depicted right-hand. 200 mM salt (KCl, see 5.2.7.1) was used for cell breakage, binding and washing of the immunoprecipitations. Cells were grown overnight in YP-galactose, diluted in YP-galactose and subsequently expression of pGAL-RPSX was shut down in YP-glucose medium for the time indicated. (**A**) Yeast strain ToY2065, in which RPS2 is under control of the GAL1 promoter and Nob1p is TAP-tagged. (**B**) Yeast strain ToY1765, in which RPS5 is under control of the GAL1 promoter and Nob1p is TAP-tagged. (**C**) Yeast strain ToY2067, in which RPS14 is under control of the GAL1 promoter and Nob1p is TAP-tagged. (**D**) Yeast strain ToY2066, in which RPS20 is under control of the GAL1 promoter and Nob1p is TAP-tagged. (**E**) Yeast strain ToY1765, in which RPS5 is under control of the GAL1 promoter and Nob1p is TAP-tagged was transformed either with an empty vector (YEplac181) or vectors coding for HA-tagged full length rpS5 (ToP1162), rpS5-ΔC (ToP1156), rpS5-Δloop (ToP1157) or rpS5-short-loop (ToP1158) under the control of a constitutive promoter. Cells were grown overnight in selective media containing galactose, diluted in YP-galactose and subsequently expression of pGAL-RPS5 was shut down for 3 hours in YP-glucose medium. Nob1p-TAP associated SSU precursors were purified from these strains as described before. (**F**) and (**G**) Steady state (pre-) rRNA processing analyses of pGAL-RPS5 or pGAL-RPS14 with or without TAP-tagged NOB1. Cells were grown overnight in YP-galactose, diluted in YP-galactose and subsequently expression of pGAL-RPSX was shut down in YP-glucose medium for the time indicated. At each time point 1 OD(600) of cells was harvested, RNA was extracted and analyzed by Northern blotting. Probes used for detection of (pre-) rRNA species are depicted right-hand. (**F**) Yeast strains pGAL-RPS5 (ToY1659) and pGAL-RPS5 + NOB1-TAP (ToY1765). (**G**) pGAL-RPS14 (ToY1658) and pGAL-RPS14 + NOB1-TAP (ToY2067).

2.3.2 20S pre-rRNA might be stabilized through TAP-tag fusion of Nob1p

In strains depleted for rpS5 or rpS14, a potential 20S pre-rRNA processing delay or protection of this pre-rRNA species from degradation was already visible on steady state rRNA analysis (Figure 48 F and G, see also 2.3.1). Several generation times after depletion of GAL1-promoter driven rpS14 expression this effect is plainest visible, since a small amount of 20S pre-rRNA could still be detected (Figure 48 G, lane 8).

A possible explanation for the higher ratio of newly synthesized 20S to 18S rRNA when full length rpS5 was expressed (compare 20S to 18S ratio in Figure 49 A and B, lanes 5 to 8) might be reduced endonucleolytic activity of TAP-tagged Nob1p. If one compares the levels of newly made 20S pre-rRNA over time, in the strains expressing rpS5-ΔC with or without TAP-tagged Nob1p, while in both no final pre-18S rRNA maturation occurred, 20S pre-rRNA accumulated in the Nob1p-TAP strain (compare 20S levels in Figure 49 A and B, lanes 9 to 12).

It is tempting to speculate that Nob1p mediated D-site processing still occurs in all these cases, but maybe due to misfolded rRNAs or unstable assembly of r-proteins, the immature subunits become degraded. TAP-tag fusion of Nob1p may lead to reduced nuclease activity and thereby to an apparent stabilization of precursor subunits (see also discussion in 3.3).

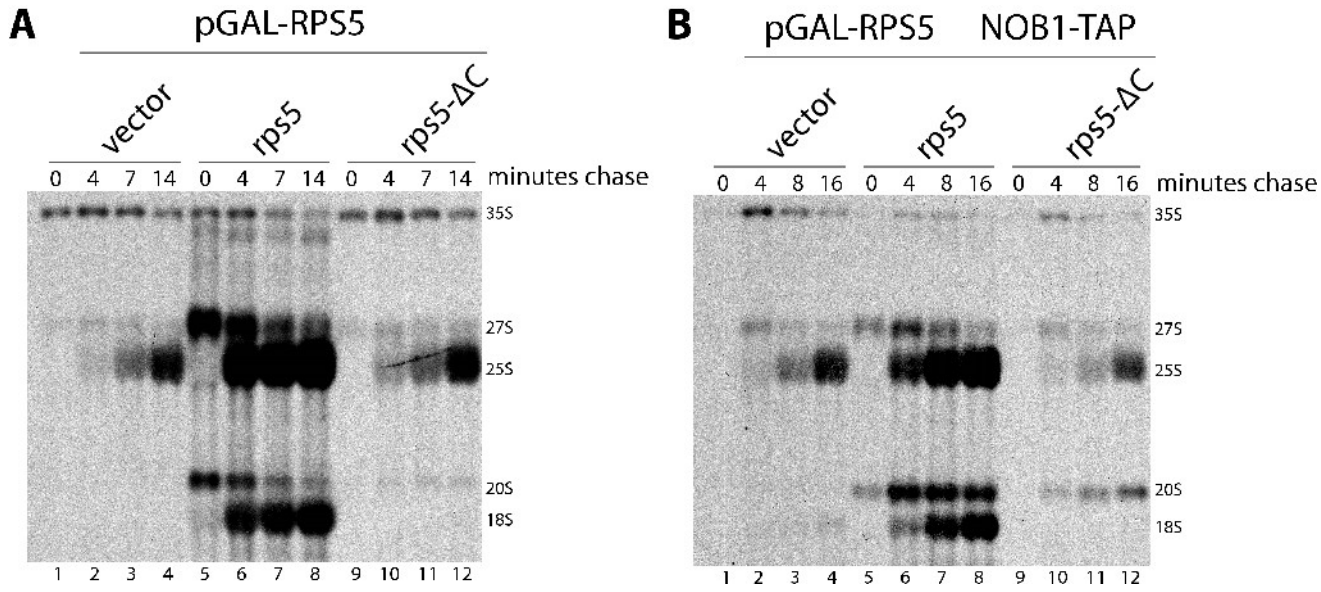

Figure 49. Pulse-chase analysis of newly synthesized rRNA in pGAL-RPS5 with or without NOB1-TAP

(**A**) and (**B**) The subsequently described strains were transformed with an empty vector (YEplac181) or vectors coding for HA-tagged full length rpS5 (ToP1162) or rps5-ΔC (ToP1156) under the control of a constitutive promoter. Cells were grown overnight in selective media, diluted in YP-galactose and expression of pGAL-RPS5 was shut down for 2 hours in YP-glucose medium. The cells were pulsed with 5',6'-[^{3}H] uracil for 5 minutes at 30°C and chased with non-marked uracil for the time indicated. Total RNA was extracted and separated by gel electrophoresis, radio-labeled RNA was visualized by fluorography (see also 5.2.5.4). (**A**) Yeast strain ToY1659 (pGAL-RPS5) was transformed with the above described HA-tagged alleles and analyzed by pulse-chase labeling. (**B**) Yeast strain ToY1765 (pGAL-RPS5 + NOB1-TAP) was transformed with the above described HA-tagged alleles and analyzed by pulse-chase labeling.

3 Discussion and perspective

3.1 Conservation of r-protein – rRNA interactions between Eukarya and Archaea

Eukarya and Archaea share a large set of ribosomal proteins (see 1.2.1). 28 out of 32 r-proteins of the small subunit have homologues in the other evolutionary kingdom. Taking advantage of this vast overlap, various archaeal r-proteins were tested in this work, whether they are able to substitute their eukaryotic counterparts in some functions during ribosome biogenesis. In a broad screen, ribosomal proteins of the small subunits from *T. acidophilum* and *S. acidocaldarius*, both model organisms of Euryarcheota and Crenarchaeota, respectively, were examined for their ability to interact with (pre-) rRNA species in *S. cerevisiae*. To quite a surprise, many of the archaeal r-proteins were indeed able to co-precipitate (pre-) rRNAs when expressed in yeast (see Supplemental Table 4).

The archaeal homologue of rpS20 from *T. acidophilum* (TAS20) could actually completely substitute yeast rpS20 *in vivo*, accordingly expression of TAS20 in *S. cerevisiae* restored new synthesis of mature 18S rRNA (see 2.2.6). In contrast, the corresponding r-protein from *S. acidocaldarius* (SAS20) didn't promote 18S 3'-end maturation, yet it was stably incorporated into nascent subunits. Variants of both archaeal r-proteins also efficiently co-precipitated pre-18S rRNAs (see 2.2.6).

Two further examples of archaeal r-proteins, which strongly interacted with pre-40S subunits are the homologues of rpS15 from *T. acidophilum* – TAS15 and *S. acidocaldarius* – SAS15 (see 2.2.1.2). These variants were not only efficiently incorporated into precursor subunits, but also into mature ribosomes. At elevated temperatures the rpS15 variant from *S. acidocaldarius* complemented near-complete all the essential functions of eukaryotic rpS15 (see 2.2.1.1). A tempting explanation for this observation is that these r-proteins, derived from thermophilic organisms, are more correctly folded at higher temperatures. Of course it can not be ruled out that this effect is mediated by expression of any (RNA) chaperones, or slight mis-folding is compensated due to higher flexibility of rRNA structure. RpS15 depletion in yeast results in destabilized assembly of a subset of head domain binding r-proteins (Ferreira-Cerca et al., 2007). Two of the most affected r-proteins, rpS3 and rpS19 were again stably incorporated into 20S pre-rRNA containing precursor subunits upon expression of both archaeal r-proteins. *In vivo* assembly of the two variants apparently structures the pre-rRNA in a way that the binding sites of the missing head domain r-proteins are created or become accessible. Since rpS15 is localized at the subunit interface and in very close proximity to the mRNA channel (Bulygin et al., 2002; Chandramouli et al., 2008; Taylor et al., 2009), there is a high probability that it is also directly involved in translation. TAS15, even more than SAS15, promoted production of a small population of newly synthesized 18S rRNA at 37°C (see 2.2.1.3). First of all, a low level of 18S rRNA synthesis

conclusively is sufficient to produce functional ribosomes in adequate numbers. Maybe the *de novo* emergence of about 2000 ribosomes per minute in a logarithmically growing yeast cell is not reached (Warner, 1999), but ribosome biogenesis is fast enough to allow constant growth. Secondly, TAS15 copied the phenotype of SAS15 regarding incorporation into (pre-) 40S subunits, rRNA processing and new synthesis of 18S rRNA, but nevertheless it didn't support growth after shutdown of rpS15 (see 2.2.1.1). Hence SAS15 is most probably able to overtake additional role(s) in ribosome function.

Another approach to study conserved functions of ribosomal proteins was based on truncation of eukaryotic specific extended primary sequence parts. Deletion of the N-termini of rpS2 (see 2.2.3.1), rpS5 (see 2.2.4.1) and rpS11 (rpS11-ΔN (ΔM1-R33)) or the C-termini of rpS0 (rpS0-ΔC (ΔA216-W252)) and rpS24 (rpS24-ΔC (ΔA103-D135)) caused no lethal phenotypes. In some cases the truncated protein was slightly less incorporated into pre-40S subunits or mature ribosomes (rpS11-ΔN and rpS24-ΔC, see Supplemental Figure 4) or comprised some minor growth defects (rpS2-ΔN, see 2.2.3.1). Some truncated r-proteins showed reduced resistance to anisomycin or rapamycin (see Supplemental Figure 5). Anisomycin is a bacterial antibiotic from *Streptomyces griseolus* and, next to other effects, inhibits peptidyl-transferase activity by mimicking the amino acid chain of aminoacyl tRNAs at the A-site (Hansen et al., 2003). Rapamycin, a macrolide antibiotic from *Streptomyces hygroscopicus*, inhibits TOR (**t**arget **o**f **r**apamycin) kinases and by this, among others, ribosome biogenesis (Sabatini et al., 1994; Mayer and Grummt, 2006). So very likely the eukaryotic specific protein parts, even if they are not absolute required for growth, provide yeast cells with some advantages under non-optimal growth conditions.

Interestingly, eukaryotic rpS2 is post-translational covalently modified by an arginine methyltransferase (PRMT3, homologues in function to yeast Rmt1p), which blocks ubiquitination and following degradation (Bachand et al., 2004; Lipson et al., 2010). Deletion of some of the modification sites (see Figure 29 B, rpS2-ΔN or rpS2-RRAA) resulted in appearance of a C-terminal degradation product. Covalent modifications of r-proteins (Mangiarotti, 2002; Mazumder et al., 2003) are supposed to contribute to ribosomal pools with varying cellular functions, as proposed by the “ribosome filter hypothesis”. This hypothesis states that gene expression is as well regulated by mRNA-specific translation of heterogeneous ribosomes (Mauro and Edelman, 2002). This heterogeneity can be achieved e.g. by differences in the rRNA itself (differences in rRNA species (5.8S$_S$ or 5.8S$_L$ rRNA), nucleotide polymorphism, base modification), modifications of r-proteins, the existence of non-identical r-protein paralogs or ribosomal protein composition (non-essential r-proteins) (for recent review see (Mauro and Edelman, 2007)).

On the other hand, deletion of the vast eukaryotic specific C-termini of rpS6 (rpS6-ΔC (ΔK131-A236), see Supplemental Figure 4) and rpS17 (see 2.2.2.3) resulted in a lethal phenotype and strong pre-rRNA processing defects. Both truncated r-proteins, however, efficiently co-precipitated pre-18S rRNAs (see 2.2.2.3 and Supplemental Figure 4).

Furthermore, it could be demonstrated that the C-terminus of rpS17 is specifically required for 3'-end maturation of 18S rRNA and enhances incorporation of rpS17 into mature subunits (see 2.2.2.2 and 2.2.2.3).

Some interesting conclusions can be drawn due to the fact that archaeal r-proteins or the evolutionary conserved eukaryotic r-protein parts are solitary able to bind and structure eukaryotic ribosomal RNAs: The way of folding of the 18S rRNA core structure, meaning the part which is related to prokaryotic 16S rRNA, seems to be conserved. Apart from this, extra sequences of 18S rRNA, the so-called expansion segments, might be structured through binding of eukaryotic specific r-proteins. Yeast SSU precursor subunits which incorporated archaeal ribosomes are mostly able to leave the nucleus (see also 3.3), but are not finally matured in the cytoplasm, speaking for a very tight control of final cytoplasmic SSU maturation (see also 3.2).

3.2 The influence of ribosomal proteins on final pre-18S rRNA maturation

Previous work suggested that some SSU r-proteins assemble at a later stage of 40S biogenesis in yeast (Ferreira-Cerca et al., 2005, 2007). Strikingly, depletion of one of these r-proteins very often resulted in a 20S pre-rRNA maturation defect. This observation was an indication that these r-proteins are required for this specific processing step, yet their exact molecular function is still obscure. Ribosomal proteins, which are required for 20S pre-rRNA processing are localized all over the head domain and include the two r-proteins binding in the neck region (rpS0, rpS2) (see Figure 8). Therefore it is very unlikely that a direct contact of one of these r-proteins regulates e.g. the enzyme activity of the nuclease mediating the D-site cut. Furthermore, no one knows how their binding/absence is communicated and translated to allow/block 20S pre-rRNA processing. The variants created in this work are an ideal basis to test different hypotheses, how final pre-18S rRNA maturation might be regulated.

The two ribosomal proteins binding in the neck region – rpS0 and rpS2 – are both needed for D-site cut processing (Tabb-Massey et al., 2003; Ferreira-Cerca et al., 2005). As the analogy of SSU structure already connotes, these “neck region” r-proteins might help to stabilize the head – body orientation. And indeed mutations in the hairpin of rpS2, which interacts with head domain rRNA, attenuated the efficiency of D-site cut processing (see 2.2.3.2). Exchange of arginine and lysine residues to alanines most probably destroys the rpS2-rRNA interactions, thus rendering the 20S pre-rRNA containing particles more flexible and less defined as a substrate for processing.

Like the wobbly neck, due to mutations in the hairpin of rpS2, the consequences caused by rpS20 depletion or expression of one of its variants, likewise need to be forwarded to the

spatial distant 18S 3'-end. As already discussed, the archaeal homologue from *T. acidophilum* (TAS20) could substitute rpS20 in vivo (see 2.2.6.1). SAS20, the homologue from *S. acidocaldarius* could not rescue the loss of eukaryotic rpS20 (see 2.2.6.1). These two variants therefore offered the possibility for detailed analysis of rpS20 function(s) in ribosome biogenesis, in particular its role in 18S 3'-end maturation. Through exchange of large protein parts among themselves, it could be demonstrated that the correct molecular structure of the hairpin of rpS20 is required for efficient D-site cut processing (see 2.2.6.2). The amino acid composition at the tip of this hairpin is of special interest for r-protein function. The non-complementing variant SAS20 displays two additional positive charges at the tip (SAS20 K59 and K61). An exchange of this lysines with the corresponding residues of TAS20 and rpS20, respectively, resulted in a partly suppressed rpS20 depletion phenotype (see 2.2.6.2, SAS20-KKTT, SAS20-K59T, SAS20-K61T). Head domain assembly state remained largely unaffected upon depletion of rpS20 (see 2.2.6.3). What's more, mass spectrometric analysis of r-protein composition showed no major disturbance in precursor particles containing SAS20 (see 2.2.6.4). The difference in functional complementation of TAS20 and SAS20 is also not due to changed association of ribosome biogenesis factors. In both strains, 40S precursor particles, purified via Rio2p or the FLAG-tagged variant, were well associated with virtually all late acting biogenesis factors, including Nob1p (see 2.2.6.4). Thus most probably rpS20 is needed for formation of the correct head domain structure, thereby influencing the efficiency of D-site cut processing.

Tiny changes in r-protein structure, as well as of course absence of a r-protein are mirrored in changes of (pre-) rRNA folding and might be passed over to a “SSU defectiveness sensor”. As mentioned before, it is very unlikely that spatial distant effects (e.g. rpS20 is localized about 50Å away on the other side of the head domain in respect to the 18S 3'-end; see Figure 42), directly influence the activity of the nuclease mediating the D-site cut. Therefore a read-out mechanism has to exist, which senses the maturation state of pre-40S subunits and by this allows or blocks 18S 3'-end processing. Such a potential read-out for the maturation state of 40S precursors is the local environment around the 18S 3'-end, comprised of rpS5 and rpS14 (maybe additional other eukaryotic specific r-proteins) and several ribosome biogenesis factors.

Depletion of the platform component rpS14 leads to a strong block of sites A_0, A_1, A_2 processing and nuclear accumulation of 40S precursor subunits (Moritz et al., 1990; Jakovljevic et al., 2004; Ferreira-Cerca et al., 2005). The protein binds in close proximity to the 18S 3'-end and amino acid substitutions of positively charged C-terminal residues resulted in accumulation of cytoplasmic 20S pre-rRNA, apparently abrogating the early processing defects seen upon rpS14 depletion (Jakovljevic et al., 2004). Similar mutations of positively charged residues at the surface of rpS14 strongly delayed 20S pre-rRNA processing (see 2.2.5). These amino acids might contribute to a stable head-body orientation through direct contact with rpS5 or could help to position precursor rRNA sequences in a way

to generate a suitable substrate for processing. Although rpS14 is one of the primary binders of the 18S central domain and is required to build the platform, it is also required for D-site cut processing. In this case physical proximity correlates directly with function in pre-rRNA processing.

Ribosomal proteins for which this correlation might as well be true are other potential components of the local environment around the 18S 3'-end. One of these could be rpS26, which is predicted to bind next to rpS14 at the platform (Malygin et al., 2009). Interestingly rpS26, as a platform binding r-protein, is not required for early pre-rRNA processing steps and nuclear export of pre-SSUs, giving another argument for late assembly (Ferreira-Cerca et al., 2005). A further possible constituent is rpS28, whose stable assembly with SSU precursors depends to some extent on the presence of the C-terminus of rpS5 (see 2.2.4.6). Site directed cross-linking of individual mRNA nucleotides in translation initiation complexes with ribosomal proteins and rRNA suggested that both proteins bind in the neighborhood of rpS5 and rpS14 (Pisarev et al., 2008a).

The first essential role of rpS5, the primary binder of the SSU head domain, is nucleation of head domain folding and thereby stabilizing the incorporation of other head domain r-proteins, which leads to efficient 20S pre-rRNA production and nuclear export competence of pre-SSUs (Ferreira-Cerca et al., 2005, 2007). In this work, a second role for rpS5 as a component of the local environment around the 18S 3'-end could be shown. Both, shortening of the rpS5 hairpin (rpS5-short-loop) and its highly conserved C-terminal helix (rpS5-ΔC) resulted in restoration of new synthesis of 20S pre-rRNA (see 2.2.4.2 and 2.2.4.3). While the hairpin of rpS5 was required for stable incorporation into mature subunits (see 2.2.4.2), its C-terminal part was negligible for stable incorporation into (pre-) 40S subunits (see 2.2.4.3). What's more, the 20S pre-rRNA containing precursor particles were exported when expressing the rpS5-ΔC or rpS5-short-loop variant, though with delayed kinetics (see 2.2.4.4). This delay is maybe due to destabilization of stable incorporation of certain r-proteins into nascent SSUs when expressing the rpS5-short-loop variant, in particular the secondary binders rpS15 and rpS16 (see 2.2.4.5). The truncation of the seven C-terminal amino acids had only mild effects on the SSU assembly status, i.e. rpS28 was the only head domain r-protein, whose binding remained largely destabilized (see 2.2.4.6). Taken together, the results suggest that the globular domain of rpS5 is sufficient for incorporation into nascent ribosomes and formation of a crude head domain assembly, as well as to allow a basal level of nuclear export and new synthesis of 20S pre-rRNA. The C-terminus of rpS5, on the other hand, is specifically required for processing of 20S pre-rRNA in the cytoplasm.

The question remains, which prerequisite for proceeding 18S 3'-end maturation is missing? One possible explanation would be absence of non-ribosomal factors that are required for this particular pre-rRNA processing step. The kinase Rio2p (Vanrobays et al., 2003), together with other ribosome biogenesis factors, many of them required for efficient 20S pre-rRNA processing, is part of a cytoplasmic protein complex (Merl et al., 2010). This complex

includes another kinase Hrr25p (Schäfer et al., 2006), the snoRNA binding protein Enp1p (Chen et al., 2003), the rRNA interacting factors Krr1p (Sasaki et al., 2000) and Tsr1p (Gelperin et al., 2001), the methyltransferase Dim1p (Lafontaine et al., 1994, 1995) and the non-essential protein Ltv1p (Seiser et al., 2006a; Fassio et al., 2010b). It was suggested that this protein complex forms independently of pre-rRNA synthesis (Merl et al., 2010). Nob1p, a PIN-domain containing nuclease (Fatica et al., 2003, 2004) and its interacting factor Pno1p/Dim2p (Vanrobays et al., 2004) were as well associated with the Rio2p complex, but in a pre-rRNA dependent manner (Merl et al., 2010). Purification of Rio2p-TAP associated RNPs in yeast strains expressing different r-protein variants and comparison of their protein contents indicated that all just mentioned biogenesis factors are more or less quantitative associated with precursor particles containing the variant r-proteins (see 2.2.4.7 and 2.2.6.4). FLAG-tag purifications of r-protein variants fully support these observations (see Table 11, Table 12 and Table 15).

Biogenesis factors that are possible constituents of the local environment around the 18S 3'-end are Nob1p and its co-factor Pno1p/Dim2p. Nob1p protects rRNA sequence around the D-site from chemical modification and is believed to be the endonuclease for D-site cut processing (Fatica et al., 2003, 2004; Lamanna et al., 2009; Pertschy et al., 2009a). Dim1p, whose putative bacterial orthologue KsgA crosslinks nearby with SSU rRNA (Xu et al., 2008), is another possible component. Furthermore, the transient interaction of rpS14 and Fap7p suggests binding of the latter one in proximity to the 18S 3'-end (Granneman et al., 2005). It was postulated that D-site cut processing is happening concurrent with a larger conformational change of 3'-18S rRNA and ITS1 pre-rRNA sequences, maybe mediated by the helicase Prp43p, which in addition shows genetic interactions with Nob1p (Lebaron et al., 2005; Pertschy et al., 2009b; Bohnsack et al., 2009).

To summarize, transient binding of all these components might protect the head-platform interface in a chaperone-like way from non-productive interactions with abundant cytoplasmic (translation related) factors, thereby opening a time window for final folding and assembly events. Remarkably, also in prokaryotes, final in vivo maturation of SSUs was suggested to depend on factor mediated assembly and/or folding events in the head-platform interface (Sharma et al., 2005).

The interaction of Nob1p, the nuclease presumably responsible for final 18S rRNA maturation, with nascent SSUs seems to be independent of platform or head domain r-protein assembly state. RNA co-immunoprecipitation experiments showed that after depletion of rpS5 or rpS14, both primary binders of their respective domain, TAP-tagged Nob1p still very efficiently interacted with the remaining 20S pre-rRNA (see 2.3.1). Interestingly, the co-immunoprecipitation experiments suggested that Nob1p exists in only sub-stoichiometrically amounts and that binding could be saturated with 20S pre-rRNA (see 2.3.1). Depletion of other head domain r-proteins (see 2.3.1, rpS2 and rpS20) or expression of rpS5 variants (see 2.3.1, E) seem not to interfere with pre-SSU binding of Nob1p. In

agreement with this, Nob1p solely binds *in vitro* with certain specificity pre-rRNA model substrates, while its endonucleolytic activity appears to be rather weak under these conditions (Lamanna et al., 2009; Pertschy et al., 2009a).

Taken these results into account, the simple presence of the putative nuclease does not mandatory lead to processing of pre-rRNA. The activity of the processing enzyme is in all probabilities modulated by the correct substrate conformation, rather than by regulating the enzyme itself. Such a mechanism was proposed for the maturation of 5S rRNA by RNase M5 (Pace et al., 1984; Stahl et al., 1984) and 23S rRNA by RNase Mini-III (Redko et al., 2009) in *Bacillus subtilis*. Binding of the r-proteins L18 and L3, respectively, is the prerequisite for establishment of a RNP conformation, appropriate for processing.

Most probably, a correctly formed head-platform interface, comprised of several r-proteins (rpS5, rpS14, rpS26, rpS28) and biogenesis factors (Nob1p, Pno1p/Dim2p, Dim1p), generates a local environment around the 18S 3'-end so that final conformational changes, possibly mediated by the helicase Prp43p, can take place and pre-rRNA cleavage by Nob1p is triggered. Since the formation of the head-platform interface will depend on the general assembly and folding state of the SSU head domain, the pre-rRNA processing phenotypes observed in many head domain assembly mutants can be explained hereby.

3.3 The role of ribosomal proteins in nuclear export and surveillance of nascent eukaryotic ribosomes

Previous observations already proposed that a well assembled head domain is one major prerequisite for efficient nuclear export of precursor subunits (Léger-Silvestre et al., 2004; Ferreira-Cerca et al., 2005, 2007). *In vivo* depletion of rpS5, the primary binder of the head domain, or the depletion of the secondary binder rpS15 results in a huge destabilization of binding of other head domain r-proteins (Ferreira-Cerca et al., 2007). Strikingly, none of the head domain r-proteins is absolutely required for early pre-rRNA cleavage events, leading to 20S pre-rRNA. New synthesis of 20S pre-rRNA is strongly delayed in strains depleted of rpS5 and rpS16, but a small amount of residual 20S pre-rRNA is still visible after depletion of both. On the other hand, the stable incorporation of r-proteins binding in the 5'- or central domain is not dependent on an assembled head domain (Ferreira-Cerca et al., 2007), while they are strictly required for generation of 20S pre-rRNA (Ferreira-Cerca et al., 2005). Yet these analyses have not shown, whether assembly of all or only a subset of head domain r-proteins are required for nuclear export of pre-40S subunits.

Many r-protein variants described in this work promoted the synthesis of 20S pre-rRNA. Although it became apparent that SSU precursors, which contained this 20S pre-rRNA, often reached the cytoplasm, they were rarely matured into final 40S subunits. These r-protein variants offered the possibility to investigate the prerequisites for nuclear export of SSU

precursors in more detail. Recent advances in mass spectrometric analyses and protein/RNP purification methods allowed comparative analyses of the protein content of different purifications. Exploiting this techniques and using RNA co-immunoprecipitation experiments of FLAG-tagged r-proteins as a complementary method, it was possible to characterize different pre-40S particles regarding their r-protein composition. Pre-SSUs which incorporated the rpS5-short-loop variant were exported, though with strongly delayed kinetics (see 2.2.4.4). In contrast, pre-SSUs which incorporated the rpS5-ΔC variant were very efficiently exported (see 2.2.4.4). Comparison of RNA co-precipitation by FLAG-epitope fused r-proteins showed that the head domain secondary binders rpS15 and rpS16 were less stable assembled in the strain expressing rpS5-short-loop (see 2.2.4.5 and 2.2.4.6). The destabilization of rpS3 binding might be an indirect effect, since its stable incorporation highly depends in the in vivo assembly of rpS15 (Ferreira-Cerca et al., 2007). RpS28 assembly on the other hands seems to be dispensable for ongoing nucleo-cytoplasmic transport of pre-SSUs (see 2.2.4.4 and 2.2.4.6). Mass spectrometric analyses of r-proteins, co-purified with TAP-tagged Rio2p, in the strains expressing either rpS5-ΔC or rpS5-short-loop were not reflecting the differences between both variants, which were observed in the RNA co-immunoprecipitations (see 2.2.4.7). A reason for this discrepancy could be that mature ribosomes often unspecific co-purify in TAP-tag purifications, thus decreasing the signal to noise ratio in the mass spectrometric analyses. In addition, it might be possible that Rio2p containing RNPs represent only a sub-population of all SSU precursor and one is selecting for example on export competent particles.

One interesting finding in this work was the observation that assembly of archaeal r-proteins promoted nuclear export of pre-40S subunits in the eukaryote S. cerevisiae. TAS15 and SAS15, both homologues of yeast rpS15 strongly interacted with 20S pre-rRNA and apparently structure SSU precursor particles in a way to restore efficient nucleo-cytoplasmic transport (see 2.2.1.4). It was shown that the stable incorporation of rpS3 and rpS19 into pre-SSUs was severely weakened upon in vivo depletion of rpS15 (Ferreira-Cerca et al., 2007). Expression of both archaeal variants restored stable assembly of these two most affected r-proteins, so most probably other head domain r-proteins can assemble as well (see 2.2.1.5). It is very unlikely that archaeal r-proteins can communicate directly with any parts of the eukaryotic import or export machinery. Therefore, upon re-establishment of head domain r-protein assembly status, potential contact sites for the export machinery, apart from the archaeal r-protein itself, emerge. Alternatively, the archaeal r-protein contributes to spatial organization of other r-proteins in a way that the hydrophilic rRNA core is shielded from the hydrophobic nuclear pore complex regions. In any case, the properties of the prokaryotic r-proteins are sufficient to promote nuclear export of pre-40S particles and no evolutionary gained functions of eukaryotic r-proteins are needed.

The endosymbiotic theory states that an eubacterial and an archaebacterial cell merged and the archaeal cell became the nucleus, gathering the advantage of motility through the

eubacterial cell (Mereschkowsky, 1905; Sagan, 1967). In this line of argumentation, ribosomes from the archaeal cell are the ancestors of the eukaryotic ones. It is not clear, which mechanism, until evolution of the nuclear pore complex, was responsible for nuclear export, in particular of ribosomal subunits. It has been speculated that a set of membrane associated export adapters, the so-called mREFs (**m**embraneous **r**ibosome **e**xport **f**actors) facilitated export through pores in the nuclear membrane during the first steps of eukaryotic evolution (Martin and Koonin, 2006; Ohyanagi et al., 2008a, 2008b). Another possibility is that a form of exocytosis could have been responsible for nucleo-cytoplasmic/archeal-eubacterial transport. To be able to regulate ribosome biogenesis independently from other processes and gain the ability of further quality control mechanisms, maybe also prevent unproductive translation in the nucleus, it might have been useful to evolve eukaryotic specific additional pre-subunit maturation events. Pre-40S subunits are finally matured in the cytoplasm (among others (Rouquette et al., 2005; Ferreira-Cerca et al., 2005)) and there is a large amount of evidence that also the large subunit undergoes final maturation not till reaching the cytoplasm (among others (Kemmler et al., 2009; Thomson and Tollervey, 2010; Panse and Johnson, 2010)). Not all of the enzymes required for these maturation events are conserved between Prokarya and Eukarya, hence this might be the reason that archaeal r-proteins promote nuclear export, but don't allow cytoplasmic pre-18S rRNA processing.

Nuclear export competence of pre-SSUs is therefore most likely a consequence of a certain head domain r-protein assembly status. Depletion of many ribosome biogenesis factors and r-proteins leads to nuclear retention of pre-ribosomal particles and subsequent degradation (see 1.4.6). By this, sensing nuclear export competence of precursor ribosomes is one critical quality control step in ribosome biogenesis.

A further quality control step, if misassembled pre-ribosomes escape nuclear degradation and reach the cytoplasm, e.g. in case of some head domain r-protein mutants, is the tight surveillance of cytoplasmic rRNA maturation events. In this work, the high significance of the head-platform interface in final 18S rRNA maturation was shown (see 3.2). In addition to its apparent importance in eukaryotic pre-rRNA processing, the head-platform interface is crucial for ribosome function. The translation initiation factors eIF1A, eIF1, eIF2A, eIF3 and eIF4G are thought to bind here (Lomakin et al., 2003; Siridechadilok et al., 2005; Pisarev et al., 2006; Passmore et al., 2007; Yu et al., 2009), rpS5 and rpS14 seem to contribute to the mRNA channel (Pisarev et al., 2008a) and rpS5 is one of the key players in IRES (internal ribosome entry site) dependent translation initiation (Fukushi et al., 2001; Laletina et al., 2006). The prokaryotic homologue of rpS5, S7 is a functional component of the E-site and crosslinks to mRNAs and tRNAs (Dontsova et al., 1991; Döring et al., 1994; Fargo et al., 2001; Kurkcuoglu et al., 2008b). Accordingly, overexpression of C-terminal mutant alleles of the prokaryotic homologues of rpS5 and rpS14, S7 respectively S11, leads to perturbed ribosome function in E. coli (Robert et al., 2003).

The accurate conformation of the head-platform interface, which mirrors the actual assembly and folding state of nascent SSUs, seems to be crucial for efficient removal of ITS1 pre-rRNA sequences and recycling of any late biogenesis factors (see 3.2). This removal in turn strongly correlates with, or might even improve the capability of pre-SSUs to enter a productive translation cycle. By this mechanism improperly assembled/folded pre-SSUs are excluded from the translation process, hence the accuracy and fidelity of translation remain unimpaired and energy waste through non-productive translation factor interactions is avoided. In support to this, 20S pre-rRNA is virtually excluded from 80S and polysomal fractions in logarithmically growing yeast cells (see 2.2.4.8 and among others (Udem and Warner, 1973; Trapman and Planta, 1976)). In several mutants, which are defective in 20S pre-rRNA processing, the amount of mature 40S subunits strongly decreases, while the pool of 60S and translation factors increases (see for example Figure 37 vector). Under these conditions substantial portions of immature, 20S pre-rRNA containing SSUs seem to associate with initiation factors, 60S subunits and mRNA (see 2.2.4.8 and (Soudet et al., 2010)).

Two examples of variant r-proteins, whose expression leads to great amounts of 20S pre-rRNA accumulating in the cytoplasm, are the archaeal homologue of rpS20 – SAS20 (see 2.2.6.1) and the rpS5 variant – rpS5-ΔC (see 2.2.4.3). Furthermore, an enzymatic impaired Nob1p variant led to an apparent stabilization of 20S pre-rRNA (see 2.3.2). If pre-18S rRNA containing subunits are indeed able to form translation initiation complexes, it is possible that Nob1p mediated cleavage occurs after mRNA binding and probably even after subunit joining. In wildtype situation these matured 40S subunits are fully functional and can go on with elongation. In non-wildtype conditions, especially when pre-SSUs are only very subtle altered (see 2.2.4.3, 2.2.6.1 and 2.3.2), Nob1p might nevertheless cut, but the originating 18S containing 40S subunits are defective in switching to elongation mode and become degraded by pathways, which detect malfunctioning ribosomes (Cole et al., 2009; Lafontaine, 2010).

In conclusion, cytoplasmic processing of pre-18S rRNA may not be strictly required for nascent SSUs to engage in translation initiation, but it correlates clearly with full translation competence of newly synthesized SSUs. In wildtype like states, not yet fully assembled or folded SSUs are largely excluded from the translation process due to numeric and kinetic disadvantages in translation initiation when competing with fully matured free 40S subunits. Defective subunits escaping nuclear degradation pathways (for recent reviews see (Houseley and Tollervey, 2009; Lafontaine, 2010)) might eventually succeed to engage in translation, but will then be eliminated by backup pathways detecting abnormal, stalled ribosomal complexes (Cole et al., 2009; Soudet et al., 2010).

4 Summary – Zusammenfassung

Summary

Single ribosomal proteins are required for specific steps in eukaryotic ribosome biogenesis. Consequently, depletion of a certain r-protein leads to a block or delay in pre-rRNA maturation and/or transport of precursor subunits. However, the exact molecular functions of the r-proteins in these processes are still obscure. To accurately investigate the molecular functions and to determine possible multiple roles, variant r-proteins with partial functionality were created and their impact on ribosome biogenesis was analyzed.

One set of variant r-proteins was created based on the conservation of r-proteins between the evolutionary kingdoms. In this approach, archaeal r-proteins were expressed in yeast and assayed for conserved functions. The functional characterization of archaeal ribosomal proteins showed the ability of many of them to assemble *in vivo* into eukaryotic pre-ribosomes. This suggests that r-protein – rRNA interactions are widely conserved between Archaea and Eukarya. Interestingly, incorporation of two archaeal r-proteins into nascent ribosomal subunits promoted their subsequent nuclear export. Apparently, the role of the homologous eukaryotic r-protein in nucleo-cytoplasmic transport is based on evolutionary conserved features and not due to a gain of function in the course of evolution.

In an alternative approach, variant r-proteins were created based on current atomic structure models of eukaryotic small subunits, possibly giving insights into structure-function correlation of certain r-proteins. Thorough analysis of rpS5, the primary binder of the head domain revealed a dual role in ribosome biogenesis: A first one in the global organization of the SSU head domain. And a second one in establishment of a highly defined spatial arrangement in the head-platform interface of nascent SSUs that is required for efficient processing of the 18S rRNA 3'-end. This interface most probably senses the overall maturation/assembly state of the head domain of pre-SSUs. Thereby, many phenotypes caused by depletion of other head domain r-proteins can be explained.

Furthermore, functional characterization of several variants of rpS2, rpS14 and rpS20 indicated that final cytoplasmic 3'-end processing of eukaryotic 18S rRNA not only depends on a certain protein composition of small ribosomal subunit precursors, but also on their exact conformational state. RNA co-immunoprecipitation experiments and mass spectrometric analyses showed that the sole assembly of the putative nuclease, mediating the final maturation step of SSU precursors, is not sufficient to trigger removal of pre-rRNA sequences. The occurrence of this processing step is therefore consequence of a highly defined assembly and folding state of nascent small ribosomal subunits and might directly correlate with their capability to function in translation.

Zusammenfassung

Einzelne ribosomale Proteine werden für spezifische Schritte in der Ribosomen Biogenese von Eukaryonten benötigt. Demzufolge führt das Fehlen eines bestimmten ribosomalen Proteins zur Verzögerung bzw. Verhinderung von Vorläufer rRNA Reifungschritten und/oder dem Transport von Vorläufer Partikeln. Bis jetzt sind die genauen molekularen Funktionen der ribosomalen Proteine jedoch noch größtenteils unbekannt. Um diese genauer zu untersuchen und eventuelle, zusätzliche Funktionen aufzudecken, wurden veränderte ribosomale Proteine mit nur partieller Funktion hergestellt und der daraus resultierende Einfluss auf die Ribosomen Biogenese untersucht.

Ein Satz von veränderten ribosomalen Proteinen wurde basierend auf der Konservierung einiger ribosomaler Proteine in den evolutionären Königreichen hergestellt. Hierzu wurden die archaeellen ribosomalen Proteine in *S. cerevisiae* exprimiert und auf konservierte Funktionen hin untersucht. Durch funktionelle Charakterisierung von archaeellen ribosomalen Proteinen konnte gezeigt werden, dass diese *in vivo* in Vorläufer Ribosomen eingebaut werden. Dies deutet darauf hin, dass die grundlegenden Interaktionen von ribosomalen Proteinen und ribosomaler RNA weitgehend konserviert sind. Interessanterweise war dieser Einbau in zwei Fällen ausreichend, um den Kernexport von Vorläufer Ribosomen zu unterstützen. Offensichtlich ist die Funktion des entsprechenden eukaryontischen ribosomalen Proteins im Kernexport auf evolutionär konservierte Merkmale zurückzuführen und nicht auf erworbene Fähigkeiten im Laufe der Evolution.

In einem parallelen Ansatz wurden Varianten ribosomaler Proteine basierend auf aktuellen Strukturmodellen erstellt. Dies sollte Hinweise auf Struktur-Funktion Korrelation bestimmter ribosomaler Protein geben. Detaillierte Analyse von rpS5, dem primären Binder der Kopfdomäne, zeigte eine doppelte Rolle dieses Proteins in der Ribosomen Biogenese: Zum einen, in der generellen Organisation der Kopfdomäne der kleinen Untereinheit. Zum anderen, in der Etablierung einer hochgradig definierten räumlichen Anordnung des Kopfdomänen-Plattform Bereichs, der für den effizienten Ablauf des letzten Reifungsschritts der 18S rRNA benötigt wird. Veränderungen im Reifungs-, oder Assemblierungszustand der Kopfdomäne von Vorläufer Untereinheiten könnten folglich zu einer Störung der Anordnung dieses Bereichs führen. Durch diesen Mechanismus lassen sich viele der Phänotypen erklären, die durch Fehlen eines ribosomalen Proteins der Kopfdomäne entstehen.

Weiterhin gab die funktionelle Charakterisierung von Varianten der ribosomalen Proteine rpS2, rpS14, und rpS20 Hinweise darauf, dass die endgültige Reifung der 18S rRNA im Zytoplasma nicht nur von einer bestimmten Protein Zusammensetzung, sondern auch von der exakten dreidimensionalen Form der Vorläufer Ribosomen abhängt. RNA Ko-Immunpräzipitationen und Analysen durch Massenspektrometrie zeigten, dass die Anwesenheit der mutmaßlichen Nuklease, die den letzten Reifungsschritt in der Biogenese

der kleinen Untereinheit katalysiert, alleine nicht ausreichend ist, um den Reifungsschritt ablaufen zu lassen. Das Ablaufen dieses letzten Reifungsschrittes ist daher Konsequenz eines im hohen Maße definierten Assemblierungs- und Faltungszustands der Vorläufer Partikel. Zusätzlich könnte diese Reifung die Grundlage der vollen Funktionalität von kleinen ribosomalen Untereinheiten in der Translation sein.

5 Materials & Methods

5.1 Materials

5.1.1 *Escherichia coli* strains

Name	Genotype	Origin
XL1-Blue	*endA1 gyrA96(nal^R) thi-1 recA1 relA1 lac glnV44 F'[::Tn10 proAB$^+$ lacI^q Δ(lacZ)M15] hsdR17(r$_K^-$ m$_K^+$)*	Stratagene
DH5α	*F$^-$ endA1 glnV44 thi-1 recA1 relA1 gyrA96 deoR nupG Φ80dlacZΔM15 Δ(lacZYA-argF)U169, hsdR17(r$_K^-$ m$_K^+$), λ–*	Grant et al., 1990

5.1.2 *Saccharomyces cerevisiae* strains

all strains are haploid

ToY	Name	Genotype	Plasmids	Origin
85	RPS15-shuffle	his3-1,leu2-0,ura3-0,YOL040c::kanMX4	pFL38-pGalRPS15	Toulouse
89	pGal-RPS15	his3-1,leu2-0,ura3-0,YOL040c::kanMX4	pFL36-pGalRPS15	Ferreira-Cerca et.al., 2005
186	RPS2-shuffle	his3-1,leu2-0,ura3-0,met15-0,lys2-0, YGL123w::kanMX4	YCplac33-RPS2	Ferreira-Cerca et.al., 2005
193	RPS20-shuffle	his3-1,leu2-0,ura3-0,met15-0, LYS2,YHL015w::kanMX4	YCplac33-RPS20	Ferreira-Cerca et.al., 2005
198	RPS5-shuffle	his3-1,leu2-0,ura3-0,lys2-0, YJR123w::kanMX4	YCplac33-RPS5	Ferreira-Cerca et.al., 2005
206	BY4741	his3-1,leu2-0,met15-0,ura3-0		Euroscarf
207	BY4742	his3-1,leu2-0,lys2-0,ura3-0		Euroscarf
256	pGAL-RPS0	his3-1,leu2-0,lys2-0,met15-0,ura3-0, YLR048w::kanMX4,YGR214w::HIS3	YCplac111pGAL-RPS 0B	Ferreira-Cerca et.al., 2005
257	pGAL-RPS1	his3-1,leu2-0,met15-0,LYS2,ura3-0, YML063w::kanMX4,YLR441c::HIS3	YCplac111pGAL-RPS 1A	Ferreira-Cerca et.al., 2005
258	pGAL-RPS6	his3-1,leu2-0,lys2-0,met15-0,ura3-0, YBR181c::kanMX4,YPL090c::HIS3	YCplac111-pGALRPS 6A	Ferreira-Cerca et.al., 2005
259	pGAL-RPS9	his3-1,leu2-0,lys2-0,met15-0,ura3-0, YBR189w::kanMX4,YPL081w::HIS3	YCplac111-pGALRPS 9A	Ferreira-Cerca et.al., 2005
260	pGAL-RPS10	his3-1,leu2-0,lys2-0,met15-0,ura3-0, YMR230w::kanMX4,YOR293w::HIS3	YCplac111-pGALRPS 10A	Ferreira-Cerca et.al., 2005
261	pGAL-RPS13	his3-1,leu2-0,ura3-0, MET15,LYS2,YDR064w::kanMX4	YCplac111-pGALRPS 13	Ferreira-Cerca et.al., 2005
262	pGAL-RPS20	his3-1,leu2-0,met15-0,ura3-0, LYS2,YHL015w::kanMX4	YCplac111-pGALRPS 20	Ferreira-Cerca et.al., 2005
263	pGAL-RPS30	his3-1,leu2-0,MET15,LYS2,ura3-0, YOR182c::kanMX4,YLR287c-a::HIS3	YCplac111-pGALRPS 30B	Ferreira-Cerca et.al., 2005
286	pGAL-RPS2	his3-1,leu2-0,ura3-0,met15-0,lys2-0, YGL123w::kanMX4	YCplac111-pGAL-RP S2	Ferreira-Cerca et.al., 2005

ToY	Name	Genotype	Plasmids	Origin
288	pGAL-RPS23	his3-1,leu2-0,LYS2,met15-0,ura3-0, YPR132w::kanMX4,YGR118w::HIS3	YCplac111-pGAL-RPS23A	Ferreira-Cerca et.al., 2005
318	pGAL-RPS16	his3-1,leu2-0,met15-0,LYS2,ura3-0, YDL083c::kanMX4, YMR143w::HIS3	YCplac111-pGAL-RPS16A	Ferreira-Cerca et.al., 2005
323	pGAL-RPS5	his3-1,leu2-0,ura3-0,lys2-0, YJR123w::kanMX4	YCplac111-pGAL-RPS5	Ferreira-Cerca et.al., 2005
325	pGAL-RPS11	his3-1,leu2-0,lys2-0,met15-0,ura3-0, YBR048w::kanMX4,YDR025w::HIS3	YCplac111-pGAL-RPS11A	Ferreira-Cerca et.al., 2005
326	pGAL-RPS27	his31,leu20,ura3-0, YHR021c::kanMX4,YKL156w::HIS3	YCplac111-pGAL-RPS27B	Ferreira-Cerca et.al., 2005
327	pGAL-RPS3	his3-1, leu2-0, ura3-0, YNL178w::kanMX4	YCplac111-pGAL-RPS3	Ferreira-Cerca et.al., 2005
336	pGAL-RPS31	his3-1,leu2-0,ura3-0,MET15,lys2-0, YLR167w::kanMX4	YCplac111-pGAL-RPS31	Ferreira-Cerca et.al., 2005
364	pGAL-RPS17	his3-1,leu2-0,ura3-0, YDR447C::kanMX,YML024W::kanMX	pFL38-pGAL-RPS17	Toulouse
365	pGAL-RPS24	his3-1,leu2-0,ura3-0, YIL069c::kanMX4,YER074w::HIS3	YCplac111-pGAL-RPS24	Ferreira-Cerca et.al., 2005
396	RPS14-shuffle	his3-1,leu2-0,met15-0,lys2-0,ura3-0, YCR031c::HIS3Mx6,YJL191w::kanMX4	YCplac33-RPS14A	Ferreira-Cerca et.al., 2005
399	pGAL-RPS14	his3-1,leu2-0,met15-0,lys2-0,ura3-0, YCR031c::HIS3Mx6,YJL191w::kanMX4	YCplac111-pGAL-RPS14A	Ferreira-Cerca et.al., 2005
566	pGAL-RPS17	his3-1,leu2-0,ura3-0, YDR447C::kanMX,YML024W::kanMX	YCplac111-pGAL-RPS17A	ToY364, this study
567	pGAL-RPS19	ura3-0,leu2-0,his3-1, YOL121c::kanMX4,YNL302c::kanMX4	YCplac111-pGAL-RPS19A	ToY343, this study
595	pRPS28-FLAG-TAS20	his3-1,leu2-0,ura3-0,met15-0, YHL015w::kanMX4	YEplac195-pRPS28-FLAG-TAS20	ToY262, this study
845	pGAL-RPS20 (TRP)	his3-1,leu2-0,ura3-0,met15-0, LYS2,YHL015w::kanMX4	YCplac22-pGAL-RPS20	ToY193, this study
1198	pGAL-RPS20_new	his3-1,leu2-0,ura3-0,met15-0, LYS2,YHL015w::kanMX4	YCplac111-pGAL-RPS20_new	ToY193, this study
1217	pGAL-RPS15 (TRP)	his3-1,leu2-0,ura3-0,YOL040c::kanMX4	YCplac22-RPS15	ToY85, this study
1420	pGAL-RPS15 (TRP) TSR1-3Myc	his3-1,leu2-0,ura3-0, YOL040c::kanMX4,TSR1::Myc-HIS3	YCplac22-RPS15	ToY1217, this study
1422	pGAL-RPS15 (TRP) NOC4-HA3	his3-1,leu2-0,ura3-0, YOL040c::kanMX4,NOC4::HA3-HIS3	YCplac22-RPS15	ToY1217, this study
1497	pGAL-RPS17 (TRP)	his3-1,leu2-0,ura3-0, YDR447C::kanMX,YML024W::kanMX	YCplac22-pGAL-RPS17	ToY364, this study
1498	pRPS28-FLAG-RPS0	his3-1,leu2-0,lys2-0,met15-0,ura3-0, YLR048w::kanMX4,YGR214w::HIS3	YEplac195-pRPS28-FLAG-RPS0	ToY256, this study
1499	pRPS28-FLAG-RPS0 deltaC	his3-1,leu2-0,lys2-0,met15-0,ura3-0, YLR048w::kanMX4,YGR214w::HIS3	YEplac195-pRPS28-FLAG-RPS0deltaC	ToY256, this study
1500	pRPS28-FLAG-RPS2	his3-1,leu2-0,ura3-0,met15-0,lys2-0, YGL123w::kanMX4	YEplac195-pRPS28-FLAG-RPS2	ToY286, this study
1501	pRPS28-FLAG-RPS2 deltaN	his3-1,leu2-0,ura3-0,met15-0,lys2-0, YGL123w::kanMX4	YEplac195-pRPS28-FLAG-RPS2deltaN	ToY286, this study

ToY	Name	Genotype	Plasmids	Origin
1502	pRPS28-FLAG-RPS5	his3-1,leu2-0,ura3-0,lys2-0, YJR123w::kanMX4	YEplac195-pRPS28-FLAG-RPS5	ToY323, this study
1503	pRPS28-FLAG-RPS5 deltaN	his3-1,leu2-0,ura3-0,lys2-0, YJR123w::kanMX4	YEplac195-pRPS28-FLAG-RPS5deltaN	ToY323, this study
1504	pRPS28-FLAG-RPS11	his3-1,leu2-0,lys2-0,met15-0,ura3-0, YBR048w::kanMX4,YDR025w::HIS3	YEplac195-pRPS28-FLAG-RPS11	ToY325, this study
1505	pRPS28-FLAG-RPS11 deltaN	his3-1,leu2-0,lys2-0,met15-0,ura3-0, YBR048w::kanMX4,YDR025w::HIS3	YEplac195-pRPS28-FLAG-RPS11deltaN	ToY325, this study
1506	pRPS28-FLAG-RPS24	his3-1,leu2-0,ura3-0, YIL069c::kanMX4,YER074w::HIS3	YEplac195-pRPS28-FLAG-RPS24	ToY365, this study
1507	pRPS28-FLAG-RPS24deltaC	his3-1,leu2-0,ura3-0, YIL069c::kanMX4,YER074w::HIS3	YEplac195-pRPS28-FLAG-RPS24deltaC	ToY365, this study
1657	pGAL-RPS2 (TRP)	his3-1,leu2-0,ura3-0,met15-0,lys2-0, YGL123w::kanMX4	YCplac22-pGAL-RPS2	ToY186, this study
1658	pGAL-RPS14 (TRP)	his3-1,leu2-0,met15-0,lys2-0,ura3-0, YCR031c::HIS3Mx6,YJL191w::kanMX4	YCplac22-pGAL-RPS14A	ToY396, this study
1659	pGAL-RPS5 (TRP)	his3-1,leu2-0,ura3-0,lys2-0, YJR123w::kanMX4	YCplac22-pGAL-RPS5	ToY198, this study
1739	pGAL-RPS5 (TRP) RIO2-TAP	his3-1,leu2-0,ura3-0,lys2-0, YJR123w::kanMX4,YNL207W-TAP (URA3-KL)	YCplac22-pGAL-RPS5	ToY1659, this study
1740	pGAL-RPS5 (TRP) ENP1-TAP	his3-1,leu2-0,ura3-0,lys2-0, YJR123w::kanMX4,YBR247C-TAP (URA3-KL)	YCplac22-pGAL-RPS5	ToY1659, this study
1741	pGAL RPS20 (TRP) RIO2-TAP	his3-1,leu2-0,ura3-0,met15-0, LYS2,YHL015w::kanMX4,YNL207W-TAP (URA3-KL)	YCplac22-pGAL-RPS20	ToY845, this study
1742	pGAL-RPS2 (TRP) RIO2-TAP	his3-1,leu2-0,ura3-0,met15-0,lys2-0, YGL123w::kanMX4,YNL207W-TAP (URA3-KL)	YCplac22-pGAL-RPS2	ToY1657, this study
1765	pGAL-RPS5 (TRP) NOB1-TAP	his3-1,leu2-0,ura3-0,lys2-0, YJR123w::kanMX4,YOR056C-TAP (URA3-KL)	YCplac22-pGAL-RPS5	ToY1659, this study
2065	pGAL-RPS2 (TRP) NOB1-TAP	his3-1,leu2-0,ura3-0,met15-0,lys2-0, YGL123w::kanMX4,YOR056C-TAP (URA3-KL)	YCplac22-pGAL-RPS2	ToY1657, this study
2066	pGAL-RPS20 (TRP) NOB1-TAP	his3-1,leu2-0,ura3-0,met15-0, LYS2,YHL015w::kanMX4,YOR056C-TAP (URA3-KL)	YCplac22-pGAL-RPS20	ToY845, this study
2067	pGAL-RPS14 (TRP) NOB1-TAP	his3-1,leu2-0,met15-0,lys2-0,ura3-0, YCR031c::HIS3Mx6,YJL191w::kanMX4, YOR056C-TAP (URA3-KL)	YCplac22-pGAL-RPS14A	ToY1658, this study

5.1.3 Oligonucleotides

5.1.3.1 Oligonucleotides used for cloning

ToO	Name	Gene	Sequence
700	TAS0-BamHI-Start	TAS0	TTTTTTGGATCCATGGATGAAGAGATGCTAATT
701	TAS0-Stop-PstI	TAS0	TTTTTTCTGCAGTTAAATCTGGGCCTCGAAATC
702	TAS1-BamHI-Start-f	TAS1	TTTTTTGGATCCATGGCTGGCGAAAAAGCACAG
703	TAS1-Stop-PstI-r	TAS1	TTTTTTCTGCAGTCAGTTCTGGGCTATTGCCTC
704	TAS2-Stop-PstI-r	TAS2	TTTTTTGGATCCATGAGTGAAGAATGGGTTCCA
705	TAS2-BamHI-Start-f	TAS2	TTTTTTCTGCAGCTAATCCTTATGACCGCTAAC
706	TAS3-Stop-PstI-r	TAS3	TTTTTTGGATCCATGAAGGAGAGAAAGTTCATT
707	TAS3-BamHI-Start-f	TAS3	TTTTTTCTGCAGTTAAGATTCTTCAGCGTTTCC
708	TAS5-Stop-HindIII-r	TAS5	TTTTTTGGATCCATGCTATTCAACAAATACGAT
709	TAS5-BamHI-Start-f	TAS5	TTTTTTAAGCTTTTACCTTGCGGACTGTGCAAC
742	TAS31-Frame-PstI-r	TAS31	TTTTTTCTGCAGTGATTTACTTTTCTTTGCCTT
743	TAS31-BamHI-Start-f	TAS31	TTTTTTGGATCCATGCAGAAGAGAGAACTTTAT
744	TAS27-Stop-PstI-r	TAS27	TTTTTTCTGCAGTCATAGTACCTCTACTACCTC
745	TAS27-BamHI-Start-f	TAS27	TTTTTTGGATCCATGGCGGATGTTAAATTCGTA
746	TAS24-Frame-PstI-r	TAS24	TTTTTTCTGCAGTTTTGCCTCTTTCTGCTTCAA
747	TAS24-BamHI-ATGVal-f	TAS24	TTTTTTGGATCCATGGTGGATCTGATAATCAAGGAA
748	TAS20-XbaI-Start-f	TAS20	TTTTTTTCTAGAATGGTCTCCTATAAGGCAAGG
749	TAS20-Stop-PstI-r	TAS20	TTTTTTCTGCAGTTAACTTTTGATCTGTATCTC
750	TAS19-Stop-PstI-r	TAS19	TTTTTTCTGCAGTCAGATGAATTTCTGGAACGC
751	TAS19-BamHI-Start-f	TAS19	TTTTTTGGATCCATGGTTAGTGTCAAATACGTT
752	TAS17-Stop-PstI-r	TAS17	TTTTTTCTGCAGTCAGTTGAGAGAATTCTCCTC
753	TAS17-BamHI-Start-f	TAS17	TTTTTTGGATCCATGGGAAGTATCAGACCATTC
754	TAS16-Stop-PstI-r	TAS16	TTTTTTCTGCAGTCACCTGTAGGACTTCTGCTT
755	TAS16-BamHI-Val-f	TAS16	TTTTTTGGATCCGTGATAACTACCGGTAAGAGA
756	TAS15-Stop-PstI-r	TAS15	TTTTTTCTGCAGTCACTTCAGCGGCATGAACTT
757	TAS15-BamHI-Start-f	TAS15	TTTTTTGGATCCATGGTCGTTAATAAGCAGGGT
758	TAS14-Stop-PstI-r	TAS14	TTTTTTCTGCAGTCAGACCCTTCTCCCTCTCTT
759	TAS14-BamHI-Val-f	TAS14	TTTTTTGGATCCGTGAGACAGATGAATAAGACT
760	TAS13-Stop-PstI-r	TAS13	TTTTTTCTGCAGTCATCTCAGAACCTTACTTAG
761	TAS13-BamHI-Start-f	TAS13	TTTTTTGGATCCATGGCACGAATGCACACAAGA
762	TAS11-Stop-PstI-r	TAS11	TTTTTTCTGCAGTCATTGATTCACCTTTTCAAC
763	TAS11-BamHI-Start-f	TAS11	TTTTTTGGATCCATGTATACGCGTAATATTGGA
764	TAS9-BamHI-Start-f	TAS9	TTTTTTGGATCCATGGGAGATCCTAAATTTCAT
765	TAS8-Stop-PstI-r	TAS8	TTTTTTCTGCAGTTACTTCAGCAGCTTTGCGTT
766	TAS8-BamHI-Start-f	TAS8	TTTTTTGGATCCATGACGATATTTCAGGGTAAA
767	TAS6-BamHI-Start-f	TAS6	TTTTTTGGATCCATGGCTAATTCATTGGCAATC
768	TAS6-Flag-HindIII-r	TAS6	TTTTTTAAGCTTTTACTTATCGTCGTCATCCTTGTAATCCATAGCTTGC TGATCATCTTTCTT

ToO	Name	Gene	Sequence
769	TAS9-Flag-HindIII-r	TAS9	TTTTTTAAGCTTTTACTTATCGTCGTCATCCTTGTAATCCATTTCATCT GTCTCACCCTCCTC
848	rps0_deltaC_PstI	RPS0	TTACTGCAGTTAGATGGACCATGGTTGA
849	rps2_deltaN_BamHI	RPS2	TAAGGATCCATGGAAGAAAAGGGATGGG
850	rps11_deltaN_BamHI	RPS11	TAAGGATCCATGTGGTACAAGAATGCCG
851	rps11_rev_PstI	RPS11	CGCCTGCAGAAGATTCATGACTTTAAA
852	rps17_deltaC_PstI	RPS17	TTACTGCAGTTATTGCAATTTGAAAGAG
854	rps20_rev_PstI	RPS20	GCGCTGCAGGTAAATATGAATAGAA
855	rps16_rev_PstI	RPS16	GCGCTGCAGAAGTTGAATCGGTTTA
856	TAS17_SOE_revers	RPS17	TCTCTTTCTTCTTCGTTGAGAGAATTCT
857	TAS17_SOE_forward	RPS17	AGAATTCTCTCAACGAAGAAGAAAGAGA
858	TAS17+RPS17CTerm_rev_PstI	RPS17	GCGCTGCAGTTAAACTCTCTTTCTGTA
859	K349_PCR_Mut_for		AATGGATTACAAGGATGACGACGATAAGGGTACCGGATCC
860	K349_PCR_Mut_rev		CAGCTATGACCATGATTACGCCAAGCTTGCATGCCTGCAG
871	RPS20 GAL F	RPS20	CGCCGCGGATCCATGTCTGACTTTCAAAAG
902	RPS5delN_for_BamHI	RPS5	CGCGGATCCTTGTTCAACAAATGGTC
903	RPS5_rev_PstI	RPS5	GCGCTGCAGGTAGAGTGACTTAGAAA
904	RPS6delC_rev_PstI	RPS6	GCGCTGCAGTGGAACAGTAGTGTCAG
905	RPS24delC_rev_PstI	RPS24	GCGCTGCAGCTTTTCAACCTTTTCAGCC
932	SOE_TAS6_for	RPS6	AAAGATGATCAGCAAGCTAAGAGATTGGGTCCAAAG
933	SOE_TAS6_rev	RPS6	CTTTGGACCCAATCTCTTAGCTTGCTGATCATCTTT
934	SOE_RPS6CT_FLAG_rev_HindIII	RPS6	CGCAAGCTTTTACTTATCGTCGTCATCCTTGTAATCCATAGCCTTCAA AGAAGAAGC
1003	RPS6delC+5_rev_PstI	RPS6	GCGCTGCAGTGGACCCAATCTCTT
1004	SAS3_for_BamHI	RPS3	CGCGGATCCATGGTTCTTATAAAG
1005	SAS3_rev_PstI	RPS3	GCGCTGCAGTCAACTTCCAGAGGC
1006	SAS5_for_BamHI	RPS5	CGCGGATCCATGGTTGAGAATATT
1007	SAS5_rev_PstI	RPS5	GCGCTGCAGTTACCTAGAGCTTAA
1008	SAS20_for_BamHI	RPS20	CGCGGATCCATGCCTACTAAAGCC
1009	SAS20_rev_PstI	RPS20	GCGCTGCAGTCAAATTAGCTCAAT
1010	SAS26_for_BglII	RPS26	CGCAGATCTATGTTGCCAAAGAAG
1011	SAS26_rev_PstI	RPS26	GCGCTGCAGATACAATTTGGCTTT
1012	SAS27_for_BamHI	RPS27	CGCGGATCCATGAAGGCAAAGTTT
1013	SAS27_rev_PstI	RPS27	GCGCTGCAGTTAACCTAGTATTCT
1014	SAS30_for_BamHI	RPS30	CGCGGATCCATGCCTTCGCACGGT
1015	SAS30_rev_PstI	RPS30	GCGCTGCAGCCTTGCCACTGCTCT
1037	SOE20_1_for	TAS20 RPS20	ACAGAGTGGTTGACTTCGTGGTTAATCA
1038	SOE20_1_rev	SAS20 RPS20	TGATTAACCACGAAGTCAACCACTCTGT
1039	SOE20_2_N-Term-rev	TAS20 RPS20	GCGCCATGGGGACTCTTCCTGACAG

ToO	Name	Gene	Sequence
1069	SOE20_2_for	TAS20 RPS20	TCAGGAAGAGTCCTCATGGTGAGGGAAA
1070	SOE20_2_rev	SAS20 RPS20	TTTCCCTCACCATGAGGACTCTTCCTGA
1071	RPS3-S6A_for_BamHI	RPS3	CGCGGATCCATGGTCGCTTTAATCGCTAAGAAAAGAAAGC
1072	RPS3-T42+44A_for	RPS3	GAAGTCCGTGTCGCTCCAGCCAAGACCGAAGTT
1073	RPS3-T42+44A_rev	RPS3	AACTTCGGTCTTGGCTGGAGCGACACGGACTTC
1074	RPS3-T207A_for	RPS3	CCAGATGCTGTCGCCATCATTGAACCA
1075	RPS3-T207A_rev	RPS3	TGGTTCAATGATGGCGACAGCATCTGG
1076	RPS3-S221A_for	RPS3	ATTCTTGCTCCAGCTGTCAAGGACTAC
1077	RPS3-S221A_rev	RPS3	GTAGTCCTTGACAGCTGGAGCAAGAAT
1085	SAS13_for_BamHI	RPS13	CGCGGATCCTTGAATAAGAAGAGG
1086	SAS13_rev_PstI	RPS13	GCGCTGCAGTCAGTAGAGGGAACC
1087	SAS14_for_BamHI	RPS14	CGCGGATCCATGTCGAGCAGGCGT
1088	SAS14_rev_PstI	RPS14	GCGCTGCAGTTATACTCTTCTTCC
1089	SAS15_for_BamHI	RPS15	CGCGGATCCATGTCACCCGAAATT
1090	SAS15_rev_PstI	RPS15	GCGCTGCAGTCATCCCTTCATTGC
1091	SAS16_for_BamHI	RPS16	CGCGGATCCATGAGTCAGGCTGAA
1092	SAS16_rev_PstI	RPS16	GCGCTGCAGTCACCTGTACGCTTT
1099	SOE20_3_#1	RPS20	ATTCCTTTGCCGACAAAGAGGCTGGTGGTA
1100	SOE20_3_#2	RPS20	TACCACCAGCCTCTTTGTCGGCAAAGGAAT
1101	SOE20_3_#3	RPS20	CACTGGGAGATGAGAGTACATAAGAGAATA
1102	SOE20_3_#4	RPS20	TATTCTCTTATGTACTCTCATCTCCCAGTG
1134	SOE15_1_for	TAS15 SAS15	ATTTCTAGAGAAGGAAAGCAGAATAAAGTAGTGAAGACACAC
1135	SOE15_1_rev	TAS15 SAS15	ATTCTGCTTTCCTTCTCTAGAAATCTTTCTAAGCTTCTCCAT
1179	SAS20_KKTT_for	SAS20	CCCCATGGTGAGGGAACGAAAACGTGGGAGCATTGGGAA
1180	SAS20_KKTT_rev	SAS20	TTCCCAATGCTCCCACGTTTTCGTTCCCTCACCATGGGG
1260	SAS20_K59S_for	SAS20	CCCCATGGTGAGGGATCGAAAAAGTGGGAGCA
1261	SAS20_K59S_rev	SAS20	TGCTCCCACTTTTTCGATCCCTCACCATGGGG
1262	rps2_RRAA_for	RPS2	TTCAAAAGCAAACCGCAGCCGGTCAAGCAACCAGATTTAAGGC
1263	rps2_RRAA_rev	RPS2	GCCTTAAATCTGGTTGCTTGACCGGCTGCGGTTTGCTTTTGAA
1264	rps9_KKAA_for	RPS9	TTCGGTTTGAAGAACGCGGCGGAAATTTACAGAATT
1265	rps9_KKAA_rev	RPS9	AATTCTGTAAATTTCCGCCGCGTTCTTCAAACCGAA
1268	S5_R111A_for	RPS5	ATTAAAGGCTGTTGCAATCATCAAGCAC
1269	S5_R111A_rev	RPS5	GTGCTTGATGATTGCAACAGCCTTTAAT
1270	S5_RKAA_for	RPS5	GAAGCTGCTTTCGCAAACATCGCGACCATTGCTGAA
1271	S5_RKAA_rev	RPS5	TTCAGCAATGGTCGCGATGTTTGCGAAAGCAGCTTC
1365	RPS20T78A_for	RPS20	GGTGAAGGTTCTAAGGCTTGGGAAACCTACG
1366	RPS20T78A_rev	RPS20	CGTAGGTTTCCCAAGCCTTAGAACCTTCACC

ToO	Name	Gene	Sequence
1367	RPS20T78K_for	RPS20	GTGAAGGTTCTAAGAAGTGGGAAACCTACGAA
1368	RPS20T78K_rev	RPS20	TTCGTAGGTTTCCCACTTCTTAGAACCTTCAC
1369	SAS20_K59T_for	SAS20	CCATGGTGAGGGAACGAAAAAGTGGGAGC
1370	SAS20_K59T_rev	SAS20	GCTCCCACTTTTTCGTTCCCTCACCATGG
1371	SAS20_K61T_for	SAS20	AGGGAAAGAAAACGTGGGAGCATTG
1372	SAS20_K61T_rev	SAS20	CAATGCTCCCACGTTTTCTTTCCCT
1377	rps6delC+10	RPS6	GCGCTGCAGGTTGTTAGCTCTCTTT
1378	S2_full_del_for	RPS2	GACGAAGTCATGAACATCAAGGCTGTTGTCGTTGTT
1379	S2_full_del_rev	RPS2	AACAACGACAACAGCCTTGATGTTCATGACTTCGTC
1380	RPS2_APA_for	RPS2	GACGAAGTCATGAACATCGCTCCAGCTAAGGCTGTTGTCGTTGTT
1381	RPS2_APA_rev	RPS2	AACAACGACAACAGCCTTAGCTGGAGCGATGTTCATGACTTCGTC
1382	S2_short_loop_for	RPS2	CAAACCAGAGCCGGTCAAAGATTTAAGGCTGTTGTCGTTGTTGGTG ACTCTAACG
1383	S2_short_loop_rev	RPS2	TTGACCGGCTCTGGTTTGCTTCTTGATGTTCATGACTTCGTCTTGCAA ACCTGGC
1581	T15delN-15	TAS15	CGCGGATCCATGGCCAGGAAATCAAAG
1582	T15delN-30	TAS15	CGCGGATCCATGACATACAAGGGATAC
1587	RPS20S76K_for	RPS20	CAAATGGTGAAGGTAAGAAGACTTGGGAAAC
1588	RPS20S76K_rev	RPS20	GTTTCCCAAGTCTTCTTACCTTCACCATTTG
1589	RPS20S76A_for	RPS20	CAAATGGTGAAGGTGCTAAGACTTGGGAAAC
1590	RPS20S76A_rev	RPS20	GTTTCCCAAGTCTTAGCACCTTCACCATTTG
1591	RPS20_STKK_for	RPS20	CCAAATGGTGAAGGTAAGAAGAAGTGGGAAACCTACGAA
1592	RPS20_STKK_rev	RPS20	TTCGTAGGTTTCCCACTTCTTCTTACCTTCACCATTTGG
1818	ext_ITS1_1	ITS1	TGTATTGAAACGGTTTTAATT
1819	ext_ITS1_2	ITS1	GTAAAAGCTCTCATGCTCTTGCC
1828	Noc4_integr_for	Noc4	GACGGCGATAGCGAAGCGTC
1829	Tsr1_integr_for	Tsr1	CCTTGTACAAACGTATGTGGCCC
1830	RPS17delN_for_BamHI	RPS17	GCGGGATCCGAAGAAGAAAGAGAAAGA
1831	SAS17_for_BamHI	RPS17 SAS17	GCGGGATCCATGGGTAATGTATACACG
1832	SAS17_rev_PstI	RPS17 SAS17	GCGCTGCAGTTATGTTTCACTCTCTAAA
1880	nat1_for	NAT1	CGCGCTAGCTTAATTAAGGCGCGCCAGATC
1881	nat1_rev	NAT1	GCGGCTAGCATTACAACAGGTGTTGTCCTC
1913	S2-KRRAAA_for	RPS2	CAGTTCAAGCGCAAACCGCAGCCGGTC
1914	S2-KRRAAA_rev	RPS2	TGCGGTTTGCGCTTGAACTGGCTTGATG
1915	hph_for	hph HIS3MX6	ATGGGTAGGAGGGCTTTTGTAGAAAGAAATACGAACGAAACGAAA GCTAGCTTAATTAAGGCGCGCCA
1916	hph_rev	hph HIS3MX6	CAACACTCCCTTCGTGCTTGGGACTTCAGAACTTCCAGTAAGACTG CTAGCGTTAAAGCCTTCGAGCG
1917	S5delloopGG_rev	RPS5	TGGAGAACCACCTGGACCAGTGTTGGTGATAG
1918	S5delloopGG_for	RPS5	GGTCCAGGTGGTTCTCCATTGAGAAGAGTTAA

ToO	Name	Gene	Sequence
1919	S5delloop_rev	RPS5	AATGGAGATGGACCAGTGTTGGTGATAGC
1920	S5delloop_for	RPS5	CTGGTCCATCTCCATTGAGAAGAGTTAAC
1923	S14R133A_for	RPS14	GAAAGAAGGGTGGTAGAGCAGGTAGAAGATTATGAG
1924	S14R133A_rev	RPS14	CTCATAATCTTCTACCTGCTCTACCACCCTTCTTTC
1925	S14-464851_for	RPS14	AGTTACTGGTGGTATGGCGGTTGCGGCTGACGCAGATGAATCTTCTC CAT
1926	S14-464851_rev	RPS14	ATGGAGAAGATTCATCTGCGTCAGCCGCAACCGCCATACCACCAGT AACT
1927	S14-6971_for	RPS14	CCCAAGATGTTGCCGCTGCGTGTGCGGAAGTCGGTATCACTG
1928	S14-6971_rev	RPS14	CAGTGATACCGACTTCCGCACACGCAGCGGCAACATCTTGGG
1929	S14_for_BamHI	RPS14	CGCGGATCCATGTCTAACGTTGTTCAAG
1939	S5delC_rev	RPS5	GCGCTGCAGTTATTCCAATTCATCCTTCTTC
1940	S5_R147A_rev	RPS5	CCACCGACTGCGGTGGTGTCTTCTCTTG
1941	S5_R147A_for	RPS5	GACACCACCGCAGTCGGTGGTGGTGGTG
1942	S5_RR155156AA_for	RPS5	GGTGCTGCTGCTGCTCAAGCTGTCGATGTTTCTCC
1943	S5_RR155156AA_rev	RPS5	GACAGCTTGAGCAGCAGCAGCACCACCACCACCG
2221	NOB1_TAP_f	NOB1	GAAGCAGCATAACGTCCGCATTGGTAAGGGAAGGTACGTCAACAGT TCCAAAAGGAGAAGTTCCATGGAAAAGAGAAG
2222	NOB1_TAP_r	NOB1	GAAAAAGAAAAAGGGCAGCTGCCAACTAGTACACACTACACAGATA TTTATGAAAAACATACGACTCACTATAGGG
2223	NOB1_int_for	NOB1	GCGGTGGACAGGGTACCTTATT
2224	NOB1_int_rev	NOB1	ATGGTACCGTTTGTCATTGCGTCTCTGCAC
2229	NOB1_seq_rev	NOB1	CATCAGCATCCTCGAATACTTC
2316	RIO2-pBS1479-INT-UP	RIO2	GGTGTTGAAAATCTAAAAATGGATAAACTAGGAAACTATATACTAGA GTCCATGGAAAAGAGAAG
2317	RIO2-pBS1479-INT-DO	RIO2	GGATAACAACTTGATTATTTGCGGCCATTTATGCAGTCGTCTAAACTA AATACGACTCACTATAGGG
2318	ENP1-pBS1479-INT-UP	ENP1	TTTGTTGATCCACAGGAAGCTAATGATGATTTAATGATTGATGTCAAT TCCATGGAAAAGAGAAG
2319	ENP1-pBS1479-INT-DO	ENP1	GGGAAAGACCGAGCGATATAAAATTGATGAAAAATTGATATTACAGC ATACGACTCACTATAGGG

5.1.3.2 Oligonucleotides used as probes

ToO	Name	Sequence
204	o1-5'A0	GGTCTCTCTGCTGCCGG
205	o2-18S	CATGGCTTAATCTTTGAGAC
206	o3-D/A2	CGGTTTTAATTGTCCTA
207	o4-A2/A3	TGTTACCTCTGGGCCC
208	o5-A3/B1	AATTTCCAGTTACGAAAATTCTTG
209	o6-5.8	TTTCGCTGCGTTCTTCATC
210	o7-E/C2	GGCCAGCAATTTCAAGTTA
211	o8-C1/C2	GAACATTGTTCGCCTAGA
212	o9-25S	CTCCGCTTATTGATATGC
378	ITS1-Forward	GTTTTGGCAAGAGCATGAGAGC
441	T7-Prom-ITS1.r	TAATACGACTCACTATAGGG TGTATTGAAACGGTTTTAATTGTCC
1818	ext_ITS1_1	TGTATTGAAACGGTTTTAATT
1819	ext_ITS1_2	GTAAAAGCTCTCATGCTCTTGCC
	ITS1-Cy3	TT*GCACAGAAATCTCT*CACCGTTTGGAAT*AGCAAGAAAGAAACT*TACAA GCT*T (where T* represents amino-modified deoxythymidine conjugated to Cy3)

5.1.4 Plasmids

ToP	Name	Gene	Marker	Features	Origin
48	YCplac22-pGAL		AmpR, TRP1	CEN4, ARS1	
52	YCplac111		AmpR, LEU2	CEN4, ARS1	
90	YEplac181		AmpR, LEU2	2µ	
94	pfl36-pGAL-RPS15	RPS15	AmpR, LEU2	CEN6, ARS1	Toulouse
230	YCplac111-pGAL		AmpR, LEU2	CEN4, ARS1	Ferreira-Cerca et.al., 2005
232	YEplac181-pGAL		AmpR, LEU2	2µ	Ferreira-Cerca et.al., 2005
236	YEplac181-pGAL-RPS15	RPS15	AmpR, LEU2	2µ	Ferreira-Cerca et.al., 2005
251	YCplac111-pGAL-RPS0B	RPS0B	AmpR, LEU2	CEN4, ARS1	Ferreira-Cerca et.al., 2005
254	YCplac111-pGAL-RPS1A	RPS1A	AmpR, LEU2	CEN4, ARS1	Ferreira-Cerca et.al., 2005
255	YCplac111-pGAL-RPS2	RPS2	AmpR, LEU2	CEN4, ARS1	Ferreira-Cerca et.al., 2005
257	YCplac111-pGAL-RPS3	RPS3	AmpR, LEU2	CEN4, ARS1	Ferreira-Cerca et.al., 2005
259	YCplac111-pGAL-RPS5	RPS5	AmpR, LEU2	CEN4, ARS1	Ferreira-Cerca et.al., 2005
261	YCplac111-pGAL-RPS6A	RPS6A	AmpR, LEU2	CEN4, ARS1	Ferreira-Cerca et.al., 2005
264	YCplac111-pGAL-RPS9A	RPS9A	AmpR, LEU2	CEN4, ARS1	Ferreira-Cerca et.al., 2005
266	YCplac111-pGAL-RPS10A	RPS10A	AmpR, LEU2	CEN4, ARS1	Ferreira-Cerca et.al., 2005
268	YCplac111-pGAL-RPS11A	RPS11A	AmpR, LEU2	CEN4, ARS1	Ferreira-Cerca et.al., 2005
270	YCplac111-pGAL-RPS13	RPS13	AmpR, LEU2	CEN4, ARS1	Ferreira-Cerca et.al., 2005
272	YCplac111-pGAL-RPS16A	RPS16A	AmpR, LEU2	CEN4, ARS1	Ferreira-Cerca et.al., 2005
274	YCplac111-pGAL-RPS20	RPS20	AmpR, LEU2	CEN4, ARS1	Ferreira-Cerca et.al., 2005
276	YCplac111-pGAL-RPS23	RPS23	AmpR, LEU2	CEN4, ARS1	Ferreira-Cerca et.al., 2005

ToP	Name	Gene	Marker	Features	Origin
278	YCplac111-pGAL-RPS26	RPS26	AmpR, LEU2	CEN4, ARS1	Ferreira-Cerca et.al., 2005
280	YCplac111-pGAL-RPS27	RPS27	AmpR, LEU2	CEN4, ARS1	Ferreira-Cerca et.al., 2005
283	YCplac111-pGAL-RPS30B	RPS30B	AmpR, LEU2	CEN4, ARS1	Ferreira-Cerca et.al., 2005
285	YCplac111-pGAL-RPS31	RPS31	AmpR, LEU2	CEN4, ARS1	Ferreira-Cerca et.al., 2005
322	YEplac195		AmpR, URA3	2µ	
338	YCplac111-pGAL-RPS14A	RPS14A	AmpR, LEU2	CEN4, ARS1	Ferreira-Cerca et.al., 2005
349	YEplac195-pRPS28-FLAG		AmpR, URA3	2µ	Ferreira-Cerca et.al., 2005
479	YCplac111-pGAL-RPS17	RPS17	AmpR, LEU2	CEN4, ARS1	this study
485	YCplac111-pGAL-RPS19	RPS19A	AmpR, LEU2	CEN4, ARS1	this study
496	YEplac195-pRPS28-FLAG-TAS0	TAS0	AmpR, URA3	2µ	this study
497	YEplac195-pRPS28-FLAG-TAS1	TAS1	AmpR, URA3	2µ	this study
498	YEplac195-pRPS28-FLAG-TAS2	TAS2	AmpR, URA3	2µ	this study
499	YEplac195-pRPS28-FLAG-TAS3	TAS3	AmpR, URA3	2µ	this study
500	YEplac195-pRPS28-FLAG-TAS5	TAS5	AmpR, URA3	2µ	this study
501	YEplac195-pRPS28-TAS6-FLAG	TAS6	AmpR, URA3	2µ	this study
502	YEplac195-pRPS28-TAS9-FLAG	TAS9	AmpR, URA3	2µ	this study
503	YEplac195-pRPS28-FLAG-TAS11	TAS11	AmpR, URA3	2µ	this study
504	YEplac195-pRPS28-FLAG-TAS13	TAS13	AmpR, URA3	2µ	this study
505	YEplac195-pRPS28-FLAG-TAS14	TAS14	AmpR, URA3	2µ	this study
506	YEplac195-pRPS28-FLAG-TAS15	TAS15	AmpR, URA3	2µ	this study
507	YEplac195-pRPS28-FLAG-TAS16	TAS16	AmpR, URA3	2µ	this study
508	YEplac195-pRPS28-FLAG-TAS17	TAS17	AmpR, URA3	2µ	this study
509	YEplac195-pRPS28-FLAG-TAS19	TAS19	AmpR, URA3	2µ	this study
510	YEplac195-pRPS28-FLAG-TAS20	TAS20	AmpR, URA3	2µ	this study
511	YEplac195-pRPS28-TAS24-FLAG	TAS24	AmpR, URA3	2µ	this study
512	YEplac195-pRPS28-FLAG-TAS27	TAS27	AmpR, URA3	2µ	this study
513	YEplac195-pRPS28-TAS31-FLAG	TAS31	AmpR, URA3	2µ	this study
514	YEplac195-pRPS28-FLAG-RPS0deltaC	RPS0	AmpR, URA3	2µ	this study
515	YEplac195-pRPS28-FLAG-RPS11deltaN	RPS11	AmpR, URA3	2µ	this study
516	YEplac195-pRPS28-FLAG-RPS2deltaN	RPS2	AmpR, URA3	2µ	this study
517	YEplac195-pRPS28-FLAG-RPS17deltaC	RPS17	AmpR, URA3	2µ	this study
520	YEplac195-pRPS28		AmpR, URA3	2µ	Ferreira-Cerca
542	YEplac195-pRPS28-TAS0	TAS0	AmpR, URA3	2µ	this study
543	YEplac195-pRPS28-TAS1	TAS1	AmpR, URA3	2µ	this study
544	YEplac195-pRPS28-TAS2	TAS2	AmpR, URA3	2µ	this study
545	YEplac195-pRPS28-TAS3	TAS3	AmpR, URA3	2µ	this study
546	YEplac195-pRPS28-TAS11	TAS11	AmpR, URA3	2µ	this study
547	YEplac195-pRPS28-TAS13	TAS13	AmpR, URA3	2µ	this study
548	YEplac195-pRPS28-TAS14	TAS14	AmpR, URA3	2µ	this study
549	YEplac195-pRPS28-TAS15	TAS15	AmpR, URA3	2µ	this study

ToP	Name	Gene	Marker	Features	Origin
550	YEplac195-pRPS28-TAS16	TAS16	AmpR, URA3	2µ	this study
551	YEplac195-pRPS28-TAS17	TAS17	AmpR, URA3	2µ	this study
552	YEplac195-pRPS28-TAS19	TAS19	AmpR, URA3	2µ	this study
553	YEplac195-pRPS28-TAS27	TAS27	AmpR, URA3	2µ	this study
556	YEplac181-pGAL-TAS0	TAS0	AmpR, LEU2	2µ	this study
557	YEplac181-pGAL-TAS13	TAS13	AmpR, LEU2	2µ	this study
558	YEplac181-pGAL-TAS14	TAS14	AmpR, LEU2	2µ	this study
559	YEplac181-pGAL-TAS15	TAS15	AmpR, LEU2	2µ	this study
560	YEplac181-pGAL-TAS19	TAS19	AmpR, LEU2	2µ	this study
561	YEplac181-pGAL-FLAG-TAS0	TAS0	AmpR, LEU2	2µ	this study
562	YEplac181-pGAL-FLAG-TAS13	TAS13	AmpR, LEU2	2µ	this study
563	YEplac181-pGAL-FLAG-TAS14	TAS14	AmpR, LEU2	2µ	this study
564	YEplac181-pGAL-FLAG-TAS15	TAS15	AmpR, LEU2	2µ	this study
565	YEplac181-pGAL-FLAG-TAS19	TAS19	AmpR, LEU2	2µ	this study
572	YEplac195-pRPS28-FLAG-RPS5deltaN	RPS5	AmpR, URA3	2µ	this study
573	YEplac195-pRPS28-RPS6deltaC-FLAG	RPS6	AmpR, URA3	2µ	this study
574	YEplac195-pRPS28-RPS24deltaC-FLAG	RPS24	AmpR, URA3	2µ	this study
575	pRPS28-FLAG-Fusion-TAS/RPS17	RPS17	AmpR, URA3	2µ	this study
576	pRPS28-Fusion-TAS/RPS6-FLAG	RPS6	AmpR, URA3	2µ	this study
585	YEplac181-pGAL-Flag-TAS1	TAS1	AmpR, LEU2	2µ	this study
586	YEplac181-pGAL-Flag-TAS2	TAS2	AmpR, LEU2	2µ	this study
587	YEplac181-pGAL-Flag-TAS3	TAS3	AmpR, LEU2	2µ	this study
588	YEplac181-pGAL-Flag-TAS11	TAS11	AmpR, LEU2	2µ	this study
589	YEplac181-pGAL-Flag-TAS16	TAS16	AmpR, LEU2	2µ	this study
590	YEplac181-pGAL-Flag-TAS17	TAS17	AmpR, LEU2	2µ	this study
591	YEplac181-pGAL-Flag-TAS27	TAS27	AmpR, LEU2	2µ	this study
592	YEplac181-pGAL-TAS1	TAS1	AmpR, LEU2	2µ	this study
593	YEplac181-pGAL-TAS2	TAS2	AmpR, LEU2	2µ	this study
594	YEplac181-pGAL-TAS3	TAS3	AmpR, LEU2	2µ	this study
595	YEplac181-pGAL-TAS11	TAS11	AmpR, LEU2	2µ	this study
596	YEplac181-pGAL-TAS16	TAS16	AmpR, LEU2	2µ	this study
597	YEplac181-pGAL-TAS17	TAS17	AmpR, LEU2	2µ	this study
598	YEplac181-pGAL-TAS27	TAS27	AmpR, LEU2	2µ	this study
603	YEplac181-pGAL-Flag-TAS5	TAS5	AmpR, LEU2	2µ	this study
604	YEplac181-pGAL-TAS6-Flag	TAS6	AmpR, LEU2	2µ	this study
605	YEplac181-pGAL-TAS9-Flag	TAS9	AmpR, LEU2	2µ	this study
606	YEplac181-pGAL-TAS24-Flag	TAS24	AmpR, LEU2	2µ	this study
607	YEplac181-pGAL-TAS31-Flag	TAS31	AmpR, LEU2	2µ	this study
608	YCplac111GAL-RPS20-SE	RPS20	AmpR, LEU2	CEN4, ARS1	this study
662	YEplac195-pRPS28-FLAG-SAS3	SAS3	AmpR, URA3	2µ	this study

ToP	Name	Gene	Marker	Features	Origin
663	YEplac195-pRPS28-FLAG-SAS5	SAS5	AmpR, URA3	2µ	this study
664	YEplac195-pRPS28-FLAG-SAS20	SAS20	AmpR, URA3	2µ	this study
665	YEplac195-pRPS28-FLAG-SAS26	SAS26	AmpR, URA3	2µ	this study
666	YEplac195-pRPS28-FLAG-SAS27	SAS27	AmpR, URA3	2µ	this study
667	YEplac195-pRPS28-FLAG-SAS30	SAS30	AmpR, URA3	2µ	this study
706	YEplac195-pRPS28-FLAG-SAS13	SAS13	AmpR, URA3	2µ	this study
707	YEplac195-pRPS28-FLAG-SAS14	SAS14	AmpR, URA3	2µ	this study
708	YEplac195-pRPS28-FLAG-SAS15	SAS15	AmpR, URA3	2µ	this study
709	YEplac195-pRPS28-FLAG-SAS16	SAS16	AmpR, URA3	2µ	this study
752	YEplac195-pRPS28-FLAG-SOE20_1	TAS20 SAS20	AmpR, URA3	2µ	this study
753	YEplac195-pRPS28-FLAG-SOE20_2	TAS20 SAS20	AmpR, URA3	2µ	this study
754	YEplac195-pRPS28-FLAG-SOE20_3	TAS20 SAS20	AmpR, URA3	2µ	this study
787	YCplac22-pGAL-RPS15	RPS15	AmpR, TRP1	CEN4, ARS1	this study
788	YCplac22-pGAL-RPS20	RPS20	AmpR, TRP1	CEN4, ARS1	this study
859	YEplac181-pGAL-RPS15	RPS15	AmpR, LEU2	2µ	this study
861	YEplac181-pGAL-RPS15-pRPS28-TAS15	RPS15 TAS15	AmpR, LEU2	2µ	this study
863	YEplac181-pGAL-RPS15-pRPS28-SAS15	RPS15 SAS15	AmpR, LEU2	2µ	this study
972	YCplac111-pGAL-RPS20_new	RPS20	AmpR, LEU2	CEN4, ARS1	this study
973	YCplac22-pGAL-RPS15	RPS15	AmpR, TRP1	CEN4, ARS1	this study
991	YEplac195-pRPS28-FLAG-RPS0	RPS0	AmpR, URA3	2µ	Ferreira-Cerca et.al., 2005
992	YEplac195-pRPS28-FLAG-RPS1-SE	RPS1	AmpR, URA3	2µ	Ferreira-Cerca et.al., 2005
993	YEplac195-pRPS28-FLAG-RPS2-SE	RPS2	AmpR, URA3	2µ	Ferreira-Cerca et.al., 2005
994	YEplac195-pRPS28-FLAG-RPS3-SE	RPS3	AmpR, URA3	2µ	Ferreira-Cerca et.al., 2005
995	YEplac195-pRPS28-FLAG-RPS4	RPS4	AmpR, URA3	2µ	Steffen Jakob
996	YEplac195-pRPS28-FLAG-RPS5-SE	RPS5	AmpR, URA3	2µ	Ferreira-Cerca et.al., 2005
997	YEplac195-pRPS28-RPS6A-FLAG	RPS6A	AmpR, URA3	2µ	Ferreira-Cerca et.al., 2005
998	YEplac195-pRPS28-FLAG-RPS7	RPS7A	AmpR, URA3	2µ	Ferreira-Cerca et.al., 2005
999	YEplac195-pRPS28-RPS9A-FLAG	RPS9A	AmpR, URA3	2µ	Ferreira-Cerca et.al., 2005
1000	YEplac195-pRPS28-RPS10A-FLAG	RPS10A	AmpR, URA3	2µ	Ferreira-Cerca et.al., 2005
1001	YEplac195-pRPS28-FLAG-RPS11	RPS11	AmpR, URA3	2µ	Ferreira-Cerca et.al., 2005
1002	YEplac195-pRPS28-FLAG-RPS13-SE	RPS13	AmpR, URA3	2µ	Ferreira-Cerca et.al., 2005
1003	YEplac195-pRPS28-FLAG-RPS14A	RPS14A	AmpR, URA3	2µ	Ferreira-Cerca et.al., 2005
1004	YEplac195-pRPS28-FLAG-RPS15	RPS15	AmpR, URA3	2µ	Ferreira-Cerca et.al., 2005
1005	YEplac195-pRPS28-FLAG-RPS16-SE	RPS16	AmpR, URA3	2µ	Ferreira-Cerca et.al., 2005
1006	YEplac195-pRPS28-FLAG-RPS17	RPS17	AmpR, URA3	2µ	Ferreira-Cerca et.al., 2005
1007	YEplac195-pRPS28 FLAG RPS18B	RPS18B	AmpR, URA3	2µ	Ferreira-Cerca et.al., 2005

ToP	Name	Gene	Marker	Features	Origin
1008	YEplac195-pRPS28-FLAG-RPS19	RPS19	AmpR, URA3	2µ	Ferreira-Cerca et.al., 2005
1009	YEplac195-pRPS28-FLAG-RPS20	RPS20	AmpR, URA3	2µ	Ferreira-Cerca et.al., 2005
1010	YEplac195-pRPS28-FLAG-RPS21	RPS21	AmpR, URA3	2µ	Steffen Jakob
1011	YEplac195-pRPS28-FLAG-RPS22	RPS22	AmpR, URA3	2µ	Steffen Jakob
1012	YEplac195-pRPS28-RPS24-FLAG	RPS24	AmpR, URA3	2µ	Ferreira-Cerca et.al., 2005
1013	YEplac195-pRPS28-RPS26A-FLAG	RPS26A	AmpR, URA3	2µ	Ferreira-Cerca et.al., 2005
1014	YEplac195-pRPS28-FLAG-RPS27-SE	RPS27	AmpR, URA3	2µ	Ferreira-Cerca et.al., 2005
1015	YEplac195-pRPS28-FLAG-RPS28	RPS28	AmpR, URA3	2µ	Ferreira-Cerca et.al., 2005
1016	YEplac195-pRPS28-FLAG-RPS29	RPS29	AmpR, URA3	2µ	Steffen Jakob
1017	YEplac195-pRPS28-RPS30-FLAG	RPS30	AmpR, URA3	2µ	Ferreira-Cerca et.al., 2005
1018	YEplac195-pRPS28-RPS31-FLAG	RPS31	AmpR, URA3	2µ	Ferreira-Cerca et.al., 2005
1058	YCplac22-pGAL-RPS17	RPS17	AmpR, TRP1	CEN4, ARS1	this study
1070	YEplac195-pRPS28-FLAG-RPS2 RRAA	RPS2	AmpR, URA3	2µ	this study
1071	YEplac195-pRPS28-FLAG-RPS5 RKAA	RPS5	AmpR, URA3	2µ	this study
1072	YEplac195-pRPS28-FLAG-RPS5 R112A	RPS5	AmpR, URA3	2µ	this study
1073	YEplac195-pRPS28-FLAG-RPS9 KKAA	RPS9	AmpR, URA3	2µ	this study
1074	YEplac195-pRPS28-FLAG-RPS3-S6A	RPS3	AmpR, URA3	2µ	this study
1075	YEplac195-pRPS28-FLAG-RPS3-TTAA	RPS3	AmpR, URA3	2µ	this study
1076	YEplac195-pRPS28-FLAG-RPS3-T207A	RPS3	AmpR, URA3	2µ	this study
1077	YEplac195-pRPS28-FLAG-RPS3-S221A	RPS3	AmpR, URA3	2µ	this study
1078	YCplac22-pGAL-RPS17 NAT1	RPS17 natNT2	AmpR, TRP1	CEN4, ARS1	this study
1098	YEplac195-pRPS28-FLAG-RPS5 del loop	RPS5	AmpR, URA3	2µ	this study
1099	YEplac195-pRPS28-FLAG-RPS5 del loop GG	RPS5	AmpR, URA3	2µ	this study
1100	YEplac195-pRPS28-FLAG-RPS5 truncated	RPS5	AmpR, URA3	2µ	this study
1101	YEplac195-pRPS28-FLAG-RPS5deltaC	RPS5	AmpR, URA3	2µ	this study
1102	YEplac195-pRPS28-FLAG-RPS5 R148A	RPS5	AmpR, URA3	2µ	this study
1103	YEplac195-pRPS28-FLAG-RPS5 RRAA	RPS5	AmpR, URA3	2µ	this study
1104	YEplac195-pRPS28-FLAG-RPS2 del loop	RPS2	AmpR, URA3	2µ	this study
1105	YEplac195-pRPS28-FLAG-RPS2 del loop APA	RPS2	AmpR, URA3	2µ	this study
1106	YEplac195-pRPS28-FLAG-RPS2 short loop	RPS2	AmpR, URA3	2µ	this study
1107	YEplac195-pRPS28-FLAG-RPS2 KRRAAA	RPS2	AmpR, URA3	2µ	this study
1108	YEplac195-pRPS28-FLAG-RPS14A R133A	RPS14A	AmpR, URA3	2µ	this study
1109	YEplac195-pRPS28-FLAG-RPS14A KKRAAA	RPS14A	AmpR, URA3	2µ	this study

ToP	Name	Gene	Marker	Features	Origin
1110	YEplac195-pRPS28-FLAG-RPS14A KKAA	RPS14A	AmpR, URA3	2µ	this study
1111	YEplac195-pRPS28-FLAG-RPS14A-SE	RPS14A	AmpR, URA3	2µ	this study
1155	YCplac22-pGAL-RPS5 NAT1	RPS5, natNT2	AmpR, TRP1	CEN4, ARS1	this study
1156	YEplac181-pRPS28-5xHA-RPS5deltaC	RPS5	AmpR, LEU2	2µ	this study
1157	YEplac181-pRPS28-5xHA-RPS5-delta-loop	RPS5	AmpR, LEU2	2µ	this study
1158	YEplac181-pRPS28-5xHA-RPS5-delta-loop+GG	RPS5	AmpR, LEU2	2µ	this study
1159	YCplac22-pGAL-RPS14 NAT1	RPS14, natNT2	AmpR, TRP1	CEN4, ARS1	this study
1160	YCplac22-pGAL-RPS2 NAT1	RPS2, natNT2	AmpR, TRP1	CEN4, ARS1	this study
1161	YEplac181-pRPS28-5xHA-RPS2	RPS2	AmpR, LEU2	2µ	this study
1162	YEplac181-pRPS28-5xHA-RPS5	RPS5	AmpR, LEU2	2µ	this study
1163	YEplac181-pRPS28-5xHA-RPS2-short-loop	RPS2	AmpR, LEU2	2µ	this study
1164	YEplac181-pRPS28-5xHA-RPS2-KRRAAA	RPS2	AmpR, LEU2	2µ	this study
1171	YEplac181-pRPS28-TAS15	TAS15	AmpR, LEU2	2µ	this study
1172	YEplac181-pRPS28-SAS15	SAS15	AmpR, LEU2	2µ	this study
1173	YEplac181-pRPS28-RPS15	RPS15	AmpR, LEU2	2µ	this study
1174	YEplac181-pRPS28-5xHA-TAS15	TAS15	AmpR, LEU2	2µ	this study
1175	YEplac181-pRPS28-5xHA-SAS15	SAS15	AmpR, LEU2	2µ	this study
1176	YEplac181-pRPS28-5xHA-RPS15	RPS15	AmpR, LEU2	2µ	this study
1177	YEplac195-pRPS28-FLAG-SAS20-KKTT	SAS20	AmpR, URA3	2µ	this study
1178	YEplac195-pRPS28-FLAG-SAS20-K59S	SAS20	AmpR, URA3	2µ	this study
1179	YEplac195-pRPS28-FLAG-SAS20-K59T	SAS20	AmpR, URA3	2µ	this study
1180	YEplac195-pRPS28-FLAG-SAS20-K61T	SAS20	AmpR, URA3	2µ	this study
1181	YEplac195-pRPS28-FLAG-RPS20-S76K	RPS20	AmpR, URA3	2µ	this study
1182	YEplac195-pRPS28-FLAG-RPS20-T78K	RPS20	AmpR, URA3	2µ	this study
1183	YEplac195-pRPS28-FLAG-RPS20-STKK	RPS20	AmpR, URA3	2µ	this study
1278	YEplac181-pRPS28-5xHA-TAS20	TAS20	AmpR, LEU2	2µ	this study
1279	YEplac181-pRPS28-5xHA-SAS20	SAS20	AmpR, LEU2	2µ	this study
1280	YEplac181-pRPS28-5xHA-SOE20_3	TAS20 SAS20	AmpR, LEU2	2µ	this study
1283	YEplac195-pRPS28-Nt-FLAG-SAS17	SAS17	AmpR, URA3	2µ	this study
1284	YEplac195-pRPS28-Nt-FLAG-RPS17deltaN	RPS17	AmpR, URA3	2µ	this study
1285	YEplac181-pRPS28-5xHA-RPS17deltaN	RPS17	AmpR, LEU2	2µ	this study
1286	YEplac181-pRPS28-5xHA-SAS17	SAS17	AmpR, LEU2	2µ	this study
1287	YEplac181-pRPS28-5xHA-RPS17	RPS17	AmpR, LEU2	2µ	this study

ToP	Name	Gene	Marker	Features	Origin
1288	YEplac181-pRPS28-5xHA-RPS17deltaC	RPS17	AmpR, LEU2	2µ	this study
1289	YEplac181-pRPS28-5xHA-TAS17	TAS17	AmpR, LEU2	2µ	this study
1290	YEplac181-pRPS28-5xHA-Fusion-TAS/RPS17-	RPS17 TAS17	AmpR, LEU2	2µ	this study
1413	YEplac195-pRPS28-FLAG-RPS20-T78A	RPS20	AmpR, URA3	2µ	this study
1414	YEplac195-pRPS28-FLAG-RPS20-S76A	RPS20	AmpR, URA3	2µ	this study

5.1.5 Enzymes

Enzyme	Origin
Antarctic Phosphatase	New England Biolabs
Calf Intestinal Phosphatase	New England Biolabs
iProof high-fidelity DNA polymerase	Bio-Rad
Restriction Endonucleases	New England Biolabs
T4 DNA ligase	New England Biolabs
Taq DNA polymerase	New England Biolabs
Trypsin, modified, sequencing grade, from bovine pancreas	Roche
Zymolyase 100T	Seikagaku Corporation

5.1.6 Antibodies

Antibody	Species	Dilution	Origin
Alexa-Fluor-488, goat anti mouse	goat	1:500	Molecular probes
Alexa-Fluor-488, goat anti rat	goat	1:500	Molecular probes
Alexa-Fluor-594, goat anti mouse	goat	1:500	Molecular probes
Alexa-Fluor-594, goat anti rabbit	goat	1:500	Molecular probes
α-A43	rabbit	1:50000	A. Sentenac, Paris (Buhler et al., 1980)
α-DIG (Fab fragments)	sheep	1:7500	Roche
α-FLAG (M2)	mouse	1:5000	Sigma
α-FLAG (polyclonal)	rabbit	1:1000	Sigma
α-HA (12CA5)	mouse	1:1000	Kremmer, Helmholtz Zentrum München
α-HA (16B12)	rat	1:1000	HISS
α-HA (3F10)	mouse	1:1000	Roche
α-ProteinA (P-3775)	rabbit	1:10000-1:50000	Sigma
α-Tubulin (AB6161)	rat	1:400	Abcam

5.1.7 Chemicals

Chemicals were purchased at the highest available purity from Sigma-Aldrich, Merck, Fluka, Roth or J.T.Baker, except:

5-FOA	Toronto Research Chemicals
agarose (electrophoresis grade)	Invitrogen
amino acid supplements	Bio101®Systems, Sunrise Science Products
Bacto™ Agar	BD Biosciences
Bacto™ Peptone	BD Biosciences
Bacto™ Tryptone	BD Biosciences
Bacto™ Yeast Extract	BD Biosciences
bromine phenol blue	Serva
complete supplement mixtures (CSM)	Sunrise Science Products
Ficoll (Typ400)	Pharmacia
milk powder	Sukofin
MOWIOL® 4-88	Calbiochem
Nonidet P-40 substitute (NP40)	USB Corporation
Paraformaldehyde 16%, EM Grade	Electron Microscopy Sciences
Tris ultrapure	USB Corporation
Tween 20	Serva
Yeast nitrogen base (YNB)	Bio101®Systems
α-cyano-4-hydroxycinnamic acid (>98%, TLC)	Sigma-Aldrich

5.1.8 Other Materials

Material	**Origin**
3MM filter-papers	Millipore
BM Chemiluminescence Blotting Substrate (POD)	Roche
Broad Range Protein Markers	New England Biolabs
DNA ladders	New England Biolabs
kits used for cloning techniques	Qiagen, Invitrogen
Mobicol columns	MoBiTec
PositiveTM Membrane	Qbiogen
PVDF membrane Immobilion P 0.45µm	Millipore
radioactive chemicals	Amersham, Hartmann-Analytics
Salmon sperm DNA (10 mg/ml)	Invitrogen
sterile filters 0.22µm	Millipore
Sulfolobus acidocaldarius DSM 639 genomic DNA	kind gift of Dr. H. Huber and Prof. Dr. M. Thomm, Lehrstuhl für Mikrobiologie & Archaeenzentrum, Regensburg
Thermoplasma acidophilum genomic DNA 122-1B2 [AMRC C165, DSM 1728]	ATCC™
Yeast genomic DNA (strain S288C)	Invitrogen

5.1.9 Media

YPD	1% (w/v) Bacto Yeast Extract, 2% (w/v) Bacto Peptone, 2% (w/v) Glucose
YPG	1% (w/v) Bacto Yeast Extract, 2% (w/v) Bacto Peptone, 2% (w/v) Galactose
YPAD, YPAG	YPD or YPD + 100 mg/l adenine
SDC or SGC	6,7 g/l YNB, CSM dropout according to label, 2 % (w/v) sugar (Glucose for SDC, Galactose for SGC), amino acid supplements according to following table
5-FOA	added 0,1% (w/v)
Nourseothricin	added 100 µg/ml
Hygromycin B	added 200 µg/ml
LB (Luria Broth)	1% (w/v) Bacto Tryptone, 0,5% (w/v) Bacto Yeast Extract, 0,5% (w/v) NaCl
LB_{Amp}	LB + 100 µg/ml ampicillin

All media was sterilized for 20 minutes at 110°C. Supplements were added after cooling to approximately 60°C. For plate media 2% (w/v) were added before autoclaving.

Amino acid supplementation according to Bio101®Systems

CSM Formation	**mg/liter**
Adenine	10*
Arginine	50
Aspartic Acid	80
Histidine	20
Isoleucine	50
Leucine	100
Lysine	50
Methionine	20**
Phenylalanine	50
Threonine	100**
Tryptophan	50
Tyrosine	50
Uracil	20
Valine	140

* Minimum quantity for healthy growth and yet optimized to promote red color in certain adenine auxotrophs. CSM formulations are available that contain 20 or 40 mg/liter of adenine.
** 80 mg/liter of Homoserine is substituted for Threonine in mixtures where Methionine is dropped-out.

5-FOA-Selection:
5-FOA is converted by the orotidine-5'-phosphate decarboxylase encoded by the URA3 gene in S. cerevisiae into the toxic product 5' fluorouridine monophosphate, which inhibits cell growth (Boeke et al., 1984). Therefore 5-FOA selection can be used to screen for loss (of function) of the URA3 gene in yeast.

5.1.10 Equipment

Device	Manufacturer
4700 Proteomics Analyzer MALDI-TOF/TOF	Applied Biosystems
Alpha 2-4 lyophilizer	Christ
BAS 1000 Raytest	Fujifilm
BAS Cassette 2040	Fujifilm
BAS-III Imaging Plate	Fujifilm
Biofuge Fresco refrigerated tabletop centrifuge	Hereaus
Biofuge Pico tabletop centrifuge	Hereaus
C412 centrifuge	Jouan
Centrikon T-1170 ultracentrifuge	Kontron Instruments
Centrikon T-324 centrifuge	Kontron Instruments
CT422 refrigerated centrifuge	Jouan
Electrophoresis system model 45-2010-i	Peqlab Biotechnologie GmBH
FLA-3000 fluorescent image analyzer	Fujifilm
Gel Max UV transilluminator	Intas
IKA-Vibrax VXR	IKA
Incubators	Memmert
LAS-3000 chemiluminescence image analyzer	Fujifilm
Liquid Scintillation analyzer 1600 TR	Packard
MicroPulser electroporation apparatus	Bio-Rad
Mini-PROTEAN 3 electrophoresis system	Bio-Rad
NanoDrop ND-1000 spectrophotometer	Peqlab Biotechnologie GmbH
Optima L-80 X ultracentrifuge	Beckman Coulter
PCR Sprint thermocycler	Hybaid
Power Pac 3000 power supplies	Bio-Rad
Pulverisette 6 planetary mono mill	Fritsch
Roto-Shake Genie	Scientific Industries
Shake incubators Multitron / Minitron	Infors
Speed Vac Concentrator	Savant
Sub-Cell® GT Agarose Gel Electrophoresis System	Biorad
Thermomixer compact	Eppendorf
Trans-Blot SD Semi-dry transfer cell	Bio-Rad
UltiMate 3000 NanoHPLC	Dionex
Ultrospec 3100pro spectrophotometer	Amersham
XCell SureLock Mini-Cell electrophoresis system	Invitrogen
Zeiss Axiovert 200M microscope	Carl Zeiss

5.1.11 Software

Software	Producer
4000 Series Explorer v.3.6	Applied Biosystems
Accelrys DS Visualizer 2 and 2.5	Accelrys Software Inc.
AIDA	Raytest
Axiovision rel. 4.7	Carl Zeiss
Chromeleon v.6.70	Dionex
Data Explorer v.4.5 C	Applied Biosystems
DeepView Swiss-PdbViewer 4.01	Swiss Institute for Bioinformatics
Gimp	gimp.org
GPS Explorer v.3.5	Applied Biosystems
Image Reader LAS-3000 v.1.12	Fujifilm
ImageGauge	Fujifilm
IrfanView	Irfan Skiljan
Mascot	Matrix Science
ND-1000 v.3.5.2	Peqlab Biotechnologie GmbH
OpenOffice 3	openoffice.org
POV-Ray 3.6	Persistance of Vision Team
Vector NTI Advance 10.0	Invitrogen

5.2 Methods

5.2.1 Work with *Escherichia coli*

All *E. coli* strains were grown at 37°C, unless other temperature indicated. For liquid cultures 1x Luria-Bertani (LB) media was used. For solid media 2% Bacto-agar was added. Ampicillin resistant bacteria were selected by addition of 100 µg/ml ampicillin.

5.2.1.1 Competent cells for electroporation

XL1-blue and DH5a strains were used as a host for amplification of plasmid DNA. Only electro-competent *E. coli* cells were used in this work. Cells are grown in SOB (2% Bacto-Trypton, 0.5% Bacto-Yeast extract, 8.55 mM NaCl, 2.5mM KCl, 10 mM $MgCl_2$, pH 7) at 37°C to mid-log phase (OD600= 0.35 – 0.6), chilled on ice for 15 min and harvested. Cells are washed 3 times with ice-cold sterile water to reduce the ionic strength of the cell suspension. The cells are resuspended in 10% sterile glycerol (on average $1\text{-}3 \cdot 10^{10}$ cells per ml), aliquoted and stored at –80°C.

5.2.1.2 Transformation with plasmid DNA

Electro-competent cells (see 5.2.1.1) are thaw on ice, incubated for 1 min with DNA on ice, and transfered into electroporation cuvette (Biorad). Cells are exposed to a short high voltage discharge (2.5 kV, 5-6 ms) using a Biorad Micropulser. Cells are resuspended in LB media, incubated for 30 min at 37°C and platted on the appropriated selection medium (in this work on LB plates containing Ampicillin) and grow overnight at 37°C.

5.2.1.3 Extraction and purification of plasmid DNA

Isolation of plasmid DNA from bacteria were performed according to the manufacturer's manual (Invitrogen, Quick Plasmid Miniprep Kit).
Briefly, cells are lysed, cell debris is removed and plasmid DNA is bound to a silica-matrix. The bound plasmid DNA is washed with an alcohol-based buffer, and eluted from the matrix by a pH step with pre-warmed (65°C) 2 mM Tris buffered water.

5.2.2 Work with *Saccharomyces cerevisiae*

All *S. cerevisiae* strains were grown at 30°C, unless other temperature is indicated.

5.2.2.1 Preparation of transformation competent yeast cells

Fifty milliliter of mid-log phase growing cells (OD600 0.5-0.7) are harvested and washed once with sterile water. Yeast cells are further washed twice with sterile filtrated lithium-sorbitol buffer (100 mM lithium acetate, 10 mM Tris-HCl pH 8, 1 mM EDTA pH 8, 1 M sorbitol, buffered to pH 8 with acetic acid). Cells are then resuspended in 360 ml lithium-sorbitol buffer and 400 mg of heat denatured salmon sperm DNA (10 mg/ml - Invitrogen), aliquoted and stored at –80°C.
Small cations such as Li^+ or K^+ induce the ability of yeast cells to uptake DNA. PEG (Polytethylene glycol) is indispensable for plasmid DNA uptake (Ito *et al.*, 1983; Hisao *et al.*, 1984)

5.2.2.2 Transformation with DNA

Transformation competent cells are thaw on ice and incubated with plasmid DNA (100-500 ng) or linear DNA (Several µg for efficient homologous recombination). After addition of 6 volumes Lithium-PEG buffer (PEG3350 (40% (w/v), 100 mM lithium acetate, 10mM Tris-Cl pH 8, 1 mM EDTA pH 8, buffered to pH 8 with acetic acid and sterile autoclaved), cells are incubated 30 min at room temperature. After incubation 1/9 th volume DMSO is added and the cells are subjected to a temperature shock at 42°C for 15 min. Cells are spun down and resuspended in 1x YNB and plated on the appropriated media.

5.2.2.3 Long-term storage

Logarithmically growing yeast cultures are harvested, supplemented with 20% (w/v) glycerol and stored at –80°C.

5.2.2.4 Preparation of yeast genomic DNA

Yeast genomic DNA was prepared according to Harju *et al.*, 2004.
Briefly, yeast cell are lysed by repeated heat-freeze cycles, DNA is extracted by Chloroform and Ethanol precipitation. The quality of DNA is sufficient to allow PCR screening of yeast cells.

5.2.3 Protein analysis

5.2.3.1 Determination of protein concentrations

The Bradford protein assay (Biorad) was used to determine the relative amount of proteins in solution. The assay is based on an absorbance shift from 465 nm to 595 nm in the dye Coomassie brilliant blue G-250 when bound to arginine and hydrophobic amino acid residues. The increase in absorbance at 595 nm is proportional to the protein concentration in the sample.
The protein concentrations [mg/ml] equals $A_{595nm} \cdot 23$, in which the factor 23 is an empirical determined constant.

5.2.3.2 Protein preparation for further analysis

Proteins from cell pellets were extracted as following:
Logarithmically growing yeast cultures are harvested and resuspended in 1 ml of sterile water. 150µl of extraction buffer (7.5% beta-mercaptoethanol, 1.85 NaOH) is added to lyse the cells. Proteins are precipitated by addition of 150µl of 55% TCA and incubation for 10 min on ice. TCA precipitate are centrifuged 10 min at 14000 rpm at 4°C. The precipitated proteins are resuspended in HU buffer (5% SDS, 200 mM Tris pH 6.8, 1 mM EDTA, 1.5% beta mercaptoethanol, 8 M urea, 0.01% bromphenolblue) and heated 15 min at 65°C. Equivalent to OD600 0.2-0.5 of cells are analyzed by SDS-PAGE and/or Western Blotting.
Alternatively, defined protein amounts from whole cell extracts after glassbeads extraction are solubilized in HU buffer and heated 15 min at 65°C followed by further analyses.

5.2.3.3 Separation of proteins by SDS-PAGE

SDS-polyacrylamide gelelectrophoresis (SDS-PAGE) allows to separate proteins according to their apparent molecular weight. Proteins and SDS (Sodium Dodecyl Sulfate) are forming negatively charged complexes depending on the length of the proteins. They are separated through the polyacrylamide gel according to the apparent SDS/protein complex's molecular weight. Molecular weights of the different proteins are estimated using protein markers of known molecular weight.
A discontinuous gel system was used in this work, with a stacking gel (6% acrylamide, 125 mM Tris-Cl pH 6.8, 0.1% SDS) and a resolving gel (8-16% acrylamide depending on the protein's molecular weight to resolve, 375 mM Tris-Cl pH 8.8, 0.1% SDS). Gels were run for 1 to 2 h at 120 V in 1x Tris-Glycine electrophoresis buffer (25 mM Tris base, 250 mM glycine, 0.1% SDS).
For better resolution of small proteins 6 M urea was added in the stacking and resolving gel.

5.2.3.4 Western Blot

Separated proteins by preceding SDS-PAGE are transferred from the gel to a membrane. The immobilized proteins can be detected with antibodies against the protein of interest allowing identification and (semi) quantification of a specific protein in complex mixtures.
In this work SDS-PAGE resolved proteins are transferred on PVDF membrane in transfer buffer (25 mM Tris, 190 mM glycine, 20% methanol, pH 8.3 with HCl) using a semi-dry blot apparatus (Biorad) for 1 h at 24 V.
Non protein decorated membrane patches are blocked for 1 h at room temperature or over-night at 4°C with blocking buffer (0.5% low-fat dry milk, 1x TBS: 0.8% NaCl, 0.3% Tris, 0.02% KCl, pH7.4). Membranes are incubated (time and temperature according to the data sheet) with the primary antibody diluted in blocking buffer, and washed 3 times 10 min at room temperature in 1x TBS. If required, membranes are incubated (time and temperature according to the data sheet) with a secondary antibody diluted in blocking buffer and washed as before.
Immuno-detection was performed using a chemi-luminescence reaction depending on the conjugated enzymatic activity. For peroxidase coupled antibodies POD-substrate (Roche) was added to the blot as described by the manufacturer. Signals were acquired and quantified using a Fuji LAS Reader 3000.

5.2.3.5 Coomassie polyacrylamide gel staining

To visualize the total protein content of a polyacrylamide gel, it was stained with SimplyBlue SafeStain (Invitrogen) according to the manufacturer's instructions. The stain is Coomassie G-250 stain.
Briefly, the gel is incubated with staining solution (50% methanol, 10% acetic acid, 0.25% (w/v) Coomassie G-250) for 30 min at room temperature. Because non-protein parts of the gel are unspecific stained, this background is reduced by partly unstaining of the gel. Therefore the gel is washed several times with destaining solution (45% methanol, 45% H_2O, 10% acetic acid).

5.2.4 DNA analysis

5.2.4.1 Polymerase chain reaction

The polymerase chain reaction allows the exponential amplification of DNA fragments *in vitro*. The isolated DNA fragments can be further used in various experiments such as cloning. The principles of PCR are widely discussed in the literature and applications are extremely versatile.
In this work, PCR were performed with yeast genomic DNA (100ng) or plasmid DNA (10-50 ng) as templates in 50µl reactions. Different polymerases were used, such as Taq, iProof or Herculase. All buffer conditions, denaturing temperature and elongation temperature, as well as primer concentration and any other supplement was carried out as described by the manufacturer.
Annealing temperature was calculated using the provided melting temperatures of each primer by MWG Biotech AG. PCR amplification cycles varied between 30 and 35.

5.2.4.2 Separation of DNA by electrophoresis

Agarose gel electrophoresis was used to separate DNA fragments of different lengths. In this work,

electrophoresis was performed in general with 1.0% (w/v) agarose in 1x TBE (90 mM tris base, 89 mM boric acid, 2 mM EDTA) gels containing 0.2 mg/ml ethidium bromide. As electrophoresis buffer 1x TBE was used. To determine the lengths of the fragments, DNA standards were used according to the manufacturer. All samples were diluted approximately 1 to 10 in DNA loading buffer (10 mM Tris-Cl pH8.0, 1 mM EDTA, 0.01% bromphenolblue, 0.01% xylencyanole, 33.3% glycerol).

5.2.4.3 Purification of DNA

DNA fragments were purified by either precipitation with ethanol or by separation in an agarose gel followed by excission of the respective band.
For precipitation 1 volume of DNA is mixed with 2.5 volumes of ethanol and 1/10 volume of 10M LiCl. DNA is dehydrated at -20°C for at least 30 min and precipitated through centrifugation at 4°C with maximum speed for at least 15 min. The pellet was resuspended in 2 mM Tris pH 8.0.
For gel extraction the Quick Gel Extraction Kit (Invitrogen) was used as described by the manufacturer. Briefly, after manual excision of the designated DNA fragment, the agarose gel was solubilized and free DNA bound to a silica matrix, washed and eluted with preheated (65°C) 2 mM Tris pH 8.0.

5.2.4.4 DNA digestion and ligation

DNA digestion with restriction endonucleases has been always performed as suggested by the manufacturer. Buffer conditions, incubation temperatures and DNA concentrations were adapted to the manual.
After purification of DNA fragments (see 5.2.4.3), plasmid DNA and insert DNA (approximate amounts plasmid:insert 1:10) were mixed and ligated with T4-Ligase in the appropriate buffer for 30 min at room temperature. An aliquot of the ligation reaction was directly transformed into XL1blue or DH5α cells (5.2.1.2).

5.2.4.5 Sequencing of DNA

Purified DNA (plasmid or PCR product) was sequenced by companies MWG Biotech AG (Ebersberg) or GENEART (Regensburg).

5.2.5 RNA analysis

5.2.5.1 RNA extraction

RNA extractions were primary performed as described previously (Schmitt *et al.*, 1990).
Briefly, cell pellets or cell extracts are resuspended to a total volume of 500 µl with AE buffer (50 mM NaAc pH 5.3, 10 mM EDTA pH 8) and mixed with same volume of AE buffer equilibrated phenol (Roth) and 1/10th volume of 10% SDS. The samples are incubated for 10 to 15 minutes at 65°C in a thermomixer and chilled on ice for at least 2 min. The aqueous phase, containing the RNA, is collected, and a second time extracted with phenol (1:1 volume) and one further extraction with chloroform (1:1 volume). RNAs are precipitated from the aqueous phase at –20°C for longer than 10 min after addition of 2.5 volume of ethanol and 1/10th volume of 3 M NaAc pH 5.3.
Precipitated RNA, analyzed by denaturing agarose gel electrophoresis (Northern blot), was solubilited in RNA loading buffer (1x MOPS buffer (see 5.2.5.2), 8% formaldehyde, 50% deionized formamid, 0.01% bromphenolblue), denatured for 15 min at 65°C and stored at –20°C. For cDNA synthesis, RNA was solubilized in Milli-Q water.

5.2.5.2 Northern Blot

RNAs were separated on a denaturating agarose gel (1.3% agarose (Invitrogen), 2% formaldehyde; 0.1 µg/ml ethidium bromide; 1x MOPS buffer (2mM sodium acetate trihydrate, 20 mM MOPS (Fluka), 1 mM EDTA, pH 7)). Gels were run for 16–18 h at 45 V in 1x MOPS and 2% formaldehyde electrophoresis buffer. After gel run, the gels were washed once 5 min in milli-Q water, once 20 min in 0.05 M NaOH to hydrolyze the RNAs and facilitate the transfer of larger RNAs, and twice 20 min in 10x SSC (1.5 M NaCl, 150 mM sodium-citrate trihydrate). RNAs were either transferred by overnight passive transfer or vacuum assisted fast transfer onto a positively charged nylon membrane. The

RNA of interest can be detected by forming a RNA/DNA hybrid with the respective probe. Digoxigenin (DIG) labeled probes were prepared according to the manufacturer's manual. Radioactive probes were end-labeled with T4 polynucleotide kinase (PNK) by adding the gamma-^{32}P-phosphate of ATP to the oligo. Ten picomol of the oligo-probe were incubated with 50 µCi of gamma-^{32}P-ATP (Amersham) in 1x PNK buffer and 10U of T4 PNK for 45 min at 37°C. Reactions were stopped by addition of 1µl of 0.5 M EDTA pH 8. Probes were purified by gel exclusion column (Micro Bio Spin6 - Biorad). For hybridization membranes were pre-incubated for 1 h at the respective temperature in hybridization buffer (50% formamide; 5x SSC; 0.5% SDS; 5x Denhards (1% Ficoll typ 400-Pharmacia, 1% Polyvinylpyrrolidone, 1% BSA Fraction V-Sigma)). After addition of the probe, the blots were incubated with motion overnight at the respective temperature, appropriate for forming the RNA/DNA hybrid. For radioactive detection, the membranes were washed three times with 2x SSC at the used temperature and afterwards exposed onto a PhosphoImager screen and/ or onto BioMax MS/MR films (all FujiFilm). For non-radioactive probe detection the blots were washed after hybridization 2 times with hybridization buffer and two times with 0.1xSSC, 0.1%SDS at the used temperature. The membrane is shortly washed in DIG washing buffer (100 mM maleic acid, 150 mM NaCl, pH 7.5 and 0.3% N-lauroylsarcosin) and afterwards blocked for 1 hour with 1xblocking reagent (Roche) in 100 mM maleic acid, 150 mM NaCl, pH 7.5. Next, 0.75 U/ml of anti-DIG antibody conjugated to the alkaline phosphatase (Roche) in blocking buffer was added and incubated for further 45 minutes at RT. The membranes were washed three times in DIG washing buffer and incubated more than 5 minutes in reaction buffer (100 mM Tris pH 9.5, 100 mM NaCl, 5 mM MgCl2). 1% CDP-star in reaction buffer (Roche) was added and the chemiluminescence signals were detected with a Fuji LAS Reader 3000.

5.2.5.3 RNA co-immuno-precipitation

Logarithmically growing cells were harvested and washed with milli-Q water. Cells were disrupted by vortexing at 4°C with glass beads (0.75-1 mm Roth) in lysis buffer (usually buffer A200 (200 mM KCl, 20 mM Tris-HCl pH 8.0, 5 mM MgAc, 1 mM DTT, 1 mM PMSF, 2 mM benzamidine, 20 U/ml of RNasin (NEB)). To clear the extracts from large debris and insoluble material, the extract was twice centrifuged at 14000 rpm for 5 minutes at 4°C. Triton X-100 was added to the supernatants to a final volume of 0.2% (v/v). Five mg of whole cells extract (determined by Bradford assay see 5.2.3.1) were incubated with 50 µl of agarose coupled anti-Flag M2 beads (Sigma) for 90 min at 4°C. Beads were washed 5 times with 2 ml of buffer A200 plus Triton (0.2% v/v) and 1 time with 10 ml of buffer A200 plus Triton (0.2% v/v). RNAs were extracted from a volume of cell extract supernatant (input), corresponding to 1% of the volume loaded on the beads, and beads after washing (IP). Same volume percentage of extracted RNAs (see 5.2.5.1) were loaded on denaturing agarose gels (see 5.2.5.2).

5.2.5.4 Analysis of newly synthesized RNA

1 OD_{600} of logarithmically growing cells was harvested and resuspended in 100 µl of recovery buffer (2% glucose, 1% bacto peptone, 0.6% malt extract, 0.01% yeast extract, 12% mannitol, 17.8 mM magnesium acetate). 20 µCi of 5',6'-[^{3}H] uracil were added and the cells were incubated for 15 to 30 min at 30°C. RNA was extracted (see 5.2.5.1) and same amounts of radioactivity (as counted with a scintillation counter (Packard Tri-Carb 1600TR)) was loaded on a denaturating agarose gel (see 5.2.5.2). After transfer, the membrane was sprayed with an enhancer spray (EN3HANCE spray surface, Perkin Elmer) to overcome the quenching effect of non-radioactive 25S and 18S rRNAs. The membranes were exposed to a BAS-TR 2040 screen or BioMax MS films (all FujiFilm).
For pulse-chase experiments same volume percentage of 2mg/ml uracil in YPD was added to the pulsed samples and the samples were further incubated for the time required. RNA was extracted (see 5.2.5.1) and same volume percentage of samples were loaded on a denaturating agarose gel (see 5.2.5.2). The membranes were handled as described above.

5.2.5.5 Subcellular fractionation

30 OD600 of logarithmically growing cells were harvested and washed twice with 25 ml of milli-Q water. Cells were resuspended in 50 ml of buffer Z (10 mM citrate pH 7.5; 2 mM $MgCl_2$ hexa-hydrate and 12% (w(v) mannitol) with 9 mM beta-mercaptoethanol and incubated for 30 min at 37°C. 2 mg zymolyase 100T was added and the cells were further incubated at 37°C for 15 to 20 minutes. Cells are chilled on ice and washed twice with ice-cold buffer Z (8 min; 4000 rpm). For depletion of

galactose-promotor driven protein, the spheroplasts are resuspended in 25 ml of YPD supplemented with 12% (w/v) mannitol. The suspension is incubated for 30 to 35 minutes at 30°C and pelleted by centrifugation for 8 minutes at 4000 rpm. Spheroplasts are washed once with 0.5 ml of recovery buffer (2% glucose, 1% bacto peptone, 0.6% malt extract, 0.01% yeast extract, 12% mannitol, 17.8 mM magnesium acetate) and resuspended in 0.2 ml of recovery buffer. If newly synthesized RNA should be analyzed, the spheroplasts were at this step pulsed with 20 µCi of 5',6'-[^{3}H] uracil and incubated for 20 min at 30°C. In each case, the spheroplasts were pelleted and resuspended in 0.7 ml of 0.03% (w/v) Trition X-100 in PVP (8% Polyvinylpyrrolidon; 1 mM $MgCl_2$ hexa-hydrate; 20 mM potassium-phosphate buffer pH6.5; 10 mM EDTA pH8; titrated with potassium-phosphate buffer to pH 6.5). The spheroplasts are fractionated with a tight douncer (25-75µm clearance) and 0.7 ml of 0.6 M sucrose in PVP was added. The mixture was layered on top of 0.45 M sucrose cushion and centrifuged for 10 minutes at 4500 rpm and 4°C in a swing out rotor. 0.5 ml of the top layer was collected (cytoplasm). The remaining sucrose gradient was removed and the pellet (nuclei) was resuspended in 300 µl of 0.45 M sucrose in PVP. RNA from 200 µl of the cytoplasmic fraction (14%) and 100 µl of the nuclear fraction (33%) was extracted and subjected to further analysis.

5.2.5.6 RNA analysis by sucrose gradient fractionation

To 100 ml of logarithmically growing cells a total amount of 10 mg cycloheximide (CHX) was added. The cells were shook rapidly for 30 seconds and poured in a centrifugation bottle with same amounts of ice. After centrifugation, the cells were washed twice with lysis buffer (10 mM Tris-Cl pH 7.5; 0.1 M NaCl; 30 mM $MgCl_2$ hexa-hydrate) supplemented with 0.1 mg/ml CHX and 0.2 mg/ml heparin. The cells are lysed in lysis buffer and the extracted was cleared by two centrifugations. 0.5 µg protein was layered on top of a 12 ml 10-50% (w/v) sucrose gradient (10% or 50% sucrose solutions in 50 mM tris-acetate pH 7.0; 50 mM NH_4Cl; 12 mM $MgCl_2$ hexa-hydrate; 1 mM DTT; mixed with a Biocomp Gradient Master$_{IP}$). The gradients were centrifuged in a SW40 swing out rotor for 2.7 hours at 39000 rpm and the spektra were collected using a BioLogic UV detection system (254 nm) connected to a FPLC-Pharmacia LKB-P500 (flow: 0.5 ml/min). Signals were recorded using the LP analysis software (Biorad). Or the gradients were apportioned into 0.5 ml fractions. From 50% of each fraction either RNA or proteins were extracted. For RNA extraction, 110 µl of AE buffer and 40 µl of 10% SDS were added (see 5.2.5.1). 1 ml of a 1:1 phenol:chloroform mixture was added and incubated at 65°C for 10 minutes. The suspension was centrifuged and again extracted with 0.9 ml of a 1:1 phenol:chloroform mixture. RNA was precipitated as described in 5.2.5.1. Proteins were precipitated by addition of 375 µl of 7:2 acetone:H_2O to 250 µl of gradient fractions. The solution is placed on -20°C for longer than 30 minutes and afterwards centrifuged. The pellet is resuspended in protein solubilization buffer and analyzed by Western blotting.

5.2.6 Cell biological methods

5.2.6.1 Immunofluorescence

To 5ml of logarithmically growing yeast cells 500µl 37% Formaldehyde (stabilized with 10% Methanol) were added and incubated for 1 hour at the temperature used for cultivation. The cells were pelleted and resuspended in 1 ml of 0.1 M potassium-phosphate buffer pH 7.5 containing 28,6 mM beta-mercaptoethanol and 50 µg zymolyase 100T (Medac GmBH). The suspension was incubated at 30°C for 30-45 minutes with agitation. The spheroplasts are pelleted and resuspended in 1 ml TBS. At this point the cells can be stored at -20°C or subjected to immuno cytochemistry.
50 µl of the spheroplast suspension is applied on poly-L-Lysin coated coverslips. The cells adhered for 5 minutes at RT onto the coverslips. Excess suspension is aspirated and the spheroplasts are washed three times with with 50 µl TBS. The spheroplasts are covered with 50 µl 2% BSA in 1x TBS and incubated for 30 min at RT in a wet chamber. Excess suspension is aspirated and the spheroplasts are covered with the primary antibody, diluted in 50µl 0.1% BSA in 1x TBS. After incubation for 1 hour at RT, the spheroplasts are washed 4 times with 50 µl 1x TBS. Afterwards the spheroplasts are covered with secondary antibody, diluted in 50 µl 0.1% BSA in 1x TBS. The coverslips are incubated for 1 hour at RT in a dark and wet chamber. Finally spheroplasts are mounted in 2-3 µl 0.1 µg/ml DAPI in moviol and stored at 4°C in the dark.

5.2.6.2 Fluorescence in situ hybridization

15 ml exponentially growing cells are centrifuged 5 min at 3000 rpm. The supernatant is discarded, leaving 3 ml in the tube.1 ml of 16% para-formaldehyde is added on the 3 ml of the culture (4% final concentration). The cells are fixed for 30 minutes at RT and washed once with 10 ml buffer B (1.2 M sorbitol in 1x TBS). The cells are pelleted and resuspended in 0.5 ml of spheroplasting buffer (2 mM Vanadium Ribonucleoside Complex; 0.2 µM PMSF; 28.6 mM beta-mercaptoethanol; 50µg/ml zymolyase 100T (Medac GmBH); in buffer B). The suspension is incubated for 30 minutes at 30°C, pelleted and the supernatant is discarded. The spheroplasts are once washed with 1 ml buffer B and resuspended in 200-800 µl buffer B. From now humid chambers are used for incubations. 50µl of spheroplast suspension is dropped on poly-L-lysin treated coverslips and incubated for 30 minutes on 4°C. 4 ml ice-cold 70% ethanol is added and incubated overnight at -20°C. The spheroplast are washed twice with each 4 ml 2xSSC pH 7.0 for 5 minutes at RT and once for 5 minutes at RT in 2x SSC with 10% (v/v) formamide. The probe is prepared as follows: 2 µl probe (10 ng/µl); 4 µl formamide; 2 µl 2x SSC, 2 µl tRNA (10 mg/ml); 10 µl H_2O; the mixture is incubated for 5 minutes at 99°C and cooled rapidly in an ice/water bath. 20 µl 20% dextrane sulfate (in 4x SSC), 1µl BSA (2 mg/ml) and 2 µl Vanadium Ribonucleoside Complex (200 mM) is added. 20 µl of the probe solution is droped on each coverslip and incubated for 3 hours to overnight incubation at 37°C. The coverslips are washed 2 times for 15 minutes with 4 ml 2x SSC/10% formamide at 37°C, once with 2x SSC/0.1% Triton X-100 (w/v) at RT, twice with 1x SSC at RT and once with 1x TBS. The spheroplast are mounted in 2-5 µl of DAPI (0.1 µg/ml) in moviol.

5.2.7 Protein identification using MALDI-TOF/TOF mass spectrometry

5.2.7.1 Purification of (pre-) ribosomal particles

(Pre-) ribosomal particles are either purified by immuno-precipitation of FLAG-epitope or protein A (TAP-tag) epitope tagged proteins. In each case cell extracts are prepared like described in 5.2.5.3.
For FLAG-tagged proteins, the immuno-precipitation was carried out like described in 5.2.5.3 with following exceptions: the protein amount loaded on the M2 beads was in the range of 40 to 80 mg; the volume of beads was adjusted. After washing with A200 plus Triton (0.2% v/v), the beads were washed twice with 1 ml of desalting buffer AC (0.1 M ammonium acetate pH 7.4; 0.1 mM $MgCl_2$ hexa-hydrate) and the proteins are eluted through a basic pH step by two times washing with each 0.5 ml of 0.5 M ammonium hydroxide. The supernatants of the elutions are pooled and lyophilized.
For TAP-tagged proteins, immuno-precipitation was carried out as described for FLAG-tagged proteins with following exceptions: buffer MB is buffer A200, supplemented with Triton X-100 (0.5% v/v) and Tween 20 (0.1% v/v); the precipitation matrix is magnetic beads (1 µm BcMagEpoxy, Bioclone Inc.) coupled to rabbit IgG (Sigma-Aldrich). 200 µl of coupled beads are used for each precipitation experiment (pre-washed 3 times with buffer MB). Binding is carried out at 4°C for 1 hour. The beads are washed in a McMag magnetic separator (Bioclone Inc.) 3 times with buffer MB and 2 times with buffer AC (see before), each 0.7 ml. Elution is done like described before (see FLAG-tag purification). The eluates are pooled and lyophilized.

5.2.7.2 Analysis of purified (pre-) ribosomal particles by mass spectrometry

The lyophilized protein purifications (5.2.7.1) are resuspended in 20-50 µl of 50 mM ammonium carbonate pH 7.5 and 6 µl trypsin (1 mg/ml, Roche) is added. The proteins are digested overnight at 37°C. Once again the peptides are lyophilized and the pellet is resuspended in 20-50 µl of 0.1% TFA. The solution is centrifuged for 10 minutes at full speed and the supernatant is transferred into a HPLC cup. 10 to 15 µl of the peptide solution is separated on a nano-flow HPLC system (Dionex) with a Pep-Map C18–reversed phase column (LC-Packings/Dionex). Separation is done with a 5% to 95% gradient of 80% Acetonitril, 0.05% TFA (flow 0,3 µl/min). The fractions are mixed at real time with 5 times volume of MALDI matrix (CHCA α-cyano-4-hydroxycinnamic acid, 2 mg/ml in 70% acetonitril/0.1%TFA) and spotted onto a MALDI sample plate (SS, 192 well, Applied Biosystems) by a Dionex Probot system. The samples were analyzed by a MALDI-TOF/TOF 4800 series (Applied Biosystems). For standardization a Cal 4700 standard peptide mixture was used (Applied Biosystems). For the MS mode, 1000 shots with suitable energy were appointed. The six peaks with

highest intensity were further fragmented in the MSMS mode (2500 shots, 20% more energy than MS mode). Identification of peptides was done by a database search by the mass/ionization rate (MASCOT or NCBI database).

5.2.7.3 Quantitative analysis of purified pre-ribosomal particles by mass spectrometry

The lyophilized protein purifications (5.2.7.1) were subjected to iTRAQ labeling according to the manufacturer's instructions. Briefly, the pellets were resuspended, side chains (disulfide bonds) reduced, cysteins blocked, digested with trypsin, labeled with the corresponding iTRAQ reagent and lyophilized. The labeled peptides are resuspended in 20-50 µl of 0.1% TFA. Starting from this step, the protocol followed exactly the one from non-labeled peptides (see 5.2.7.2). Identification of peptides was done by a database search (MASCOT or NCBI database) including the peptide modifications (reduction, blocking, labeling). Quantification was done by intensity comparison of the iTRAQ area peaks (114 to 117 daltons). The quantitative data were normalized to the ratio of bait protein in the different purifications.

6 Appendix

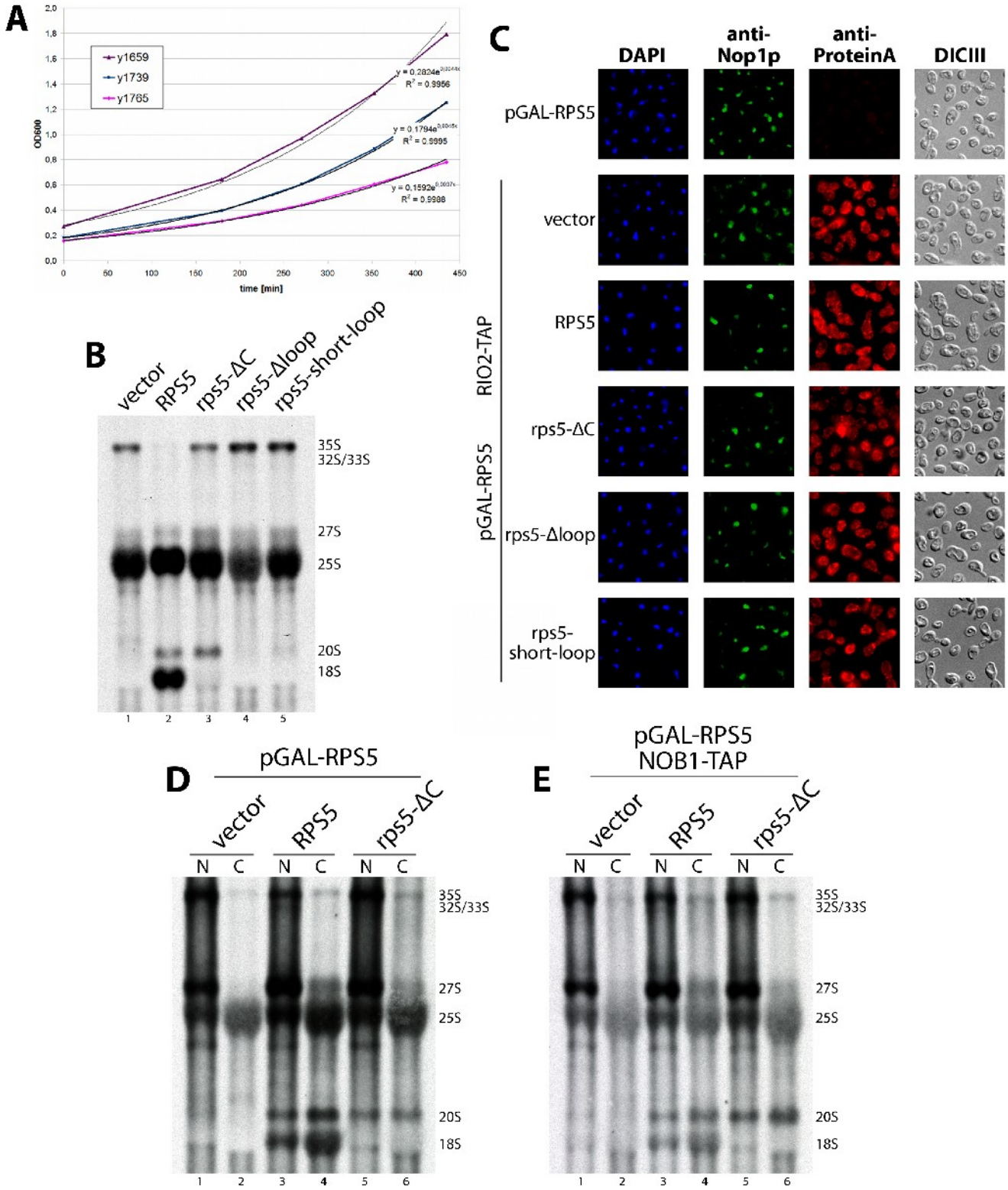

Supplemental Figure 1. Analyses of HA-tagged rpS5 variants

(**A**) Growth kinetics of yeast strains ToY1659 (pGAL-RPS5), ToY1739 (pGAL-RPS5, RIO2-TAP) and ToY1765 (pGAL-RPS5, NOB1-TAP). Logarithmically growing yeast cells (YP-galactose pre-culture) were diluted to the indicated OD(600) at time point 0 minutes and further grown in YP-galactose media. The best fits for the growth

curves are shown. Following doubling times in YP-galactose were calculated: ToY1659 – 158 minutes; ToY1739 – 154 minutes; ToY1765 – 187 minutes. (**B**)-(**E**) All experiments were performed in yeast strains, in which full length rpS5 is encoded under the control of the galactose inducible GAL1 promoter. The strains were either transformed with an empty vector (YEplac181) or vectors coding for HA-tagged full length rpS5 (ToP1162), rps5-ΔC (ToP1156), rps5-Δloop (ToP1157) or rps5-short-loop (ToP1158) under the control of a constitutive promoter. (**B**) and (**C**) Cells were grown overnight in selective media containing galactose, diluted in YP-galactose and subsequently expression of pGAL-RPS5 was shut down for 2 hours in YP-glucose medium. The experiments were performed in yeast strain ToY1659 (pGAL-RPS5). (**B**) 5',6'-[^{3}H] uracil metabolic labeling of newly synthesized RNA. Cells were pulsed for 30 minutes at 30°C. Total RNA was extracted and separated by gel electrophoresis, radio-labeled RNA was visualized by fluorography. (**C**) Steady state distribution of precursor subunits. Total DNA (DAPI) and rRNA precursors containing ITS1-sequences between site D and A2 (ITS1-Cy3) were detected as described in 5.2.6.2. (**D**) and (**E**) Cell fractionation after metabolic RNA labeling. Cells were grown overnight in in YP-galactose media, diluted in YP-galactose and grown for 1 hour in YP-glucose media before starting with the fractionation protocol (see 5.2.5.5). (**D**) The experiment was performed in yeast strain ToY1659 (pGAL-RPS5). After shut down of pGAL-RPS5 expression, newly synthesized RNA was labeled with 5',6'-[^{3}H] uracil for 20 minutes. Nuclear (N) and cytoplasmic (C) cellular fractions were subsequently separated, RNA was extracted, separated by gel electrophoresis and newly synthesized RNA was visualized by fluorography. (**E**) The experiment was performed in yeast strain ToY1765 (pGAL-RPS5, NOB1-TAP). After shut down of pGAL-RPS5 expression, newly synthesized RNA was labeled with 5',6'-[^{3}H] uracil for 20 minutes. Nuclear (N) and cytoplasmic (C) cellular fractions were subsequently separated, RNA was extracted, separated by gel electrophoresis and newly synthesized RNA was visualized by fluorography.

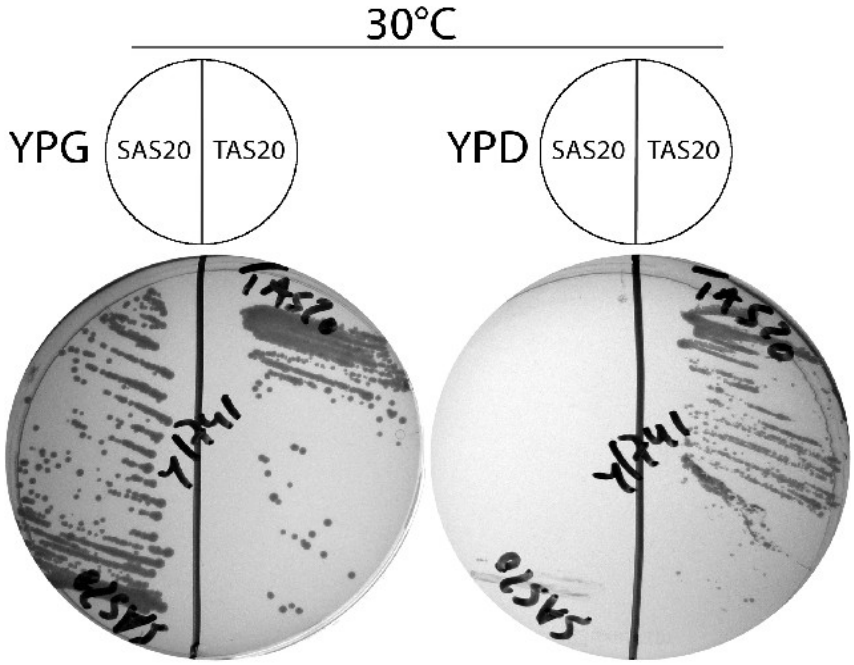

Supplemental Figure 2. Complementation analysis of HA-tagged TAS20 and SAS20
HA-tagged, constitutive expressed alleles of TAS20 (ToP1278) and SAS20 (ToP1279) were tested for rpS20 substitution in strain ToY845, where RPS20 is under control of a galactose inducible GAL1 promoter. The plates containing galactose (YPG) and glucose (YPD) were incubated for 3 days at 30°C.

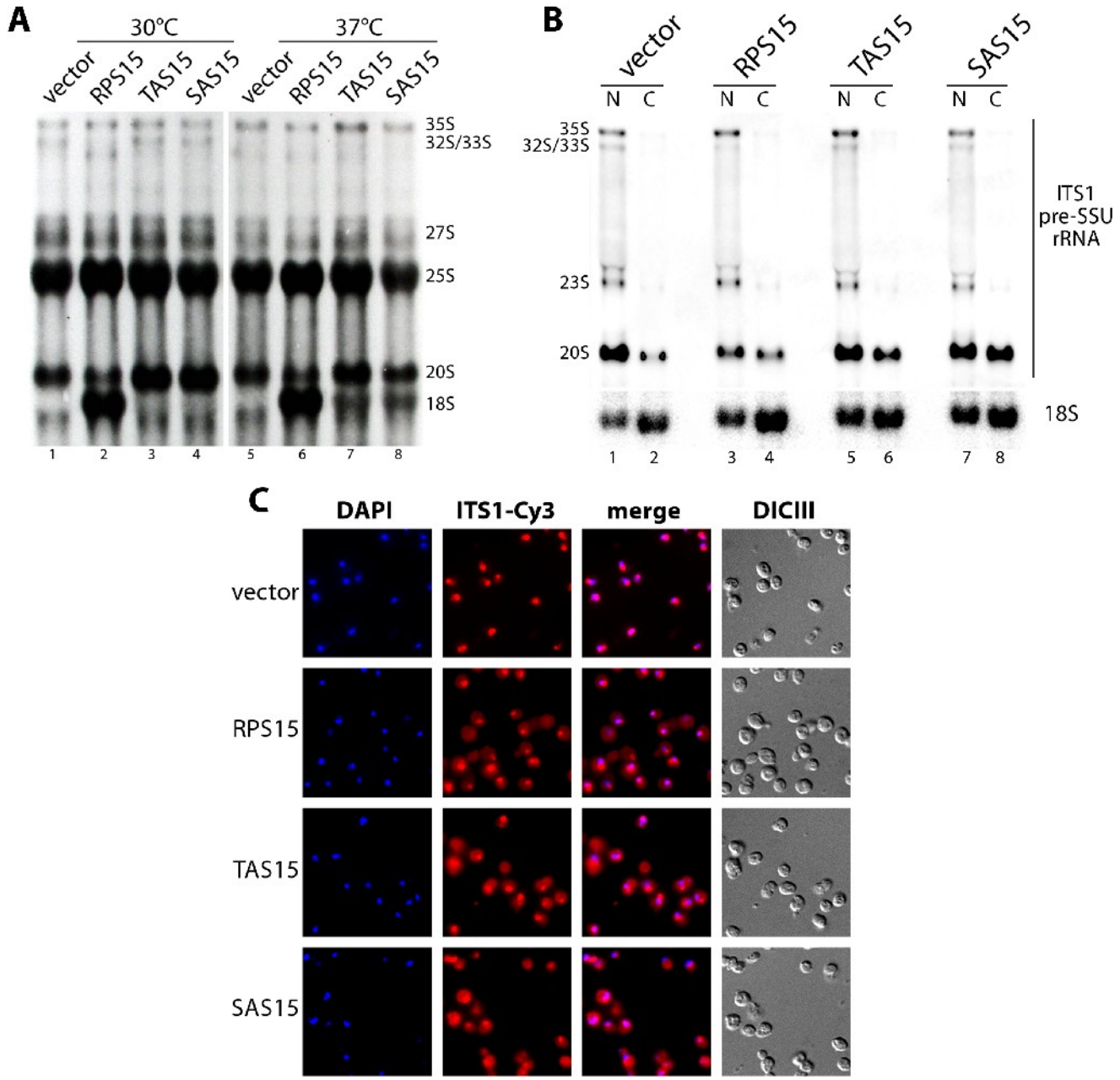

Supplemental Figure 3. Analyses of HA-tagged rpS15 variants

(**A**)-(**C**) All experiments were performed in yeast strain pGAL-RPS15 (ToY1217), in which full length rpS15 is encoded under the control of the galactose inducible GAL1 promoter. The strain was either transformed with an empty vector (YEplac181) or vectors coding for HA-tagged full length rpS15 (ToP1173), TAS15 (ToP1171) or SAS15 (ToP1172) under the control of a constitutive promoter. Cells were grown overnight in selective media containing galactose, diluted in YP-galactose and subsequently expression of pGAL-RPS15 was shut down for 2 hours in YP-glucose medium. The cultures were cultivated at the respective temperature of the later experiment. (**A**) 5',6'-[^{3}H] uracil metabolic labeling of newly synthesized RNA. Cells were pulsed for 30 minutes at 30°C or 37°C. Total RNA was extracted and separated by gel electrophoresis, radio-labeled RNA was visualized by fluorography. (**B**) Steady state analysis of pre-rRNA in sub-cellular fractions. Cells were grown for 1.5 hours in YPD before starting with the fractionation protocol (see 5.2.5.5). Cells were spheroplasted and subsequently fractionated in nuclei and cytoplasm. RNA was extracted and 2.4 times more volume of nuclear than cytoplasmic fractions were separated by gel electrophoresis and analyzed by northern blotting. Probes for detection of rRNA species are depicted right-hand. N – nuclear fraction; C – cytoplasmic fraction. (**C**) Steady state distribution of precursor subunits analyzed by FISH experiments. Total DNA (DAPI) and rRNA precursors containing ITS1-sequences between site D and A2 (ITS1-Cy3) were detected as described in 5.2.6.2.

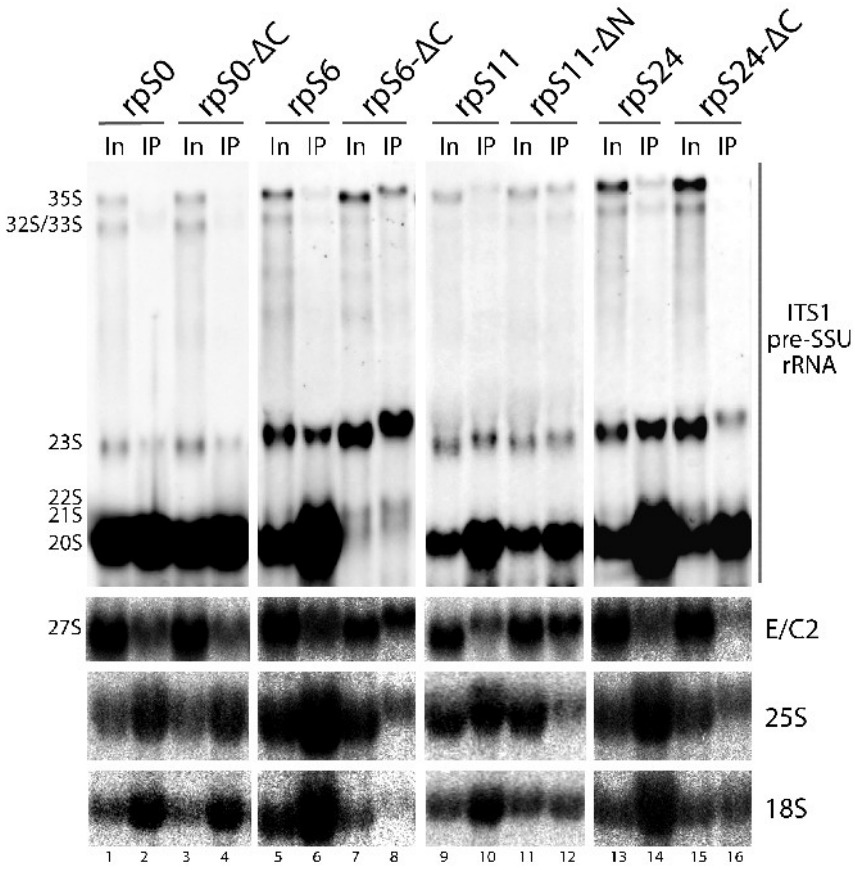

Supplemental Figure 4. RNA co-immunoprecipitation of FLAG-tagged truncated rpS proteins
All experiments were performed in the corresponding pGAL-RPSX strains (pGAL-RPS0 ToY256; pGAL-RPS6 ToY258; pGAL-RPS11 ToY325; pGAL-RPS24 ToY365). The strains were either transformed with vectors coding for FLAG-tagged full length rpSX or the truncated variant, both under the control of a constitutive promoter (rpS0 ToP991; rpS0-ΔC ToP514; rpS6 ToP997; rpS6-ΔC ToP573; rpS11 ToP1001; rpS11-ΔN ToP515; rpS24 ToP1012; rpS24-ΔC ToP574). Cells were grown overnight in selective media containing galactose, diluted in YP-galactose and subsequently expression of pGAL-RPSX was shut down for 3 hours in YP-glucose medium. RNA was extracted from Input (In) and immuno-purified (IP) fractions. Probes used for detection of (pre-) rRNA species are depicted right-hand. 200 mM salt (KCl, see 5.2.5.3) was used for cell breakage, binding and washing of the immunoprecipitations.

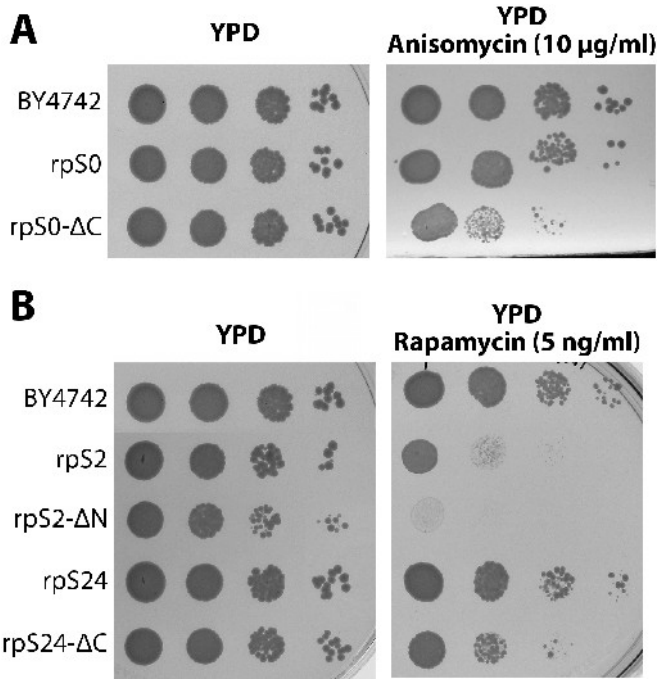

Supplemental Figure 5. Changed antibiotic resistance of some truncated rpS proteins
(**A**)-(**B**) Serial dilutions of the indicated transformants on YP-glucose (YPD) and YP-glucose mixed with indicated drugs containing plates. Plates were incubated for 2 days at 30°C. All yeast strains depend solely on the indicated FLAG-tagged constitutive expressed alleles. BY4742 is the isogenic wildtype background strain. (**A**) Strains ToY1498 (rpS0) and ToY1499 (rpS0-ΔC) (**B**) Strains ToY1500 (rpS2), ToY1501 (rpS2-ΔN), ToY1506 (rpS24) and ToY1507 (rpS24-ΔC). The spot tests were performed by U. Ohmayer during a practical course, instructed by A. Neueder.

Supplemental Table 1. FLAG-rpS5-ΔC associated proteins

A typical FLAG-tag purification of rpS5-ΔC containing SSU precursors. Basic elution, tryptic digest and identification by mass spectrometry (MALDI TOF/TOF)

	protein	peptides	total ion score %	SGD description
ribosome biogenesis factors	Arb1p	3	100	ATPase of the ATP-binding cassette (ABC) family involved in 40S and 60S ribosome biogenesis, has similarity to Gcn20p; shuttles from nucleus to cytoplasm, physically interacts with Tif6p, Lsg1p
	Bfr2p	1	79.4	Essential protein that is a component of 90S preribosomes; may be involved in rRNA processing; multicopy suppressor of sensitivity to Brefeldin A; expression is induced during lag phase and also by cold shock
	Bms1p	2	100	Essential conserved nucleolar GTP-binding protein required for synthesis of 40S ribosomal subunits and for processing of the 35S pre-rRNA at sites A0, A1, and A2; interacts with Rcl1p, has similarity to Tsr1p
	Dbp2p	9	100	Essential ATP-dependent RNA helicase of the DEAD-box protein family, involved in nonsense-mediated mRNA decay and rRNA processing
	Dim1p	1	99.8	Essential 18S rRNA dimethylase (dimethyladenosine transferase), responsible for conserved m6(2)Am6(2)A dimethylation in 3'-terminal loop of 18S rRNA, part of 90S and 40S pre-particles in nucleolus, involved in pre-ribosomal RNA processing
	Ecm16p (Dhr1p)	1	94.4	Essential DEAH-box ATP-dependent RNA helicase specific to the U3 snoRNP, predominantly nucleolar in distribution, required for 18S rRNA synthesis
	Enp1p	2	100	Protein associated with U3 and U14 snoRNAs, required for pre-rRNA processing and 40S ribosomal subunit synthesis; localized in the nucleus and concentrated in the nucleolus
	Kre33p	2	100	Essential protein of unknown function; heterozygous mutant shows haploinsufficiency in K1 killer toxin resistance
	Kri1p	1	92.5	Essential nucleolar protein required for 40S ribosome biogenesis; physically and functionally interacts with Krr1p
	Krr1p	2	100	Essential nucleolar protein required for the synthesis of 18S rRNA and for the assembly of 40S ribosomal subunit
	Ltv1p	5	100	Component of the GSE complex, which is required for proper sorting of amino acid permease Gap1p; required for ribosomal small subunit export from nucleus; required for growth at low temperature
	Mrt4p	2	100	Protein involved in mRNA turnover and ribosome assembly, localizes to the nucleolus
	Nob1p	2	100	Essential nuclear protein involved in proteasome maturation and synthesis of 40S ribosomal subunits; required for cleavage of the 20S pre-rRNA to generate the mature 18S rRNA
	Nog1p	1	99.2	Putative GTPase that associates with free 60S ribosomal subunits in the nucleolus and is required for 60S ribosomal subunit biogenesis; constituent of 66S pre-ribosomal particles; member of the ODN family of nucleolar G-proteins
	Nop1p	1	96.1	Nucleolar protein, component of the small subunit processome complex, which is required for processing of pre-18S rRNA; has similarity to mammalian fibrillarin
	Nop56p (Sik1p)	1	90	Essential evolutionarily-conserved nucleolar protein component of the box C/D snoRNP complexes that direct 2'-O-methylation of pre-rRNA during its maturation; overexpression causes spindle orientation defects
	Nop58p (Nop5p)	1	100	Protein involved in pre-rRNA processing, 18S rRNA synthesis, and snoRNA synthesis; component of the small subunit processome complex, which is required for processing of pre-18S rRNA
	Pno1p (Dim2p)	2	100	Essential nucleolar protein required for pre-18S rRNA processing, interacts with Dim1p, an 18S rRNA dimethyltransferase, and also with Nob1p, which is involved in proteasome biogenesis; contains a KH domain
	Prp43p	2	100	RNA helicase in the DEAH-box family, functions in both RNA polymerase I and polymerase II transcript metabolism, involved in release of the lariat-intron from the spliceosome (1, 2, 3, 4) Also known as: JA1
	Rex2p	4	100	3'-5' RNA exonuclease; involved in 3'-end processing of U4 and U5 snRNAs, 5S and 5.8S rRNAs, and RNase P and RNase MRP RNA; localized to mitochondria and null suppresses escape of mtDNA to nucleus in yme1 yme2 mutants; RNase D exonuclease
	Rio2p	2	100	Essential serine kinase involved in the processing of the 20S pre-rRNA into mature 18S rRNA; has similarity to Rio1p
	Sof1p	1	100	Essential protein required for biogenesis of 40S (small) ribosomal subunit; has similarity to the beta subunit of trimeric G-proteins and the splicing factor Prp4p
	Tsr1p	4	100	Protein required for processing of 20S pre-rRNA in the cytoplasm, associates with pre-40S ribosomal particles
	Utp2p (Nop14p / Noc5p)	1	100	Nucleolar protein, forms a complex with Noc4p that mediates maturation and nuclear export of 40S ribosomal subunits; also present in the small subunit processome complex, which is required for processing of pre-18S rRNA

	Utp12p (Dip2p)	1	96.7	Nucleolar protein, specifically associated with the U3 snoRNA, part of the large ribonucleoprotein complex known as the small subunit (SSU) processome, required for 18S rRNA biogenesis, part of the active pre-rRNA processing complex
	Utp14p	1	100	Subunit of U3-containing Small Subunit (SSU) processome complex involved in production of 18S rRNA and assembly of small ribosomal subunit
	Utp15p	1	95.5	Nucleolar protein, component of the small subunit (SSU) processome containing the U3 snoRNA that is involved in processing of pre-18S rRNA
	Utp21p	1	100	Subunit of U3-containing 90S preribosome and Small Subunit (SSU) processome complexes involved in production of 18S rRNA and assembly of small ribosomal subunit; synthetic defect with STI1 Hsp90 cochaperone; human homolog linked to glaucoma
	Utp22p	2	100	Possible U3 snoRNP protein involved in maturation of pre-18S rRNA, based on computational analysis of large-scale protein-protein interaction data
translation associated factors	eIF3	3	100	eukaryotic translation initiation factor 3
	eIF4A	7	100	Translation initiation factor eIF4A, identical to Tif1p; DEA(D/H)-box RNA helicase that couples ATPase activity to RNA binding and unwinding; forms a dumbbell structure of two compact domains connected by a linker; interacts with eIF4G
	EF-1 alpha	7	100	Translational elongation factor EF-1 alpha; functions in the binding reaction of aminoacyl-tRNA (AA-tRNA) to ribosomes
	EF-2 (Eft2p)	5	100	Elongation factor 2 (EF-2), also encoded by EFT1; catalyzes ribosomal translocation during protein synthesis; contains diphthamide, the unique posttranslationally modified histidine residue specifically ADP-ribosylated by diphtheria toxin
	EF-3	1	99.9	Translational elongation factor 3, stimulates the binding of aminoacyl-tRNA (AA-tRNA) to ribosomes by releasing EF-1 alpha from the ribosomal complex; contains two ABC cassettes; binds and hydrolyses ATP
	eRF1	1	83.4	Polypeptide release factor (eRF1) in translation termination
	Ded1p	1	100	ATP-dependent DEAD (Asp-Glu-Ala-Asp)-box RNA helicase, required for translation initiation of all yeast mRNAs; mutations in human DEAD-box DBY are a frequent cause of male infertility
nucleo-cytoplasmic transport	Hrb1p	1	86.2	Poly(A+) RNA-binding protein, involved in the export of mRNAs from the nucleus to the cytoplasm; similar to Gbp2p and Npl3p
	Kap123p	5	100	Karyopherin beta, mediates nuclear import of ribosomal proteins prior to assembly into ribosomes and import of histones H3 and H4; localizes to the nuclear pore, nucleus, and cytoplasm; exhibits genetic interactions with RAI1
	Seh1p	1	100	Nuclear pore protein that is part of the evolutionarily conserved Nup84p complex (Nup84p, Nup85p, Nup120p, Nup145p, and Seh1p); homologous to Sec13p
	Sub2p	1	100	Component of the TREX complex required for nuclear mRNA export; member of the DEAD-box RNA helicase superfamily and is involved in early and late steps of spliceosome assembly; homolog of the human splicing factor hUAP56
	Yra1p	2	100	Nuclear protein that binds to RNA and to Mex67p, required for export of poly(A)+ mRNA from the nucleus; member of the REF (RNA and export factor binding proteins) family; another family member, Yra2p, can substitute for Yra1p function
	Yrb1p	1	90	Ran GTPase binding protein; involved in nuclear protein import and RNA export, ubiquitin-mediated protein degradation during the cell cycle; shuttles between the nucleus and cytoplasm; is essential; homolog of human RanBP1
other factors	H2B	1	100	Histone H2B
	Swi3p	1	85.4	Subunit of the SWI/SNF chromatin remodeling complex, which regulates transcription by remodeling chromosomes; required for transcription of many genes, including ADH1, ADH2, GAL1, HO, INO1 and SUC2
	RPC40	1	95.5	RNA polymerase subunit, common to RNA polymerase I and III
	Rtf1p	3	100	Subunit of the RNA polymerase II-associated Paf1 complex; directly or indirectly regulates DNA-binding properties of Spt15p and relative activities of different TATA elements; involved in telomere maintenance
	Tap42p	2	100	Essential protein involved in the TOR signaling pathway; physically associates with the protein phosphatase 2A and the SIT4 protein phosphatase catalytic subunits
	Ssb2p	1	100	Cytoplasmic ATPase that is a ribosome-associated molecular chaperone, functions with J-protein partner Zuo1p; may be involved in the folding of newly-synthesized polypeptide chains; member of the HSP70 family; homolog of SSB1
	Bmh1p	1	99.1	14-3-3 protein, major isoform; controls proteome at post-transcriptional level, binds proteins and DNA, involved in regulation of many processes including exocytosis, vesicle transport, Ras/MAPK signaling, and rapamycin-sensitive signaling

Supplemental Table 2. FLAG-rpS5-short-loop associated proteins

A typical FLAG-tag purification of rpS5-short-loop containing SSU precursors. Basic elution, tryptic digest and identification by mass spectrometry (MALDI TOF/TOF)

	protein	peptides	total ion score %	SGD description
ribosome biogenesis factors	Arb1p	1	100	ATPase of the ATP-binding cassette (ABC) family involved in 40S and 60S ribosome biogenesis, has similarity to Gcn20p; shuttles from nucleus to cytoplasm, physically interacts with Tif6p, Lsg1p
	Enp1p	7	100	Protein associated with U3 and U14 snoRNAs, required for pre-rRNA processing and 40S ribosomal subunit synthesis; localized in the nucleus and concentrated in the nucleolus
	Ltv1p	4	100	Component of the GSE complex, which is required for proper sorting of amino acid permease Gap1p; required for ribosomal small subunit export from nucleus; required for growth at low temperature
	Nmd3p	1	96.4	Protein involved in nuclear export of the large ribosomal subunit; acts as a Crm1p-dependent adapter protein for export of nascent ribosomal subunits through the nuclear pore complex
	Nob1p	3	100	Essential nuclear protein involved in proteasome maturation and synthesis of 40S ribosomal subunits; required for cleavage of the 20S pre-rRNA to generate the mature 18S rRNA
	Nop58p (Nop5p)	1	99.5	Protein involved in pre-rRNA processing, 18S rRNA synthesis, and snoRNA synthesis; component of the small subunit processome complex, which is required for processing of pre-18S rRNA
	Rex2p	4	100	3'-5' RNA exonuclease; involved in 3'-end processing of U4 and U5 snRNAs, 5S and 5.8S rRNAs, and RNase P and RNase MRP RNA; localized to mitochondria and null suppresses escape of mtDNA to nucleus in yme1 yme2 mutants; RNase D exonuclease
	Rio2p	3	100	Essential serine kinase involved in the processing of the 20S pre-rRNA into mature 18S rRNA; has similarity to Rio1p
	Tif6p	1	91.1	Constituent of 66S pre-ribosomal particles, has similarity to human translation initiation factor 6 (eIF6); may be involved in the biogenesis and or stability of 60S ribosomal subunits
	Tsr1p	7	100	Protein required for processing of 20S pre-rRNA in the cytoplasm, associates with pre-40S ribosomal particles
translation associated factors	eIF3	3	100	eukaryotic translation initiation factor 3
	eIF4A (Tif2p)	6	100	Translation initiation factor eIF4A, identical to Tif1p; DEA(D/H)-box RNA helicase that couples ATPase activity to RNA binding and unwinding; forms a dumbbell structure of two compact domains connected by a linker; interacts with eIF4G
	eIF4E	1	98.8	Cytoplasmic mRNA cap binding protein and translation initiation factor eIF4E
	EF-1 alpha	10	100	Translational elongation factor EF-1 alpha; functions in the binding reaction of aminoacyl-tRNA (AA-tRNA) to ribosomes
	EF-2 (Eft2p)	8	100	Elongation factor 2 (EF-2), also encoded by EFT1; catalyzes ribosomal translocation during protein synthesis; contains diphthamide, the unique posttranslationally modified histidine residue specifically ADP-ribosylated by diphtheria toxin
	EF-3	9	100	Translational elongation factor 3, stimulates the binding of aminoacyl-tRNA (AA-tRNA) to ribosomes by releasing EF-1 alpha from the ribosomal complex; contains two ABC cassettes; binds and hydrolyses ATP
nucleo-cytoplasmic transport	Gsp2p	1	99.4	GTP binding protein (mammalian Ranp homolog) involved in the maintenance of nuclear organization, RNA processing and transport; interacts with Kap121p, Kap123p and Pdr6p (karyophilin betas); Gsp1p homolog that is not required for viability
	Kap123	8	100	Karyopherin beta, mediates nuclear import of ribosomal proteins prior to assembly into ribosomes and import of histones H3 and H4; localizes to the nuclear pore, nucleus, and cytoplasm; exhibits genetic interactions with RAI1
	Sub2p	1	99.9	Component of the TREX complex required for nuclear mRNA export; member of the DEAD-box RNA helicase superfamily and is involved in early and late steps of spliceosome assembly; homolog of the human splicing factor hUAP56
other factors	RPA34	3	100	RNA polymerase I subunit A34.5
	Rtf1p	5	100	Subunit of the RNA polymerase II-associated Paf1 complex; directly or indirectly regulates DNA-binding properties of Spt15p and relative activities of different TATA elements; involved in telomere maintenance
	Ssb2p	1	100	Cytoplasmic ATPase that is a ribosome-associated molecular chaperone, functions with J-protein partner Zuo1p; may be involved in the folding of newly-synthesized polypeptide chains; member of the HSP70 family; homolog of SSB1
	Bmh1p	2	100	14-3-3 protein, major isoform; controls proteome at post-transcriptional level, binds proteins and DNA, involved in regulation of many processes including exocytosis, vesicle transport, Ras/MAPK signaling, and rapamycin-sensitive signaling

Supplemental Table 3. FLAG-SAS20 associated proteins

A typical FLAG-tag purification of SAS20 containing SSU precursors. Basic elution, tryptic digest and identification by mass spectrometry (MALDI TOF/TOF)

	protein	peptides	total ion score %	SGD description
ribosome biogenesis factors	Arb1p	7	100	ATPase of the ATP-binding cassette (ABC) family involved in 40S and 60S ribosome biogenesis, has similarity to Gcn20p; shuttles from nucleus to cytoplasm, physically interacts with Tif6p, Lsg1p
	Bfr2p	1	100	Essential protein that is a component of 90S preribosomes; may be involved in rRNA processing; multicopy suppressor of sensitivity to Brefeldin A; expression is induced during lag phase and also by cold shock
	Dbp2p	6	100	Essential ATP-dependent RNA helicase of the DEAD-box protein family, involved in nonsense-mediated mRNA decay and rRNA processing
	Drs1p	1	100	Nucleolar DEAD-box protein required for ribosome assembly and function, including synthesis of 60S ribosomal subunits; constituent of 66S pre-ribosomal particles
	Ecm16p (Dhr1p)	1	97.5	Essential DEAH-box ATP-dependent RNA helicase specific to the U3 snoRNP, predominantly nucleolar in distribution, required for 18S rRNA synthesis
	Enp1p	10	100	Protein associated with U3 and U14 snoRNAs, required for pre-rRNA processing and 40S ribosomal subunit synthesis; localized in the nucleus and concentrated in the nucleolus
	Gar1p	1	100	Protein component of the H/ACA snoRNP pseudouridylase complex, involved in the modification and cleavage of the 18S pre-rRNA
	Has1p	1	99.6	ATP-dependent RNA helicase; localizes to both the nuclear periphery and nucleolus; highly enriched in nuclear pore complex fractions; constituent of 66S pre-ribosomal particles
	Kre33p	3	100	Essential protein of unknown function; heterozygous mutant shows haploinsufficiency in K1 killer toxin resistance
	Ltv1p	6	100	Component of the GSE complex, which is required for proper sorting of amino acid permease Gap1p; required for ribosomal small subunit export from nucleus; required for growth at low temperature
	Mrt4p	3	100	Protein involved in mRNA turnover and ribosome assembly, localizes to the nucleolus
	Nob1p	9	100	Essential nuclear protein involved in proteasome maturation and synthesis of 40S ribosomal subunits; required for cleavage of the 20S pre-rRNA to generate the mature 18S rRNA
	Nog1p	1	100	Putative GTPase that associates with free 60S ribosomal subunits in the nucleolus and is required for 60S ribosomal subunit biogenesis; constituent of 66S pre-ribosomal particles; member of the ODN family of nucleolar G-proteins
	Nop58p (Nop5p)	1	100	Protein involved in pre-rRNA processing, 18S rRNA synthesis, and snoRNA synthesis; component of the small subunit processome complex, which is required for processing of pre-18S rRNA
	Nug1p	2	100	GTPase that associates with nuclear 60S pre-ribosomes, required for export of 60S ribosomal subunits from the nucleus
	Pno1p (Dim2p)	4	100	Essential nucleolar protein required for pre-18S rRNA processing, interacts with Dim1p, an 18S rRNA dimethyltransferase, and also with Nob1p, which is involved in proteasome biogenesis; contains a KH domain
	Rio2p	8	100	Essential serine kinase involved in the processing of the 20S pre-rRNA into mature 18S rRNA; has similarity to Rio1p
	Rrp3p	2	100	Protein involved in rRNA processing; required for maturation of the 35S primary transcript of pre-rRNA and for cleavage leading to mature 18S rRNA; homologous to eIF-4a, which is a DEAD box RNA-dependent ATPase with helicase activity
	Rrp8p	1	100	Nucleolar protein involved in rRNA processing, pre-rRNA cleavage at site A2; also involved in telomere maintenance; mutation is synthetically lethal with a gar1 mutation
	Rrp12p	2	100	Protein required for export of the ribosomal subunits; associates with the RNA components of the pre-ribosomes; contains HEAT-repeats
	Tif6p	1	100	Constituent of 66S pre-ribosomal particles, has similarity to human translation initiation factor 6 (eIF6); may be involved in the biogenesis and or stability of 60S ribosomal subunits
	Tsr1p	9	100	Protein required for processing of 20S pre-rRNA in the cytoplasm, associates with pre-40S ribosomal particles

translation associated factors	Ded1p	4	100	ATP-dependent DEAD (Asp-Glu-Ala-Asp)-box RNA helicase, required for translation initiation of all yeast mRNAs; mutations in human DEAD-box DBY are a frequent cause of male infertility
	eIF3	17	100	eukaryotic translation initiation factor 3
	eIF4A (Tif2p)	18	100	Translation initiation factor eIF4A, identical to Tif1p; DEA(D/H)-box RNA helicase that couples ATPase activity to RNA binding and unwinding; forms a dumbbell structure of two compact domains connected by a linker; interacts with eIF4G
	eIF4E	2	100	Cytoplasmic mRNA cap binding protein and translation initiation factor eIF4E
	eIF5B	2	100	GTPase, required for general translation initiation by promoting Met-tRNAiMet binding to ribosomes and ribosomal subunit joining; homolog of bacterial IF2
	EF-1 alpha	16	100	Translational elongation factor EF-1 alpha; functions in the binding reaction of aminoacyl-tRNA (AA-tRNA) to ribosomes
	EF-1 gamma	1	100	Translation elongation factor EF-1 gamma
	EF-2 (Eft2p)	15	100	Elongation factor 2 (EF-2), also encoded by EFT1; catalyzes ribosomal translocation during protein synthesis; contains diphthamide, the unique posttranslationally modified histidine residue specifically ADP-ribosylated by diphtheria toxin
	EF-3	23	100	Translational elongation factor 3, stimulates the binding of aminoacyl-tRNA (AA-tRNA) to ribosomes by releasing EF-1 alpha from the ribosomal complex; contains two ABC cassettes; binds and hydrolyses ATP
	eRF1	2	100	Polypeptide release factor (eRF1) in translation termination
	eRF3	2	100	Translation termination factor eRF3
transcription associated factors	Rtf1p	6	100	Subunit of the RNA polymerase II-associated Paf1 complex; directly or indirectly regulates DNA-binding properties of Spt15p and relative activities of different TATA elements; involved in telomere maintenance
	Rvb1p	1	100	Essential protein involved in transcription regulation; component of chromatin remodeling complexes; required for assembly and function of the INO80 complex; also referred to as pontin; member of the RUVB-like protein family
	Rvb2p	1	100	Essential protein involved in transcription regulation; component of chromatin remodeling complexes; required for assembly and function of the INO80 complex; also referred to as pontin; member of the RUVB-like protein family
nucleo-cytoplasmic transport	Dhh1p	1	97.7	Cytoplasmic DExD/H-box helicase, stimulates mRNA decapping, coordinates distinct steps in mRNA function and decay, interacts with both the decapping and deadenylase complexes, may have a role in mRNA export and translation
	Kap123p	5	100	Karyopherin beta, mediates nuclear import of ribosomal proteins prior to assembly into ribosomes and import of histones H3 and H4; localizes to the nuclear pore, nucleus, and cytoplasm; exhibits genetic interactions with RAI1
	Sub2p	3	100	Component of the TREX complex required for nuclear mRNA export; member of the DEAD-box RNA helicase superfamily and is involved in early and late steps of spliceosome assembly; homolog of the human splicing factor hUAP56
	Yra1p	2	100	Nuclear protein that binds to RNA and to Mex67p, required for export of poly(A)+ mRNA from the nucleus; member of the REF (RNA and export factor binding proteins) family; another family member, Yra2p, can substitute for Yra1p function
other factors	Ssb2p	1	100	Cytoplasmic ATPase that is a ribosome-associated molecular chaperone, functions with J-protein partner Zuo1p; may be involved in the folding of newly-synthesized polypeptide chains; member of the HSP70 family; homolog of SSB1
	Bmh1p	3	100	14-3-3 protein, major isoform; controls proteome at post-transcriptional level, binds proteins and DNA, involved in regulation of many processes including exocytosis, vesicle transport, Ras/MAPK signaling, and rapamycin-sensitive signaling
	H2A	2	100	Histone H2A
	H4	3	100	Histone H4
	RPA34	3	100	RNA polymerase I subunit A34.5

Supplemental Table 4. List of examined archaeal r-proteins

A list of all examined archaeal r-proteins, derived from *T. acidophilum* or *S. acidocaldarius*. All alleles were cloned in a multicopy yeast vector under control of a constitutive promoter. The relative strength of r-protein interaction with 20S pre-rRNA is given: – no interaction; +/- weak interaction; + strong interaction

Homologue of yeast rpS	*T. acidophilum*		*S. acidocaldarius*	
		pre-rRNA interaction		pre-rRNA interaction
0	✓	+/-		
1	✓	+/-		
2	✓	+/-		
3	✓	+/-	✓	--
5	✓	+/-	✓	--
6	✓	+/-		
9	✓	+		
11	✓	+/-		
13	✓	+	✓	+/-
14	✓	+/-	✓	+/-
15	✓	+	✓	+
16	✓	--	✓	--
17	✓	--		
19	✓	+		
20	✓	+	✓	+
24	✓	--		
26			✓	--
27	✓	--	✓	--
30			✓	--
31	✓	--		

7 References

Abovich, N., Gritz, L., Tung, L., and Rosbash, M. (1985). Effect of RP51 gene dosage alterations on ribosome synthesis in Saccharomyces cerevisiae. Mol. Cell. Biol *5*, 3429-3435.

Abovich, N., and Rosbash, M. (1984). Two genes for ribosomal protein 51 of Saccharomyces cerevisiae complement and contribute to the ribosomes. Mol. Cell. Biol *4*, 1871-1879.

Adilakshmi, T., Bellur, D. L., and Woodson, S. A. (2008). Concurrent nucleation of 16S folding and induced fit in 30S ribosome assembly. Nature *455*, 1268-1272.

Adilakshmi, T., Ramaswamy, P., and Woodson, S. A. (2005). Protein-independent folding pathway of the 16S rRNA 5' domain. J. Mol. Biol *351*, 508-519.

Agalarov, S. C., Zheleznyakova, E. N., Selivanova, O. M., Zheleznaya, L. A., Matvienko, N. I., Vasiliev, V. D., and Spirin, A. S. (1998). In vitro assembly of a ribonucleoprotein particle corresponding to the platform domain of the 30S ribosomal subunit. Proc. Natl. Acad. Sci. U.S.A *95*, 999-1003.

Agirrezabala, X., and Frank, J. (2009). Elongation in translation as a dynamic interaction among the ribosome, tRNA, and elongation factors EF-G and EF-Tu. Q. Rev. Biophys *42*, 159-200.

Alberts, B., Bray, D., Lewis, J., Raff, M., Roberts, K., and Watson, J. D. (1989). Molecular Biology of the Cell (New York, NY: Garland Publishing, Inc.).

Alksne, L. E., Anthony, R. A., Liebman, S. W., and Warner, J. R. (1993a). An accuracy center in the ribosome conserved over 2 billion years. Proc. Natl. Acad. Sci. U.S.A *90*, 9538-9541.

Alksne, L. E., Anthony, R. A., Liebman, S. W., and Warner, J. R. (1993b). An accuracy center in the ribosome conserved over 2 billion years. Proc. Natl. Acad. Sci. U.S.A *90*, 9538-9541.

Allmang, C., and Tollervey, D. (1998). The role of the 3' external transcribed spacer in yeast pre-rRNA processing. J. Mol. Biol *278*, 67-78.

Arenas, J. E., and Abelson, J. N. (1997). Prp43: An RNA helicase-like factor involved in spliceosome disassembly. Proc. Natl. Acad. Sci. U.S.A *94*, 11798-11802.

Auger-Buendia, M. A., Longuet, M., and Tavitian, A. (1979). Kinetic studies on ribosomal proteins assembly in preribosomal particles and ribosomal subunits of mammalian cells. Biochim. Biophys. Acta *563*, 113-128.

Bachand, F., and Silver, P. A. (2004). PRMT3 is a ribosomal protein methyltransferase that affects the cellular levels of ribosomal subunits. EMBO J *23*, 2641-2650.

Ban, N., Nissen, P., Hansen, J., Moore, P. B., and Steitz, T. A. (2000). The complete atomic structure of the large ribosomal subunit at 2.4 A resolution. Science *289*, 905-920.

Baudin-Baillieu, A., Tollervey, D., Cullin, C., and Lacroute, F. (1997a). Functional analysis of Rrp7p, an essential yeast protein involved in pre-rRNA processing and ribosome assembly. Mol. Cell. Biol *17*, 5023-5032.

Baudin-Baillieu, A., Tollervey, D., Cullin, C., and Lacroute, F. (1997b). Functional analysis of Rrp7p, an essential yeast protein involved in pre-rRNA processing and ribosome assembly. Mol. Cell. Biol *17*, 5023-5032.

Baxter-Roshek, J. L., Petrov, A. N., and Dinman, J. D. (2007). Optimization of ribosome structure and function by rRNA base modification. PLoS ONE *2*, e174.

van Beekvelt, C. A., de Graaff-Vincent, M., Faber, A. W., van't Riet, J., Venema, J., and Raué, H. A. (2001). All three functional domains of the large ribosomal subunit protein L25 are required for both early and late pre-rRNA processing steps in Saccharomyces cerevisiae. Nucleic Acids Res *29*, 5001-5008.

van Beekvelt, C. A., Jeeninga, R. E., van't Riet, J., Venema, J., and Raué, H. A. (2001). Identification of cis-acting elements involved in 3'-end formation of Saccharomyces cerevisiae 18S rRNA. RNA *7*, 896-903.

Bell, S. D., and Jackson, S. P. (1998). Transcription and translation in Archaea: a mosaic of eukaryal and bacterial features. Trends Microbiol *6*, 222-228.

Beltrame, M., and Tollervey, D. (1992). Identification and functional analysis of two U3 binding sites on yeast pre-ribosomal RNA. EMBO J *11*, 1531-1542.

Benelli, D., and Londei, P. (2009). Begin at the beginning: evolution of translational initiation. Res. Microbiol *160*, 493-501.

Berger, A. B., Decourty, L., Badis, G., Nehrbass, U., Jacquier, A., and Gadal, O. (2007). Hmo1 is required for TOR-dependent regulation of ribosomal protein gene transcription. Mol. Cell. Biol *27*, 8015-8026.

Beringer, M., and Rodnina, M. V. (2007). The ribosomal peptidyl transferase. Mol. Cell *26*, 311-321.

Bernander, R., and Poplawski, A. (1997). Cell cycle characteristics of thermophilic archaea. J. Bacteriol *179*, 4963-4969.

Bohnsack, M. T., Martin, R., Granneman, S., Ruprecht, M., Schleiff, E., and Tollervey, D. (2009). Prp43 bound at different sites on the pre-rRNA performs distinct functions in ribosome synthesis. Mol. Cell *36*, 583-592.

Boisvert, F., van Koningsbruggen, S., Navascués, J., and Lamond, A. I. (2007). The multifunctional nucleolus. Nat. Rev. Mol. Cell Biol *8*, 574-585.

Bouchoux, C., Hautbergue, G., Grenetier, S., Carles, C., Riva, M., and Goguel, V. (2004). CTD kinase I is involved in RNA polymerase I transcription. Nucleic Acids Res *32*, 5851-5860.

Bradatsch, B., Katahira, J., Kowalinski, E., Bange, G., Yao, W., Sekimoto, T., Baumgärtel, V., Boese, G., Bassler, J., Wild, K., et al. (2007). Arx1 functions as an unorthodox nuclear export receptor for the 60S preribosomal subunit. Mol. Cell *27*, 767-779.

Brandt, R., and Gualerzi, C. O. (1992). Ribosomal localization of the mRNA in the 30S initiation complex as revealed by UV crosslinking. FEBS Lett *311*, 199-202.

Braunstein, S., Karpisheva, K., Pola, C., Goldberg, J., Hochman, T., Yee, H., Cangiarella, J., Arju, R., Formenti, S. C., and Schneider, R. J. (2007). A hypoxia-controlled cap-dependent to cap-independent translation switch in breast cancer. Mol. Cell *28*, 501-512.

Brock, T. D., Brock, K. M., Belly, R. T., and Weiss, R. L. (1972). Sulfolobus: a new genus of sulfur-oxidizing bacteria living at low pH and high temperature. Arch Mikrobiol *84*, 54-68.

Brodersen, D. E., Clemons, W. M., Carter, A. P., Wimberly, B. T., and Ramakrishnan, V. (2002). Crystal structure of the 30 S ribosomal subunit from Thermus thermophilus: structure of the proteins and their interactions with 16 S RNA. J. Mol. Biol *316*, 725-768.

Brodersen, D. E., and Nissen, P. (2005). The social life of ribosomal proteins. FEBS J *272*, 2098-2108.

Buchhaupt, M., Meyer, B., Kötter, P., and Entian, K. (2006). Genetic evidence for 18S rRNA binding and an Rps19p assembly function of yeast nucleolar protein Nep1p. Mol. Genet. Genomics *276*, 273-284.

Bulygin, K. N., Repkova, M. N., Ven'yaminova, A. G., Graifer, D. M., Karpova, G. G., Frolova, L. Y., and Kisselev, L. L. (2002). Positioning of the mRNA stop signal with respect to polypeptide chain release factors and ribosomal proteins in 80S ribosomes. FEBS Lett *514*, 96-101.

Bunner, A. E., Beck, A. H., and Williamson, J. R. (2010). Kinetic cooperativity in Escherichia coli 30S ribosomal subunit reconstitution reveals additional complexity in the assembly landscape. Proc Natl Acad Sci U S A. Available at: http://www.ncbi.nlm.nih.gov/pubmed/20207951 [Accessed March 19, 2010].

Bunner, A. E., Nord, S., Wikström, P. M., and Williamson, J. R. (2010a). The Effect of Ribosome Assembly Cofactors on In Vitro 30S Subunit Reconstitution. J Mol Biol. Available at: http://www.ncbi.nlm.nih.gov/pubmed/20188109 [Accessed March 19, 2010].

Bunner, A. E., Nord, S., Wikström, P. M., and Williamson, J. R. (2010b). The Effect of Ribosome Assembly Cofactors on In Vitro 30S Subunit Reconstitution. J Mol Biol. Available at: http://www.ncbi.nlm.nih.gov/pubmed/20188109 [Accessed March 22, 2010].

Cabezón, T., Herzog, A., De Wilde, M., Villarroel, R., and Bollen, A. (1976). Cooperative control of translational fidelity by ribosomal proteins in Escherichia coli. III. A ram mutation in the structural gene for protein S5 (rpx E). Mol. Gen. Genet *144*, 59-62.

Chandramouli, P., Topf, M., Ménétret, J., Eswar, N., Cannone, J. J., Gutell, R. R., Sali, A., and Akey, C. W. (2008). Structure of the mammalian 80S ribosome at 8.7 A resolution. Structure *16*, 535-548.

Charette, M., and Gray, M. W. (2000). Pseudouridine in RNA: what, where, how, and why. IUBMB Life *49*, 341-351.

Chaudhuri, S., Vyas, K., Kapasi, P., Komar, A. A., Dinman, J. D., Barik, S., and Mazumder, B. (2007). Human ribosomal protein L13a is dispensable for canonical ribosome function but indispensable for efficient rRNA methylation. RNA *13*, 2224-2237.

Chen, D., and Huang, S. (2001). Nucleolar components involved in ribosome biogenesis cycle between the nucleolus and nucleoplasm in interphase cells. J. Cell Biol *153*, 169-176.

Chen, L., Brügger, K., Skovgaard, M., Redder, P., She, Q., Torarinsson, E., Greve, B., Awayez, M., Zibat, A., Klenk, H., et al. (2005). The genome of Sulfolobus acidocaldarius, a model organism of the Crenarchaeota. J. Bacteriol *187*, 4992-4999.

Chen, W., Bucaria, J., Band, D. A., Sutton, A., and Sternglanz, R. (2003). Enp1, a yeast protein associated with U3 and U14 snoRNAs, is required for pre-rRNA processing and 40S subunit synthesis. Nucleic Acids Res *31*, 690-699.

Chiocchetti, A., Zhou, J., Zhu, H., Karl, T., Haubenreisser, O., Rinnerthaler, M., Heeren, G., Oender, K., Bauer, J., Hintner, H., et al. (2007). Ribosomal proteins Rpl10 and Rps6 are potent regulators of yeast replicative life span. Exp. Gerontol *42*, 275-286.

Chooi, W. Y., and Leiby, K. R. (1981). An electron microscopic method for localization of ribosomal proteins during transcription of ribosomal DNA: a method for studying protein assembly. Proc. Natl. Acad. Sci. U.S.A *78*, 4823-4827.

Ciammaruconi, A., and Londei, P. (2001). In vitro processing of the 16S rRNA of the thermophilic archaeon Sulfolobus solfataricus. J. Bacteriol *183*, 3866-3874.

Cisterna, B., Malatesta, M., Dieker, J., Muller, S., Prosperi, E., and Biggiogera, M. (2009). An active mechanism flanks and modulates the export of the small ribosomal subunits. Histochem. Cell Biol *131*, 743-753.

Cisterna, B., Necchi, D., Prosperi, E., and Biggiogera, M. (2006). Small ribosomal subunits associate with nuclear myosin and actin in transit to the nuclear pores. FASEB J *20*, 1901-1903.

Claypool, J. A., French, S. L., Johzuka, K., Eliason, K., Vu, L., Dodd, J. A., Beyer, A. L., and Nomura, M. (2004). Tor pathway regulates Rrn3p-dependent recruitment of yeast RNA polymerase I to the promoter but does not participate in alteration of the number of active genes. Mol. Biol. Cell *15*, 946-956.

Clemons, W. M., May, J. L., Wimberly, B. T., McCutcheon, J. P., Capel, M. S., and Ramakrishnan, V. (1999). Structure of a bacterial 30S ribosomal subunit at 5.5 A resolution. Nature *400*, 833-840.

Cole, S. E., LaRiviere, F. J., Merrikh, C. N., and Moore, M. J. (2009). A convergence of rRNA and mRNA quality control pathways revealed by mechanistic analysis of nonfunctional rRNA decay. Mol. Cell *34*, 440-450.

Cybulski, N., and Hall, M. N. (2009). TOR complex 2: a signaling pathway of its own. Trends Biochem. Sci *34*, 620-627.

Dai, M., Arnold, H., Sun, X., Sears, R., and Lu, H. (2007). Inhibition of c-Myc activity by ribosomal protein L11. EMBO J *26*, 3332-3345.

Dai, M., Sun, X., and Lu, H. (2010). Ribosomal protein L11 associates with c-Myc at 5S rRNA and tRNA genes and regulates their expression. J Biol Chem. Available at: http://www.ncbi.nlm.nih.gov/pubmed/20194507 [Accessed March 25, 2010].

Dammann, R., Lucchini, R., Koller, T., and Sogo, J. M. (1995). Transcription in the yeast rRNA gene locus: distribution of the active gene copies and chromatin structure of their flanking regulatory sequences. Mol. Cell. Biol *15*, 5294-5303.

Darland, G., Brock, T. D., Samsonoff, W., and Conti, S. F. (1970). A thermophilic, acidophilic mycoplasma isolated from a coal refuse pile. Science *170*, 1416-1418.

Demianova, M., Formosa, T. G., and Ellis, S. R. (1996). Yeast proteins related to the p40/laminin

receptor precursor are essential components of the 40 S ribosomal subunit. J. Biol. Chem *271*, 11383-11391.

Dennis, P. P., Omer, A., and Lowe, T. (2001). A guided tour: small RNA function in Archaea. Mol. Microbiol *40*, 509-519.

Dennis, P. P., Ehrenberg, M., and Bremer, H. (2004). Control of rRNA synthesis in Escherichia coli: a systems biology approach. Microbiol. Mol. Biol. Rev *68*, 639-668.

Derenzini, M., Montanaro, L., and Treré, D. (2009). What the nucleolus says to a tumour pathologist. Histopathology *54*, 753-762.

Dez, C., Houseley, J., and Tollervey, D. (2006). Surveillance of nuclear-restricted pre-ribosomes within a subnucleolar region of Saccharomyces cerevisiae. EMBO J *25*, 1534-1546.

Dontsova, O., Kopylov, A., and Brimacombe, R. (1991). The location of mRNA in the ribosomal 30S initiation complex; site-directed cross-linking of mRNA analogues carrying several photo-reactive labels simultaneously on either side of the AUG start codon. EMBO J *10*, 2613-2620.

Döring, T., Mitchell, P., Osswald, M., Bochkariov, D., and Brimacombe, R. (1994). The decoding region of 16S RNA; a cross-linking study of the ribosomal A, P and E sites using tRNA derivatized at position 32 in the anticodon loop. EMBO J *13*, 2677-2685.

Dragon, F., Gallagher, J. E. G., Compagnone-Post, P. A., Mitchell, B. M., Porwancher, K. A., Wehner, K. A., Wormsley, S., Settlage, R. E., Shabanowitz, J., Osheim, Y., et al. (2002a). A large nucleolar U3 ribonucleoprotein required for 18S ribosomal RNA biogenesis. Nature *417*, 967-970.

Dragon, F., Gallagher, J. E. G., Compagnone-Post, P. A., Mitchell, B. M., Porwancher, K. A., Wehner, K. A., Wormsley, S., Settlage, R. E., Shabanowitz, J., Osheim, Y., et al. (2002b). A large nucleolar U3 ribonucleoprotein required for 18S ribosomal RNA biogenesis. Nature *417*, 967-970.

Dresios, J., Panopoulos, P., and Synetos, D. (2006). Eukaryotic ribosomal proteins lacking a eubacterial counterpart: important players in ribosomal function. Mol. Microbiol *59*, 1651-1663.

Dundr, M., Hebert, M. D., Karpova, T. S., Stanek, D., Xu, H., Shpargel, K. B., Meier, U. T., Neugebauer, K. M., Matera, A. G., and Misteli, T. (2004). In vivo kinetics of Cajal body components. J. Cell Biol *164*, 831-842.

Dunn, J. J., and Studier, F. W. (1973). T7 early RNAs and Escherichia coli ribosomal RNAs are cut from large precursor RNAs in vivo by ribonuclease 3. Proc. Natl. Acad. Sci. U.S.A *70*, 3296-3300.

Durovic, P., and Dennis, P. P. (1994a). Separate pathways for excision and processing of 16S and 23S rRNA from the primary rRNA operon transcript from the hyperthermophilic archaebacterium Sulfolobus acidocaldarius: similarities to eukaryotic rRNA processing. Mol. Microbiol *13*, 229-242.

Durovic, P., and Dennis, P. P. (1994b). Separate pathways for excision and processing of 16S and 23S rRNA from the primary rRNA operon transcript from the hyperthermophilic archaebacterium Sulfolobus acidocaldarius: similarities to eukaryotic rRNA processing. Mol. Microbiol *13*, 229-242.

Eisinger, D. P., Dick, F. A., and Trumpower, B. L. (1997). Qsr1p, a 60S ribosomal subunit protein, is required for joining of 40S and 60S subunits. Mol. Cell. Biol *17*, 5136-5145.

El Hage, A., Sbaï, M., and Alix, J. H. (2001). The chaperonin GroEL and other heat-shock proteins, besides DnaK, participate in ribosome biogenesis in Escherichia coli. Mol. Gen. Genet *264*, 796-808.

Elion, E. A., and Warner, J. R. (1986). An RNA polymerase I enhancer in Saccharomyces cerevisiae. Mol. Cell. Biol *6*, 2089-2097.

Fargo, D. C., Boynton, J. E., and Gillham, N. W. (2001). Chloroplast ribosomal protein S7 of Chlamydomonas binds to chloroplast mRNA leader sequences and may be involved in translation initiation. Plant Cell *13*, 207-218.

Fassio, C. A., Schofield, B. J., Seiser, R. M., Johnson, A. W., and Lycan, D. E. (2010a). Dominant Mutations in the Late 40S Biogenesis Factor Ltv1 Affect Cytoplasmic Maturation of the Small

Ribosomal Subunit in S. cerevisiae. Genetics. Available at: http://www.ncbi.nlm.nih.gov/pubmed/20215468 [Accessed March 12, 2010].

Fassio, C. A., Schofield, B. J., Seiser, R. M., Johnson, A. W., and Lycan, D. E. (2010b). Dominant Mutations in the Late 40S Biogenesis Factor Ltv1 Affect Cytoplasmic Maturation of the Small Ribosomal Subunit in S. cerevisiae. Genetics. Available at: http://www.ncbi.nlm.nih.gov/pubmed/20215468 [Accessed March 19, 2010].

Fatica, A., Oeffinger, M., Dlakić, M., and Tollervey, D. (2003). Nob1p is required for cleavage of the 3' end of 18S rRNA. Mol. Cell. Biol *23*, 1798-1807.

Fatica, A., Tollervey, D., and Dlakić, M. (2004). PIN domain of Nob1p is required for D-site cleavage in 20S pre-rRNA. RNA *10*, 1698-1701.

Fei, J., Kosuri, P., MacDougall, D. D., and Gonzalez, R. L. (2008). Coupling of ribosomal L1 stalk and tRNA dynamics during translation elongation. Mol. Cell *30*, 348-359.

Ferreira-Cerca, S., Pöll, G., Gleizes, P., Tschochner, H., and Milkereit, P. (2005). Roles of eukaryotic ribosomal proteins in maturation and transport of pre-18S rRNA and ribosome function. Mol. Cell *20*, 263-275.

Ferreira-Cerca, S., Pöll, G., Kühn, H., Neueder, A., Jakob, S., Tschochner, H., and Milkereit, P. (2007). Analysis of the in vivo assembly pathway of eukaryotic 40S ribosomal proteins. Mol. Cell *28*, 446-457.

Fiserova, J., and Goldberg, M. W. (2010). Nucleocytoplasmic transport in yeast: a few roles for many actors. Biochem. Soc. Trans *38*, 273-277.

Fox, G. W., and Woese, C. R. (1975). 5S RNA secondary structure. Nature *256*, 505-507.

Frank, J., and Agrawal, R. K. (2000). A ratchet-like inter-subunit reorganization of the ribosome during translocation. Nature *406*, 318-322.

Fukushi, S., Okada, M., Stahl, J., Kageyama, T., Hoshino, F. B., and Katayama, K. (2001). Ribosomal protein S5 interacts with the internal ribosomal entry site of hepatitis C virus. J. Biol. Chem *276*, 20824-20826.

Fumagalli, S., Di Cara, A., Neb-Gulati, A., Natt, F., Schwemberger, S., Hall, J., Babcock, G. F., Bernardi, R., Pandolfi, P. P., and Thomas, G. (2009). Absence of nucleolar disruption after impairment of 40S ribosome biogenesis reveals an rpL11-translation-dependent mechanism of p53 induction. Nat. Cell Biol *11*, 501-508.

Gadal, O., Labarre, S., Boschiero, C., and Thuriaux, P. (2002). Hmo1, an HMG-box protein, belongs to the yeast ribosomal DNA transcription system. EMBO J *21*, 5498-5507.

Gallagher, J. E. G., Dunbar, D. A., Granneman, S., Mitchell, B. M., Osheim, Y., Beyer, A. L., and Baserga, S. J. (2004). RNA polymerase I transcription and pre-rRNA processing are linked by specific SSU processome components. Genes Dev *18*, 2506-2517.

Ganapathi, K. A., and Shimamura, A. (2008). Ribosomal dysfunction and inherited marrow failure. Br. J. Haematol *141*, 376-387.

Gaspin, C., Cavaillé, J., Erauso, G., and Bachellerie, J. P. (2000). Archaeal homologs of eukaryotic methylation guide small nucleolar RNAs: lessons from the Pyrococcus genomes. J. Mol. Biol *297*, 895-906.

Geerlings, T. H., Faber, A. W., Bister, M. D., Vos, J. C., and Raué, H. A. (2003). Rio2p, an evolutionarily conserved, low abundant protein kinase essential for processing of 20 S Pre-rRNA in Saccharomyces cerevisiae. J. Biol. Chem *278*, 22537-22545.

Gelperin, D., Horton, L., Beckman, J., Hensold, J., and Lemmon, S. K. (2001). Bms1p, a novel GTP-binding protein, and the related Tsr1p are required for distinct steps of 40S ribosome biogenesis in yeast. RNA *7*, 1268-1283.

Gerbasi, V. R., Weaver, C. M., Hill, S., Friedman, D. B., and Link, A. J. (2004). Yeast Asc1p and mammalian RACK1 are functionally orthologous core 40S ribosomal proteins that repress gene expression. Mol. Cell. Biol *24*, 8276-8287.

Granneman, S., and Baserga, S. J. (2004). Ribosome biogenesis: of knobs and RNA processing. Exp. Cell Res *296*, 43-50.

Granneman, S., Nandineni, M. R., and Baserga, S. J. (2005). The putative NTPase Fap7 mediates cytoplasmic 20S pre-rRNA processing through a direct interaction with Rps14. Mol. Cell. Biol *25*, 10352-10364.

Green, R., and Noller, H. F. (1996). In vitro complementation analysis localizes 23S rRNA posttranscriptional modifications that are required for Escherichia coli 50S ribosomal subunit assembly and function. RNA *2*, 1011-1021.

Hall, D. B., Wade, J. T., and Struhl, K. (2006). An HMG protein, Hmo1, associates with promoters of many ribosomal protein genes and throughout the rRNA gene locus in Saccharomyces cerevisiae. Mol. Cell. Biol *26*, 3672-3679.

Hansen, J. L., Moore, P. B., and Steitz, T. A. (2003). Structures of five antibiotics bound at the peptidyl transferase center of the large ribosomal subunit. J. Mol. Biol *330*, 1061-1075.

Hansen, M., Taubert, S., Crawford, D., Libina, N., Lee, S., and Kenyon, C. (2007). Lifespan extension by conditions that inhibit translation in Caenorhabditis elegans. Aging Cell *6*, 95-110.

Hayes, F., and Vasseur, M. (1976). Processing of the 17-S Escherichia coli precursor RNA in the 27-S pre-ribosomal particle. Eur. J. Biochem *61*, 433-442.

Henis-Korenblit, S., Strumpf, N. L., Goldstaub, D., and Kimchi, A. (2000). A novel form of DAP5 protein accumulates in apoptotic cells as a result of caspase cleavage and internal ribosome entry site-mediated translation. Mol. Cell. Biol *20*, 496-506.

Henras, A. K., Soudet, J., Gérus, M., Lebaron, S., Caizergues-Ferrer, M., Mougin, A., and Henry, Y. (2008). The post-transcriptional steps of eukaryotic ribosome biogenesis. Cell. Mol. Life Sci *65*, 2334-2359.

Henras, A. K., Bertrand, E., and Chanfreau, G. (2004). A cotranscriptional model for 3'-end processing of the Saccharomyces cerevisiae pre-ribosomal RNA precursor. RNA *10*, 1572-1585.

Herold, M., and Nierhaus, K. H. (1987). Incorporation of six additional proteins to complete the assembly map of the 50 S subunit from Escherichia coli ribosomes. J. Biol. Chem *262*, 8826-8833.

Hinnebusch, A. G. (2005). Translational regulation of GCN4 and the general amino acid control of yeast. Annu. Rev. Microbiol *59*, 407-450.

Hjort, K., and Bernander, R. (2001). Cell cycle regulation in the hyperthermophilic crenarchaeon Sulfolobus acidocaldarius. Mol. Microbiol *40*, 225-234.

Ho, J. H., Kallstrom, G., and Johnson, A. W. (2000). Nmd3p is a Crm1p-dependent adapter protein for nuclear export of the large ribosomal subunit. J. Cell Biol *151*, 1057-1066.

Hoagland, M. B., Stephenson, M. L., Scott, J. F., Hecht, L. I., and Zamecnik, P. C. (1958). A soluble ribonucleic acid intermediate in protein synthesis. J. Biol. Chem *231*, 241-257.

Hofer, A., Bussiere, C., and Johnson, A. W. (2007). Mutational analysis of the ribosomal protein Rpl10 from yeast. J. Biol. Chem *282*, 32630-32639.

Hoffmann, A., Bukau, B., and Kramer, G. (2010). Structure and function of the molecular chaperone Trigger Factor. Biochim Biophys Acta. Available at: http://www.ncbi.nlm.nih.gov/pubmed/20132842 [Accessed March 19, 2010].

Hölzle, A., Fischer, S., Heyer, R., Schütz, S., Zacharias, M., Walther, P., Allers, T., and Marchfelder, A. (2008). Maturation of the 5S rRNA 5' end is catalyzed in vitro by the endonuclease tRNase Z in the archaeon H. volcanii. RNA *14*, 928-937.

van Hoof, A., Lennertz, P., and Parker, R. (2000). Three conserved members of the RNase D family have unique and overlapping functions in the processing of 5S, 5.8S, U4, U5, RNase MRP and RNase P RNAs in yeast. EMBO J *19*, 1357-1365.

Hosokawa, K., Fujimura, R. K., and Nomura, M. (1966). Reconstitution of functionally active ribosomes from inactive subparticles and proteins. Proc. Natl. Acad. Sci. U.S.A *55*, 198-204.

Houseley, J., and Tollervey, D. (2009). The many pathways of RNA degradation. Cell *136*, 763-776.

Hughes, J. M., and Ares, M. (1991a). Depletion of U3 small nucleolar RNA inhibits cleavage in the 5' external transcribed spacer of yeast pre-ribosomal RNA and impairs formation of 18S ribosomal RNA. EMBO J *10*, 4231-4239.

Hughes, J. M., and Ares, M. (1991b). Depletion of U3 small nucleolar RNA inhibits cleavage in the 5' external transcribed spacer of yeast pre-ribosomal RNA and impairs formation of 18S ribosomal RNA. EMBO J *10*, 4231-4239.

Hung, N., Lo, K., Patel, S. S., Helmke, K., and Johnson, A. W. (2008). Arx1 is a nuclear export receptor for the 60S ribosomal subunit in yeast. Mol. Biol. Cell *19*, 735-744.

Jackson, R. J., Hellen, C. U. T., and Pestova, T. V. (2010). The mechanism of eukaryotic translation initiation and principles of its regulation. Nat. Rev. Mol. Cell Biol *11*, 113-127.

Jacob, F., and Monod, J. (1961). Genetic regulatory mechanisms in the synthesis of proteins. J. Mol. Biol *3*, 318-356.

Jacobs, K. L., and Grogan, D. W. (1997). Rates of spontaneous mutation in an archaeon from geothermal environments. J. Bacteriol *179*, 3298-3303.

Jacq, B. (1981). Sequence homologies between eukaryotic 5.8S rRNA and the 5' end of prokaryotic 23S rRNa: evidences for a common evolutionary origin. Nucleic Acids Res *9*, 2913-2932.

Jakovljevic, J., de Mayolo, P. A., Miles, T. D., Nguyen, T. M., Léger-Silvestre, I., Gas, N., and Woolford, J. L. (2004). The carboxy-terminal extension of yeast ribosomal protein S14 is necessary for maturation of 43S preribosomes. Mol. Cell *14*, 331-342.

Jang, S. K., Kräusslich, H. G., Nicklin, M. J., Duke, G. M., Palmenberg, A. C., and Wimmer, E. (1988). A segment of the 5' nontranslated region of encephalomyocarditis virus RNA directs internal entry of ribosomes during in vitro translation. J. Virol *62*, 2636-2643.

Johannes, G., Carter, M. S., Eisen, M. B., Brown, P. O., and Sarnow, P. (1999). Identification of eukaryotic mRNAs that are translated at reduced cap binding complex eIF4F concentrations using a cDNA microarray. Proc. Natl. Acad. Sci. U.S.A *96*, 13118-13123.

Johannes, G., and Sarnow, P. (1998). Cap-independent polysomal association of natural mRNAs encoding c-myc, BiP, and eIF4G conferred by internal ribosome entry sites. RNA *4*, 1500-1513.

Kaczanowska, M., and Rydén-Aulin, M. (2007). Ribosome biogenesis and the translation process in Escherichia coli. Microbiol. Mol. Biol. Rev *71*, 477-494.

Keller, E. B., Zamecnik, P. C., and Loftfield, R. B. (1954). The role of microsomes in the incorporation of amino acids into proteins. J. Histochem. Cytochem *2*, 378-386.

Kelley, L. A., and Sternberg, M. J. E. (2009). Protein structure prediction on the Web: a case study using the Phyre server. Nat Protoc *4*, 363-371.

Kemmler, S., Occhipinti, L., Veisu, M., and Panse, V. G. (2009). Yvh1 is required for a late maturation step in the 60S biogenesis pathway. J. Cell Biol *186*, 863-880.

King, T. H., Liu, B., McCully, R. R., and Fournier, M. J. (2003). Ribosome structure and activity are altered in cells lacking snoRNPs that form pseudouridines in the peptidyl transferase center. Mol. Cell *11*, 425-435.

Kirthi, N., Roy-Chaudhuri, B., Kelley, T., and Culver, G. M. (2006). A novel single amino acid change in small subunit ribosomal protein S5 has profound effects on translational fidelity. RNA *12*, 2080-2091.

Kitahara, K., and Suzuki, T. (2009). The ordered transcription of RNA domains is not essential for ribosome biogenesis in Escherichia coli. Mol. Cell *34*, 760-766.

Kjems, J., and Garrett, R. A. (1988). Novel splicing mechanism for the ribosomal RNA intron in the archaebacterium Desulfurococcus mobilis. Cell *54*, 693-703.

Kjems, J., and Garrett, R. A. (1991). Ribosomal RNA introns in archaea and evidence for RNA conformational changes associated with splicing. Proc. Natl. Acad. Sci. U.S.A *88*, 439-443.

Klein, C., and Struhl, K. (1994). Protein kinase A mediates growth-regulated expression of yeast ribosomal protein genes by modulating RAP1 transcriptional activity. Mol. Cell. Biol *14*, 1920-1928.

Koš, M., and Tollervey, D. (2010). Yeast Pre-rRNA Processing and Modification Occur Cotranscriptionally. Mol Cell *37*, 809-820.

Koulis, A., Cowan, D. A., Pearl, L. H., and Savva, R. (1996). Uracil-DNA glycosylase activities in

hyperthermophilic micro-organisms. FEMS Microbiol. Lett *143*, 267-271.

Kraft, C., Deplazes, A., Sohrmann, M., and Peter, M. (2008). Mature ribosomes are selectively degraded upon starvation by an autophagy pathway requiring the Ubp3p/Bre5p ubiquitin protease. Nat. Cell Biol *10*, 602-610.

Kraft, C., and Peter, M. (2008). Is the Rsp5 ubiquitin ligase involved in the regulation of ribophagy? Autophagy *4*, 838-840.

Krüger, T., Zentgraf, H., and Scheer, U. (2007). Intranucleolar sites of ribosome biogenesis defined by the localization of early binding ribosomal proteins. J. Cell Biol *177*, 573-578.

Kruiswijk, T., Planta, R. J., and Krop, J. M. (1978). The course of the assembly of ribosomal subunits in yeast. Biochim. Biophys. Acta *517*, 378-389.

Krzyzosiak, W., Denman, R., Nurse, K., Hellmann, W., Boublik, M., Gehrke, C. W., Agris, P. F., and Ofengand, J. (1987). In vitro synthesis of 16S ribosomal RNA containing single base changes and assembly into a functional 30S ribosome. Biochemistry *26*, 2353-2364.

Kurkcuoglu, O., Doruker, P., Sen, T. Z., Kloczkowski, A., and Jernigan, R. L. (2008a). The ribosome structure controls and directs mRNA entry, translocation and exit dynamics. Phys Biol *5*, 46005.

Kurkcuoglu, O., Doruker, P., Sen, T. Z., Kloczkowski, A., and Jernigan, R. L. (2008b). The ribosome structure controls and directs mRNA entry, translocation and exit dynamics. Phys Biol *5*, 46005.

Lafontaine, D., Delcour, J., Glasser, A. L., Desgrès, J., and Vandenhaute, J. (1994). The DIM1 gene responsible for the conserved m6(2)Am6(2)A dimethylation in the 3'-terminal loop of 18 S rRNA is essential in yeast. J. Mol. Biol *241*, 492-497.

Lafontaine, D., Vandenhaute, J., and Tollervey, D. (1995). The 18S rRNA dimethylase Dim1p is required for pre-ribosomal RNA processing in yeast. Genes Dev *9*, 2470-2481.

Lafontaine, D. L. J. (2010). A 'garbage can' for ribosomes: how eukaryotes degrade their ribosomes. Trends Biochem Sci. Available at: http://www.ncbi.nlm.nih.gov/pubmed/20097077 [Accessed February 12, 2010].

Lake, J. A. (1976). Ribosome structure determined by electron microscopy of Escherichia coli small subunits, large subunits and monomeric ribosomes. J. Mol. Biol *105*, 131-139.

Laletina, E., Graifer, D., Malygin, A., Ivanov, A., Shatsky, I., and Karpova, G. (2006). Proteins surrounding hairpin IIIe of the hepatitis C virus internal ribosome entry site on the human 40S ribosomal subunit. Nucleic Acids Res *34*, 2027-2036.

Lam, Y. W., Lamond, A. I., Mann, M., and Andersen, J. S. (2007). Analysis of nucleolar protein dynamics reveals the nuclear degradation of ribosomal proteins. Curr. Biol *17*, 749-760.

Lamanna, A. C., and Karbstein, K. (2009). Nob1 binds the single-stranded cleavage site D at the 3'-end of 18S rRNA with its PIN domain. Proc. Natl. Acad. Sci. U.S.A *106*, 14259-14264.

Langer, D., Hain, J., Thuriaux, P., and Zillig, W. (1995). Transcription in archaea: similarity to that in eucarya. Proc. Natl. Acad. Sci. U.S.A *92*, 5768-5772.

LaRiviere, F. J., Cole, S. E., Ferullo, D. J., and Moore, M. J. (2006). A late-acting quality control process for mature eukaryotic rRNAs. Mol. Cell *24*, 619-626.

Lebaron, S., Froment, C., Fromont-Racine, M., Rain, J., Monsarrat, B., Caizergues-Ferrer, M., and Henry, Y. (2005). The splicing ATPase prp43p is a component of multiple preribosomal particles. Mol. Cell. Biol *25*, 9269-9282.

Lee, Y., and Nazar, R. N. (1997). Ribosomal 5 S rRNA maturation in Saccharomyces cerevisiae. J. Biol. Chem *272*, 15206-15212.

Léger-Silvestre, I., Milkereit, P., Ferreira-Cerca, S., Saveanu, C., Rousselle, J., Choesmel, V., Guinefoleau, C., Gas, N., and Gleizes, P. (2004). The ribosomal protein Rps15p is required for nuclear exit of the 40S subunit precursors in yeast. EMBO J *23*, 2336-2347.

Lempiäinen, H., and Shore, D. (2009). Growth control and ribosome biogenesis. Curr. Opin. Cell Biol *21*, 855-863.

Li, H., Tsang, C. K., Watkins, M., Bertram, P. G., and Zheng, X. F. S. (2006). Nutrient regulates Tor1

nuclear localization and association with rDNA promoter. Nature *442*, 1058-1061.

Li, Z., and Deutscher, M. P. (1995). The tRNA processing enzyme RNase T is essential for maturation of 5S RNA. Proc. Natl. Acad. Sci. U.S.A *92*, 6883-6886.

Li, Z., Pandit, S., and Deutscher, M. P. (1999a). Maturation of 23S ribosomal RNA requires the exoribonuclease RNase T. RNA *5*, 139-146.

Li, Z., Pandit, S., and Deutscher, M. P. (1999b). RNase G (CafA protein) and RNase E are both required for the 5' maturation of 16S ribosomal RNA. EMBO J *18*, 2878-2885.

Liang, W. Q., and Fournier, M. J. (1997). Synthesis of functional eukaryotic ribosomal RNAs in trans: development of a novel in vivo rDNA system for dissecting ribosome biogenesis. Proc. Natl. Acad. Sci. U.S.A *94*, 2864-2868.

Liang, X., Liu, Q., and Fournier, M. J. (2007). rRNA modifications in an intersubunit bridge of the ribosome strongly affect both ribosome biogenesis and activity. Mol. Cell *28*, 965-977.

Lindström, M. S. (2009). Emerging functions of ribosomal proteins in gene-specific transcription and translation. Biochem. Biophys. Res. Commun *379*, 167-170.

Link, A. J., Eng, J., Schieltz, D. M., Carmack, E., Mize, G. J., Morris, D. R., Garvik, B. M., and Yates, J. R. (1999). Direct analysis of protein complexes using mass spectrometry. Nat. Biotechnol *17*, 676-682.

Lipson, R. S., Webb, K. J., and Clarke, S. G. (2010). Rmt1 catalyzes zinc-finger independent arginine methylation of ribosomal protein Rps2 in Saccharomyces cerevisiae. Biochem Biophys Res Commun *391*, 1658-1662.

Lo, K., and Johnson, A. W. (2009). Reengineering ribosome export. Mol. Biol. Cell *20*, 1545-1554.

Loar, J. W., Seiser, R. M., Sundberg, A. E., Sagerson, H. J., Ilias, N., Zobel-Thropp, P., Craig, E. A., and Lycan, D. E. (2004). Genetic and biochemical interactions among Yar1, Ltv1 and Rps3 define novel links between environmental stress and ribosome biogenesis in Saccharomyces cerevisiae. Genetics *168*, 1877-1889.

Lodmell, J. S., and Dahlberg, A. E. (1997). A conformational switch in Escherichia coli 16S ribosomal RNA during decoding of messenger RNA. Science *277*, 1262-1267.

Lomakin, I. B., Kolupaeva, V. G., Marintchev, A., Wagner, G., and Pestova, T. V. (2003). Position of eukaryotic initiation factor eIF1 on the 40S ribosomal subunit determined by directed hydroxyl radical probing. Genes Dev *17*, 2786-2797.

Louvet, E., Junéra, H. R., Le Panse, S., and Hernandez-Verdun, D. (2005). Dynamics and compartmentation of the nucleolar processing machinery. Exp. Cell Res *304*, 457-470.

Lumsden, T., Bentley, A. A., Beutler, W., Ghosh, A., Galkin, O., and Komar, A. A. (2009). Yeast strains with N-terminally truncated ribosomal protein S5: implications for the evolution, structure and function of the Rps5/Rps7 proteins. Nucleic Acids Res. Available at: http://www.ncbi.nlm.nih.gov/pubmed/19969550 [Accessed February 17, 2010].

Mager, W. H., Retél, J., Planta, R. J., Bollen, G. H., De Regt, V. C., and Hoving, H. (1977). Transcriptional units for ribosomal proteins in yeast. Eur. J. Biochem *78*, 575-583.

Magnusson, L. U., Farewell, A., and Nyström, T. (2005). ppGpp: a global regulator in Escherichia coli. Trends Microbiol *13*, 236-242.

Maki, J. A., and Culver, G. M. (2005). Recent developments in factor-facilitated ribosome assembly. Methods *36*, 313-320.

Malygin, A. A., and Karpova, G. G. (2009). Structural motifs of the bacterial ribosomal proteins S20, S18 and S16 that contact rRNA present in the eukaryotic ribosomal proteins S25, S26 and S27A, respectively. Nucleic Acids Res. Available at: http://www.ncbi.nlm.nih.gov/pubmed/20034956 [Accessed February 15, 2010].

Mandiyan, V., Tumminia, S. J., Wall, J. S., Hainfeld, J. F., and Boublik, M. (1991). Assembly of the Escherichia coli 30S ribosomal subunit reveals protein-dependent folding of the 16S rRNA domains. Proc. Natl. Acad. Sci. U.S.A *88*, 8174-8178.

Mangiarotti, G., Turco, E., Ponzetto, A., and Altruda, F. (1974). Precursor 16S RNA in active 30S ribosomes. Nature *247*, 147-148.

Mangiarotti, G. (2002). Synthesis of ribosomal proteins in developing Dictyostelium discoideum cells is controlled by the methylation of proteins S24 and S31. Biochem. Cell Biol *80*, 261-270.

Martin, A., Schneider, S., and Schwer, B. (2002). Prp43 is an essential RNA-dependent ATPase required for release of lariat-intron from the spliceosome. J. Biol. Chem *277*, 17743-17750.

Martin, W., and Koonin, E. V. (2006). Introns and the origin of nucleus-cytosol compartmentalization. Nature *440*, 41-45.

Mauro, V. P., and Edelman, G. M. (2002). The ribosome filter hypothesis. Proc. Natl. Acad. Sci. U.S.A *99*, 12031-12036.

Mauro, V. P., and Edelman, G. M. (2007). The ribosome filter redux. Cell Cycle *6*, 2246-2251.

Mayer, C., and Grummt, I. (2006). Ribosome biogenesis and cell growth: mTOR coordinates transcription by all three classes of nuclear RNA polymerases. Oncogene *25*, 6384-6391.

Mayer, C., Zhao, J., Yuan, X., and Grummt, I. (2004). mTOR-dependent activation of the transcription factor TIF-IA links rRNA synthesis to nutrient availability. Genes Dev *18*, 423-434.

Mazumder, B., Sampath, P., Seshadri, V., Maitra, R. K., DiCorleto, P. E., and Fox, P. L. (2003). Regulated release of L13a from the 60S ribosomal subunit as a mechanism of transcript-specific translational control. Cell *115*, 187-198.

McConkey, E. H., Bielka, H., Gordon, J., Lastick, S. M., Lin, A., Ogata, K., Reboud, J. P., Traugh, J. A., Traut, R. R., Warner, J. R., et al. (1979). Proposed uniform nomenclature for mammalian ribosomal proteins. Mol. Gen. Genet *169*, 1-6.

McQuillen, K., Roberts, R. B., and Britten, R. J. (1959). SYNTHESIS OF NASCENT PROTEIN BY RIBOSOMES IN ESCHERICHIA COLI. Proc. Natl. Acad. Sci. U.S.A *45*, 1437-1447.

Mereschkowsky, C. (1905). Über Natur und Ursprung der Chromatophoren im Pflanzenreiche. *25*, 593-604.

Merl, J., Jakob, S., Ridinger, K., Hierlmeier, T., Deutzmann, R., Milkereit, P., and Tschochner, H. (2010). Analysis of ribosome biogenesis factor-modules in yeast cells depleted from pre-ribosomes. Nucleic Acids Res. Available at: http://www.ncbi.nlm.nih.gov/pubmed/20100801 [Accessed February 17, 2010].

Merz, K., Hondele, M., Goetze, H., Gmelch, K., Stoeckl, U., and Griesenbeck, J. (2008). Actively transcribed rRNA genes in S. cerevisiae are organized in a specialized chromatin associated with the high-mobility group protein Hmo1 and are largely devoid of histone molecules. Genes Dev *22*, 1190-1204.

Mitchell, S. A., Brown, E. C., Coldwell, M. J., Jackson, R. J., and Willis, A. E. (2001). Protein factor requirements of the Apaf-1 internal ribosome entry segment: roles of polypyrimidine tract binding protein and upstream of N-ras. Mol. Cell. Biol *21*, 3364-3374.

Mizushima, S., and Nomura, M. (1970). Assembly mapping of 30S ribosomal proteins from E. coli. Nature *226*, 1214.

Moehle, C. M., and Hinnebusch, A. G. (1991). Association of RAP1 binding sites with stringent control of ribosomal protein gene transcription in Saccharomyces cerevisiae. Mol. Cell. Biol *11*, 2723-2735.

Moore, J., Jacobs, H. T., and Kaiser, K. (1995). The relationship between mRNA half-life and gene function in the yeast Saccharomyces cerevisiae. Gene *166*, 145-149.

Moradi, H., Simoff, I., Bartish, G., and Nygård, O. (2008). Functional features of the C-terminal region of yeast ribosomal protein L5. Mol. Genet. Genomics *280*, 337-350.

Morgan, A. R., Wells, R. D., and Khorana, H. G. (1966). STUDIES ON POLYNUCLEOTIDES, LIX. FURTHER CODON ASSIGNMENTS FROM AMINO ACID INCORPORATIONS DIRECTED BY RIBOPOLYNUCLEOTIDES CONTAINING REPEATING TRINUCLEOTIDE SEQUENCES. Proc. Natl. Acad. Sci. U.S.A *56*, 1899-1906.

Moritz, M., Paulovich, A. G., Tsay, Y. F., and Woolford, J. L. (1990). Depletion of yeast ribosomal proteins L16 or rp59 disrupts ribosome assembly. J. Cell Biol *111*, 2261-2274.

Morrissey, J. P., and Tollervey, D. (1995). Birth of the snoRNPs: the evolution of RNase MRP and the eukaryotic pre-rRNA-processing system. Trends Biochem. Sci *20*, 78-82.

Moss, T., Langlois, F., Gagnon-Kugler, T., and Stefanovsky, V. (2007). A housekeeper with power of attorney: the rRNA genes in ribosome biogenesis. Cell. Mol. Life Sci *64*, 29-49.

Moy, T. I., and Silver, P. A. (1999). Nuclear export of the small ribosomal subunit requires the ran-GTPase cycle and certain nucleoporins. Genes Dev *13*, 2118-2133.

Murayama, A., Ohmori, K., Fujimura, A., Minami, H., Yasuzawa-Tanaka, K., Kuroda, T., Oie, S., Daitoku, H., Okuwaki, M., Nagata, K., et al. (2008). Epigenetic control of rDNA loci in response to intracellular energy status. Cell *133*, 627-639.

Nagai, K., Oubridge, C., Ito, N., Avis, J., and Evans, P. (1995). The RNP domain: a sequence-specific RNA-binding domain involved in processing and transport of RNA. Trends Biochem. Sci *20*, 235-240.

Nagai, K., Oubridge, C., Ito, N., Jessen, T. H., Avis, J., and Evans, P. (1995). Crystal structure of the U1A spliceosomal protein complexed with its cognate RNA hairpin. Nucleic Acids Symp. Ser, 1-2.

Nazar, R. N. (2004). Ribosomal RNA processing and ribosome biogenesis in eukaryotes. IUBMB Life *56*, 457-465.

Ni, J., Tien, A. L., and Fournier, M. J. (1997). Small nucleolar RNAs direct site-specific synthesis of pseudouridine in ribosomal RNA. Cell *89*, 565-573.

Nierhaus, K. H. (1991). The assembly of prokaryotic ribosomes. Biochimie *73*, 739-755.

Nirenberg, M. W., and Matthaei, J. H. (1961). The dependence of cell-free protein synthesis in E. coli upon naturally occurring or synthetic polyribonucleotides. Proc. Natl. Acad. Sci. U.S.A *47*, 1588-1602.

Noller, H. F., Kop, J., Wheaton, V., Brosius, J., Gutell, R. R., Kopylov, A. M., Dohme, F., Herr, W., Stahl, D. A., Gupta, R., et al. (1981). Secondary structure model for 23S ribosomal RNA. Nucleic Acids Res *9*, 6167-6189.

Nomura, M. (1999). Regulation of ribosome biosynthesis in Escherichia coli and Saccharomyces cerevisiae: diversity and common principles. J. Bacteriol *181*, 6857-6864.

Nomura, M., and Erdmann, V. A. (1970). Reconstitution of 50S ribosomal subunits from dissociated molecular components. Nature *228*, 744-748.

Oeffinger, M., Dlakic, M., and Tollervey, D. (2004). A pre-ribosome-associated HEAT-repeat protein is required for export of both ribosomal subunits. Genes Dev *18*, 196-209.

Ohyanagi, H., Ikeo, K., and Gojobori, T. (2008a). Eukaryotic nuclear structure explains the evolutionary rate difference of ribosome export factors. Gene *421*, 7-13.

Ohyanagi, H., Ikeo, K., and Gojobori, T. (2008b). The origin of nucleus: rebuild from the prokaryotic ancestors of ribosome export factors. Gene *423*, 149-152.

Omer, A. D., Lowe, T. M., Russell, A. G., Ebhardt, H., Eddy, S. R., and Dennis, P. P. (2000a). Homologs of small nucleolar RNAs in Archaea. Science *288*, 517-522.

Omer, A. D., Lowe, T. M., Russell, A. G., Ebhardt, H., Eddy, S. R., and Dennis, P. P. (2000b). Homologs of small nucleolar RNAs in Archaea. Science *288*, 517-522.

Orengo, C. A., and Thornton, J. M. (1993). Alpha plus beta folds revisited: some favoured motifs. Structure *1*, 105-120.

Pace, B., Stahl, D. A., and Pace, N. R. (1984). The catalytic element of a ribosomal RNA-processing complex. J. Biol. Chem *259*, 11454-11458.

Palade, G. E. (1955). A small particulate component of the cytoplasm. J Biophys Biochem Cytol *1*, 59-68.

Panse, V. G., and Johnson, A. W. (2010). Maturation of eukaryotic ribosomes: acquisition of functionality. Trends Biochem Sci. Available at: http://www.ncbi.nlm.nih.gov/pubmed/20137954 [Accessed February 12, 2010].

Pape, T., Wintermeyer, W., and Rodnina, M. V. (1998). Complete kinetic mechanism of elongation factor Tu-dependent binding of aminoacyl-tRNA to the A site of the E. coli ribosome. EMBO J *17*, 7490-7497.

Passmore, L. A., Schmeing, T. M., Maag, D., Applefield, D. J., Acker, M. G., Algire, M. A., Lorsch, J.

R., and Ramakrishnan, V. (2007). The eukaryotic translation initiation factors eIF1 and eIF1A induce an open conformation of the 40S ribosome. Mol. Cell *26*, 41-50.

Pellagatti, A., Hellström-Lindberg, E., Giagounidis, A., Perry, J., Malcovati, L., Della Porta, M. G., Jädersten, M., Killick, S., Fidler, C., Cazzola, M., et al. (2008). Haploinsufficiency of RPS14 in 5q- syndrome is associated with deregulation of ribosomal- and translation-related genes. Br. J. Haematol *142*, 57-64.

Pelletier, J., and Sonenberg, N. (1988). Internal initiation of translation of eukaryotic mRNA directed by a sequence derived from poliovirus RNA. Nature *334*, 320-325.

Pertschy, B., Saveanu, C., Zisser, G., Lebreton, A., Tengg, M., Jacquier, A., Liebminger, E., Nobis, B., Kappel, L., van der Klei, I., et al. (2007). Cytoplasmic recycling of 60S preribosomal factors depends on the AAA protein Drg1. Mol. Cell. Biol *27*, 6581-6592.

Pertschy, B., Schneider, C., Gnädig, M., Schäfer, T., Tollervey, D., and Hurt, E. (2009a). RNA helicase Prp43 and its co-factor Pfa1 promote 20S to 18S rRNA processing catalyzed by the endonuclease Nob1. J. Biol. Chem. Available at: http://www.ncbi.nlm.nih.gov/pubmed/19801658 [Accessed October 22, 2009].

Pertschy, B., Schneider, C., Gnädig, M., Schäfer, T., Tollervey, D., and Hurt, E. (2009b). RNA helicase Prp43 and its co-factor Pfa1 promote 20S to 18S rRNA processing catalyzed by the endonuclease Nob1. J. Biol. Chem. Available at: http://www.ncbi.nlm.nih.gov/pubmed/19801658 [Accessed October 22, 2009].

Peters, R. (2005). Translocation through the nuclear pore complex: selectivity and speed by reduction-of-dimensionality. Traffic *6*, 421-427.

Piepersberg, W., Böck, A., and Wittmann, H. G. (1975a). Effect of different mutations in ribosomal protein S5 of Escherichia coli on translational fidelity. Mol. Gen. Genet *140*, 91-100.

Piepersberg, W., Böck, A., and Wittmann, H. G. (1975b). Effect of different mutations in ribosomal protein S5 of Escherichia coli on translational fidelity. Mol. Gen. Genet *140*, 91-100.

Pisarev, A. V., Kolupaeva, V. G., Pisareva, V. P., Merrick, W. C., Hellen, C. U. T., and Pestova, T. V. (2006). Specific functional interactions of nucleotides at key -3 and +4 positions flanking the initiation codon with components of the mammalian 48S translation initiation complex. Genes Dev *20*, 624-636.

Pisarev, A. V., Kolupaeva, V. G., Yusupov, M. M., Hellen, C. U. T., and Pestova, T. V. (2008a). Ribosomal position and contacts of mRNA in eukaryotic translation initiation complexes. EMBO J *27*, 1609-1621.

Pisarev, A. V., Kolupaeva, V. G., Yusupov, M. M., Hellen, C. U. T., and Pestova, T. V. (2008b). Ribosomal position and contacts of mRNA in eukaryotic translation initiation complexes. EMBO J *27*, 1609-1621.

Pisarev, A. V., Kolupaeva, V. G., Yusupov, M. M., Hellen, C. U. T., and Pestova, T. V. (2008c). Ribosomal position and contacts of mRNA in eukaryotic translation initiation complexes. EMBO J *27*, 1609-1621.

Planta, R. J., and Mager, W. H. (1998). The list of cytoplasmic ribosomal proteins of Saccharomyces cerevisiae. Yeast *14*, 471-477.

Politz, J. C. R., Tuft, R. A., and Pederson, T. (2003). Diffusion-based transport of nascent ribosomes in the nucleus. Mol. Biol. Cell *14*, 4805-4812.

Pöll, G., Braun, T., Jakovljevic, J., Neueder, A., Jakob, S., Woolford, J. L., Tschochner, H., and Milkereit, P. (2009). rRNA maturation in yeast cells depleted of large ribosomal subunit proteins. PLoS ONE *4*, e8249.

Potter, S., Durovic, P., and Dennis, P. P. (1995). Ribosomal RNA precursor processing by a eukaryotic U3 small nucleolar RNA-like molecule in an archaeon. Science *268*, 1056-1060.

Potter, S., Durovic, P., Russell, A., Wang, X., de Jong-Wong, D., and Dennis, P. P. (1995). Preribosomal RNA processing in archaea: characterization of the RNP endonuclease mediated processing of precursor 16S rRNA in the thermoacidophile Sulfolobus acidocaldarius. Biochem. Cell Biol *73*, 813-823.

Powers, T., and Walter, P. (1999). Regulation of ribosome biogenesis by the rapamycin-sensitive

TOR-signaling pathway in Saccharomyces cerevisiae. Mol. Biol. Cell *10*, 987-1000.

Prangishvilli, D., Zillig, W., Gierl, A., Biesert, L., and Holz, I. (1982). DNA-dependent RNA polymerase of thermoacidophilic archaebacteria. Eur. J. Biochem *122*, 471-477.

Ramakrishnan, V., and Moore, P. B. (2001). Atomic structures at last: the ribosome in 2000. Curr. Opin. Struct. Biol *11*, 144-154.

Rauch, T., Hundley, H. A., Pfund, C., Wegrzyn, R. D., Walter, W., Kramer, G., Kim, S., Craig, E. A., and Deuerling, E. (2005). Dissecting functional similarities of ribosome-associated chaperones from Saccharomyces cerevisiae and Escherichia coli. Mol. Microbiol *57*, 357-365.

Redko, Y., and Condon, C. (2009). Ribosomal protein L3 bound to 23S precursor rRNA stimulates its maturation by Mini-III ribonuclease. Mol. Microbiol *71*, 1145-1154.

Ree, H. K., Cao, K. M., Thurlow, D. L., and Zimmermann, R. A. (1989). The structure and organization of the 16S ribosomal RNA gene from the archaebacterium Thermoplasma acidophilum. Can. J. Microbiol *35*, 124-133.

Ree, H. K., and Zimmermann, R. A. (1990). Organization and expression of the 16S, 23S and 5S ribosomal RNA genes from the archaebacterium Thermoplasma acidophilum. Nucleic Acids Res *18*, 4471-4478.

Retèl, J., van den Bos, R. C., and Planta, R. J. (1969). Characteristics of the methylation in vivo of ribosomal RNA in yeast. Biochim. Biophys. Acta *195*, 370-380.

Rheinberger, H. J., Sternbach, H., and Nierhaus, K. H. (1981). Three tRNA binding sites on Escherichia coli ribosomes. Proc. Natl. Acad. Sci. U.S.A *78*, 5310-5314.

Robert, F., and Brakier-Gingras, L. (2003). A functional interaction between ribosomal proteins S7 and S11 within the bacterial ribosome. J. Biol. Chem *278*, 44913-44920.

Roberts, J. W., Shankar, S., and Filter, J. J. (2008). RNA polymerase elongation factors. Annu. Rev. Microbiol *62*, 211-233.

Roberts, P., Moshitch-Moshkovitz, S., Kvam, E., O'Toole, E., Winey, M., and Goldfarb, D. S. (2003). Piecemeal microautophagy of nucleus in Saccharomyces cerevisiae. Mol. Biol. Cell *14*, 129-141.

Roberts, R. (1958). Microsomal particles and protein synthesis papers presented at the First Symposium of the Biophysical Society, at the Massachusetts Institute of Technology, Cambridge, February 5, 6, and 8, 1958. (New York: Published on behalf of the Washington Academy of Sciences Washington D.C. by Pergamon Press).

Robledo, S., Idol, R. A., Crimmins, D. L., Ladenson, J. H., Mason, P. J., and Bessler, M. (2008). The role of human ribosomal proteins in the maturation of rRNA and ribosome production. RNA *14*, 1918-1929.

Rodnina, M. V., Savelsbergh, A., Katunin, V. I., and Wintermeyer, W. (1997). Hydrolysis of GTP by elongation factor G drives tRNA movement on the ribosome. Nature *385*, 37-41.

Rodnina, M. V., and Wintermeyer, W. (2009). Recent mechanistic insights into eukaryotic ribosomes. Curr. Opin. Cell Biol *21*, 435-443.

Roeben, A., Kofler, C., Nagy, I., Nickell, S., Hartl, F. U., and Bracher, A. (2006). Crystal structure of an archaeal actin homolog. J. Mol. Biol *358*, 145-156.

Rosado, I. V., Kressler, D., and de la Cruz, J. (2007). Functional analysis of Saccharomyces cerevisiae ribosomal protein Rpl3p in ribosome synthesis. Nucleic Acids Res *35*, 4203-4213.

Rosen, K. V., Alexander, R. W., Wower, J., and Zimmermann, R. A. (1993). Mapping the central fold of tRNA2(fMet) in the P site of the Escherichia coli ribosome. Biochemistry *32*, 12802-12811.

Rosset, R., and Gorini, L. (1969). A ribosomal ambiguity mutation. J. Mol. Biol *39*, 95-112.

Röther, S., and Strässer, K. (2007). The RNA polymerase II CTD kinase Ctk1 functions in translation elongation. Genes Dev *21*, 1409-1421.

Rouquette, J., Choesmel, V., and Gleizes, P. (2005). Nuclear export and cytoplasmic processing of precursors to the 40S ribosomal subunits in mammalian cells. EMBO J *24*, 2862-2872.

Rudra, D., Mallick, J., Zhao, Y., and Warner, J. R. (2007). Potential interface between ribosomal protein production and pre-rRNA processing. Mol. Cell. Biol *27*, 4815-4824.

Ruepp, A., Graml, W., Santos-Martinez, M. L., Koretke, K. K., Volker, C., Mewes, H. W., Frishman, D., Stocker, S., Lupas, A. N., and Baumeister, W. (2000). The genome sequence of the thermoacidophilic scavenger Thermoplasma acidophilum. Nature *407*, 508-513.

Ruggero, D., and Pandolfi, P. P. (2003). Does the ribosome translate cancer? Nat. Rev. Cancer *3*, 179-192.

Sabatini, D. M., Erdjument-Bromage, H., Lui, M., Tempst, P., and Snyder, S. H. (1994). RAFT1: a mammalian protein that binds to FKBP12 in a rapamycin-dependent fashion and is homologous to yeast TORs. Cell *78*, 35-43.

Sagan, L. (1967). On the origin of mitosing cells. J. Theor. Biol *14*, 255-274.

Samaha, R. R., O'Brien, B., O'Brien, T. W., and Noller, H. F. (1994). Independent in vitro assembly of a ribonucleoprotein particle containing the 3' domain of 16S rRNA. Proc. Natl. Acad. Sci. U.S.A *91*, 7884-7888.

Sasaki, T., Toh-E, A., and Kikuchi, Y. (2000). Yeast Krr1p physically and functionally interacts with a novel essential Kri1p, and both proteins are required for 40S ribosome biogenesis in the nucleolus. Mol. Cell. Biol *20*, 7971-7979.

Schäfer, T., Maco, B., Petfalski, E., Tollervey, D., Böttcher, B., Aebi, U., and Hurt, E. (2006). Hrr25-dependent phosphorylation state regulates organization of the pre-40S subunit. Nature *441*, 651-655.

Schmeing, T. M., Huang, K. S., Kitchen, D. E., Strobel, S. A., and Steitz, T. A. (2005). Structural insights into the roles of water and the 2' hydroxyl of the P site tRNA in the peptidyl transferase reaction. Mol. Cell *20*, 437-448.

Schmeing, T. M., Voorhees, R. M., Kelley, A. C., Gao, Y., Murphy, F. V., Weir, J. R., and Ramakrishnan, V. (2009). The crystal structure of the ribosome bound to EF-Tu and aminoacyl-tRNA. Science *326*, 688-694.

Schnabel, H., Schnabel, R., Yeats, S., Tu, J., Gierl, A., Neumann, H., and Zillig, W. (1984). Genome organization and transcription in archaebacteria. Folia Biol. (Praha) *30 Spec No*, 2-6.

Schneider, D. A., Michel, A., Sikes, M. L., Vu, L., Dodd, J. A., Salgia, S., Osheim, Y. N., Beyer, A. L., and Nomura, M. (2007). Transcription elongation by RNA polymerase I is linked to efficient rRNA processing and ribosome assembly. Mol. Cell *26*, 217-229.

Searcy, D. G., Stein, D. B., and Green, G. R. (1978). Phylogenetic affinities between eukaryotic cells and a thermophilic mycoplasma. BioSystems *10*, 19-28.

Seiser, R. M., Sundberg, A. E., Wollam, B. J., Zobel-Thropp, P., Baldwin, K., Spector, M. D., and Lycan, D. E. (2006a). Ltv1 is required for efficient nuclear export of the ribosomal small subunit in Saccharomyces cerevisiae. Genetics *174*, 679-691.

Seiser, R. M., Sundberg, A. E., Wollam, B. J., Zobel-Thropp, P., Baldwin, K., Spector, M. D., and Lycan, D. E. (2006b). Ltv1 is required for efficient nuclear export of the ribosomal small subunit in Saccharomyces cerevisiae. Genetics *174*, 679-691.

Semrad, K., Green, R., and Schroeder, R. (2004). RNA chaperone activity of large ribosomal subunit proteins from Escherichia coli. RNA *10*, 1855-1860.

Sharma, M. R., Barat, C., Wilson, D. N., Booth, T. M., Kawazoe, M., Hori-Takemoto, C., Shirouzu, M., Yokoyama, S., Fucini, P., and Agrawal, R. K. (2005). Interaction of Era with the 30S ribosomal subunit implications for 30S subunit assembly. Mol. Cell *18*, 319-329.

Shou, W., Sakamoto, K. M., Keener, J., Morimoto, K. W., Traverso, E. E., Azzam, R., Hoppe, G. J., Feldman, R. M., DeModena, J., Moazed, D., et al. (2001). Net1 stimulates RNA polymerase I transcription and regulates nucleolar structure independently of controlling mitotic exit. Mol. Cell *8*, 45-55.

Siekevitz, P. (1952). Uptake of radioactive alanine in vitro into the proteins of rat liver fractions. J. Biol. Chem *195*, 549-565.

Silvera, D., Arju, R., Darvishian, F., Levine, P. H., Zolfaghari, L., Goldberg, J., Hochman, T., Formenti, S. C., and Schneider, R. J. (2009). Essential role for eIF4GI overexpression in the pathogenesis of inflammatory breast cancer. Nat. Cell Biol *11*, 903-908.

Simonetti, A., Marzi, S., Jenner, L., Myasnikov, A., Romby, P., Yusupova, G., Klaholz, B. P., and

Yusupov, M. (2009). A structural view of translation initiation in bacteria. Cell. Mol. Life Sci *66*, 423-436.

Siridechadilok, B., Fraser, C. S., Hall, R. J., Doudna, J. A., and Nogales, E. (2005). Structural roles for human translation factor eIF3 in initiation of protein synthesis. Science *310*, 1513-1515.

Sirri, V., Urcuqui-Inchima, S., Roussel, P., and Hernandez-Verdun, D. (2008). Nucleolus: the fascinating nuclear body. Histochem. Cell Biol *129*, 13-31.

Skorvaga, M., Raven, N. D., and Margison, G. P. (1998). Thermostable archaeal O6-alkylguanine-DNA alkyltransferases. Proc. Natl. Acad. Sci. U.S.A *95*, 6711-6715.

Song, X., and Nazar, R. N. (2002). Modification of rRNA as a 'quality control mechanism' in ribosome biogenesis. FEBS Lett *523*, 182-186.

Soudet, J., Gélugne, J., Belhabich-Baumas, K., Caizergues-Ferrer, M., and Mougin, A. (2010). Immature small ribosomal subunits can engage in translation initiation in Saccharomyces cerevisiae. EMBO J *29*, 80-92.

Spahn, C. M., Beckmann, R., Eswar, N., Penczek, P. A., Sali, A., Blobel, G., and Frank, J. (2001). Structure of the 80S ribosome from Saccharomyces cerevisiae--tRNA-ribosome and subunit-subunit interactions. Cell *107*, 373-386.

Squires, C. L., and Zaporojets, D. (2000). Proteins shared by the transcription and translation machines. Annu. Rev. Microbiol *54*, 775-798.

Stahl, D. A., Pace, B., Marsh, T., and Pace, N. R. (1984). The ribonucleoprotein substrate for a ribosomal RNA-processing nuclease. J. Biol. Chem *259*, 11448-11453.

Steffen, K. K., MacKay, V. L., Kerr, E. O., Tsuchiya, M., Hu, D., Fox, L. A., Dang, N., Johnston, E. D., Oakes, J. A., Tchao, B. N., et al. (2008). Yeast life span extension by depletion of 60s ribosomal subunits is mediated by Gcn4. Cell *133*, 292-302.

Stein, D. B., and Searcy, D. G. (1978). Physiologically important stabilization of DNA by a prokaryotic histone-like protein. Science *202*, 219-221.

Steitz, T. A. (2008). A structural understanding of the dynamic ribosome machine. Nat. Rev. Mol. Cell Biol *9*, 242-253.

Stern, S., Powers, T., Changchien, L. M., and Noller, H. F. (1989). RNA-protein interactions in 30S ribosomal subunits: folding and function of 16S rRNA. Science *244*, 783-790.

Suthers, P. F., Gourse, R. L., and Yin, J. (2007). Rapid responses of ribosomal RNA synthesis to nutrient shifts. Biotechnol. Bioeng *97*, 1230-1245.

Sykes, M. T., and Williamson, J. R. (2009). A complex assembly landscape for the 30S ribosomal subunit. Annu Rev Biophys *38*, 197-215.

Synetos, D., Frantziou, C. P., and Alksne, L. E. (1996a). Mutations in yeast ribosomal proteins S28 and S4 affect the accuracy of translation and alter the sensitivity of the ribosomes to paromomycin. Biochim. Biophys. Acta *1309*, 156-166.

Synetos, D., Frantziou, C. P., and Alksne, L. E. (1996b). Mutations in yeast ribosomal proteins S28 and S4 affect the accuracy of translation and alter the sensitivity of the ribosomes to paromomycin. Biochim. Biophys. Acta *1309*, 156-166.

Szeberényi, J., Roy, M. K., Vaidya, H. C., and Apirion, D. (1984). 7S RNA, containing 5S ribosomal RNA and the termination stem, is a specific substrate for the two RNA processing enzymes RNase III and RNase E. Biochemistry *23*, 2952-2957.

Szymanski, M., Barciszewska, M. Z., Erdmann, V. A., and Barciszewski, J. (2002). 5S Ribosomal RNA Database. Nucleic Acids Res *30*, 176-178.

Tabb-Massey, A., Caffrey, J. M., Logsden, P., Taylor, S., Trent, J. O., and Ellis, S. R. (2003). Ribosomal proteins Rps0 and Rps21 of Saccharomyces cerevisiae have overlapping functions in the maturation of the 3' end of 18S rRNA. Nucleic Acids Res *31*, 6798-6805.

Takahashi, Y., Hirayama, S., and Odani, S. (2005). Ribosomal proteins cross-linked to the initiator AUG codon of a mRNA in the translation initiation complex by UV-irradiation. J. Biochem *138*, 41-46.

Talkington, M. W. T., Siuzdak, G., and Williamson, J. R. (2005). An assembly landscape for the 30S

ribosomal subunit. Nature *438*, 628-632.

Tang, T. H., Rozhdestvensky, T. S., d'Orval, B. C., Bortolin, M., Huber, H., Charpentier, B., Branlant, C., Bachellerie, J., Brosius, J., and Hüttenhofer, A. (2002). RNomics in Archaea reveals a further link between splicing of archaeal introns and rRNA processing. Nucleic Acids Res *30*, 921-930.

Tang, T., Bachellerie, J., Rozhdestvensky, T., Bortolin, M., Huber, H., Drungowski, M., Elge, T., Brosius, J., and Hüttenhofer, A. (2002). Identification of 86 candidates for small non-messenger RNAs from the archaeon Archaeoglobus fulgidus. Proc. Natl. Acad. Sci. U.S.A *99*, 7536-7541.

Taylor, D. J., Devkota, B., Huang, A. D., Topf, M., Narayanan, E., Sali, A., Harvey, S. C., and Frank, J. (2009). Comprehensive molecular structure of the eukaryotic ribosome. Structure *17*, 1591-1604.

The Royal Swedish Academy of Sciences (2009). The Nobel Prize in Chemistry 2009. Press Release.

Thomas, F., and Kutay, U. (2003). Biogenesis and nuclear export of ribosomal subunits in higher eukaryotes depend on the CRM1 export pathway. J. Cell. Sci *116*, 2409-2419.

Thomson, E., and Tollervey, D. (2010). The final step in 5.8S rRNA processing is cytoplasmic in Saccharomyces cerevisiae. Mol. Cell. Biol *30*, 976-984.

Tollervey, D., Lehtonen, H., Jansen, R., Kern, H., and Hurt, E. C. (1993). Temperature-sensitive mutations demonstrate roles for yeast fibrillarin in pre-rRNA processing, pre-rRNA methylation, and ribosome assembly. Cell *72*, 443-457.

Trapman, J., and Planta, R. J. (1976). Maturation of ribosomes in yeast. I Kinetic analysis by labelling of high molecular weight rRNA species. Biochim. Biophys. Acta *442*, 265-274.

Traub, P., and Nomura, M. (1968). Structure and function of E. coli ribosomes. V. Reconstitution of functionally active 30S ribosomal particles from RNA and proteins. Proc. Natl. Acad. Sci. U.S.A *59*, 777-784.

Tschochner, H., and Hurt, E. (2003). Pre-ribosomes on the road from the nucleolus to the cytoplasm. Trends Cell Biol *13*, 255-263.

Tu, J., and Zillig, W. (1982). Organization of rRNA structural genes in the archaebacterium Thermoplasma acidophilum. Nucleic Acids Res *10*, 7231-7245.

Udem, S. A., and Warner, J. R. (1973). The cytoplasmic maturation of a ribosomal precursor ribonucleic acid in yeast. J. Biol. Chem *248*, 1412-1416.

Vanrobays, E., Gelugne, J., Gleizes, P., and Caizergues-Ferrer, M. (2003). Late cytoplasmic maturation of the small ribosomal subunit requires RIO proteins in Saccharomyces cerevisiae. Mol. Cell. Biol *23*, 2083-2095.

Vanrobays, E., Gélugne, J., Caizergues-Ferrer, M., and Lafontaine, D. L. J. (2004). Dim2p, a KH-domain protein required for small ribosomal subunit synthesis. RNA *10*, 645-656.

Vanrobays, E., Leplus, A., Osheim, Y. N., Beyer, A. L., Wacheul, L., and Lafontaine, D. L. J. (2008). TOR regulates the subcellular distribution of DIM2, a KH domain protein required for cotranscriptional ribosome assembly and pre-40S ribosome export. RNA *14*, 2061-2073.

Venema, J., and Tollervey, D. (1995). Processing of pre-ribosomal RNA in Saccharomyces cerevisiae. Yeast *11*, 1629-1650.

Volkin, E., and Astrachan, L. (1956). Phosphorus incorporation in Escherichia coli ribo-nucleic acid after infection with bacteriophage T2. Virology *2*, 149-161.

Wagner, R. (2002). Regulation of ribosomal RNA synthesis in E. coli: effects of the global regulator guanosine tetraphosphate (ppGpp). J. Mol. Microbiol. Biotechnol *4*, 331-340.

Warner, J. R. (1999). The economics of ribosome biosynthesis in yeast. Trends Biochem. Sci *24*, 437-440.

Warner, J. R., and McIntosh, K. B. (2009). How common are extraribosomal functions of ribosomal proteins? Mol. Cell *34*, 3-11.

Weis, K. (2007). The nuclear pore complex: oily spaghetti or gummy bear? Cell *130*, 405-407.

Weisberg, R. A. (2008). Transcription by moonlight: structural basis of an extraribosomal activity of

ribosomal protein S10. Mol. Cell *32*, 747-748.

Weitzmann, C. J., Cunningham, P. R., Nurse, K., and Ofengand, J. (1993). Chemical evidence for domain assembly of the Escherichia coli 30S ribosome. FASEB J *7*, 177-180.

Wery, M., Ruidant, S., Schillewaert, S., Leporé, N., and Lafontaine, D. L. J. (2009). The nuclear poly(A) polymerase and Exosome cofactor Trf5 is recruited cotranscriptionally to nucleolar surveillance. RNA *15*, 406-419.

West, M., Hedges, J. B., Chen, A., and Johnson, A. W. (2005). Defining the order in which Nmd3p and Rpl10p load onto nascent 60S ribosomal subunits. Mol. Cell. Biol *25*, 3802-3813.

Wilson, D. N., and Nierhaus, K. H. (2005). Ribosomal proteins in the spotlight. Crit. Rev. Biochem. Mol. Biol *40*, 243-267.

Wimberly, B. T., Brodersen, D. E., Clemons, W. M., Morgan-Warren, R. J., Carter, A. P., Vonrhein, C., Hartsch, T., and Ramakrishnan, V. (2000). Structure of the 30S ribosomal subunit. Nature *407*, 327-339.

Woese, C. R., Magrum, L. J., Gupta, R., Siegel, R. B., Stahl, D. A., Kop, J., Crawford, N., Brosius, J., Gutell, R., Hogan, J. J., et al. (1980). Secondary structure model for bacterial 16S ribosomal RNA: phylogenetic, enzymatic and chemical evidence. Nucleic Acids Res *8*, 2275-2293.

Wolf, S., Lottspeich, F., and Baumeister, W. (1993). Ubiquitin found in the archaebacterium Thermoplasma acidophilum. FEBS Lett *326*, 42-44.

Wood, E. R., Ghané, F., and Grogan, D. W. (1997). Genetic responses of the thermophilic archaeon Sulfolobus acidocaldarius to short-wavelength UV light. J. Bacteriol *179*, 5693-5698.

Woodson, S. A. (2008). RNA folding and ribosome assembly. Curr Opin Chem Biol *12*, 667-673.

Wu, B., Yee, A., Huang, Y. J., Ramelot, T. A., Cort, J. R., Semesi, A., Jung, J., Lee, W., Montelione, G. T., Kennedy, M. A., et al. (2008). The solution structure of ribosomal protein S17E from Methanobacterium thermoautotrophicum: a structural homolog of the FF domain. Protein Sci *17*, 583-588.

Xu, Z., O'Farrell, H. C., Rife, J. P., and Culver, G. M. (2008). A conserved rRNA methyltransferase regulates ribosome biogenesis. Nat. Struct. Mol. Biol *15*, 534-536.

Yao, W., Roser, D., Köhler, A., Bradatsch, B., Bassler, J., and Hurt, E. (2007). Nuclear export of ribosomal 60S subunits by the general mRNA export receptor Mex67-Mtr2. Mol. Cell *26*, 51-62.

Yu, Y., Marintchev, A., Kolupaeva, V. G., Unbehaun, A., Veryasova, T., Lai, S., Hong, P., Wagner, G., Hellen, C. U. T., and Pestova, T. V. (2009). Position of eukaryotic translation initiation factor eIF1A on the 40S ribosomal subunit mapped by directed hydroxyl radical probing. Nucleic Acids Res *37*, 5167-5182.

Zebarjadian, Y., King, T., Fournier, M. J., Clarke, L., and Carbon, J. (1999). Point mutations in yeast CBF5 can abolish in vivo pseudouridylation of rRNA. Mol. Cell. Biol *19*, 7461-7472.

Zemp, I., Wild, T., O'Donohue, M., Wandrey, F., Widmann, B., Gleizes, P., and Kutay, U. (2009). Distinct cytoplasmic maturation steps of 40S ribosomal subunit precursors require hRio2. J. Cell Biol *185*, 1167-1180.

Zhang, Y., Wolf, G. W., Bhat, K., Jin, A., Allio, T., Burkhart, W. A., and Xiong, Y. (2003). Ribosomal protein L11 negatively regulates oncoprotein MDM2 and mediates a p53-dependent ribosomal-stress checkpoint pathway. Mol. Cell. Biol *23*, 8902-8912.

Zillig, W., Stetter, K. O., and Janeković, D. (1979). DNA-dependent RNA polymerase from the archaebacterium Sulfolobus acidocaldarius. Eur. J. Biochem *96*, 597-604.

8 Abbreviations

abbreviation	meaning
5-FOA	5-fluoro-orothic acid
Å	angstrom
ARS	autonomous replication sequence
bp	base pair
C-terminal	carboxy terminal
cs	cold sensitive
Cy3	member of the cyanine dye family (excitation 550 nm, emission 570 nm)
Da	dalton
DAPI	4'-6-Diamino-2-phenylindol-dihydrochlorid
DIC, DICIII	differential interference contrast, differential interference contrast III objective (Zeiss)
DNA	desoxyribonucleic acid
E. coli	Escherichia coli
EM	electron microscopy
ETS	external transcribed spacer
FISH	fluorescence *in situ* hybridization
GAL	galactose
GLC	glucose
IP	immuno-precipitation
ITS	internal transcribed spacer
M	molar [mol/l]
MALDI	matrix assisted laser desorption/ionization
mRNA	messenger RNA
MS	mass spectrometry
MS/MS	tandem mass spectrometry
N-terminal	amino terminal
nano HPLC	nano high pressure liquid chromatography
NES	nuclear export sequence
NLS	nuclear localization sequence
NTS	non-transcribed spacer
o/n	overnight
OD(600)	optical density at 600 nm
ORF	open reading frame
PAGE	polyacrylamide gel electrophoresis
PCR	polymerase chain reaction
pGAL	galactose inducible promoter (in this work usually GAL1-promoter)
pH	negative decadic logarithm of the molar concentration of dissolved hydrogen ions
rDNA	ribosomal DNA

abbreviation	meaning
RNA	ribonucleic acid
rpL	ribosomal protein of the large subunit
rpm	rotations per minute
rpS	ribosomal protein of the small subunit
rRNA	ribosomal RNA
RT	room termperature
S. cerevisiae	Saccharomyces cerevisiae
SAS	*Sulfolobus acidocaldarius* small subunit protein
snoRNP	small nucleolar ribonucleoprotein
SOE	splicing by overlap extension
TAP	tandem affinity purification tag
TAS	*Thermoplasma acidophilum* small subunit protein
tRNA	transfer RNA
ts	temperature sensitive
WT	wildtype

Elements, chemical compounds, physical variables and units are abbreviated according to international rules.

The one letter amino acid code is used.

9 Publications

Neueder, A., Jakob, S., Pöll, G., Linnemann J., Deutzmann R., Tschochner, H., and Milkereit, P. (2010). A local role for the small ribosomal subunit primary binder rpS5 in final 18S rRNA processing in yeast. PLoS ONE *5(4),* e10194.

Pöll, G., Braun, T., Jakovljevic, J., **Neueder, A.**, Jakob, S., Woolford, J. L., Tschochner, H., and Milkereit, P. (2009). rRNA maturation in yeast cells depleted of large ribosomal subunit proteins. PLoS ONE *4*, e8249.

Ferreira-Cerca, S., Pöll, G., Kühn, H., **Neueder, A.**, Jakob, S., Tschochner, H., and Milkereit, P. (2007). Analysis of the in vivo assembly pathway of eukaryotic 40S ribosomal proteins. Mol. Cell *28*, 446-457.

Danksagung

An erster Stelle möchte ich mich bei meinem Mentor Dr. Philipp Milkereit für die interessante Fragestellung, die professionelle Betreuung dieser Arbeit und anregende Diskussionen bedanken.

Bei Prof. Herbert Tschochner bedanke ich mich für die vielen guten Anregungen und das große Interesse an meiner Arbeit. Ich möchte mich aber auch für die vielen gemeinsamen Stunden am Fels und im Schnee bedanken. Ich werde unsere Abenteuer sehr vermissen, Herbert!

Allen ehemaligen und aktuellen Mitgliedern der “Milkereit Gruppe“ herzlichen Dank für die Hilfsbereitschaft und das nette Arbeitsklima. Insbesondere Gisela Pöll möchte ich für ihre unendliche Bereitschaft immer und überall zu helfen hier danken.

Meinen drei Praktikant(innen) Claudia Seidl, Katrin Mücke und Uli Ohmayer gilt Dank für ihre Hilfe bei dieser Arbeit. Viel Spaß und Erfolg weiterhin!

Mein Dank gilt auch allen anderen Mitgliedern des “house of the ribosome”, die hier nicht ausdrücklich erwähnt werden und speziell denen, die etwas zum Gelingen dieser Arbeit beigetragen haben.

Mein herzlichster Dank gilt meiner Familie, die mich bedingungslos unterstützt hat. Vielen lieben Dank, ohne euch wäre ich wohl nie so weit gekommen.

Meinen beiden besten Freunden möchte ich für ein immer offenes Ohr, Hilfe jeglicher Art und noch vieles mehr Danke sagen. Ich weiß es sehr zu schätzen, dass wir uns getroffen haben.

Die Dinge, für die ich mich bei meiner Freundin bedanken möchte, würden den Rahmen der Danksagung sprengen. Ich hoffe du weißt das auch so!